Morphological and spatial influences on molluscan macroevolution

by

Lucy M. Chang

A dissertation submitted in partial satisfaction of the

requirements for the degree of

Doctor of Philosophy

in

Integrative Biology

in the

Graduate Division

of the

University of California, Berkeley

Committee in charge:

Dr. Charles Marshall, Chair
Dr. Rosemary Gillespie
Dr. David Lindberg
Dr. Seth Finnegan

Summer 2017

Morphological and spatial influences on molluscan macroevolution

Lucy M. Chang

Abstract

Morphological and spatial influences on molluscan macroevolution

by

Lucy M. Chang

Doctor of Philosophy in Integrative Biology

University of California, Berkeley

Dr. Charles Marshall, Chair

Predicting the capacity of a lineage to survive, disperse, or diversify when faced with a changing environment is a fundamental aim in both ecology and evolution and one that is increasingly critical in a rapidly altered world. Here, by using morphological and phylogenetic measures of similarity as proxies for ecological similarity, I examine how the presence and absence of similar taxa across both space and time impacts extinction risk, morphological evolution, and colonization success. Through use of temporal and taxonomic replicates, the consistency of these patterns can be characterized, leading to a better understanding of the degree to which biotic responses to novel conditions are predictable.

Chapter 1 examines the degree to which predictors of extinction risk remain consistent over time. I approach this using the fossil record of ammonites across the Cretaceous Period (145-66 Ma), incorporating measures of morphological similarity, in addition to classical descriptors of shell coiling and non-morphological traits, into stage-level extinction models. I find that predictors of background extinction are highly variable in importance and magnitude of selectivity from stage to stage with few consistent relationships that can be applied predictively across time. These results highlight the temporally variable nature of background extinction, the importance of context, and the challenge this poses in the search for generalizable rules of extinction.

Chapter 2 assesses whether occupation of a newly-formed environment coincided with consistent morphological shifts independently across taxa. I use ammonite occurrences in and around the North American Western Interior Seaway (WIS) during its formative stage and outline analysis of shell aperture shapes to test whether species inhabiting a deepening seaway occupy similar positions in morphospace relative to their congeneric, non-seaway counterparts. I find that some genera spanning the boundary between the Western Interior Seaway and the Gulf and Atlantic Coast region to the seaway's south exhibit similar shape differences between the two regions, indicating some predictability in the direction of morphological evolution given access to the same environment. This spatial pattern, however, is not reflected within wide-ranging species. The consistency across multiple taxa suggests that the onset of novel environmental conditions may be capable of influencing the trajectory of morphological evolution in a clade as a whole.

Chapter 3 characterizes the relationship between evolutionary relatedness to native taxa and successful colonization within a late Cenozoic embayment. Darwin's naturalization hypothesis predicts that potential colonizers more closely related to incumbent taxa are less likely to successfully establish due to competition and limiting similarity. I approach this using a large phylogeny of extant bivalve genera and the rich fossil record of bivalves along the Pacific Coast of North America. Specifically, I examine patterns of colonization from the open ocean, through restricted connections, into the embayment formerly present in the San Joaquin Basin of central California from 27 Ma to 2.5 Ma. By comparing the relatedness of successful colonizers to the native fauna in the basin with the relatedness expected through random assembly, I find that colonization success in the San Joaquin Basin is not strongly linked with unusually close or unusually distant relatedness in any of the time bins considered.

TABLE OF CONTENTS

Acknowledgments

This dissertation is truly the product of the generosity and patience shown to me by many individuals. First and foremost, I cannot fully express how grateful I am to have had the support, guidance, and friendship of my advisor, Charles Marshall, throughout these years. The breadth and depth of his thinking and his dedication to his students and the communities which he is a part of never fail to inspire. The many impromptu conversations have been an integral part of my development both as a scientist and as a person, as has his willingness to let me wander. None of this would have been possible if not for his encouragement, his patience, and, in a big way, his confidence in me. It has been a tremendous joy and a privilege.

I would also like to thank my committee members for their support throughout this process and their contributions to my scientific training. David Lindberg, Seth Finnegan, and Rosemary Gillespie, for the many years of feedback and encouragement that have enabled me to keep on going, and Tony Barnosky and David Ackerly, for the discussions and guidance early in my graduate career that shaped what was to come. I could not have asked for a brighter group of mentors, and I have benefitted immensely from each of their wisdom and experiences.

I would like to thank the following people for all they did to facilitate my visits to the collections at their respective institutions: Kevin McKinney (United States Geological Survey), Bushra Hussaini (American Museum of Natural History), Talia Karim (University of Colorado Museum of Natural History), and Kathy Hollis, Mark Florence, and Daniel Levin (Smithsonian Institute National Museum of Natural History). I would also like to extend my greatest thanks to Aaron Bagnell, Margaret Yacobucci, and Phillip Skipwith for generously offering their time, resources, and knowledge, without which portions of this work would not have been possible.

I gratefully acknowledge several agencies and institutions that have enabled me to pursue this work: the National Science Foundation (DGE-1106400), the University of California, Berkeley (the Reshetko Family Scholarship, Roy Leeper Scholarship, and additional Department of Integrative Biology and Graduate Division student grants), the University of California Museum of Paleontology (the William B. N. Berry Memorial Research Fund, Dorothy K. Palmer Fund, and Annie Alexander Fund), and the Geological Society of America Cordilleran Section.

For everything they have taught me and for their crucial roles in maintaining my health and sanity, I owe an incredible debt of gratitude to so many past and present graduate students of Integrative Biology and members of the University of California Museum of Paleontology community, notably the Marshall Lab family (Camilla Souto, Jun Ying Lim, and Daniel Latorre) and, especially, Ashley Poust. The sincere kindness, boundless support, and incredible trove of knowledge contained in each one of these entities is nothing short of astounding. I don't know where I'd be without the laughter and camaraderie, but I am truly lucky to have had both in plenty.

Finally, I thank my parents, Tony and May, and my sister, Nancy, for their unconditional support. There was never a shortage of curiosity and stubbornness in the Chang household, and I owe more to that than I can begin to express.

Chapter 1

Morphological predictors of background extinction risk for ammonites through the Cretaceous

Introduction

Evaluations of extinction selectivity provide one of the most compelling approaches for disentangling the relative contributions of ecology, environment, and chance in driving biodiversity patterns. Though progress has been made identifying taxonomic (e.g., Alroy 2008) and ecological (e.g., Ezard et al. 2011, Clapham and Payne 2011, Finnegan et al. 2016) selectivity in the fossil record, these features capture only a portion of the underlying biological change associated with fluctuating diversity.

The use of morphospaces allows for reproducible measures of morphological disparity and distinctness, which have been used in studies of development, radiations, and the evolution of ecological diversity (Erwin 2007). Previous applications of morphospaces in macroevolutionary studies have primarily focused on the degree of coupling between a clade's diversity and overall disparity without explicitly addressing an individual taxon's probability of going extinct or originating (Foote 1993, Foote 1994, Villier and Korn 2004). In many cases, these kinds of studies attempt to identify nonrandom trimming in morphospace as evidence of selectivity or measure how the occupation of morphospace is impacted by extinction rather than the other way around. Additional analyses linking morphological disparity to extinction noted patterns in genus-specific longevity associated with overall deviation from the mean morphology (Baumiller 1993, Liow 2006) and differential post-mass extinction recovery rate associated with specific regions in morphospace (Lockwood 2004). While an extensive body of literature regarding selectivity analyses has focused on major events in life history such as mass extinctions, background extinction has received less attention despite recognition that the drivers behind both scenarios likely differ in magnitude, direction, and identity (Jablonski 1986, Payne and Finnegan 2007). An improved understanding of factors that drive background extinction, however, provides a baseline with which to identify unusual deviations from those drivers and subsequently predict its outcomes.

In general, the incorporation of measures of relative morphological distinctness, such as the degree of packing in morphospace and morphological deviance, into time-specific models of extinction and origination has been limited. Such approaches would allow for taxon-free assessment of extinction risk by focusing on quantitative measures of dissimilarity rather than discrete ecological differences or post-hoc delineation of morphospace regions. The role of dissimilarity in driving diversification patterns has deep roots in ecological theory concerning the outcomes of competition and specialization. The competitive exclusion principle (also known as Gause's Law), for example, posits that similarity between two taxa can have far-reaching evolutionary consequences through competition, resource limitation, and subsequent extinction (Hardin 1960, Krause 1986). By extension, sparsely occupied regions of morphospace may indicate ecological opportunity and vacant niches, which are thought to promote diversification (Van Valkenburg 1991, Foote 1999, Schluter 2000). Competition, however, is notoriously difficult to detect in the fossil record and has been largely inferred using the coincident rise and

decline of entire clades (Sepkoski 1981, Benton 1987, Krause 1986, Van Valkenburg 1991, Liow et al. 2015). On the other hand, specialization has also been proposed to produce evolutionary "dead-ends" (Colles et al. 2009, Van Valkenburg et al. 2004), though it has been found to be associated with both increased and decreased genus longevities (Baumiller 1993, Van Valkenburg et al. 2004, Liow 2006). By considering only contemporary subsets of taxa, I focus on linking how a taxon experiences its extrinsic biotic and abiotic landscape to its immediate extinction risk.

Ammonoids are a model group with which to conduct high-resolution morphological and evolutionary studies. For over 300 million years until the group's extinction at the Cretaceous/Paleogene boundary, the group exhibited high rates of taxonomic turnover and a broad, labile range of morphologies. Taphonomic, biomechanical, and isotopic studies have suggested a strong relationship between the shape of the organism's external, chambered shell and its preferred position in the water column and degree of mobility (see Ritterbush et al. 2014 for review). Using a series of simple linear measurements to capture shell geometry, Raup (1966) established a theoretical morphospace for coil-shelled organisms, which he then applied to planispiral ammonites to determine the degree to which the group occupied their feasible range of morphologies (Raup 1967). This framework has been foundational in morphological studies of ammonoids, which have since made use of the theory or method with limited modification to examine changes in disparity over time as well (e.g., Moyne and Neige 2007, Saunders et al. 2008, Gerber 2011, Neige et al. 2013), selectivity at and recovery following mass extinction events (e.g., Villier and Korn 2004, Brosse et al. 2013), and links between morphology, mode of life, and environment (e.g., Westermann 1996).

Despite approaching their demise, ammonoids show high taxonomic and morphological diversity of both planispiral and heteromorphic forms for much of the Cretaceous Period (145-66 Ma). This period is characterized greenhouse Earth conditions and a continental configuration that resembles relatively closely that of modern day. Eustatic sea level rise driven by global warming and tectonic activity during this period led to the formation of large epeiric seas on most continents by the start of the Late Cretaceous, which persisted until the end Cretaceous. This climatic backdrop was furthermore punctuated by several well-documented oceanic anoxic events (OAEs) that yielded widespread oxygen-deficient bottom water conditions (Jenkyns 2010). The more severe OAEs, such as that at the Cenomanian/Turonian boundary, roughly coincided with pulses of elevated extinction in several groups of marine organisms, including ammonites (Elder 1989, Leckie et al. 2002). The study of morphological extinction selectivity and its ecological underpinnings is particularly relevant in the Cretaceous given the observed escalation in interaction-driven, morphological innovation in marine invertebrate biota across the era, recognized as the Mesozoic Marine Revolution (Vermeij 1977).

Here I establish a global morphospace for genera of ammonites across the Cretaceous Period. I apply a machine learning approach to fit predictive models of extinction for 11 stages of the Cretaceous and determine the strength and nature of the relationship between a suite of morphological and taxonomic predictors and taxon-specific extinction. I further examine the consistency of these relationships over time by assessing the ability of each interval-specific model to predict extinction in each of the other stages. Identification of taxon-free metrics such as morphological distinctness and degree of crowding that may predict selectivity at times of

biotic turnover would better allow for assessment of extinction vulnerability across biological groups and time periods.

Methods

Data sources

Stratigraphic ranges and morphological data were collected primarily from Wright et al.'s Treatise on Invertebrate Paleontology, part L, Revised. Mollusca 4: Cretaceous Ammonoidea (1996). The taxonomic scope of this study was limited to suborder Ammonitina, a diverse group consisting of planispiral ammonoid forms. Wright et al. (1996) provides a standardized treatment of ammonoid genera known at time of publication to exist during the Cretaceous, including genus and subgenus stratigraphic ranges and figures of exemplar specimens. Because the taxonomy presented in Wright et al. (1996) is resolved to the subgenus level, I treated subgenera as taxonomic units hierarchically equivalent to genera. Taxa of uncertain taxonomic status (denoted in Wright et al. [1996] with a "?") or without reported stratigraphic ranges were excluded from this study.

For the included taxa, stratigraphic first and last appearances reported in Wright et al. (1996) were resolved to the stage level and assumed to range through reported intervals. For eleven taxa, first and last stages were reported as uncertain and trimmed from the overall stratigraphic durations, providing conservative representations of true durations and leading to the exclusion of four of these taxa whose ranges could not be resolved at all following this schema. Range endpoints reported as Ryazanian or Late Volgian were reassigned to be of Berriasian age. In the end, I noted stratigraphic durations for 479 genera and subgenera of Ammonitina.

Morphological data were collected from exemplar figures published in Wright et al. (1996) for each taxon using an open-source image measurement web applet (available at https://github.com/lucymchang/webmorph). Each genus or subgenus is usually represented by one specimen to prioritize achieving taxonomic breadth. These data consist of four linear measurements: maximum diameter of the shell (*D*), maximum height of the last visible whorl (*a*), height of the whorl 180° from *a* (*a'*), and maximum width of the last visible whorl (*b*) (Figure 1.1). Because the apertural and side views of the whorl are both needed to obtain complete set of measurements, data collected from multiple figures of the same specimen were scaled to each other to provide a complete measurement set. For those genera with reported stratigraphic ranges but incomplete measurement sets, additional measurements were collected from the primary literature (Appendix A.1). Those that were unable to be supplemented were excluded from the remainder of the morphometric study. In the end, 379 taxa were included in subsequent morphospace generation and extinction models. Representation of taxa in the morphological dataset was even across stages, ranging between 75% of taxa present in the Maastrichtian to 89% of taxa present in the Barremian (Figure 1.2).

Morphospace generation

Three shell-coiling parameters based off of Raup's (1967) work were then calculated from the four linear measurements obtained from each exemplar specimen (Figure 1.1). These parameters

take the form of dimensionless ratios and have been widely used both theoretically and quantitatively to classify the gross morphology of coil-shelled organisms, including foraminifera, gastropods, and ammonoids. They consist of the umbilical ratio (U) where:

$$U = UD/D \quad (1)$$

the whorl expansion rate (w) where:

$$w = (a/a')^2 \quad (2)$$

and the shell inflation (S) where:

$$S = b/a \quad (3)$$

The biological interpretations of these parameters are discussed in more detail in the following section.

In cases where multiple specimens were figured for one genus or subgenus, the mean values of U, w, and S were used to represent the taxon (Appendix A.2). Though not completely independent, the three parameters are only somewhat correlated in the dataset. I then conducted principal component analysis using the three coiling parameters scaled to unit variance to generate an empirical morphospace for Cretaceous ammonites, which serves as the basis for the extinction models. Because only three variables were used to generate the morphospace, I retain all axes from the resulting principal component analysis and all distances calculated within this space were based on all three dimensions.

To examine the how occupation of morphospace changes over time, I follow the recommendations of Foote (1993), Ciampaglio et al. (2001), and Erwin (2007). I calculated morphological disparity in each stage as the mean pairwise distances between taxa in morphospace. Because this metric is sensitive to sample size, I rarefied each stage to the lowest diversity in any Cretaceous stage (n = 12 in the Maastrichtian) and calculated disparity as well as centroid position in principal component space for the rarefied subset of taxa. This was repeated 1,000 times.

Potential predictors of extinction

Each genus was assigned a suite of ten predictors thought to potentially influence a taxon's extinction rink. This was done independently in each stage, taking into account what taxa coexisted with the genus and where in the morphospace they are.

Four morphological descriptors, the three original coiling parameters (U, w, and S) and size, were noted for each genus in the suite of potential extinction predictors. These values do not change from stage to stage. The coiling parameters were included because of their theoretically and experimentally derived associations with ecological and physiological aspects of the organism such as swimming velocities (Chamberlain 1981, Jacobs 1992, Jacobs et al. 1994, Jacobs and Chamberlain 1996), shell strength and depth tolerance (Hewitt 1996), buoyancy (Saunders and Shapiro 1986), and orientation of the aperture (Swan and Saunders 1987, Klug and Korn 2004). The parameters serve to describe the gross morphology of the ammonite shell and how the organism is hypothesized to have interacted with its physical environment.

1. *Umbilical ratio (U)*. The umbilical ratio describes the exposure of the umbilicus or degree the whorl overlaps previous whorls during growth (involution). Adult ammonoids

with higher values of *U* have more exposed umbilici and are thought to have experienced higher drag, making them less likely to be fast-moving swimmers.

2. *Whorl expansion rate (w)*. The expansion rate of the whorl describes the change in the size of the whorl as the shell grows. High values of *w* indicate large increases in size with shell growth, which has been associated with more horizontal aperture orientation, increased maneuverability, and greater maximum swimming velocities.
3. *Shell inflation (S)*. The shell inflation value captures the aspect ratio of the aperture. Low values of *S* indicate more compressed shells, which have been experimentally shown to reduce drag on the shells of adult ammonoids.
4. *Size*. Size is calculated as the maximum measurement, typically the diameter, in millimeters taken from the lateral view of the shell. If multiple specimens were imaged for a genus or subgenus, the largest value among them was taken. Size is frequently used in macroevolutionary and macroecological studies as a proxy for metabolic, reproductive, and trophic characteristics of an organism and size selectivity in extinction events has been noted across the numerous groups (McKinney 1997, Lyons et al. 2004, Van Valkenburgh et al. 2004), though less attention has been paid towards exploring the relationship between size selectivity and background extinction. In many of these cases, large-bodied organisms experienced elevated extinction rates, which are attributed to their low reproductive rates and higher trophic positions.

In addition to the original coiling parameters and size, I derived four predictors from the generated three-dimensional morphospace in order to capture ways in which each genus occupies the morphospace differently than its contemporaries do. These predictors, described below, vary depending on the interval in question and include the taxon's distance to the interval centroid, degree of local crowding, distance to the current family centroid, and current family disparity. The inclusion of predictors generated from family subsets explores the possibility of clade-level effects due to relatedness and phylogenetically conserved ecologies. Allowing for differences that stem from clade identity may improve models of extinction (Harnik 2011).

5. *Distance to interval centroid*. The distance to the interval centroid is calculated as the Mahalanobis distance (the Euclidean distance in principal component space when axes have been scaled to unit variance) between the taxon and morphospace centroid calculated using the positions of all taxa present in that interval. Greater deviation from the mean morphology of contemporary taxa is often interpreted as increased ecological specialization, which is generally linked in theory to increased extinction risk. However, this link is neither consistent nor straightforward (Schluter 2000, Colles et al. 2009) and morphological deviation has been linked to both decreased and increased longevity (Baumiller 1993, Liow 2006).
6. *Degree of local crowding*. The degree of local crowding is calculated as the kernel density estimate (KDE) for each taxon's position in an interval's morphospace. This provides a relative measure of crowding in multivariate space given the distribution of taxa in morphospace for that interval. This was estimated using Gaussian distributed kernels. A genus with a high value of KDE indicates it is located in a more densely occupied region of morphospace relative to genera with lower values of KDE. If morphologically similar taxa are more likely to compete directly and indirectly for resources, then generally speaking taxa occupying more densely occupied morphospace

should experience increased competitive pressures. Contour plot of multidimensional KDEs for example interval (Cenomanian) is provided in Appendix A.3.

7. *Distance to family centroid*. Distance to the family centroid is calculated as the Mahalanobis distance between the taxon and the centroid calculated using the positions of all members of the same family present in that interval, standardized to the root mean square of distances within each family. Similar to the distance to the interval centroid, this metric measures overall morphological uniqueness, but differs in that it suggests that morphological deviation relative to closely related taxa may have a stronger effect on extinction probabilities than overall deviation from the overall mean morphology, assuming that taxonomy coarsely reflects phylogeny. As distance to the family centroid increases, taxa become less subjected to high competitive pressures. This hypothesis was first proposed by Darwin and stems from the idea that more closely related taxa are more ecologically similar, thus leading to increased competition intensity between them (Cavender-Bares et al. 2009). However, a growing number of studies in community ecology have shown this hypothesis infrequently holds true (e.g., Cahill et al. 2008, Godoy et al. 2014).
8. *Family disparity*. Family disparity is calculated here as the mean pairwise distance between taxa of the same family in each interval. If taxonomy is assumed to broadly reflect phylogeny, family disparity can be thought to reflect a clade's evolutionary variability. A clade that shows a higher diversity of forms may contain taxa more buffered against extinction due to an increased ability to adapt (Van Valkenburgh 1991, Kolbe et al. 2011), and morphological variability has been associated with species and genus longevity (Liow 2007).

An additional two non-morphological features were included in the extinction models for each genus, based on an extensive body of literature suggesting their strong influences on taxon longevity or extinction risk. These features are current taxon age and current family diversity and each taxon's values vary from stage to stage.

9. *Taxon age*. Taxon age is defined here as the cumulative number of stages the taxon has been recorded as extant including the stage of analysis (Figure 1.3). The Law of Constant Extinction proposed by Van Valen (1973) posits that a taxon's probability of extinction remains constant irrespective of its age. This may be due to the persistent challenge to stay alive through a constantly changing environment, an idea he termed the Red Queen hypothesis. If the Law of Constant Extinction were upheld in this case, age should be a poor predictor of extinction risk, as older taxa would be equally at risk of extinction as younger taxa.
10. *Family diversity*. Family diversity is a value assigned to each genus referring to the number of confamilial genera coexisting in the given interval. The degree to which diversity dependence regulates extinction and origination in clades remains a topic of wide discussion in macroevolutionary studies (Rabosky 2013, Marshall and Quental 2016). Under a framework of diversity dependence, the per lineage probability of becoming extinct increases with clade diversity until the carrying capacity is met. Though this predictor only coarsely approximates this process in the models and assumes a similar extinction regime across families, support for such a relationship would be compelling evidence for a prominent role of diversity dependence as a regulating factor.

Several additional predictors were considered but were found to be either highly correlated to one listed above (e.g., mean distance to confamilial genera) or unable to be compared if applied to taxonomic subdivisions (e.g., KDEs at the family level).

Extinction modeling

I applied stochastic gradient boosting to model the strength and nature of the relationships between the predictor variables and extinction response. Gradient boosting is a machine-learning technique that uses an ensemble of weak models, typically regression or classification trees, to iteratively optimize a cost function. Though the final model may be composed of several thousand weakly predictive trees, making them difficult to visualize, gradient boosting frequently has shown improved predictive power over other classification methods such as logistic regression and random forests in commercial applications, while the advantages of gradient boosting for biology continue to be explored (as discussed in Elith et al. 2008). Because gradient boosting selects features during the fitting process by reducing the effect of unimportant predictors to zero, inclusion of additional predictors does not necessarily force a trade-off in relative influence of predictors. They are also capable of fitting non-linear relationships between explanatory and response variables and these effects are generally insensitive to feature collinearity. Despite this insensitivity, I identified features that were highly correlated within each interval (Pearson's *r* magnitude greater than 0.9) and iteratively excluded the one with the highest mean absolute correlation with all other features until remaining features show no correlations above the cutoff value (Figure 1.4). The excluded features tended to be metrics related to family-level characteristics and resulted in the exclusion of family disparity as a predictor in the Berriasian and the Barremian stages and additionally distance to the family centroid in the Barremian, all of which highly correlate with family diversity in these two intervals.

Extinction was modeled independently in each stage of the Cretaceous, excluding the Maastrichtian, which cannot be modeled due to lack of variation in the response variable. Model training hyperparameters - interaction depth, number of iterations, learning rate, number of minimum observations per node - were allowed to vary between a set of potential values (see Elith et al. 2008 for additional descriptions of each hyperparameter). A grid search of these values was conducted using 10-fold cross-validation repeated ten times on a training dataset consisting of 60% of the genera in an interval and the set of hyperparameters that returned the greatest accuracy were used to fit the final models (Appendix A.4). Because the proportion of ammonites becoming extinct in each interval is quite high, I accounted for class imbalance in the response variable by measuring model accuracy as the area under the precision-recall curve (AUPRC) and by weighting the response variable by the frequency of each class in that interval. A subsampling rate (bag fraction) of 50% was used so that each instance of tree selection during model fitting used a random subset of the data. This reduces the potential for overfitting and improves accuracy (Friedman 2002). Final models were fit to the training dataset in each stage, and the model performance was assessed using the AUPRC of the final model applied to the remaining 40% of genera. I then examined the consistency of models through time by applying the best fitting model from each stage to all other stages of the Cretaceous and evaluating performance again using the AUPRC. All analyses in this study were conducted in the R programming environment (v3.2.4, R Core Team 2016). Grid searches and final model fitting

were implemented using the R packages caret (v6.0-73, Kuhn 2016) and gbm (v2.1.1, Ridgeway 2015).

Results

Ammonite diversity dynamics

The data obtained from Wright et al. (1996) show a slight decrease in raw genus diversity through the first half of the Early Cretaceous, a rapid increase in diversity from the Aptian to the Albian to reach Cretaceous peak diversity, followed by an overall decline from this peak diversity through the Late Cretaceous. The removal of singletons using the boundary crosser method of calculating diversity dramatically depresses these numbers, reflecting high rates of taxonomic turnover for this group across the Cretaceous. This is also reflected in age frequency distributions for taxa in each interval (Figure 1.4). Per capita extinction rates calculated according to Foote (2000) show dramatically elevated extinction in the first half of the Early Cretaceous, followed by low but gradually increasing rates towards the Late Cretaceous, and appear decoupled both in magnitude and direction from both raw and boundary crossing genus diversity (Figure 1.2).

Morphospace occupation through time

The three-dimensional morphospace generated using principal component analysis of coiling parameters depicts the range of morphologies that Cretaceous ammonites possessed (Figure 1.5). Factor loadings and summaries of variance explained by each principal component (PC) axis are provided in Table 1.1. The first PC axis of the morphospace captures 55.3% of the variability in the data with U and S being important factors negatively correlated with the first PC axis and w only slightly less important correlated positively with the first PC axis. The second PC axis captures 25.9% of the variability in the data and is predominantly influenced by w with lesser contributions from U and S. The third PC axis captures 18.8% of the variability in the data and is influenced for the most part by the remaining variation in U and S and very small contribution from w.

Despite high taxonomic turnover, total disparity shows no detectable change over time (Figure 1.6). Similarly, the position of occupied morphospace remains consistent near the morphospace mean across the Cretaceous in the first two PC axes (Figure 1.7). Exceptions to this include the Barremian in the Early Cretaceous, which shows some deviation from the morphospace center towards more positive values on the first PC axis, and the Late Cretaceous Maastrichtian, which shows deviation towards negative values on the second PC axis. These deviations, however, are minor in the context of the entire Cretaceous morphospace. The patterns of relatively little change in both disparity and centroid position across time, together with the high turnover rate, suggest continual reoccupation of vacated morphospace. This is in line with a number of studies that have documented the tendency for planispiral ammonoids to re-evolve morphologically familiar forms over the course of the clade's evolutionary history and across extinction events (Bayer and McGhee 1984, Saunders et al. 2008, Monnet et al. 2011, Monnet et al. 2015).

Extinction model performance

The ability to predict extinction using the set of predictors in this study was highly variable across time. Model performance was assessed by comparing the AUPRC of the trained model to the expected AUPRC value obtained by a random classifier when both are applied to data withheld during training. The AUPRC of a random classifier is equal to the proportion of positive observations in the dataset, irrespective of the evaluation threshold. Of the 11 stages in the Cretaceous for which models were fit, six produced best-fit models that outperformed a random classifier (Figure 1.8). These are the Valanginian, Hauterivian, Cenomanian, Turonian, Santonian, and Campanian. Subsequent interpretations of predictor effects focus on these six intervals.

When models were used to predict extinction in stages outside of the stage they were trained on, performance of the models were generally poor (Figure 1.9). Here, out of sample performance was assessed using the area under the receiver operating characteristic curve (AUROC), which is less discerning than AUPRC when assessing performance using imbalanced classes, but closely reflects AUPRC in terms of overall performance and is more straightforward to compare across intervals given that the expected AUROC of a random binary classifier is invariable (0.5). In some cases, models performed well when predicting extinction in intervals outside of the interval they were trained on. For example, the model trained using taxa present in the Hauterivian was able to predict extinction in the Albian and Turonian with relatively high accuracy. However, there is no clear pattern to when this occurs, as models appear no better at predicting temporally close intervals than intervals that are far away. This lack of apparent temporal autocorrelation in model performance suggests that extinction drivers are highly unique to specific time periods.

Predictor consistency and specific effects

The time-specific nature of extinction selectivity is further revealed in partial dependence plots of the fitted models, which depict marginal effects of a predictor when all other predictors are held constant at their sample means (Figure 1.10). The relative influences of each predictor, which are scaled but non-additive for each interval, are also depicted. The number and identities of variables with high relative influences vary dramatically from interval to interval - variables that are strong predictors of extinction in one interval are weak in another and stages may have any number of strong predictors or only one or two.

In some intervals, the range of marginal effects of each predictor in each interval is very small, unable to strongly distinguish between the extinct or not extinct response, despite supposedly high model performance. This is particularly striking in the Cenomanian, where no predictor has a large effect. The concentration of the narrow range of effects around a value of 0.5 is unusual and suggests the models are capturing relationships that are not immediately revealed through partial dependence plots, such as subtle impacts on extinction risk or interactions between predictors rather than each predictor individually. Regardless of the effect size, some temporal patterns arise in directionality of effects and variable importance, and variables found to be important in multiple intervals often show similar directionality in their effects.

The coiling parameters (*U*, *w*, and *S*), which describe the gross morphology of the shell and how the organism interacts with its environment, frequently contained the variable of highest relative influence in each interval. Whorl expansion rate (*w*) is generally of little influence. However, the Hauterivian exhibits a strong increase in extinction risk associated with moderate values of *w*. The umbilical ratio (*U*) is a relatively important predictor in the Hauterivian and Campanian, with both intervals showing increased extinction risk with more exposed umbilici (high values of *U*). All other intervals show weak relationship between *U* and extinction risk. Though most intervals show weak and non-directional relationships between extinction and shell inflation (*S*), two stages in the Late Cretaceous, the Santonian and Campanian, include *S* as an extremely important predictor, with both showing a marked peak in predicted extinction at intermediate and high values of the *S*. This relationship suggests preferential survival of more streamlined, compressed forms (low values of *S*). Thus, for the three intervals mentioned, the parameters that describe shell hydrodynamics appear to be important indicators of extinction risk and consistently point towards higher extinction vulnerability of less streamlined forms. Previous studies have repeatedly documented the trend for taxa with inflated, evolute, and highly ornamented shells present early in a clade's history to be later replaced by taxa possessing discoidal, involute, and smooth shells (Bayer and McGhee 1984). Extinction selectivity on those traits suggests this is a functional shift and, despite the prevalence of this trend across multiple clades, may be highly time-specific. The additional morphological descriptor, size, varies in importance and direction over time. Though generally of low relative importance, size appears to be quite influential in the Turonian, showing larger taxa became preferentially extinct in this interval.

Variables that capture aspects of a taxon's morphological context – distance from the interval centroid, degree of local crowding, distance from the family centroid, and family disparity – appear overall less important than the coiling parameters with strong exceptions in two intervals. Total family disparity is the variable of greatest importance in the Hauterivian, showing preferential extinction of genera in families occupying broader regions of morphospace. A similar pattern is seen in the Turonian, though the Turonian extinction model is more strongly influenced by other variables. In both cases, this response is decoupled from that of a taxon's distance to the family centroid and the number of confamilial genera, suggesting that overall clade dispersion, rather than individual-scale morphological deviance or clade dispersion as a function of diversity, can play a role in determining extinction susceptibility. The direction of this relationship, however, is opposite that which is expected if variability (measured as high family disparity) buffers taxa from extinction. Instead, families consisting of morphological dissimilar genera experience greater extinction. I do not find support for the inverse relationship in any time interval. The Turonian, furthermore, exhibits a sharp peak in predicted extinction risk associated with moderately small degrees of local crowding, supporting the idea that taxa in more sparsely occupied regions of morphospace experience greater extinction in that interval. These two patterns capture the extinction of morphological outliers and taxa on the fringes of the Turonian morphospace, which contains the most extreme taxa along both the first and second PC axes. The lack of a relationship between the distance to interval centroid and extinction risk, however, indicates proportionally strong extinction towards the center of the Turonian morphospace as well.

There is, additionally, some support for extinction selectivity of non-morphological traits. In particular, genera belonging to diverse families experience elevated extinction in the Valanginian. Notably, the relative importance of taxon age as a predictor of extinction is consistently low across all intervals. This finding is consistent with the lack of a strong relationship between extinction risk and age that has been observed previously in other taxonomic groups and does not refute the Law of Constant Extinction (Van Valen 1973).

Discussion

Using a stratigraphic and morphological dataset for Cretaceous ammonites, I was able to identify several features that appear to undergo background extinction selectivity. However, the importance of these features and the overall ability to fit extinction models across all stages varies over time. Here I discuss additional factors that may influence the ability to accurately predict extinction beyond the scope of this study.

Phylogeny

I have attempted to address the impact relatedness may have on extinction risk by including predictors calculated using family subsets. The use of groupings at different levels of the taxonomic hierarchy as an explicit substitute for formally assessed phylogenetic relationships is not uncommon (e.g., Brosse et al. 2013) and may be fruitful but should be used with caution (Soul and Friedman 2015). That said, when conducting macroevolutionary studies with morphologically-defined groups that lack suitable representation in phylogenetic trees, the use of taxonomy in lieu of phylogeny is unlikely to produce drastically different outcomes (Jablonski and Finarelli 2009). Previous studies of ammonites have noted that the recurrent evolution of forms appears to occur independent from phylogeny (Bayer and McGhee 1984, Saunders et al. 2008), suggesting that a lack of support found for family-dependent metrics in most intervals is not be unexpected.

The use of phylogenetic trees would additionally allow us to distinguish between true extinction and pseudoextinction in the dataset. This is of particular interest in ammonites, which are recognized as having possessed high rates of evolution and taxonomic turnover. Morphology, however, is an important factor for distinguishing ammonite taxa. Thus, though identification of anagenetic change would provide an added dimension to this study, its inclusion would leave the fundamental goal of detecting factors that induce the loss of morphotypes, the analyses, and the results relatively unchanged.

Time averaging

The highly variable nature of extinction documented here across stages likely extends to sub-stage timescales as well. If drivers of extinction were shifting relatively rapidly within a stage and at times in opposing directions, time averaging would mask the signal of selectivity, impairing the ability to detect strong relationships at the stage level. If this were overwhelmingly true, the ability to predict extinction would be expected to decrease with increasing stage durations. However, I do not find this to be the case (Appendix A.5), suggesting stages are a suitable timescale for studying extinction selectivity.

The effect of time averaging additionally implies that when cases of selectivity are detected, it is likely a real signal, as time averaging would only serve to dampen the relationship between predictors and extinction risk rather than strengthen them. These cases are remarkable, then, as they could only be achieved through either large pulses of selective extinction or sustained selectivity over the course of the interval.

There may, however, be instances in which time averaging can lead to multiple interpretations of selectivity patterns. For example, a pattern of strong selectivity shifting between extreme values of a variable's range within a stage could be interpreted as selection on extremes though at any given point the selection is in fact highly directional. I did not detect a pattern that could be interpreted this way, and variables that compound this information into one metric (distances to the interval and family centroids) were not found to be important variables. This effect, however, should be kept in mind when conducting and interpreting the results of similar studies.

Geographic range

The geographic range of a taxon has been noted in the literature to be one of the most consistent predictors of extinction in the fossil record (Payne and Finnegan 2007, Jablonski 2008, Harnik 2011). Though inclusion of geographic range may improve the performance of the final models, it would not necessarily alter the modeled relationships between the predictors and extinction. Completely disregarding geography may be problematic, however, as clades and ecological and physiological responses are dynamically structured across space (Jablonski 2008, Harnik 2011). Though I did not collect data on the geographic ranges of the taxa included in this study and thus did not include it as a potential predictor of extinction, underlying spatial structure in the predictor values may mask more generalizable effects on extinction risk and warrants further study through local and regional approaches.

Additional sources of morphological variation

There are a number of sources of morphological variation not captured by the scope of this study that may affect the ability to predict extinction from morphospaces. Previous studies suggest that whole shell morphology, including features such as ornamentation, ribbing, suture complexity, or siphuncular thickness, may be more sensitive to morphological selectivity across extinction events (Saunders and Swan 1984, Saunders et al. 2008) and broad trends in whole shell morphology across time have been recorded for ammonite clades (Ward 1986, Monnet et al. 2015). However, though additional characteristics of the shell have been incorporated into morphological analyses of ammonites (e.g., Ward and Signor 1983, Ward 1986, Swan and Saunders 1987, Dommergues et al. 1996, Moyne and Neige 2007, Saunders et al. 2008), these three coiling parameters capture most of the variation in whole shell morphospace (Saunders et al. 2008).

Though taxa are morphologically delineated, ammonite species are often described with multiple variants following a continuum between end-member morphologies. Additionally, some ammonite species are thought to have exhibited dramatic degrees of sexual dimorphism, differing primarily in size but in shape as well (Davis et al. 1996). Within individuals, allometric

growth and additional morphological modifications associated with development provides more dimensions on which selection can occur (Davis et al. 1996, Gerber et al. 2008). Here, I did not control for the age of the individuals, instead focusing efforts on achieving taxonomic breadth and complete measurement sets for each taxon using the images figured in Wright et al. (1996) and using supplementary sources.

How factors such as competition and developmental constraint relate to extinction risk are dependent on each one of these levels at which there is morphological variation, down to the individual. Despite these sources of variation, the genera included in this study capture the range of morphologies exhibited by this group. Thus, I expect for the overall findings of this study to remain consistent upon integration of additional morphological data and examination at lower levels of the biological hierarchy but look forward to testing this rigorously in future studies.

Heteromorphic forms

Because of the difficulty in incorporating non-planispiral forms into the Raup (1967) framework, heteromorphic ammonites were excluded from this study. However, given their considerable diversity and abundances, particularly in the Late Cretaceous, there seems to be little doubt that heteromorphic ammonites likely played a major role in the marine ecosystem at the time and served as direct and indirect competitors with planispiral ammonites for resources such as food and predator-free space. While some studies have considered these irregular forms using discrete or binned characters (Ward 1986), easily implemented, quantitative frameworks with which to conduct comparative studies the hypothesized modes of life and ecological roles of all ammonoid forms remain underdeveloped. Though inclusion of heteromorphs would not impact the ability to detect differential survival in coiling parameters, it may affect what can be detected in the other variables. Thus, the findings and interpretations presented here should be considered informative for an isolated subset of taxa that is partially representative of the biotic environment.

Conclusions

Although planispiral ammonites showed high rates of taxonomic turnover, occupied morphospace remained relatively unchanged across the Cretaceous. For five of the eleven stages, I was altogether unable to fit models of genus extinction with higher predictive power than that of a random classifier using morphological and non-morphological features. Of the remaining stages, which represent both the Early and Late Cretaceous, I find that variables involved with shell streamlining, isolation, family diversity, and size all appear to have been subject to extinction selectivity. The directionality of these relationships is often consistent during times when they found to be informative predictors of extinction. However, each variable's importance varies dramatically across time. I find no compelling evidence that a taxon's age nor its morphological deviation from the overall or family mean play important roles in determining its risk of extinction. The temporally variable nature of selectivity in background extinction documented in this study suggests complex, multi-causal relationships driving extinction in ammonites and highlights the shortfalls that may arise when studying extinction outside of a specific temporal context.

Acknowledgments

I would like to thank Seth Finnegan and Charles Marshall for their constructive suggestions. I would also like to thank Arnold Miller, Gene Hunt, and Peter Ward for providing feedback that helped shape the methods and discussion presented here.

References

Aguirre-Urreta, M.B. 1998. The ammonites *Karakaschiceras* and *Neohoploceras* (Valanginian Neocomitidae) from the Neuquén basin, west-central Argentina. Journal of Paleontology 72(1): 39-59.

Aguirre-Urreta, M.B. and Alvarez, P.P. 1999. The Berriasian genus *Groebericeras* in Argentina and the problem of its age. Scripta Geologica Special Issue 3: 15-29.

Aguirre-Urreta, M.B. and Rawson, P.F. 1999. Stratigraphic position of *Valanginites*, *Lissonia*, and *Acantholissonia* in the Lower Valanginian (Lower Cretaceous) ammonite sequence of the Neuquén basin, Argentina. Pp. 521-529 *in* Olóriz, F. and Rodriguez-Tovar, F.J. eds. Advancing Research in Living and Fossil Cephalopods. Kluwer/Plenum, New York.

Aguirre-Urreta, M.B. and Rawson, P.F. 2010. Lower Cretaceous ammonites from the Neuquén Basin, Argentina: the neocomitids of the *Pseudofavrella angulatiformis* Zone (upper Valanginian). Cretaceous Research 31(3): 321-343.

Alroy, J. 2008. Dynamics of origination and extinction in the marine fossil record. Proceedings of the National Academy of Sciences 105(Supplement 1): 11536-11542.

Alsen, P. 2006. The Early Cretaceous (Late Ryazanian-Early Hauterivian) ammonite fauna of North-East Greenland: taxonomy, biostratigraphy, and biogeography. Fossils and Strata 53: 1-229.

Anderson, F.M. 1958. Upper Cretaceous of the Pacific coast. Geological Society of America Memoir 71: 1-434.

Barragán, R., Rojas-Consuegra, R., and Szives, O. 2011. Late Albian (early Cretaceous) ammonites from the Provincial Formation of central Cuba. Cretaceous Research 32(4): 447-455.

Baumiller, T.K. 1993. Survivorship analysis of Paleozoic Crinoidea: effect of filter morphology on evolutionary rates. Paleobiology 19(3): 304-321.

Bayer, U. and McGhee, Jr., G.R. 1984. Iterative evolution of Middle Jurassic ammonite faunas. Lethaia 17(1): 1-16.

Benton, M.J. 1987. Progress and competition in macroevolution. Biological Reviews 62(3): 305-338.

Bogdanova, T.N. and Hoedemaeker, P.J. 2004. Barremian-Early Albian Deshayesitidae, Oppeliidae, Desmoceratidae and Silesitidae of Colombia. Scripta Geologica 128: 183-312.

Bose, E. 1927. Cretaceous ammonites from Texas and Northern Mexico. University of Texas Bulletin 2748, 356 pp., 18 pl.

Brosse, M., Brayard, A., Fara, E., and Neige, P. 2013. Ammonoid recovery after the Permian-Triassic mass extinction: a re-exploration of morphological and phylogenetic diversity patterns. Journal of the Geological Society, London 170: 225-236.

Cahill, Jr., J.F., Kembel, S.W., Lamb, E.G., and Keddy, P.A. 2008. Does phylogenetic relatedness influence the strength of competition among vascular plants? Perspectives in Plant Ecology, Evolution and Systematics 10: 41-50.

Casey, R. 1954. New genera and subgenera of Lower Cretaceous ammonites. Journal of the Washington Academy of Sciences 44(4): 106-115.
Cavender-Bares, J., Kozak, K.H., Fine, P.V.A., and Kembel, S.W. 2009. The merging of community ecology and phylogenetic biology. Ecology Letters 12: 693-715.
Chamberlain, Jr., J.A. 1981. Hydromechanical design of fossil cephalopods. Pp. 289-336 *in* House, M.R. and Senior, J.R. eds. The Ammonoidea. Systematics Association Special Volume 18. Academic Press, London.
Ciampaglio, C.N., Kemp, M, and McShea, D.W. 2001. Detecting changes in morphospace occupation patterns in the fossil record: characterization and analysis of measures of disparity. Paleobiology 27(4): 695-715.
Clapham, M.E. and Payne, J.L. 2011. Acidification, anoxia, and extinction: a multiple logistic regression analysis of extinction selectivity during the Middle and Late Permian. Geology 39(11): 1059-1062.
Cobban, W.A. 1988. *Tarrantoceras* Stephenson and related ammonoid genera from Cenomanian (Upper Cretaceous) rocks in Texas and the Western Interior of the United States. U.S. Geological Survey Professional Paper 1473: 1-30.
Cobban, W.A., Hook, S.C., and Kennedy, W.J. 1989. Upper Cretaceous rocks and ammonite faunas of southwestern New Mexico. New Mexico Bureau of Mines and Mineral Resources Memoir 45: 1-137.
Colles, A., Liow, L.H., and Prinzing, A. 2009. Are specialists at risk under environmental change? Neoecological, paleoecological and phylogenetic approaches. Ecology Letters 12(8): 849-863.
Davis, R.A., Landman, N.H., Dommergues, J.-L., Marchand, D, and Bucher, H. 1996. Mature modifications and dimorphism in ammonoid cephalopods. Pp. 463-539 *in* Landman, N.H., Tanabe, K., and Davis, R.A. eds. Ammonoid Paleobiology. Vol. 13 of F.G. Stehli and D.S. Jones, eds. Topics in Geobiology. Plenum, New York.
Dommergues, J.-L., Laurin, B., and Meister, C. 1996. Evolution of ammonoid morphospace during the Early Jurassic radiation. Paleobiology 22(2): 219-240.
Elder, W.P. 1989. Molluscan extinction patterns across the Cenomanian-Turonian Stage boundary in the western interior of the United States. Paleobiology 15(3): 299-320.
Elith, J., Leathwick, J.R., and Hastie, T. 2008. A working guide to boosted regression trees. Journal of Animal Ecology 77: 802-813.
Erwin, D.H. 2007. Disparity: morphological pattern and developmental context. Palaeontology 50(1): 57-73.
Ezard, T.H.G., Aze, T., Pearson, P.N., and Purvis, A. 2011. Interplay between changing climate and species' ecology drives macroevolutionary dynamics. Science 332(6027): 349-351.
Finnegan, S., Rasmussen, C.M.Ø., and Harper, D.A.T. 2016. Biogeographic and bathymetric determinants of brachiopod extinction and survival during the Late Ordovician mass extinction. Proceedings of the Royal Society of London B 283: 20160007.
Foote, M. 1993. Discordance and concordance between morphological and taxonomic diversity. Paleobiology 19(2): 185-204.
Foote, M. 1994. Morphological disparity in Ordovician-Devonian crinoids and the early saturation of morphological space. Paleobiology 20(3): 320-344.
Foote, M. 1999. Morphological diversity in the evolutionary radiation of Paleozoic and post-Paleozoic crinoids. Paleobiology 25(sp1): 1-115.

Foote, M. 2000. Origination and extinction components of taxonomic diversity: general problems. Paleobiology 26(sp4): 74-102.
Friedman, J.H. 2002. Stochastic Gradient Boosting. Computational Statistics and Data Analysis. 38(4): 367-378.
Futakami, M., Obata, I., Suzuki, T., and Watanabe, N. 2016. Revision of *Yabeiceras*, a Coniacian (Late Cretaceous) ammonite genus, based on material from the type locality in Fukushima, Japan. Cretaceous Research 61: 220-233.
Gerber, S. 2011. Comparing the differential filling of morphospace and allometric space through time: the morphological and developmental dynamics of Early Jurassic ammonoids. Paleobiology 37(3): 369-382.
Gerber, S., Elbe, G.J., and Neige, P. 2008. Allometric space and allometric disparity: a developmental perspective in the macroevolutionary analysis of morphological disparity. Evolution. 62(6): 1450-1457.
Godoy, O., Kraft, N.J.B., and Levine, J.M. 2014. Phylogenetic relatedness and the determinants of competitive outcomes. Ecology Letters 17: 836-844.
Gonzalez-Arreola, C., Pantoja-Alor, J., Oloriz, F., Villaseñor, A.B., and Garcia-Barrera, P. 1996. Lower Aptian Ammonitina *Pseudohaploceras liptoviense* (Zeuschner) in the Cumburindio Formation (Southwestern Mexico). Geobios 29(1): 35-43.
Hardin, G. 1960. The competitive exclusion principle. Science 131(3409): 1292-1297.
Harnik, P.G. 2011. Direct and indirect effects of biological factors on extinction risk in fossil bivalves. Proceedings of the National Academy of Sciences 108(33): 13594-13599.
Henderson, R.A. and McNamara, K.J. 1985. Maastrichtian non-heteromorph ammonites from the Miria Formation, Western Australia. Palaeontology 28(1): 35-88.
Hewitt, R.A. 1996. Architecture and strength of the ammonoid shell. Pp. 297-339 *in* Landman, N.H., Tanabe, K., and Davis, R.A. eds. Ammonoid Paleobiology. Vol. 13 of F.G. Stehli and D.S. Jones, eds. Topics in Geobiology. Plenum, New York.
Imlay, R.W. 1940. Neocomian faunas of northern Mexico. Geological Society of America Bulletin 51(1): 117-190.
Imlay, R.W. 1960. Early Cretaceous (Albian) Ammonites from the Chitina Valley and Talkeetna Mountains, Alaska. U.S. Geological Survey Professional Paper 354-D: 87-114.
Jacobs, D.K. 1992. Shape, drag, and power in ammonoid swimming. Paleobiology 18(2): 203-220.
Jacobs, D.K. and Chamberlain, Jr., J.A. 1996. Buoyancy and hydrodynamics in ammonoids. Pp. 169-224 *in* Landman, N.H., Tanabe, K., and Davis, R.A. eds. 1996. Ammonoid Paleobiology. Vol. 13 of F.G. Stehli and D.S. Jones, eds. Topics in Geobiology. Plenum, New York.
Jacobs, D.K., Landman, N.H., and Chamberlain, Jr., J.A. 1994. Ammonite shell shape covaries with facies and hydrodynamics: iterative evolution as a response to changes in basinal environment. Geology 22: 905-908.
Jablonski, D. 1986. Background and mass extinctions: the alternation of macroevolutionary regimes. Science 231(4734): 129-133.
Jablonski, D. 2008. Extinction and the spatial dynamics of biodiversity. Proceedings of the National Academy of Sciences 105(Supplement 1): 11528-11535.
Jablonski, D. and Finarelli, J.A. 2009. Congruence of morphologically-defined genera with molecular phylogenies. Proceedings of the National Academy of Sciences 106(20): 8262-8266.
Jenkyns, H.C. 2010. Geochemistry of oceanic anoxic events. Geochemistry, Geophysics, Geosystems. 11: Q03004.

Kennedy, W.J. 1986. Campanian and Maastrichtian ammonites from northern Aquitaine, France. Special Papers in Palaeontology 36: 1-145.
Kennedy, W.J., Bilotte, M., and Melchior, P. 2015. Turonian ammonite faunas from the southern Corbières, Aude, France. Acta Geologica Polonica 65(4): 437-494.
Kennedy, W.J. and Cobban, W.A. 1993. Lower Campanian (Upper Cretaceous) ammonites from the Merchantville Formation of New Jersey, Maryland, and Delaware. Journal of Paleontology 67(5): 828-849.
Kennedy, W.J., and Cobban, W.A. 1988. Mid-Turonian ammonite faunas from northern Mexico. Geological Magazine 125(6): 593-612.
Kennedy, W.J., Cobban, W.A., and Landman, N.H. 2001. A revision of the Turonian members of the ammonite subfamily Collignoniceratinae from the United States Western Interior and Gulf Coast. Bulletin of the American Museum of Natural History 267: 1-148.
Kennedy, W.J., Gale, A.S., Ward, D.J., and Underwood, C.J. 2008. Early Turonian ammonites from Goulmima, southern Morocco. Bulletin de l'Institut Royal des Sciences Naturelles de Belgique Sciences de la Terre 78: 149-177.
Kennedy, W.J. and Juignet, P. 1984. A revision of the ammonite faunas of the type Cenomanian. 2. The families Binneyitidae, Desmoceratidae, Engonoceratidae, Placenticeratidae, Hoplitidae, Schloenbachiidae, Lyelliceratidae and Forbesiceratidae. Cretaceous Research 5(2): 93-161.
Kennedy, W.J. and Juignet, P. 1993. A revision of the ammonite faunas of the type Cenomanian. 4. Acanthoceratinae (*Acompsoceras*, *Acanthoceras*, *Protacanthoceras*, *Cunningtoniceras* and *Thomelites*). Cretaceous Research 14(2): 145-190.
Kennedy, W.J. and Klinger, H.C. 1985. Cretaceous faunas from Zululand and Natal, South Africa. The ammonite family Kossmaticeratidae Spath, 1922. Annals of the South African Museum 95: 165-231.
Kennedy, W.J., Klinger, H.C., and Summesberger, H. 1981. Cretaceous Faunas from Zululand and Natal, South Africa: Additional Observations on the Ammonite Subfamily Texanitinae Collignon, 1948. Annals of the South African Museum 86: 115-155.
Kennedy, W.J., Landman, N.H., and Cobban, W.A. 1996. The Maastrichtian ammonites *Coahuilites sheltoni* Böse, 1928, and *Sphenodiscus pleurisepta* (Conrad, 1857), from the uppermost Pierre shale and basal Fox Hills formation of Colorado and Wyoming. American Museum Novitates 3186: 1-14.
Klug, C. and Korn, D. 2004. The origin of ammonoid locomotion. Acta Palaeontologica Polonica. 49(2): 235-242.
Kolbe, S.E., Lockwood, R., and Hunt, G. 2011. Does morphological variation buffer against extinction? A test using veneroid bivalves from the Plio-Pleistocene of Florida. Paleobiology 37(3): 355-368.
Krause, D.W. 1986. Competitive exclusion and taxonomic displacement in the fossil record: the case of rodents and multituberculates in North America. Pp. 95-118 *in* Flanagan, K.M. and Lillegraven, J.A. eds. Vertebrates, Phylogeny, and Philosophy. Contributions to Geology, University of Wyoming Special Paper 3. Department of Geology and Geophysics, University of Wyoming, Laramie, Wyoming.
Kuhn, M. 2016. caret: Classification and Regression Training. R package version 6.0-73.
Leckie, R.M., Bralower, T.J., and Cashman, R. 2002. Oceanic anoxic events and plankton evolution: biotic response to tectonic forcing during the mid-Cretaceous. Paleoceanography 17(3): 13-1-13-29.

Lehmann, J., Owen, H.G., and Beckert, W. 2013. A new ammonite fauna from NE Germany – evidence for an Early Albian cooling and the initial transgression in the Danish-Polish Trough. Neues Jahrbuch für Geologie und Paläontologie-Abhandlungen 268(2): 199-235.
Liow, L.H. 2006. Do deviants live longer? Morphology and longevity in trachyleberidid ostracodes. Paleobiology 32(1): 55-69.
Liow, L.H. 2007. Does versatility as measured by geographic range, bathymetric range and morphological variability contribute to taxon longevity? Global Ecology and Biogeography 16(1): 117-128.
Liow, L.H., Reitan, T., and Harnik, P.G. 2015. Ecological interactions on macroevolutionary time scales: clams and brachiopods are more than ships that pass in the night. Ecology Letters 18(10): 1030-1039.
Lockwood, R. 2004. The K/T event and infaunality: morphological and ecological patterns of extinction and recovery in veneroid bivalves. Paleobiology 30(4): 507-521.
Lyons, S.K., Smith, F.A., and Brown, J.H. 2004. Of mice, mastodons and men: human-mediated extinctions on four continents. Evolutionary Ecology Research 6: 339-358.
Marshall C.R. and Quental, T.B. 2016. The uncertain role of diversity dependence in species diversification and the need to incorporate time-varying carrying capacities. Philosophical Transactions of the Royal Society B 371: 20150217.
Matsumoto, T. 1959. Upper Cretaceous ammonites of California. Part II. Memoirs of the Faculty of Science, Kyushu University. Series D, Geology Special Volume 1: 1-172.
Matsumoto, T. 1991. The mid-Cretaceous ammonites of the family Kossmaticeratidae from Japan. Palaeontological Society of Japan Special Papers 33: 1-143.
McKinney, M.L. 1997. Extinction vulnerability and selectivity: combining ecological and paleontological views. Annual Review of Ecology and Systematics 28: 495-516.
Medina, F.A. and Riccardi, A.C. 2005. Desmoceratidae, Silesitidae and Kossmaticeratidae (Ammonitida) from the Upper Aptian-Albian of Patagonia (Argentina). Revue de Paléobiologie 24(1): 251.
Mojon, P.O., Musolino, A., Bucher, S., and Claude, B. 2013. Nouvelles données sur les ammonites du Valanginien-Hauterivien de la région stratotypique de Neuchâtel (Jura suisse): implications biostratigraphiques. Carnets de Geologie - Notebooks on Geology 2013(06), 237–254.
Monnet, C., De Baets, K., and Klug, C. 2011. Parallel evolution controlled by adaptation and covariation in ammonoid cephalopods. BMC Evolutionary Biology 11: 115.
Monnet, C., Klug, C., and De Baets, K. 2015. Evolutionary patterns of ammonoids: phenotypic trends, convergence, and parallel evolution. Pp. 95-142 *in* Klug, C., Korn, D., De Baets, K., Kruta, I., and Mapes, R.H. eds. Ammonoid Paleobiology: From macroevolution to paleogeography. Vol. 44 of Topics in Geobiology. Springer Netherlands, Dordrecht.
Moyne, S. and Neige, P. 2007. The space-time relationship of taxonomic diversity and morphological disparity in the Middle Jurassic ammonite radiation. Palaeogeography, Palaeoclimatology, Palaeoecology 248: 82-95.
Neige, P., Dera, G., and Dommergues, J.L. 2013. Adaptive radiation in the fossil record: a case study among Jurassic ammonoids. Palaeontology 56(6): 1247-1261.
Nikolov, T. and Breskovski, S. 1969. *Abrytusites*–nouveau genre d'ammonites barrémiennes. Bull of the Geological Institute, Ser. Paleontology, Bulgarian Academy of Sciences 18: 91-96.

Payne, J.L. and Finnegan, S. 2007. The effect of geographic range on extinction risk during background and mass extinction. Proceedings of the National Academy of Sciences 104(25): 10506-10511.
R Core Team. 2016. R: A language and environment for statistical computing. R Foundation for Statistical Computing, Vienna, Austria.
Rabosky, D.L. 2013. Diversity-dependence, ecological speciation, and the role of competition in macroevolution. Annual Review of Ecology, Evolution, and Systematics 44: 481-502.
Raup, D.M. 1966. Geometric analysis of shell coiling: general problems. Journal of Paleontology 40(5): 1178-1190.
Raup, D.M. 1967. Geometric analysis of shell coiling: coiling in ammonoids. Journal of Paleontology 41(1): 43-65.
Riccardi, A.C. 1988. The Cretaceous System of Southern South America. Geological Society of America Memoir 168: 1-161.
Ridgeway, G. 2015. gbm: Generalized Boosted Regression Models. R package version 2.1.1.
Ritterbush, K.A., Hoffmann, R., Lukeneder, A., and De Baets, K. 2014. Pelagic palaeoecology: the importance of recent constraints on ammonoid palaeobiology and life history. Journal of Zoology 292(4): 229-241.
Saunders, W.B., Greenfest-Allen, E., Work, D.M., and Nikolaeva, S.V. 2008. Morphologic and taxonomic history of Paleozoic ammonoids in time and morphospace. Paleobiology 34(1): 128-154.
Saunders, W.B. and Shapiro, E.A. 1986. Calculation and simulation of ammonoid hydrostatics. Paleobiology 12(1): 64-79.
Saunders, W.B. and Swan, A.R.H. 1984. Morphology and morphological diversity of mid-Carboniferous (Namurian) ammonoids in time and space. Paleobiology 10(2): 195-228.
Saunders, W.B., Work, D.M., and Nikolaeva, S.V. 2004. The evolutionary history of shell geometry in Paleozoic ammonoids. Paleobiology 30(1): 19-43.
Schluter, D. 2000. The ecology of adaptive radiation. Oxford University Press Inc., New York.
Sepkoski, Jr., J.J. 1981. A factor analytic description of the Phanerozoic marine fossil record. Paleobiology 7(1): 36-53.
Soul, L.C. and Friedman, M. 2015. Taxonomy and phylogeny can yield comparable results in comparative paleontological analyses. Systematic Biology 64(4): 608-620.
Swan, A.R.H. and Saunders, W.B. 1987. Function and shape in Late Paleozoic (Mid-Carboniferous) ammonoids. Paleobiology 13(3): 297-311.
Van Valen, L. 1973. A new evolutionary law. Evolutionary Theory 1: 1-30.
Van Valkenburgh, B. 1991. Iterative evolution of hypercarnivory in canids (Mammalia: Carnivora): evolutionary interactions among sympatric predators. Paleobiology 17(4): 340-362.
Van Valkenburgh, B., Wang, X., and Damuth, J. 2004. Cope's Rule, hypercarnivory, and extinction in North American canids. Science 306(5693): 101-104.
Vermeij, G.J. 1977. The Mesozoic Marine Revolution: evidence from snails, predators and grazers. Paleobiology 3(3): 245-258.
Villier, L. and Korn, D. 2004. Morphological disparity of ammonoids and the mark of Permian mass extinctions. Science 306(5694): 264-266.
Ward, P. 1986. Cretaceous ammonite shell shapes. Malacologia 27(1): 3-28.
Ward, P.D. and Signor III, P.W. 1983. Evolutionary tempo in Jurassic and Cretaceous ammonites. Paleobiology 9(2): 183-198.

Westermann, G.E.G. 1996. Ammonoid life and habit. Pp. 607-707 *in* Landman, N.H., Tanabe, K., and Davis, R.A. eds. Ammonoid Paleobiology. Vol. 13 of F.G. Stehli and D.S. Jones, eds. Topics in Geobiology. Plenum, New York.
Whitehouse, F.W. 1928. Additions to the Cretaceous ammonite fauna of eastern Australia. Part 2: Desmoceratidae. Memoirs of the Queensland Museum 9(2): 200-206.
Wiedmann, J. 1966. Stammesgeschichte und System der posttriadischen Ammonoideen. Neues Jahrbuch für Geologie und Paläontologie-Abhandlungen 125: 49-79.
Wright, C.W., Callomon, J.H., and Howarth, M.K. 1996. Cretaceous Ammonoidea *in* W. J. Arkell et al. Mollusca 4, Cephalopoda, Ammonoidea. Part L (Revised) of Moore, R.C. ed. Treatise on invertebrate paleontology. Geological Society of America, Boulder, Colo., and University of Kansas, Lawrence.
Wright, C.W., Chancellor, G.R., and Kennedy, W.J. 1983. The affinities of *Codazziceras* Etayo-Serna, 1979 (Cretaceous Ammonoidea). Cretaceous Research 4(4): 341-348.

Figure 1.1: Diagram of ammonite shell in lateral (left) and apertural (right) views showing measurements used to calculate coiling parameters. Abbreviations: *D* = diameter, *UD* = umbilical diameter, *a* = whorl height, *a′* = whorl height 180º from *a*, *b* = whorl width.

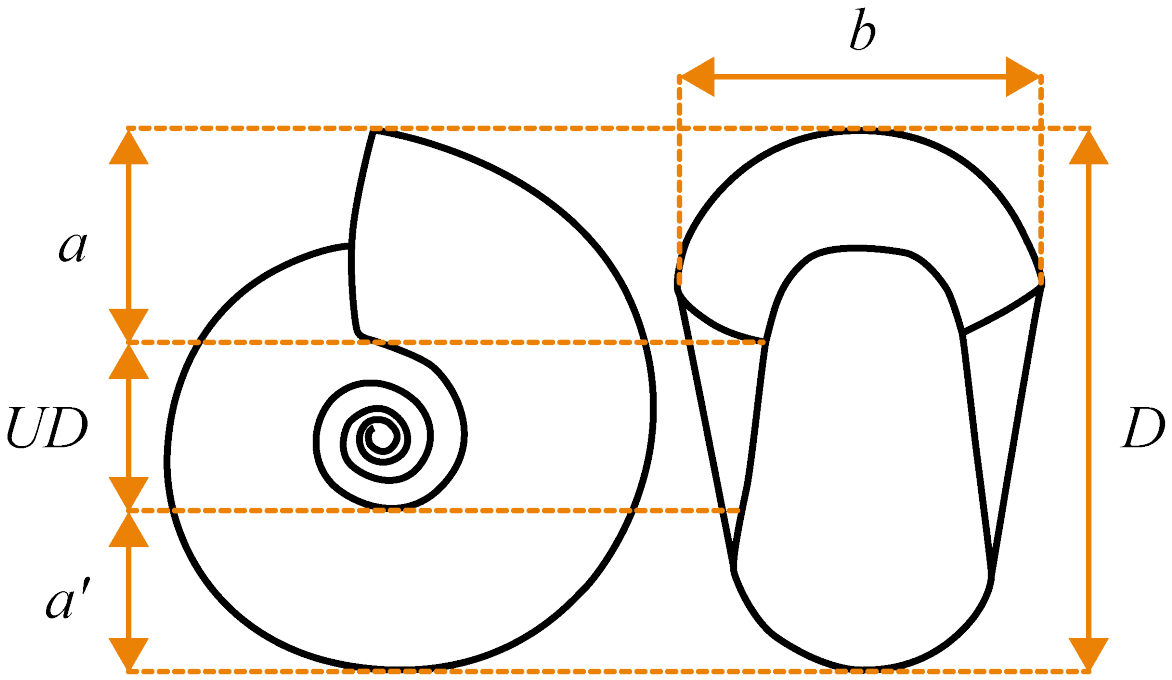

Figure 1.2: (A) Raw diversity curves and (B) per capita extinction rate for suborder Ammonitina for each stage of the Cretaceous. Black lines indicate use of the range-through method for calculating stratigraphic ranges. Orange lines indicate use of boundary crosser method. Dashed line includes all stratigraphic data obtained from Wright et al. (1996). Solid lines indicate the subset of Wright et al. (1996) for which shell measurements were collected. Per capita extinction rates are calculated according to Foote (2000). Stage abbreviations: Be = Berriasian, V = Valanginian, H = Hauterivian, Ba = Barremian, Ap = Aptian, Al = Albian, Ce = Cenomanian, T = Turonian, Co = Coniacian, S = Santonian, Ca = Campanian, M = Maastrichtian.

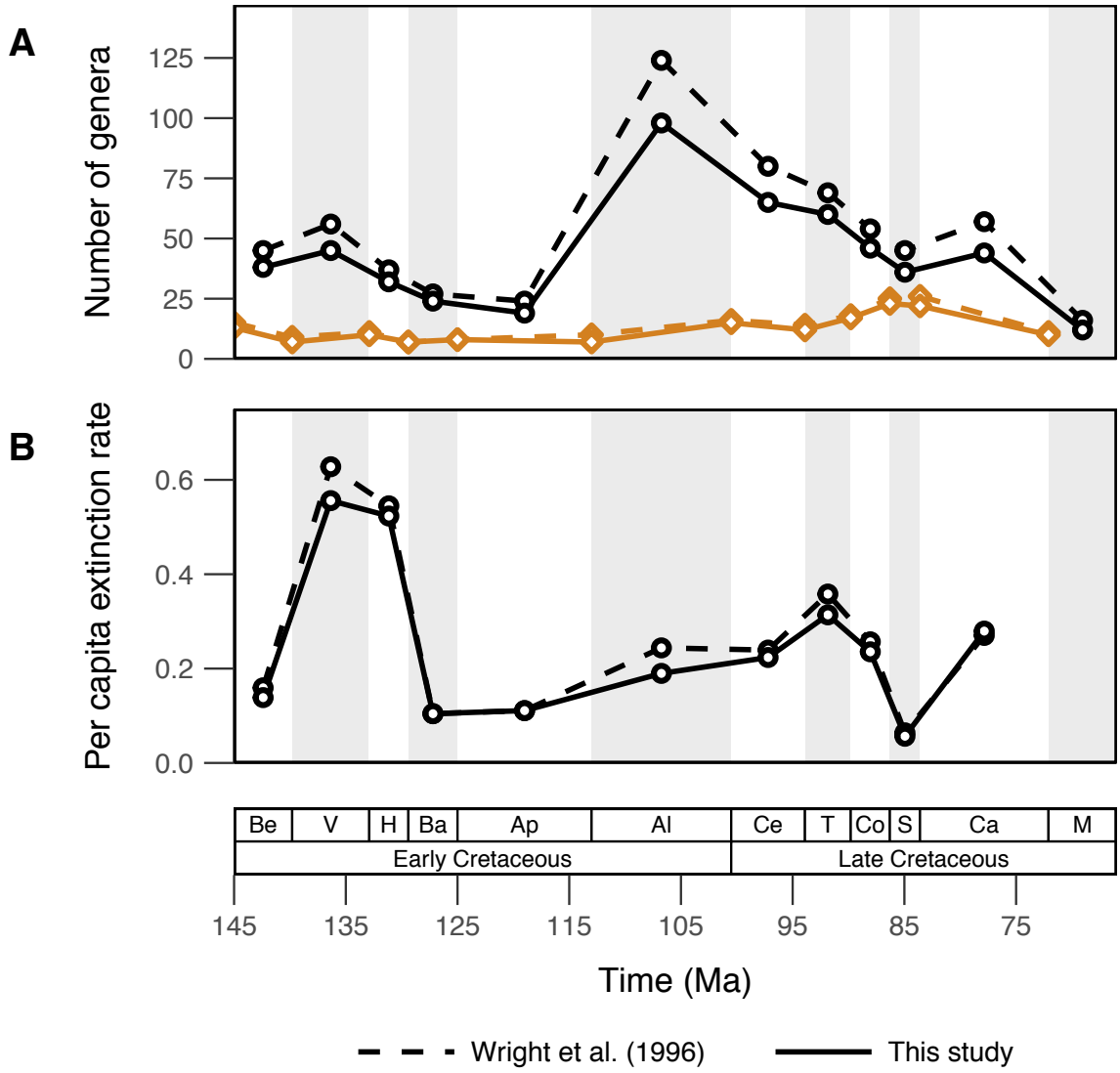

Figure 1.3: Age frequency distributions of genera included in extinction models for each Cretaceous stage. Ages are calculated as how many stages the taxon has been extant for. Gray shading indicates taxa whose last occurrence is recorded from that stage. Black shading indicates taxa that survive to the next stage. Panels are numbered in chronological order. Black and gray shadings designate taxa that do and do not survive into the following interval, respectively.

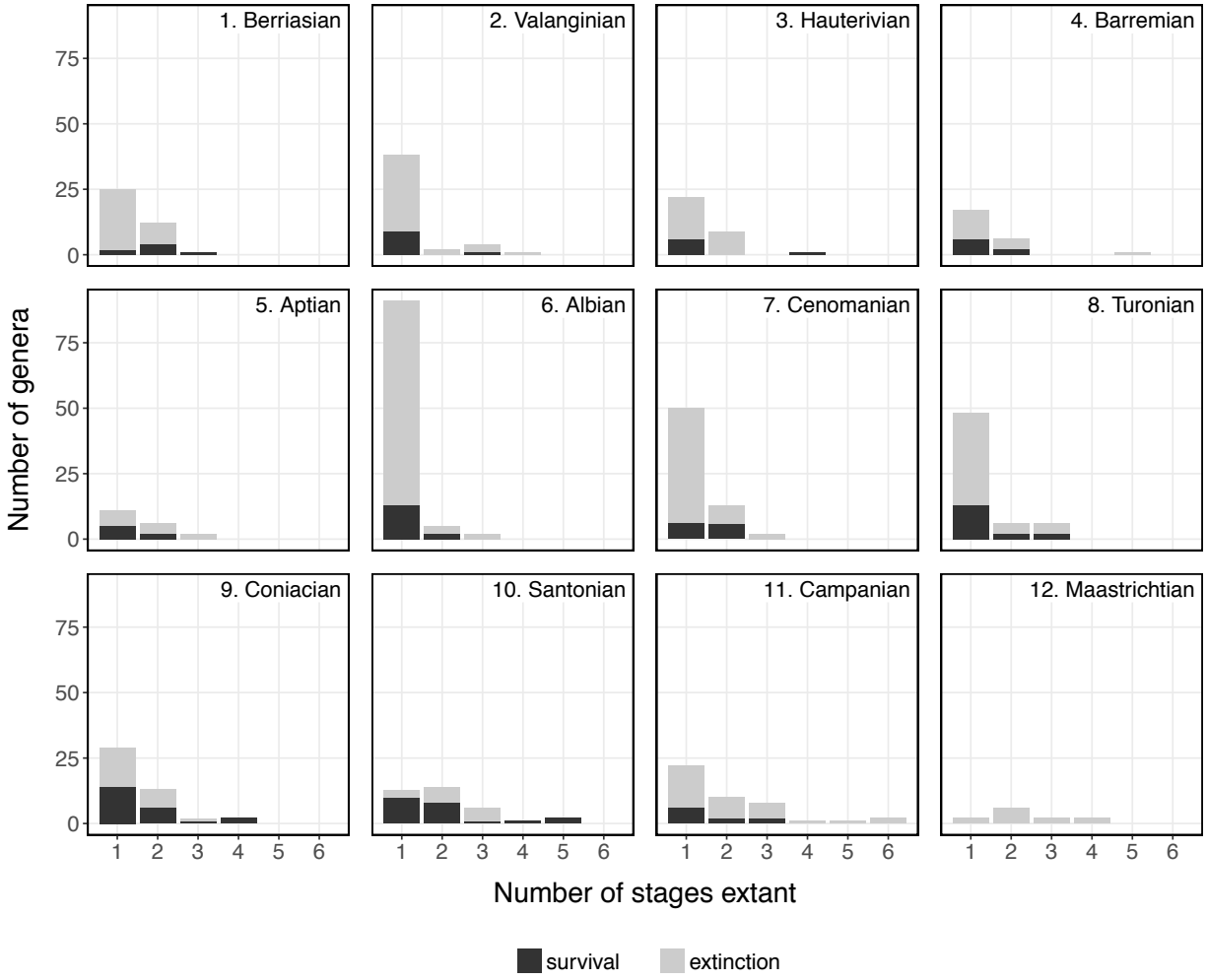

Figure 1.4: Correlations between predictors included in the extinction models. Each predictor combination contains eleven ellipses showing correlations between each pair of predictor values in a Cretaceous stage arranged temporally left to right, then top to bottom, as in Figure 1.3, (excluding the Maastrichtian, see Figure 1.2 for stage abbreviations). Color and orientation of the ellipse reflect the slope of the correlation. Eccentricity and color intensity reflect the strength of the correlation. Black boxes indicate intervals where Pearson's correlation coefficient exceeds a magnitude of 0.9.

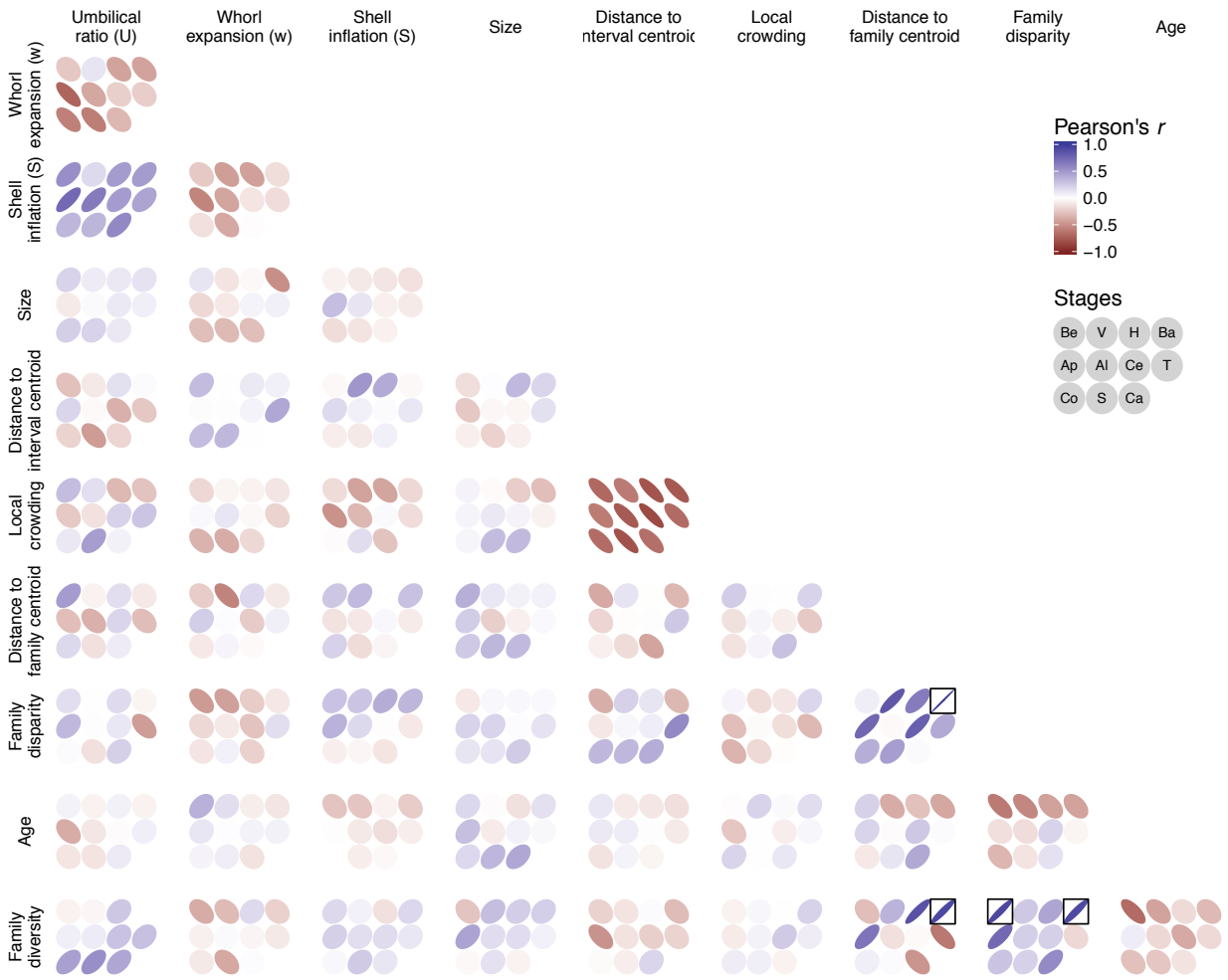

Figure 1.5: Stage-level subsets of the morphospace resulting from a principal component analysis of all Cretaceous Ammonitina. The first two principal component axes are shown. Panels are numbered in chronological order. Percentage of the total variance explained is shown for the first and second principal component axes. Circles and triangles designate taxa that do and do not survive into the following interval, respectively.

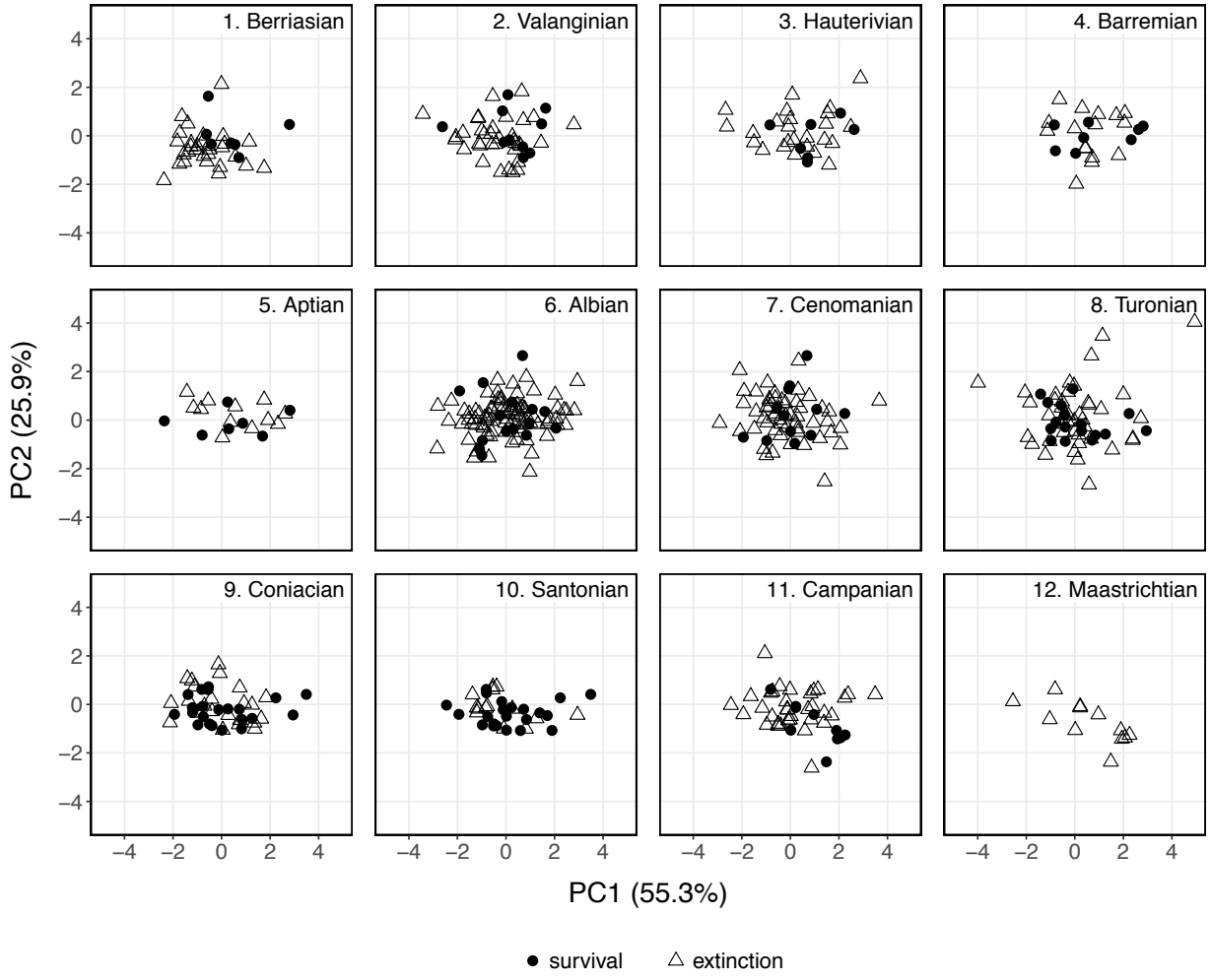

Figure 1.6: Morphological disparity in each Cretaceous stage as calculated by the mean pairwise distance between taxa after rarefaction (n = 12; 1,000 times). Error bars indicate 95% confidence intervals. See Figure 1.2 for stage abbreviations.

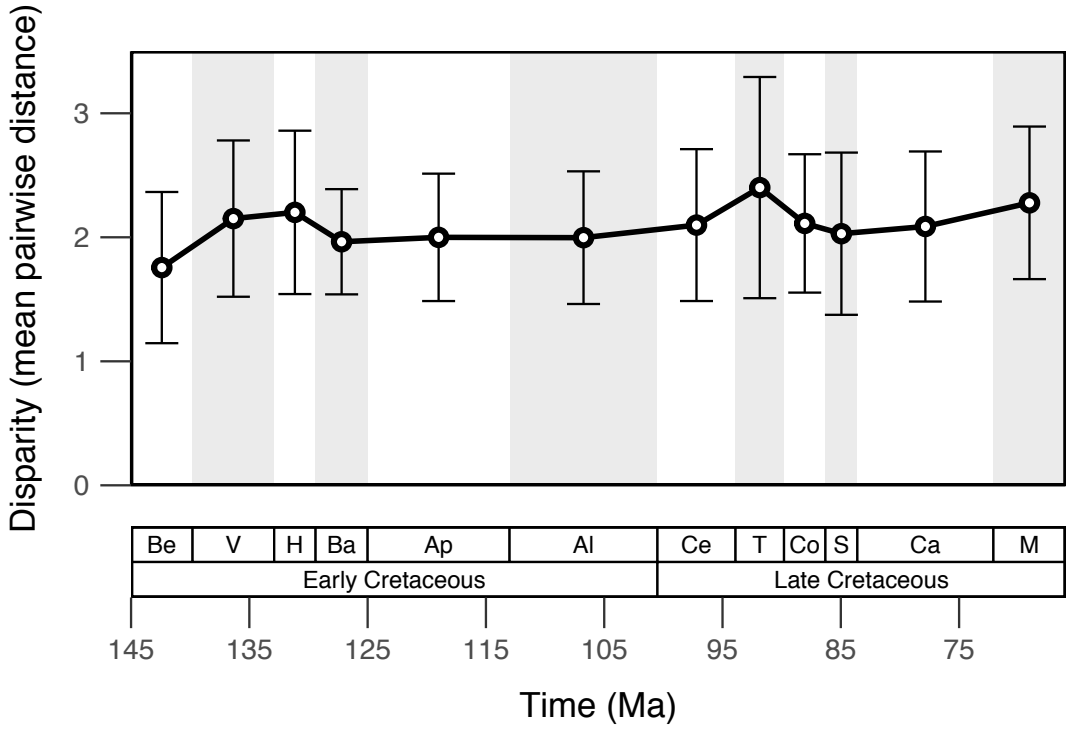

Figure 1.7: Enlarged view of the Cretaceous morphospace showing bootstrapped centroid position for stages over time. Error bars indicate 95% confidence intervals along the first and second principal component axes. Arrows point from each stage to its subsequent stage. Inset shows full morphospace including the positions of all Cretaceous taxa in gray. Black outlined box within inset indicates the enlarged region. Colors are used to visually distinguish stages. See Figure 1.2 for stage abbreviations.

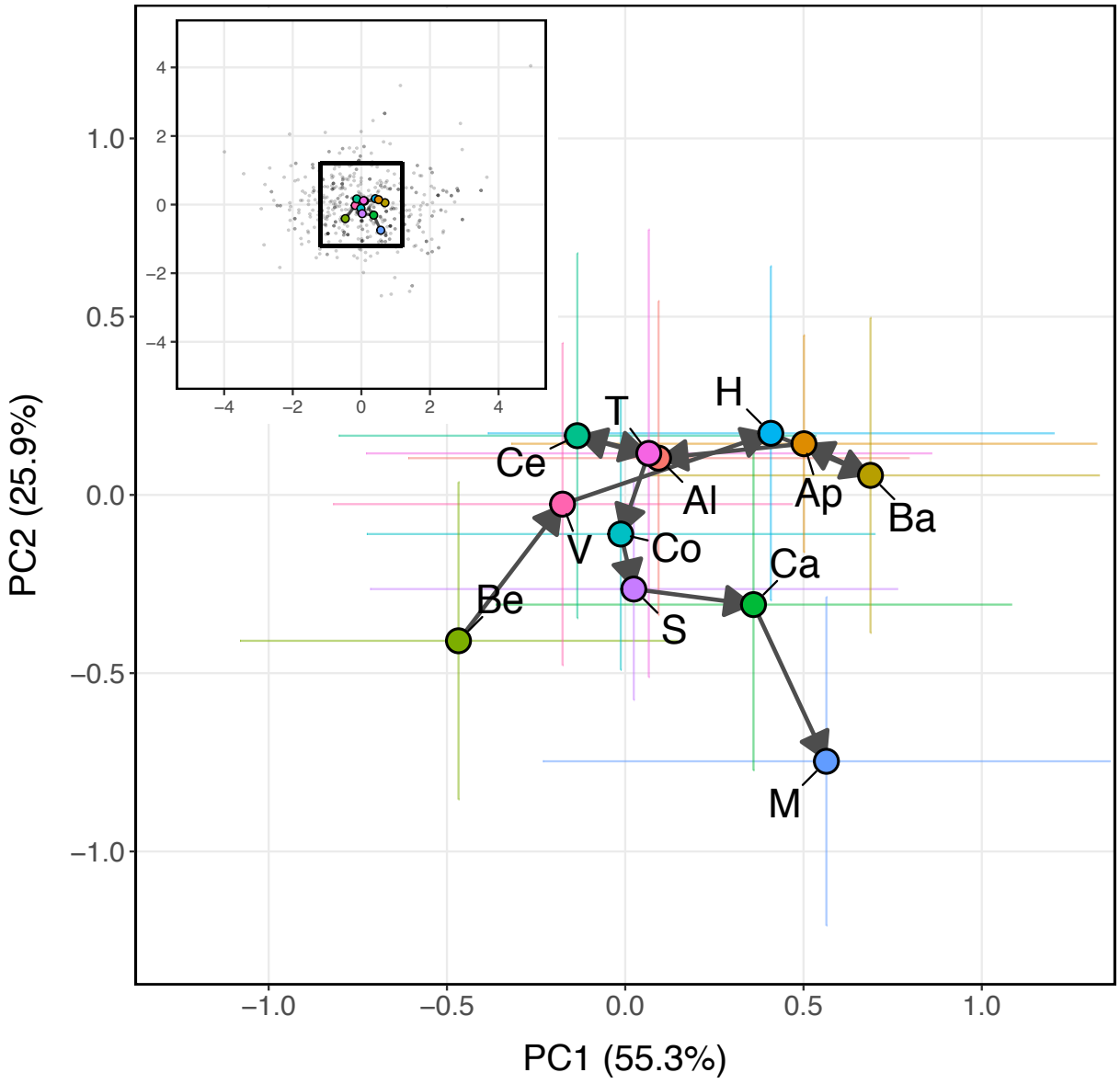

Figure 1.8: Precision-recall curves for final extinction models. Panels are arranged temporally as in Figure 1.3, excluding the Maastrichtian. Horizontal lines indicate expected precision for random classifier. The areas under the precision recall curve ("AUPRC") and the random classifier curve ("Random") are provided. Models where the AUPRC exceeds the area under a random classifier curve are considered to have performed well.

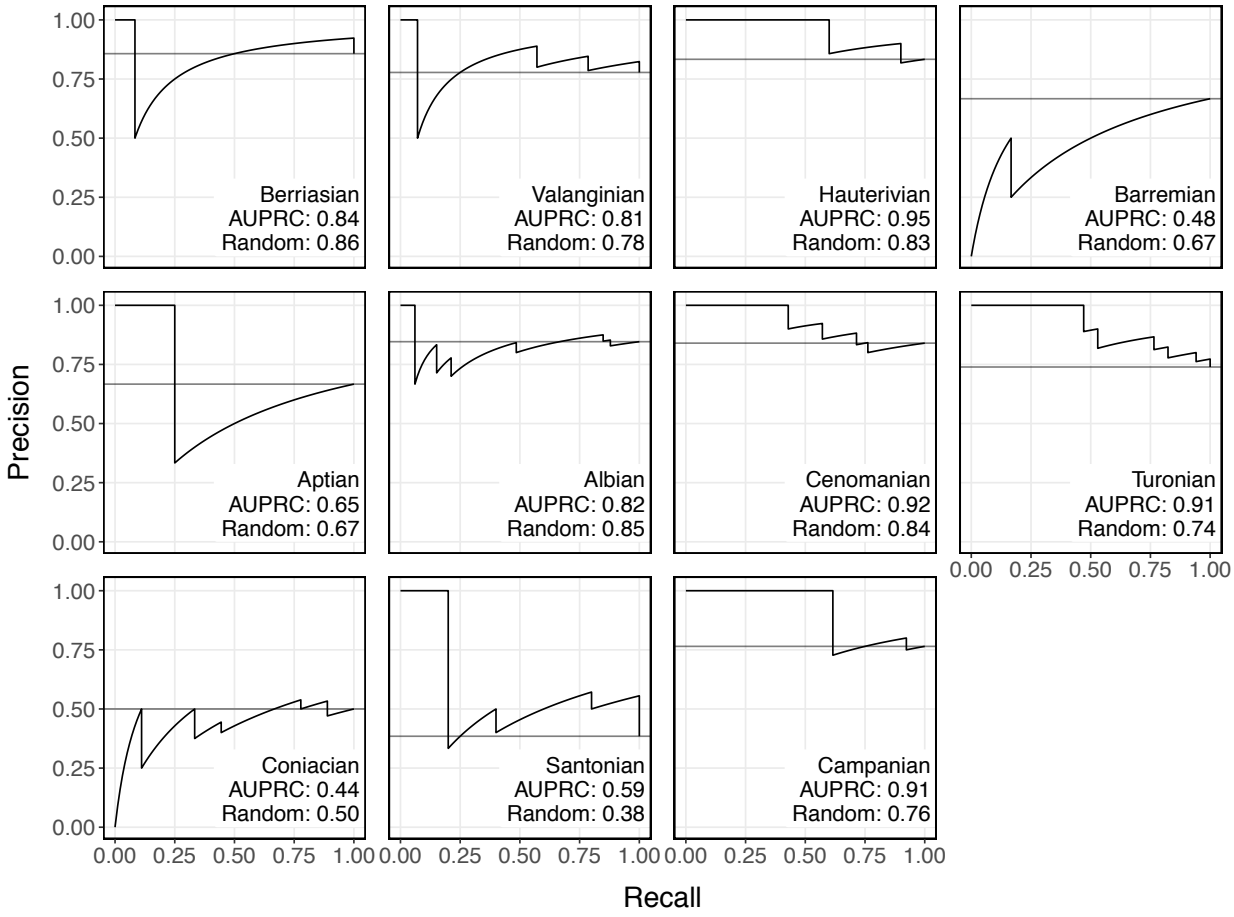

Figure 1.9: Heat map of model performance when models trained on each stage (vertical axis) are used to predict extinction in all other stages (horizontal axis). Performance within the original training interval (diagonal) was assessed using a test dataset of 40% of the original data excluded from the model training procedure. Performance is reported as the area under the receiver operating characteristic curve (AUROC) and is indicated by shading and contained values. Only performance values that exceed that expected of a random classifier (0.5) are provided.

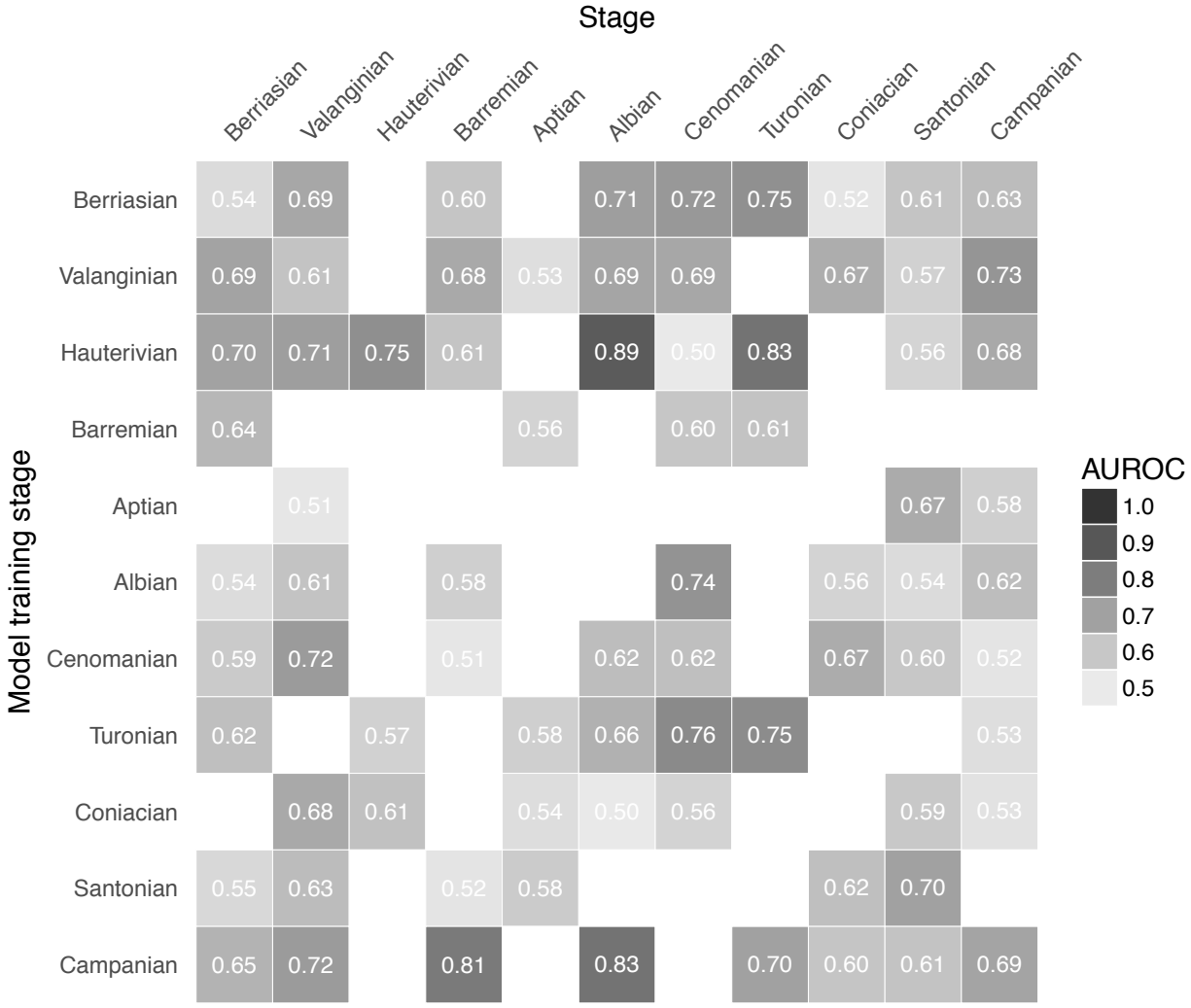

Figure 1.10: Partial dependency plots for potential extinction predictors across time (from top to bottom). If the line is above 0.5, taxa with the associated predictor values are more likely to be classified as going extinct in that interval and vice versa. Gray-scale intensity of the line indicates the relative influence of the predictor in the final model, scaled between the least informative and the most informative predictors. Partial dependencies for models that performed worse than a random classifier according to the area under the precision recall curve (AUPRC) are shown as dashed lines.

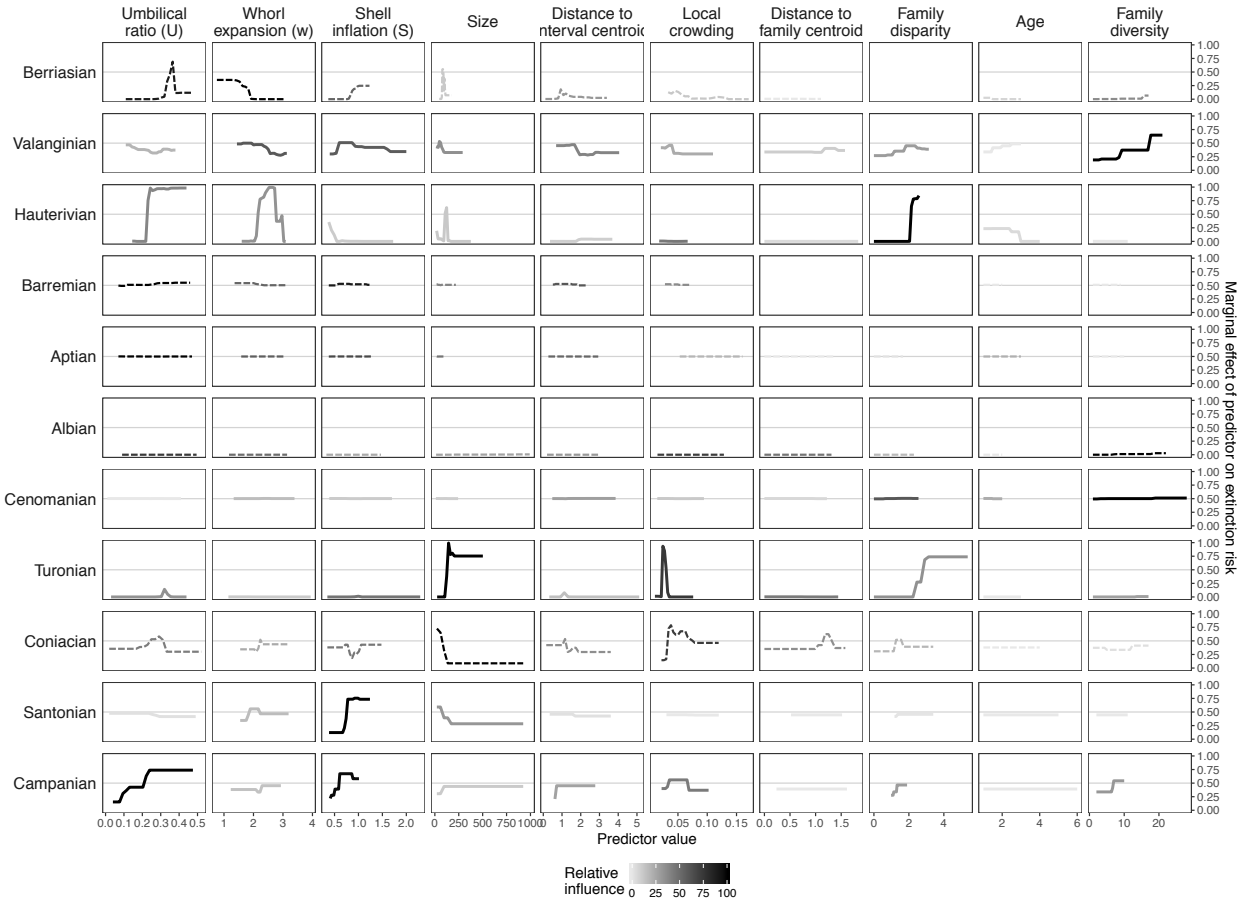

Table 1.1: Morphospace loadings and variance captured by each component. Loadings greater than the expected value of 0.577 for three equal contributing variables are shown in bold. Abbreviations: *U* = umbilical ratio, *w* = whorl expansion rate, *S* = shell inflation.

		PC1	PC2	PC3
Loadings	*U*	**-0.617**	0.302	**-0.727**
	w	0.505	**0.860**	-0.071
	S	**-0.604**	0.411	**0.683**
Proportion of Variance		0.553	0.259	0.188
Cumulative Proportion		0.553	0.812	1

Chapter 2

Testing for consistency in morphological shifts across environments for ammonites of the Western Interior Seaway

Introduction

It has been widely proposed in biology that access to temporally or spatially novel environments can have long-lasting impacts on the ecological diversity of entire clades. Though initial diversity within novel environments may be restricted due to processes such dispersal limitation and environmental filtering (Kraft et al. 2015), occupation has often been noted to subsequently promote diversification through ecological opportunity (Schluter 2000, Yoder et al. 2010). For example, establishment on oceanic islands may be a relatively infrequent event, but successful colonizers can consequently diversify into distinct ecological forms given access to new regimes of resource availability and freedom from competitors and predators. This has been documented in modern cases, such as silverswords in Hawaii (Baldwin and Sanderson. 1998) and the *Anolis* lizards across multiple Caribbean islands (Losos 1992). Novel environmental conditions may also arise in time, such as the evolution of grasses and grasslands coincident with the phenotypic diversification of Miocene horses in North America (MacFadden and Hulbert 1988). In each case, access to new environments is cited as driving ecomorphological differentiation in the one or few lineages met with the ecological opportunity. Though consideration of novel environmental conditions often refers to the abiotic environment, contemporaneous comparisons in the same geographic space allow for identification of common extrinsic factors - a combination of the biotic and abiotic environment - impacting morphology across lineages.

Determining the consistency of morphological responses to novel environmental conditions across multiple taxa can help elucidate their impacts on the ecological trajectories of the broader clade. This is complicated, however, by the fact that responses to novel environments are both individualistic and phylogenetically influenced. Well-characterized natural experiments present valuable opportunities to test how consistently novel environmental conditions shape ecological diversity on macroevolutionary timescales. Comparative frameworks using temporal or taxonomic replicates, or geographic replicates like that of Caribbean *Anolis* lizard studies (Mahler et al. 2013), can help establish baseline expectations in order to accurately measure the significance of the association between morphological differences and access to new environments, distinguishing these shifts from neutral processes. Lower-level taxonomic comparisons can also, in part, mitigate confounding effects stemming from common ancestry. The use of phylogenies and the development of phylogenetic comparative methods such as independent contrasts (Felsenstein 1984) have facilitated the construction of models of trait evolution that account for the non-independence of lineages due to shared evolutionary history. However, while modern phylogenetic methods are increasingly applied to fossil clades, they have yet to take full advantage of the rich record of life captured in the fossil record.

In this study, I assess the degree to which intraspecific and interspecific shape differences are associated with the opening up of novel environments. I do this using the North American ammonite fossil record of the Cenomanian (100.5-93.9 Ma), a formative stage of the Cretaceous Western Interior Seaway (WIS). I use outline analysis to examine the relationship between

aperture shape and latitude within species and test whether congeners spanning the biogeographic boundary separating the WIS from the Gulf and Atlantic Coast consistently fall in distinct regions of morphospace and whether taxa share common morphological responses or behave individualistically.

Study system

The formation of the WIS during the Late Cretaceous provides an ideal natural experiment with which to test the potential for novel environmental conditions to influence the ecomorphological diversity of a clade. During this time, the tectonic collision leading to the development of the Cordilleran orogenic belt along the western edge of present-day North America led to the formation of a foreland basin running primarily north-south across the continent (Slattery et al. 2015). Climatic warming and tectonic processes in the Late Cretaceous on top of existing ice-free "Greenhouse" Earth conditions led to eustatic sea level rise and the widespread formation of epeiric seas on multiple continents (Hancock and Kauffman 1979). This included the flooding of the Western Interior Foreland Basin and the formation of the WIS connecting equatorial waters of present-day Gulf of Mexico in the south to the Arctic Ocean in the north and intermittently to the Atlantic Ocean via the Hudson Seaway in the northeast. Narrow connections between the WIS and neighboring bodies of water as well as comparatively shallow depths (< 300 m; McDonough and Cross 1991) led to restricted marine conditions with the exception of brief intervals during sea level highstands (Kauffman and Caldwell 1993, Simons et al. 2003). Climate models and stratigraphic and isotopic analyses suggest the existence of latitudinal gradients in temperature and mixing regimes within the WIS linked with strong temperature- and salinity-driven stratification as a result of increased input of freshwater from continental runoff and inputs from two oceans (Slingerland et al. 1996, Fisher and Arthur 2002, Simons et al. 2003, Peterson et al. 2006, Coulson et al. 2011, Dennis et al. 2013). The first full connection of the northern and southern arms of the seaway, the Skull Creek Seaway, occurred in the Albian. This was disrupted by a fall in sea level (Williams and Stelck 1975, Slattery et al. 2015) near the Albian/Cenomanian boundary before warming and sea level rise in the early Cenomanian reconnected the WIS, which persisted to the end Cretaceous, leaving a rich and continuous fossil record that has been the subject of more than a century of extensive work. Because of its integral timing at the formation of the persistent seaway, this study focuses on the Cenomanian, which spans approximately 6.6 million years.

The early WIS opened up an expansive novel environment for fauna in adjacent environments to colonize. Using the molluscan fossil record in and near the WIS, Kauffman (1984) defined several marine biogeographic subprovinces - the temperate North, Central, and South Interior subprovinces and the subtropical Gulf and Atlantic Coast subprovince. These are characterized by faunas consisting of 10-25% endemic genera and species and have been used in biogeographic studies, for example, linking species range shifts across subprovincial boundaries during sea level fluctuations to smaller geographic range sizes (Myers et al. 2013). Similar provinciality has also been noted in the marine vertebrate record (Nicholls and Russell 1990), though its faunal compositions have been noted to be temporally and spatially complex (Cumbaa et al. 2010). The presence of biogeographic differentiation suggests that the environmental heterogeneity in and around the seaway plays an important role in structuring inhabiting communities and highlights the potential for this system in studies of response to environmental

change. Analysis of potential biases that may prevent accurate detection of paleobiogeographic patterns concluded that range sizes of WIS taxa are not significantly impacted by geographic outliers, outcrop availability, or the number of unique localities (Myers and Lieberman 2010). This suggests the paleobiogeography of WIS fauna may be well-characterized enough for use in spatial analyses.

Ammonites are ideal organisms with which to study drivers of morphological change. The diversity, abundance, and global distribution of ammonites preserved in their 300-million-year record is complemented by extensive previous work linking ammonoid morphology to ecology and mode of life through biomechanical, taphonomic, and isotopic studies. These studies suggest close ties between the shape of the ammonite's external coiled shell and the organism's swimming velocity (Chamberlain 1981, Jacobs 1992, Jacobs et al. 1994, Jacobs and Chamberlain 1996), shell strength and depth tolerance (Hewitt 1996), buoyancy (Saunders and Shapiro 1986), and vertical orientation (Swan and Saunders 1987, Klug and Korn 2004) and have led researchers to link shell shape directly to environmental conditions (Batt 1993, Westermann 1996, Kawabe 2003).

The ability to undergo rapid morphological evolution has long been recognized in ammonites from biostratigraphic and evolutionary studies. The group is commonly noted to have exhibited rapid radiations (Dommergues et al. 1996, Neige et al. 2013), evolution of similar forms repeatedly across independent lineages (Saunders et al. 2008, Monnet et al. 2011, De Baets et al. 2012, Monnet et al. 2015), repeated shifts towards more involute and compressed shells temporally within families (Bayer and McGee 1984). The partitioning of the drivers behind these patterns into developmental and environmental components has benefitted from studies of the evolution of ontogenetic shape change and its relationship to broader morphological trends and disparity (e.g., De Baets et al. 2012, Gerber 2011, Korn and Klug 2012). Assessment of potential environmental drivers, however, requires a model for how long-term morphological changes manifest themselves spatially at regional and local scales. Past studies assessing the link between adult ammonite morphology and geographic dispersion have found both strong relationship s(e.g., Brayard and Escarguel 2013) and no clear relationship (e.g., Dommergues et al. 2001). Previous studies of ammonite lineages using highly resolved stratigraphic record in basins have been promising, having identified increases in involution with invasion into basins (Klug et al. 2005, Navarro et al. 2005, Lehmann et al. 2016), morphological responses to encounters with new taxa (Yacobucci 2004), and increases in plasticity (Yacobucci 1999). However, these studies typically do not include direct morphological comparisons with source faunas, a feature of this analysis.

Methods

Selection of taxa for study

Species were targeted for sampling using a dataset of Cenomanian North American ammonoid occurrences (MacKenzie 2007) compiled from the primary literature and the Paleobiology Database. Entries of the dataset has been vetted for taxonomic validity and repeat occurrences. While the stratigraphic assignment of each occurrence is resolved to the substage level, all the occurrences were binned at the stage level for the following analyses. I limited this study to

planispiral ammonites, as it is unclear how ecologically analogous shape differences in heteromorphs may be to shape differences in planispiral forms. However, the presented approach and analyses lend themselves to any comparisons of similar anatomical features and thus may be expanded to include heteromorphs as well.

I assigned each species in the occurrence dataset a biogeographic status ("in" or "out") depending on whether any of its occurrences were located within the seaway or whether, with current sampling, it was excluded from the seaway. To better characterize similar environmental responses, I focused on WIS fauna with evolutionarily southern affinities, using the modern 37th parallel north as the geographic threshold because it roughly corresponds with the biogeographic boundary proposed by Kauffman (1984) separating the temperate Southern Interior Subprovince of the Western Interior Seaway and the more southerly subtropical Gulf and Atlantic Coast Subprovince during the Late Cretaceous. I then identified genera whose constituents included species both found within and excluded from the seaway (Figure 2.1). This restriction ensured that shape comparisons can be made directly between congeneric species representing both environments. In addition to quantifying the aperture shape, I assigned each specimen a latitude and longitude coinciding with the geographic centroid of the county in which it was collected. Three specimens were missing county locality data and thus were excluded from intraspecific shape versus latitude analyses but included in size standardization and intraspecific comparisons.

I identified museum specimens belonging to species that fit all of the biogeographic criteria above after correcting specimen records for synonymized taxonomy (Appendix B.1). I additionally targeted species with wide latitudinal ranges (greater than five degrees) to assess spatial variation in shape as well as species that were well-represented in museum collections to assess the relationship between shape change and size. In total, this study includes 115 outlines representing 25 species in 7 genera that present in or near the WIS during the Cenomanian (Table 2.1). Specimens used for this study are housed at the Smithsonian Institution National Museum of Natural History (USNM).

Quantification of aperture shape

Photographs of specimens were taken in aperture and lateral views using a Canon EOS Rebel T3i digital camera suspended facing downward from an inverted tripod. To minimize distortion of the aperture shape from camera perspective, the specimen was positioned so that the aperture was centered in the frame and the plane formed by the umbilical seam and the venter were parallel to the horizontal plane. Only specimens in which at least one half of the aperture showed an unobscured shell border when in this orientation, including an exposed coplanar dorsal contact with the overlapped whorl, were used for outline analysis. I then digitized the complete half of the aperture or, if both sides are adequately exposed, the half showing the least amount of lateral compression using image processing software (Adobe Illustrator Creative Suite 6) and assumed symmetry, reflecting the shape across the dorsal-ventral axis to form the complete aperture. For many of these specimens, the body chamber was not preserved, thus shapes were assessed using the final preserved whorl. Ribbing and ornamentation were captured in the aperture outline if no features clearly distinguish it from the chamber in any view of the shell. Though this approach introduces additional sources of variation, the resulting morphospaces

indicate features such as these are minor contributors towards the overall variation the obtained outlines.

Each aperture outline was processed using the R package Momocs (v1.1.6, Bonhomme et al. 2014), returning a set of densely spaced coordinates that closely approximate the shape of the curve. Outlines were superimposed, centered by centroid, and scaled according to centroid size. Rotation was normalized prior to image input to avoid misalignment of axes. Scaling the outlines in preparation for subsequent analyses removes size as the primary source of variation for the shape analysis. However, I obtained a measure of aperture size - the centroid size - by extracting the distance of one millimeter in the scale bar included in specimen photographs and scaling the aperture outline by this distance. The outlines were then subsampled to the fewest number of coordinates present in any outline (715 points). The centroid size of the scaled aperture was then calculated by summing of squared distances of the set of coordinates to the centroid.

I subsequently quantified the shapes of the superimposed specimen apertures using the chain-coding implementation of elliptic Fourier analysis (EFA, Kuhl and Giardina 1982). EFA treats the closed contour as a continuous periodic function which can be decomposed into sine and cosine functions of increasing frequencies called harmonics. The sum of these harmonics reconstructs the original curve and the coefficients of the sine and cosine terms, called descriptors, can be used to compare the shapes of the apertures. Each harmonic forms an ellipse and is typically characterized by four descriptors: two for each of the x and y directions. EFA is a particularly powerful approach for comparing the shapes of objects that lack clear homologous features, which makes landmarks difficult to recognize and place, and has been used to study shape differences in a variety of objects including leaves (Schmerler et al. 2012), coral sclerites (Carlo et al. 2011), and Paleolithic tools (Ioviţă 2010). The application of EFA to ammonite apertures captures much of the same morphological information as use of traditional shell coiling parameters (Raup 1967), such as degree of involution and shell inflation ratio, but also captures additional information such as the curvature of the flanks and the shape of the venter. For these reasons, EFA has been applied to whorl section views of ammonites in a number of studies to detect subtle shape differences, such as those that occur during ontogeny (e.g., Korn and Klug 2012). However, this approach requires considerably well-preserved, three dimensional specimens in order to accurately reproduce the aperture shape and so achieves objective quantification of shape at the cost of larger sample sizes.

Digitization error was assessed using outlines obtained from repeat digitization of 3 different specimens. The aperture of each specimen was digitized 5 times. Each outline was subsampled for 100 evenly spaced points, which were then aligned using Procrustes superimposition. Procrustes ANOVA (Klingenberg and McIntyre 1998, Appendix B.2) on the superimposed points revealed that inter-specimen differences were highly significant ($p << 0.01$), suggesting that the variation in shape introduced by digitization error does not affect the ability to assess variation above the specimen level. The ratio between the individual variance component and total variance, also called the repeatability of shape (Zelditch et al. 2012), was 0.97 out of 1.00.

All analyses in this study were conducted in the R programming environment (v3.4.0, R Core Team 2016). Outline quantification, EFA, and error assessment were implemented using R

packages Momocs (v1.1.6, Bonhomme et al. 2014) and geomorph (v3.0.4, Adams and Otarola-Castillo 2013).

Allometry and size standardization

An initial ammonite morphospace was generated using principal component analyses (PCA) to assess the strength and nature of allometry in the shape dataset. The morphospace used Fourier descriptors the first 7 harmonics for the digitized aperture shapes (Appendix B.3), which capture 99% of the cumulative harmonic power (Figure 2.2). The PCA thus consists of 28 dimensions for the 28 associated elliptic Fourier descriptors, four per harmonic (Figure 2.3). For ten species in the dataset with greater than three digitized specimens, I compared log-transformed centroid size against the scores of each specimen in the first three principal component axes and found that for most species shape changes linearly with size (Figure 2.4).

In order to facilitate comparison between species of the same genus, I standardized each specimen's shape to a similar size within each genus (Appendix B.4). The size used for standardization was determined to be the maximum size of the least sampled species in that genus or the mean if more than one species was represented by a single specimen. This criterion was used to minimize the need for shape estimation in species with small sample sizes where the size-shape relationship would be more poorly characterized. Because the size-shape relationship was found to be roughly linear, I used multivariate regression to predict all Fourier descriptors as a function of centroid size and estimate the mean shape for each species at the designated size. Residuals preserve deviations of each specimen from the regression line and thus the overall variation. I maintained this variation in the size-standardized shapes by adding the residuals to estimated mean shape of each species (Zelditch et al. 2012). Though the relative positions of specimens in morphospace were affected by size-standardization, the interpretations for shape differences along the major axes of variation are unchanged, indicating that size correction does not remove the major sources of variation that distinguish between taxa.

Morphological indicators such as apertural constrictions or septal approximation (i.e., a decrease in interseptal spacing) may be used to assess the maturity of the organism (Davis et al. 1996). While shape differences due to increases in size may not directly reflect shape changes due to age and maturity, specimens often do not preserve later whorls or the body chamber. Because reference shapes for mature specimens were frequently unavailable in my samples, the size-standardization undertaken here does not assume age standardization across genera but rather describes shape differences when part of the same size regime.

Testing for morphological shifts across space

I constructed a morphospace by conducting a PCA on the Fourier descriptors for size-standardized aperture shapes (Figure 2.5). I used the coefficients from first seven harmonics (28 variables total) to construct the morphospace, as they accounted for over 99% of the shape variation after size standardization. This morphospace was then used to test for relationships between shape and geographic extent both within species and between congeners.

To test for intraspecific variation across space, I used multivariate regression to examine the relationship between scores along the first two principal component axes of morphospace and latitude for widespread species. This was done in three species, *Acanthoceras amphibolum*, *Conlinoceras tarrantense*, and *Metoicoceras mosbyense*, which were sampled across a latitudinal range that exceeds five degrees. This ensured that the sampled latitudinal range of the species exceeds the latitudinal range exhibited by Kauffman's (1984) proposed WIS biogeographic subprovinces.

To test for interspecific variation across space, I identified four genera in the aperture dataset composed of both species that are found within the WIS and species that are not (*Calycoceras*, *Metoicoceras*, *Plesiacanthoceras*, and *Tarrantoceras*). For each genus, specimens were grouped by biogeographic status - in versus out of the WIS - and conducted a one-way multivariate analysis of variance (MANOVA) to test for significant shape differences between the two groups. I did not conduct MANOVA in *Plesiacanthoceras* as non-WIS group had only one case, but its occupancy in morphospace is shown. Shape comparisons were made only within genera and not across them. Significance values were adjusted using the Bonferroni correction. The direction of shape difference between groups was assessed using linear discriminant function analysis (LDA) with leave-one-out cross validation. To avoid overfitting with high dimensional data, particularly given the low sample sizes found in some groupings, I used the scores of each specimen along the first and second PC axes as low dimensional summaries of variation in aperture shapes in both analyses.

The approach taken here builds on the idea that occupants of the newly formed WIS were drawn from the regional pool of taxa in the adjacent open ocean environment that had access to seaway during and after its formation. Phylogeny can then be broadly controlled for by assuming close relatedness at lower taxonomic levels between the taxa occupying the regions of interest due to shared ancestry presumably just prior to the formation of the seaway. If occupation of the new environment had no effect on shape and, thus, was a random subset of the source pool, there would no expectation of a significant difference in morphospace occupation between WIS taxa and non-WIS taxa of the same genus. On the other hand, significant divergences in morphospace between biogeographic subregions in a common direction would suggest environmentally-driven morphological filtering independently across lineages. It is also possible for random shifts such as those caused by drift to either increase variation at higher taxonomic levels by diffusing lineages across shape space or cause seemingly directional divergence in the shape space purely by chance. The latter possibility highlights the importance of having multiple independent comparisons with which to identify commonalities in shape differences.

Results

Morphospaces

Two principal component analyses of the first seven Fourier descriptors for aperture shapes resulted in morphospaces representing ammonite aperture shapes before and after size-standardization. Prior to size-standardization, the PCA of aperture shapes captured 67.5% of the total shape variation along the first PC axis, 27.6% along the second PC axis, and 2.2% along the third (Figure 2.3). With corrections for size, the PCA of aperture shapes captured 75.2% of the

total shape variation along the first PC axis, 19.6% along the second PC axis, and 2.4% along the third (Figure 2.5). Because 95% of the total shape variation in captured in the first two PC axes in both morphospaces, subsequent analyses focus on these axes.

Though the effect of size on shape was removed when generating the second morphospace, I find that the sources of variation across all the taxa in this study remain relatively unchanged. Reconstructions of aperture shapes across both morphospaces show that the first PC axis captures differences in the degree of compression of the shell and that the second PC axis roughly corresponds to the degree of involution or how much the whorl overlaps previous whorls with growth. The third axis, which was not used for subsequent analyses, captures variation in how rounded the venter is. Much of the variation that exists in the quantified aperture shapes is driven by the inclusion of the genus *Metoicoceras*, which occupies a relatively large region of the two-dimensional morphospace at one end of the first PC axis apart from other genera.

Of the ten species for which allometry was characterized, five showed significantly non-zero linear relationships with between centroid size and scores along at least one of the first three PC axes (Figure 2.4) after correction for multiple comparisons. In all given cases, significant shape changes along the second PC axis were detected with increasing size, which corresponds to increasing degree of involution of the shell. Thus, one noticeable effect of size standardization was the reduction of the proportion of variation explained by the second PC axis.

Intra- and interspecific shape variation across space

Multivariate linear regression showed no strong support for intraspecific shape differences across latitude for species in the dataset with ranges of more than five degrees latitude (Figure 2.6). The northern extreme of the latitudinal range for *A. amphibolum* and the southern extreme of *M. mosbyense* are each represented by one relatively geographically isolated specimen. However, the shapes obtained from these specimens are well within the morphological range occupied by the other specimens of the species and are unlikely to represent a dramatic departure in shape. Exclusion of geographically outlying specimens results in a sampled latitudinal range of nearly five degrees and no apparent trend in shape across latitude in both cases (Appendix B.5).

Comparisons of morphospace occupation within genera using MANOVA show statistically significant differences between species that occupy the WIS and geographically proximate species that do not (Figure 2.7, Table 2.2). Coefficients of the linear discriminant indicate highest discriminatory power along the second PC axis for *Calycoceras* and *Tarrantoceras* (Table 2.3). The non-WIS species of *Plesiacanthoceras* are represented here by only one specimen and thus were not analyzed using MANOVA and LDA. However, the specimen lies outside the region of morphospace occupied by the *Plesiacanthoceras* WIS species (Hotelling's $T^2(2, 6) = 14.387$, p value = 0.005) and shows similar separation in morphospace along the second PC axis as *Calycoceras* and *Tarrantoceras*. In all three cases, taxa found within the WIS exhibit lesser degrees of involution than those found outside the WIS. *Metoicoceras* also shows significant shape difference between the in and out of WIS groups. However, unlike the other three genera, the coefficients of the linear discriminant for *Metoicoceras* indicate the greatest discriminatory power is in the first PC axis, with WIS species showing overall greater shell compression than non-WIS species.

Discussion

The findings presented here suggest that taxa may share common responses with exposure to the same environment but are also capable of strongly responding in clade-dependent ways. I find no evidence of consistent intraspecific shape differences across wide latitudinal ranges spanning the boundary between the WIS and the open ocean. This is in contrast to previous studies that have documented morphological changes in lineages across several European basins during the period spread and colonization of epeiric seas in the Mesozoic (e.g., Klug et al. 2005, Lehmann et al. 2016). However, I do find some evidence of separation in morphospace between in and out of seaway faunas when comparing intrageneric species. In other words, taxa that occupied the WIS and those that did not do not appear to represent random subsets of the same morphospace despite common biogeographic and, presumably, evolutionary origins. Three of the four genera examined show a common pattern, where ammonites that were present in the WIS had less involute shells compared to their open marine counterparts. The differences between groups in the fourth genus for the most part reflected variation in shell compression, with those species inside the WIS exhibiting more highly compressed shells than non-WIS species.

Sexual dimorphism

Though ammonites have been noted to exhibit sexual dimorphism (Davis et al. 1996), I do not distinguish between macro- and microconchs in this analysis. If the two forms differ primarily in size, then treatment of them separately would not change the findings of this study given the application of size-standardization. However, if the two forms exhibit different shape responses across environments or if there is spatial bias in their relative representation, then combining the two forms in the same treatment may obscure decoupled but existing intraspecific structure, warranting further investigation. Sexual dimorphism would likely have little effect on the findings from interspecific comparisons, as the position of specimens for each species in morphospace would not deviate far outside the currently occupied spaces following re-analysis using sex-specific allometric relationships. Thus, the relative positions of species would not drastically change.

Time averaging

One possible reason this study did not detect intraspecific variation as previous studies had may be the difference in temporal and stratigraphic resolution between this study – which treats all occurrences in the Cenomanian as contemporaneous – and previous studies – which commonly use time bins based on sub-stage lithostratigraphic units. Time-averaging would therefore decrease the chances of detecting intraspecific shape differences if shape evolution rapidly reaches new optima or if environmental changes were rapid and morphologies closely track them. Further partitioning of occurrence and shape datasets used in this study into finer temporal bins would better allow detection of a link, if it exists, between within lineage shape change and the flooding of the WIS, but would require much larger sample sizes than used here from which to draw conclusions.

However, if this were the case, time averaging would similarly obscure shape differences between intrageneric biogeographic groupings due to spatial averaging, geographically and in morphospace. Detection of significant between-group differences in all genera for which comparisons were made suggests that time averaging does not obscure patterns of shape differences at the genus level for the temporal resolution used in this study.

Abiotic and biotic drivers of shape change

Why these shape differences coincide with the formation of the WIS is an open question. Sea-level change, including the encroachment of more marine conditions into shallow seas, has often been invoked as a first-order driver of morphological change in ammonites (e.g., Bayer and McGhee 1984, Dommergues et al. 1996, Lehmann et al. 2016). However, the mechanism by which this would happen is unclear. It has been suggested that these patterns are passively associated with environmental conditions (Zacaï et al. 2016). Well-defined, mechanistic links between existing environmental conditions and morphology, then, are critical for determining the abiotic drivers of change if they exist. Though there exists some understanding of WIS paleooceanographic conditions across the Late Cretaceous through climate models, isotopic studies, and faunal compositions, much work remains to be done to tie together local interpretations of environments into a context within which these organisms lived. As mentioned previously, a rich body of literature exists linking an ammonoid's shell shape to how it interacts with the environment around it. For example, lower degrees of involution, like that exhibited by WIS fauna across multiple genera in this study, have been associated with increased drag and a decrease in hydrodynamic performance. Shell compression, like that shown in *Metoicoceras*, is also thought to influence the hydrodynamic properties of the shell, with more compressed shells experiencing lower drag. Thus, in just the genera included in this study, shapes differences occurred in ecologically opposing directions, suggesting complex causes of morphological evolution and no one driver of change, even across coexisting taxa.

Internal and external biotic factors are likely as important as abiotic influences in regulating shape differences across space. Work on Triassic ammonites, for example, has shown that evolute morphs tended to be more endemic than involute forms (Brayard and Escarguel 2013) and that this may be a result of dispersal ability. Early ontogenetic stages, however, may play a crucial role in structuring ammonite morphospace, as ammonites are widely thought to disperse as planktonic larvae (De Baets et al. 2012, Zacaï et al. 2016) and thus may exhibit weak associations between adult forms and the paleoenvironments in which they are found. The presence of competitors introduces another factor which may impact populations in non-straightforward ways, as character displacement has been documented in ammonites of the WIS (Yacobucci 2004). Whether these changes translate into morphological shifts at higher taxonomic levels remains to be shown in both fossil and modern systems.

Phylogeny

While comparison of congeneric species acts as an approximate methodological replacement for independent contrasts, many of the questions touched on in this study are answered best within a more formal phylogenetic framework. For example, by limiting analyses to congeners, there is the risk of excluding taxa that have become so morphologically distinct as to be assigned a new

name. Recognition of ancestor-descendant relationships and inclusion of those taxa can provide more replicates with which to test for consistent morphological responses. Detection of paraphyletic genera requires well-developed phylogenetic hypotheses and consideration of all taxa with geographic access to the new environment. However, by considering shape changes within genera, as I have done here, I focus on detecting more subtle differences small enough so as not to warrant new taxonomic assignment.

Though I consider the WIS to be a newly formed habitat, I attempt to make no assumptions about the direction of immigration. The presence of regions of high endemism in the WIS increases the possibility that genera immigrate out of the seaway into open marine waters, which requires both phylogenetic and stratigraphic consideration to determine. Thus, the aim of this study is only to identify consistent differences in shape that can then be attributable to the differences in environmental conditions between the WIS and adjacent bodies of water rather than predict the direction of change itself.

Conclusions

The Western Interior Seaway and other epeiric seas throughout Earth's history offer unique natural experiments with which to test large-scale biotic responses to habitat formation and associated ecological opportunities. I found significant differences between regions of morphospace occupied by species inhabiting the WIS compared to congeneric species not inhabiting the WIS. Examination of these differences revealed both a common pattern of shape difference across genera as well as taxon-specific shape differences. These findings suggest that morphological shifts may be consistent across taxa, that clade-level morphological trends may at least in part be driven by spatial and temporal heterogeneity in environmental conditions, and that the formation of widespread environments like the WIS impact long-term morphological trends of a clade.

Acknowledgments

I would like to thank Margaret Yacobucci for providing me access to the MacKenzie (2007) occurrence dataset and for her feedback throughout the research development and analysis. I would also like to thank Kathy Hollis, Mark Florence, and Daniel Levin for hosting me during my visits to the Smithsonian's collections, as well as Bushra Hussaini (American Museum of Natural History), Talia Karim (University of Colorado Museum of Natural History), and Kevin McKinney (United States Geological Survey) for hosting me at their respective institutions. This study received support from the William B. N. Berry Memorial Research Fund, the Reshetko Family Scholarship Fund, the Leeper Fund, the University of California Department of Integrative Biology, and the University of California Museum of Paleontology.

References

Adams, D.C. and Otarola-Castillo, E. 2013. geomorph: an R package for the collection and analysis of geometric morphometric shape data. Methods in Ecology and Evolution 4: 393-399.

Baldwin, B.G. and Sanderson, M.J. 1998. Age and rate of diversification of the Hawaiian silversword alliance (Compositae). Proceedings of the National Academy of Sciences 95(16): 9402-9406.
Batt, R. 1993. Ammonite morphotypes as indicators of oxygenation in a Cretaceous epicontinental sea. Lethaia 26(1): 49-63.
Bayer, U. and McGhee, Jr., G.R. 1984. Iterative evolution of Middle Jurassic ammonite faunas. Lethaia 17(1): 1-16.
Bonhomme, V., Picq, S, Gaucherel, C., and Claude, J. 2014. Momocs: outline analysis using R. Journal of Statistical Software 56(13): 1-24.
Brayard, A. and Escarguel, G. 2013. Untangling phylogenetic, geometric and ornamental imprints on Early Triassic ammonoid biogeography: a similarity-distance decay study. Lethaia 46(1): 19-33.
Carlo, J.M., Barbeitos, M.S., and Lasker, H.R. 2011. Quantifying complex shapes: elliptical fourier analysis of octocoral sclerites. The Biological Bulletin 220(3): 224-237.
Chamberlain, Jr., J.A. 1981. Hydromechanical design of fossil cephalopods. Pp. 289-336 *in* House, M.R. and Senior, J.R. eds. The Ammonoidea. Systematics Association Special Volume 18. Academic Press, London.
Coulson, A.B., Kohn, M.J., and Barrick, R.E. 2011. Isotopic evaluation of ocean circulation in the Late Cretaceous North American seaway. Nature Geoscience 4(12): 852-855.
Cumbaa, S.L., Shimada, K., and Cook, T.D. 2010. Mid-Cenomanian vertebrate faunas of the Western Interior Seaway of North America and their evolutionary, paleobiogeographical, and paleoecological implications. Palaeogeography, Palaeoclimatology, Palaeoecology 295(1): 199-214.
Davis, R.A., Landman, N.H., Dommergues, J.-L., Marchand, D, and Bucher, H. 1996. Mature modifications and dimorphism in ammonoid cephalopods. Pp. 463-539 *in* Landman, N.H., Tanabe, K., and Davis, R.A. eds. Ammonoid Paleobiology. Vol. 13 of F.G. Stehli and D.S. Jones, eds. Topics in Geobiology. Plenum, New York.
De Baets, K., Klug, C., Korn, D., and Landman, N.H. 2012. Early evolutionary trends in ammonoid embryonic development. Evolution 66(6): 1788-1806.
Dennis, K.J., Cochran, J.K., Landman, N.H., and Schrag, D.P. 2013. The climate of the Late Cretaceous: New insights from the application of the carbonate clumped isotope thermometer to Western Interior Seaway macrofossil. Earth and Planetary Science Letters 362: 51-65.
Dommergues, J.-L., Laurin, B., and Meister, C. 1996. Evolution of ammonoid morphospace during the Early Jurassic radiation. Paleobiology 22(2): 219-240.
Dommergues, J.-L., Laurin, B., and Meister, C., 2001. The recovery and radiation of Early Jurassic ammonoids: morphologic versus palaeobiogeographical patterns. Palaeogeography, Palaeoclimatology, Palaeoecology 165(3): 195-213.
Felsenstein, J. 1985. Phylogenies and the comparative method. The American Naturalist 125(1): 1-15.
Fisher, C.G. and Arthur, M.A. 2002. Water mass characteristics in the Cenomanian US Western Interior seaway as indicated by stable isotopes of calcareous organisms. Palaeogeography, Palaeoclimatology, Palaeoecology 188(3): 189-213.
Gerber, S. 2011. Comparing the differential filling of morphospace and allometric space through time: the morphological and developmental dynamics of Early Jurassic ammonoids. Paleobiology 37(3): 369-382.

Hancock, J.M. and Kauffman, E.G. 1979. The great transgressions of the Late Cretaceous. Journal of the Geological Society 136(2): 175-186.
Hewitt, R.A. 1996. Architecture and strength of the ammonoid shell. Pp. 297-339 *in* Landman, N.H., Tanabe, K., and Davis, R.A. eds. Ammonoid Paleobiology. Vol. 13 of F.G. Stehli and D.S. Jones, eds. Topics in Geobiology. Plenum, New York.
Ioviţă, R., 2010. Comparing stone tool resharpening trajectories with the aid of elliptical Fourier analysis. Pp. 235-253 *In* Lycett, S. and Chauhan, P. eds. New Perspectives on Old Stones. Springer Netherlands, Dordrecht.
Jacobs, D.K. 1992. Shape, drag, and power in ammonoid swimming. Paleobiology 18(2): 203-220.
Jacobs, D.K. and Chamberlain, Jr., J.A. 1996. Buoyancy and hydrodynamics in ammonoids. Pp. 169-224 *in* Landman, N.H., Tanabe, K., and Davis, R.A. eds. 1996. Ammonoid Paleobiology. Vol. 13 of F.G. Stehli and D.S. Jones, eds. Topics in Geobiology. Plenum, New York.
Jacobs, D.K., Landman, N.H., and Chamberlain, Jr., J.A. 1994. Ammonite shell shape covaries with facies and hydrodynamics: iterative evolution as a response to changes in basinal environment. Geology 22: 905-908.
Kauffman, E.G. 1984. Paleobiogeography and evolutionary response dynamic in the Cretaceous Western Interior Seaway of North America. Pp. 273-306 *in* Jurassic-Cretaceous Biochronology and Paleogeography of North America. Geological Association of Canada Special Paper 27.
Kauffman, E.G. and Caldwell, W.G.E. 1993 The Western Interior Basin in space and time. Pp. 1-30 *in* Caldwell, W.G.E. and Kauffman, E.G. eds. Evolution of the Western Interior Basin. Geological Association of Canada Special Paper 39.
Kawabe, F. 2003. Relationship between mid-Cretaceous (upper Albian–Cenomanian) ammonoid facies and lithofacies in the Yezo forearc basin, Hokkaido, Japan. Cretaceous Research 24(6): 751-763.
Klingenberg, C.P. and McIntyre, G.S. 1998. Geometric morphometrics of developmental instability: analyzing patterns of fluctuating asymmetry with Procrustes methods. Evolution 52(5): 1363-1375.
Klug, C. and Korn, D. 2004. The origin of ammonoid locomotion. Acta Palaeontologica Polonica. 49(2): 235-242.
Klug, C., Schatz, W., Korn, D., and Reisdorf, A.G. 2005. Morphological fluctuations of ammonoid assemblages from the Muschelkalk (Middle Triassic) of the Germanic Basin – indicators of their ecology, extinctions, and immigrations. Palaeogeography, Palaeoclimatology, Palaeoecology 221(1): 7-34.
Korn, D. and Klug, C. 2012. Palaeozoic ammonoids – diversity and development of conch morphology. Pp. 491-534 *in* Talent, J. ed. Earth and Life. Springer Netherlands, Dordrecht.
Kraft, N.J., Adler, P.B., Godoy, O., James, E.C., Fuller, S., and Levine, J.M. 2015. Community assembly, coexistence and the environmental filtering metaphor. Functional Ecology 29(5): 592-599.
Kuhl, F.P. and Giardina, C.R. 1982. Elliptic Fourier features of a closed contour. Computer Graphics and Image Processing 18(3): 236-258.
Lehmann, J., Bargen, D., Engelke, J., and Claßen, J. 2016. Morphological variability in response to palaeoenvironmental change – a case study on Cretaceous ammonites. Lethaia 49(1): 73-86.
Losos, J.B. 1992. The evolution of convergent structure in Caribbean *Anolis* communities. Systematic Biology 41(4): 403-420.

MacFadden, B.J. and Hulbert, R.C. 1988. Explosive speciation at the base of the adaptive radiation of Miocene grazing horses. Nature 336(6198): 466-468.
MacKenzie III, R.A. 2007. Exploring Late Cretaceous Western Interior Ammonoid Geographic Range and Its Relationship to Diversity Dynamics Using Geographic Information Systems (GIS). Unpublished M.S. thesis, Bowling Green State University, Bowling Green, OH.
Mahler, D.L., Ingram, T., Revell, L.J., and Losos, J.B. 2013. Exceptional convergence on the macroevolutionary landscape in island lizard radiations. Science 341(6143): 292-295.
McDonough, K.J. and Cross, T.A. 1991. Late Cretaceous sea level from a paleoshoreline. Journal of Geophysical Research: Solid Earth 96(B4): 6591-6607.
Monnet, C., De Baets, K., and Klug, C. 2011. Parallel evolution controlled by adaptation and covariation in ammonoid cephalopods. BMC Evolutionary Biology 11: 115.
Monnet, C., Klug, C., and De Baets, K. 2015. Evolutionary patterns of ammonoids: phenotypic trends, convergence, and parallel evolution. Pp. 95-142 *in* Klug, C., Korn, D., De Baets, K., Kruta, I., and Mapes, R.H. eds. Ammonoid Paleobiology: From macroevolution to paleogeography. Vol. 44 of Topics in Geobiology. Springer Netherlands, Dordrecht.
Myers, C.E. and Lieberman, B.S. 2010. Sharks that pass in the night: using Geographical Information Systems to investigate competition in the Cretaceous Western Interior Seaway. Proceedings of the Royal Society of London B: Biological Sciences 278: 681-689.
Myers, C.E., MacKenzie III, R.A., and Lieberman, B.S. 2012. Greenhouse biogeography: the relationship of geographic range to invasion and extinction in the Cretaceous Western Interior Seaway. Paleobiology 39(1): 135-148.
Navarro, N., Neige, P., and Marchand, D. 2005. Faunal invasions as a source of morphological constraints and innovations? The diversification of the early Cardioceratidae (Ammonoidea; Middle Jurassic). Paleobiology 31(1): 98-116.
Neige, P., Dera, G., and Dommergues, J.L. 2013. Adaptive radiation in the fossil record: a case study among Jurassic ammonoids. Palaeontology 56(6): 1247-1261.
Nicholls, E.L. and Russell, A.P. 1990. Paleobiogeography of the Cretaceous Western Interior Seaway of North America: the vertebrate evidence. Palaeogeography, Palaeoclimatology, Palaeoecology 79: 149-169.
Petersen, S.V., Tabor, C.R., Lohmann, K.C., Poulsen, C.J., Meyer, K.W., Carpenter, S.J., Erickson, J.M., Matsunaga, K.K., Smith, S.Y., and Sheldon, N.D. 2016. Temperature and salinity of the Late Cretaceous Western Interior Seaway. Geology 44(11): 903-906.
R Core Team. 2016. R: A language and environment for statistical computing. R Foundation for Statistical Computing, Vienna, Austria.
Raup, D.M. 1967. Geometric analysis of shell coiling: coiling in ammonoids. Journal of Paleontology 41(1): 43-65.
Saunders, W.B., Greenfest-Allen, E., Work, D.M., and Nikolaeva, S.V. 2008. Morphologic and taxonomic history of Paleozoic ammonoids in time and morphospace. Paleobiology 34(1): 128-154.
Saunders, W.B. and Shapiro, E.A. 1986. Calculation and simulation of ammonoid hydrostatics. Paleobiology 12(1): 64-79.
Schluter, D. 2000. The ecology of adaptive radiation. Oxford University Press Inc., New York.
Schmerler, S.B., Clement, W.L., Beaulieu, J.M., Chatelet, D.S., Sack, L., Donoghue, M.J., and Edwards, E.J. 2012. Evolution of leaf form correlates with tropical-temperate transitions in Viburnum (Adoxaceae). Proceedings of the Royal Society of London B: Biological Sciences 279(1744): 3905-3913.

Simons, D.J.H., Kenig, F., and Schröder-Adams, C.J. 2003. An organic geochemical study of Cenomanian-Turonian sediments from the Western Interior Seaway, Canada. Organic Geochemistry 34(8): 1177-1198.
Slattery, J.S., Cobban, W.A., McKinney, K.C., Harries, P.J., and Sandness, A.L. 2015. Early Cretaceous to Paleocene paleogeography of the Western Interior Seaway: the interaction of eustasy and tectonism. Wyoming Geological Association Guidebook 2015: 22-60.
Slingerland, R., Kump, L.R., Arthur, M.A., Fawcett, P.J., Sageman, B.B., and Barron, E.J. 1996. Estuarine circulation in the Turonian western interior seaway of North America. Geological Society of America Bulletin 108(8): 941-952.
Swan, A.R.H. and Saunders, W.B. 1987. Function and shape in Late Paleozoic (Mid-Carboniferous) ammonoids. Paleobiology 13(3): 297-311.
Westermann, G.E.G. 1996. Ammonoid life and habit. Pp. 607-707 *in* Landman, N.H., Tanabe, K., and Davis, R.A. eds. Ammonoid Paleobiology. Vol. 13 of F.G. Stehli and D.S. Jones, eds. Topics in Geobiology. Plenum, New York.
Williams, G.D. and Stelck, C.R. 1975. Speculations on the Cretaceous paleogeography of North America. Pp. 1-20 *in* Caldwell, W.G.E. ed. The Cretaceous System in the Western Interior of North America. Geological Association of Canada Special Paper 13.
Yacobucci, M.M. 1999. Plasticity of developmental timing as the underlying cause of high speciation rates in ammonoids. Pp. 59-76 *In* Olóriz, F. and Rodriguez-Tovar, F.J. eds. Advancing Research in Living and Fossil Cephalopods. Kluwer/Plenum, New York.
Yacobucci, M.M. 2004. *Neogastroplites* meets *Metengonoceras*: morphological response of an endemic hoplitid ammonite to a new invader in the mid-Cretaceous Mowry Sea of North America. Cretaceous Research 25(6): 927-944.
Yoder, J.B., Clancey, E., Des Roches, S., Eastman, J.M., Gentry, L., Godsoe, W., Hagey, T.J., Jochimsen, D., Oswald, B.P., Robertson, J., and Sarver, B.A.J. 2010. Ecological opportunity and the origin of adaptive radiations. Journal of Evolutionary Biology 23(8): 1581-1596.
Zacaï, A., Brayard, A., Dommergues, J.L., Meister, C., Escarguel, G., Laffont, R., Vrielynck, B., and Fara, E. 2016. Gauging scale effects and biogeographical signals in similarity distance decay analyses: an Early Jurassic ammonite case study. Palaeontology 59(5): 671-687.
Zelditch, M.L., Swiderski, D.L., and Sheets, H.D. 2012. Geometric morphometrics for biologists: a primer. Elsevier Academic Press, San Diego, CA.

Figure 2.1: Distribution of occurrences for each genus. Outlined points indicate USNM specimen localities. Species ranges are denoted using convex hulls. Red line marks the 37th north parallel, which designates the boundary between biogeographic subprovinces (see text for details). Colors indicate individual species.

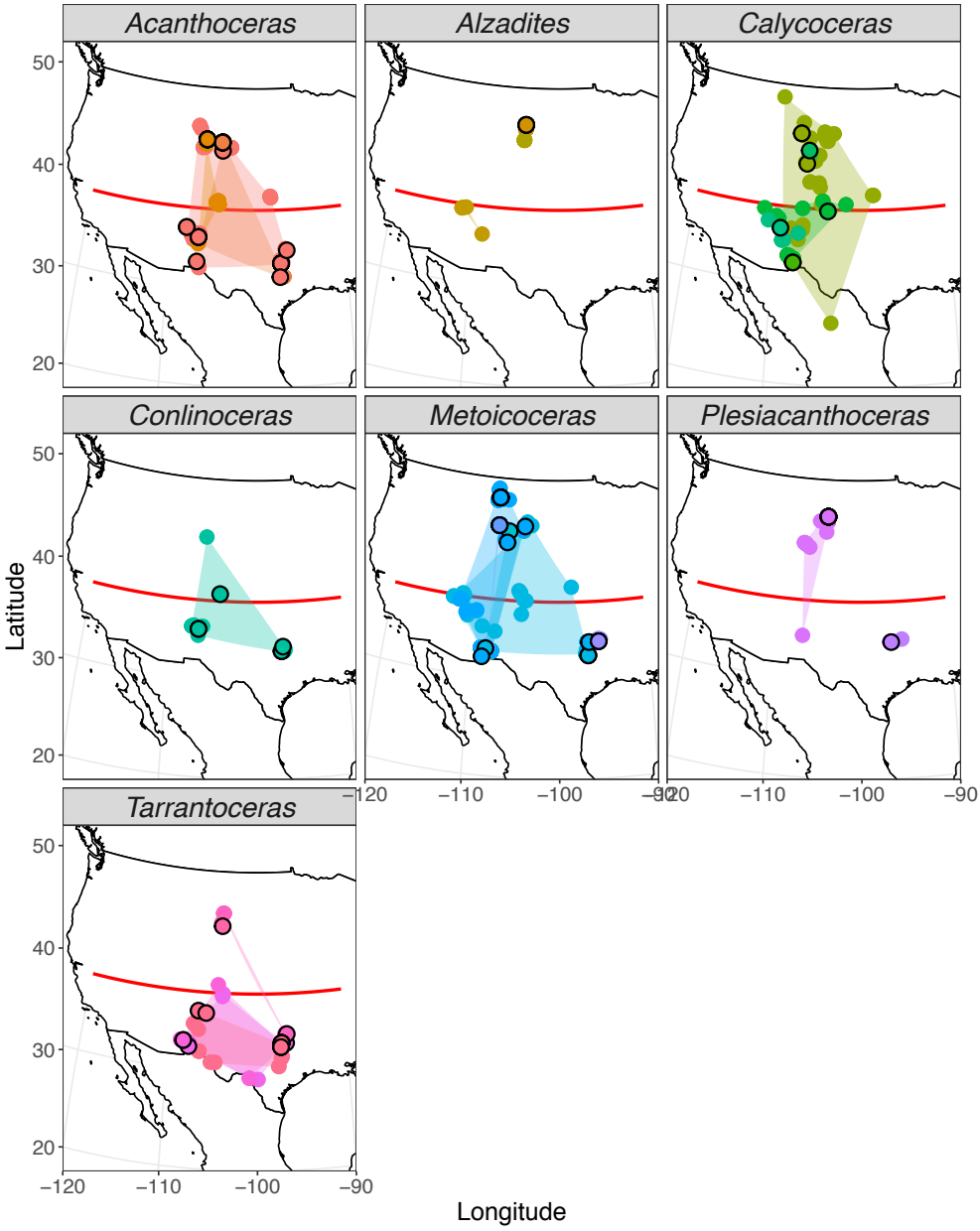

Figure 2.2. (A) Cumulative harmonic power using the first nine harmonics from an elliptic Fourier analysis of all aperture shapes before size standardization. (B) Outline reconstruction using the first nine harmonics is shown for USNM PAL 420227 (*Acanthoceras amphibolum*).

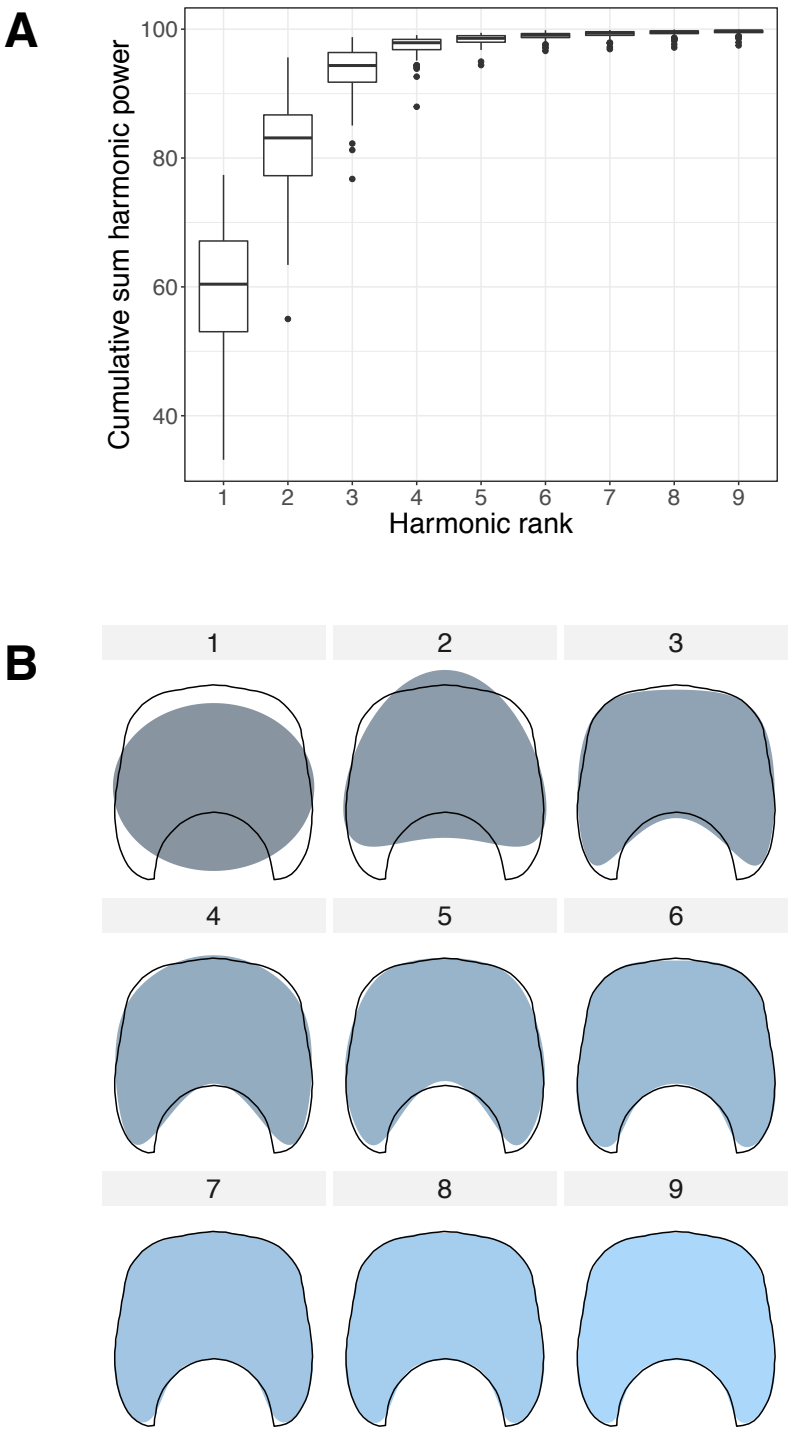

Figure 2.3: Ammonite morphospace before size standardization, shown as the first three axes of a principal components analysis of aperture shapes. Points are individual specimens with genera designated by shape and convex hull color. Hypothetical reconstructions of aperture shapes at regular intervals of the occupied morphospace are shown in the background.

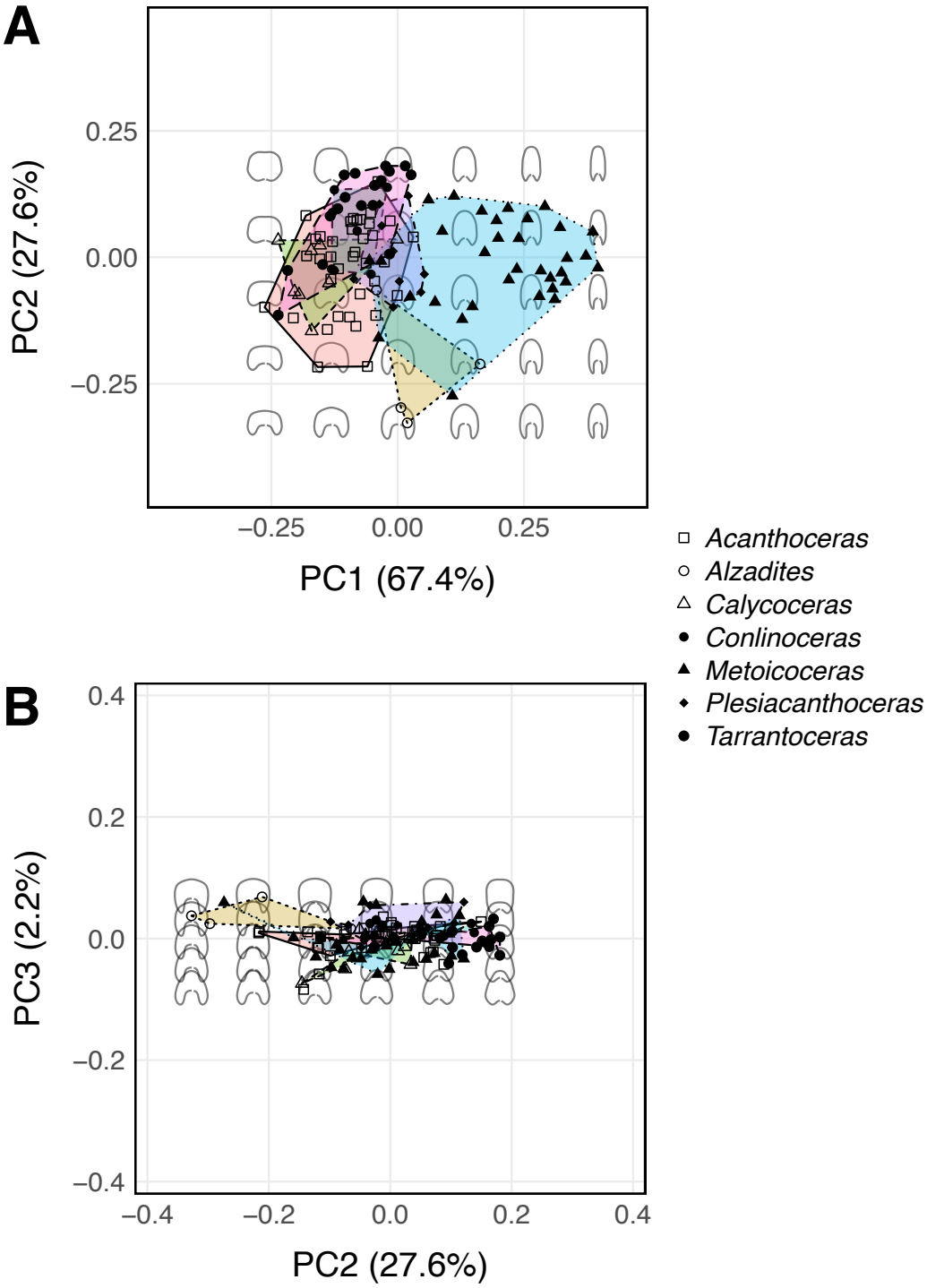

Figure 2.4: Relationship between centroid size and scores along the first three axes of a principal components analysis for species with more than three digitized specimens. The principal component analysis referenced here was conducted using non-size standardized aperture shapes. Gray shading indicates 95% confidence intervals around the regression line. Dotted lines indicate slopes indistinguishable from zero, dashed lines indicate statistically non-zero slopes before Bonferroni correction ($p \leq 0.05$) and solid lines indicate statistically non-zero slopes after correction ($p \leq 0.0017$).

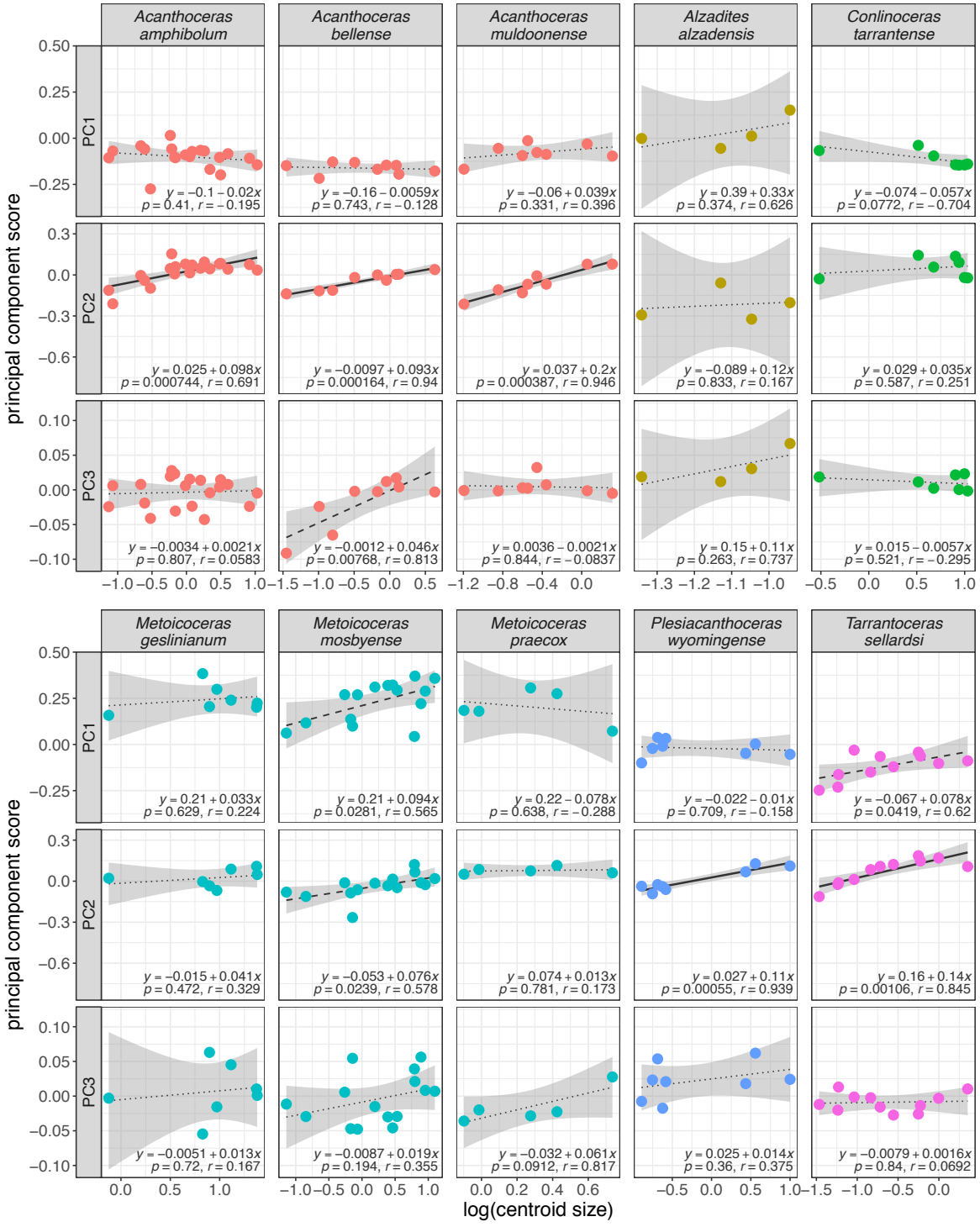

Figure 2.5: Ammonite morphospace after size standardization, shown as the first three axes of a principal components analysis of aperture shapes. Points are individual specimens with genera designated by shape and convex hull color. Hypothetical reconstructions of aperture shapes at regular intervals of the occupied morphospace are shown in the background.

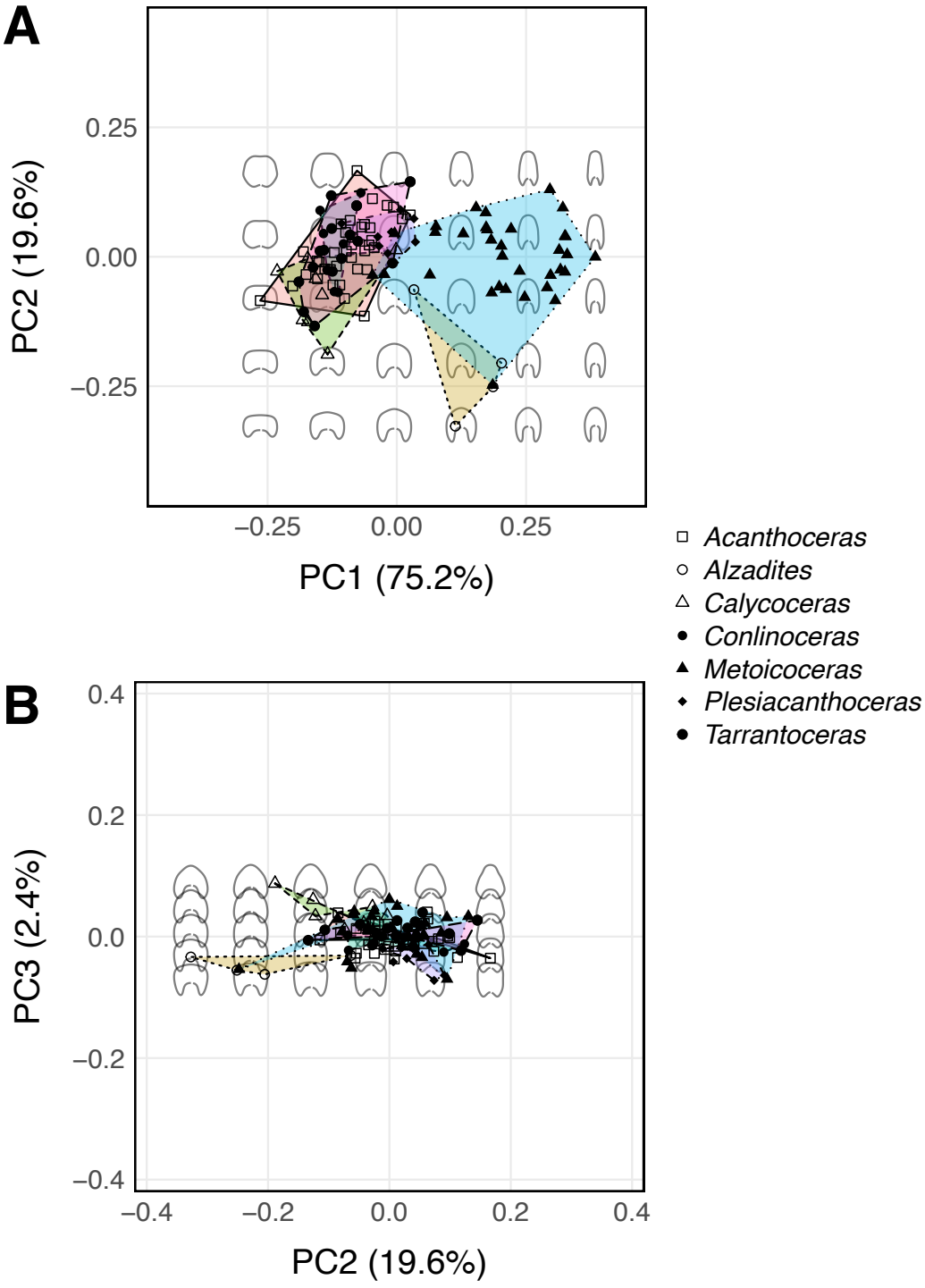

Figure 2.6: Intraspecific shape change with latitude for species with greater than five specimens. Shape is measured as scores along the first two principal components axes. Gray shading indicates 95% confidence interval around the regression line. Reported coefficients and support values are estimated using multivariate linear regression.

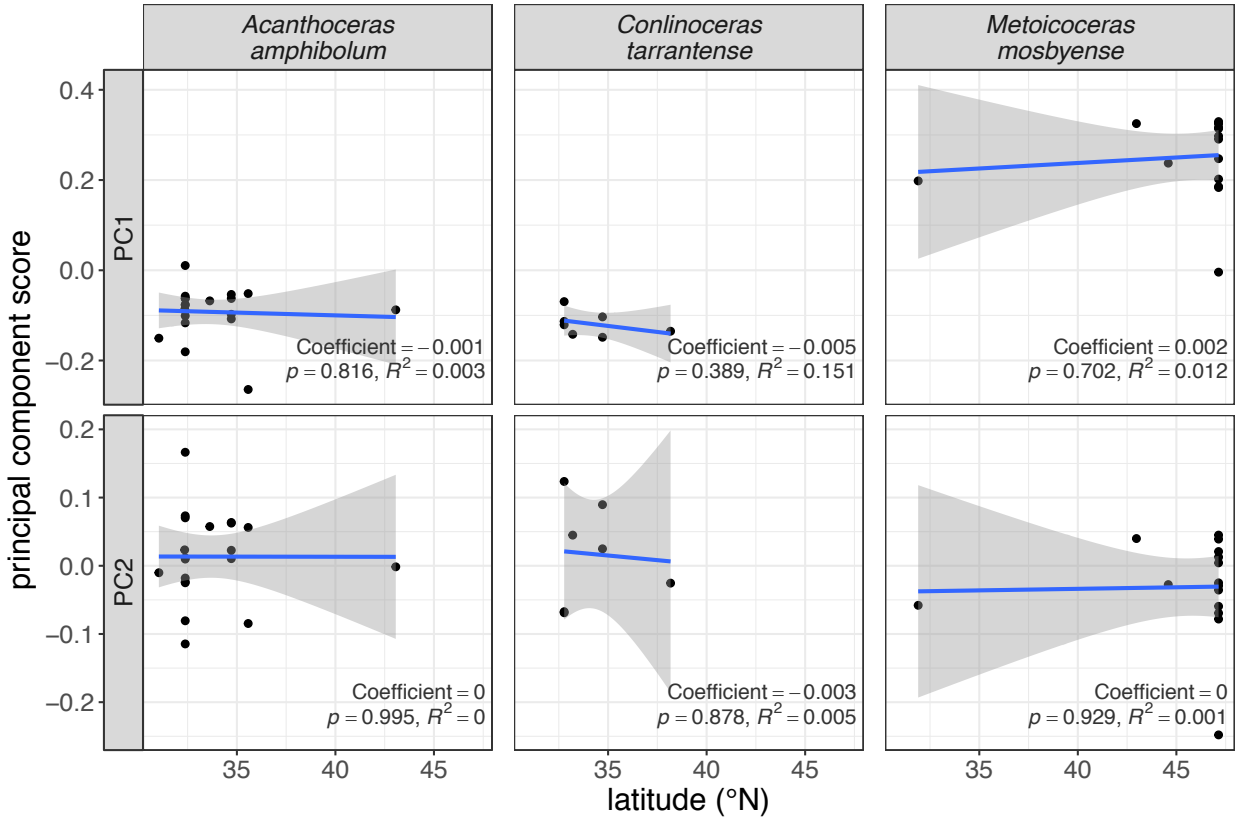

Figure 2.7: Subsets of the ammonite morphospace showing genera with both species that can be found in the WIS and not. Symbols designate biogeographic status ("in" and "out" of seaway) and convex hulls around points of common status are outlined. Colors are used to distinguish individual species. Gray dashed line indicates the decision boundary between "in" and "out" groups as determined using linear discriminant analyses. Gray outlines show shape changes between extremes of each axis.

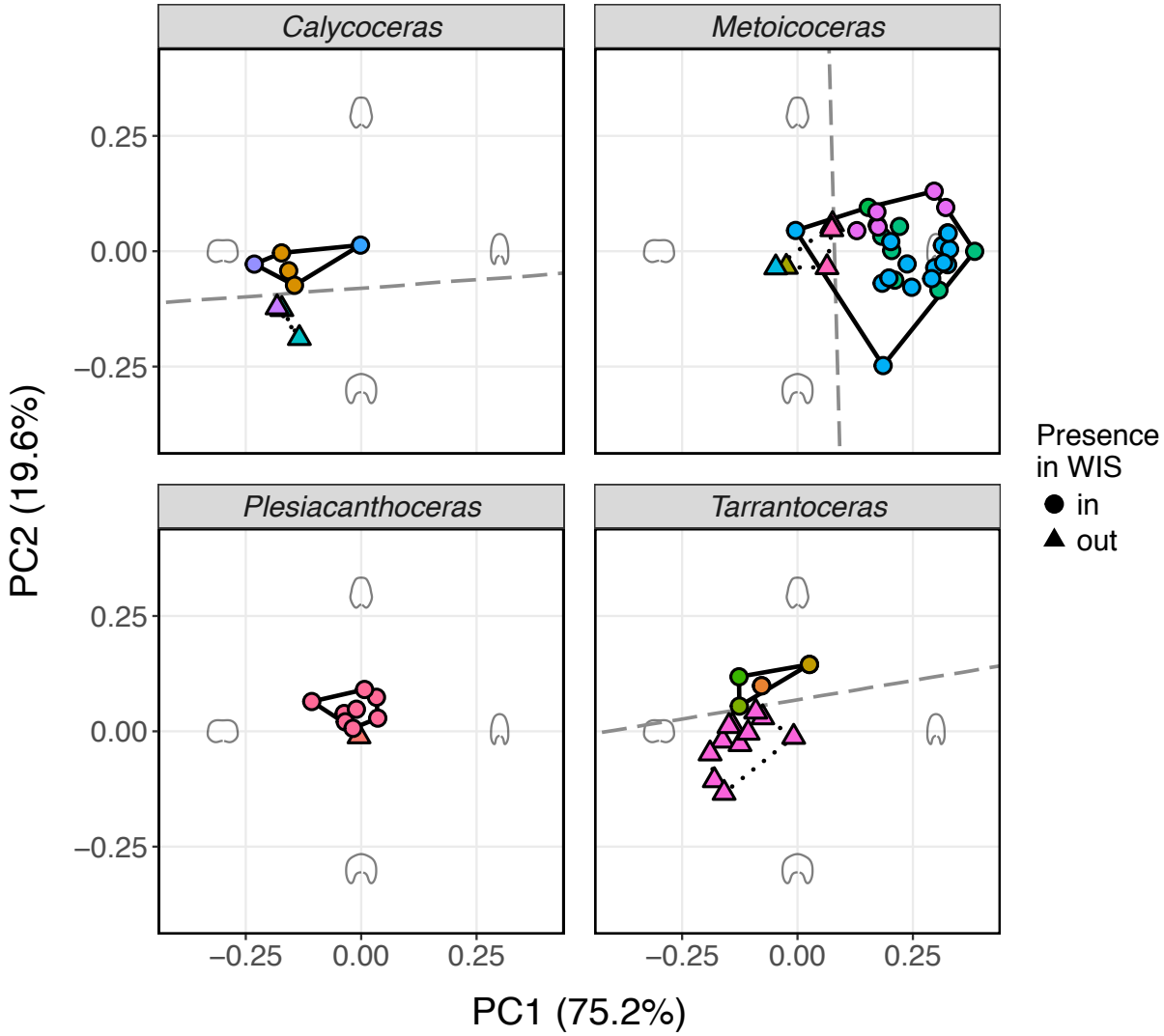

Table 2.1: Taxa included in this study. WIS status denotes whether the taxon occurred in the Western Interior Seaway ("in") or not ("out"). Parentheses indicate genus totals. Latitudinal ranges represented by the sample specimens are calculated using the centroids of the collection counties for each specimen. A complete list of specimens can be found in Appendix B.1.

species	*n* specimens	latitudinal range (º)	*n* occurrences	WIS status
Acanthoceras (NEUMAYR)	(37)		(136)	
amphibolum (MORROW)	20	12.02	78	in
bellense (ADKINS)	9	0	26	in
muldoonense (COBBAN AND SCOTT)	8	0	32	in
Alzadites (KENNEDY AND COBBAN)	(4)		(6)	
alzadensis (KENNEDY AND COBBAN)	4	0	6	in
Calycoceras (HYATT)	(8)		(137)	
canitaurinum (HAAS)	3	2.82	71	in
guerangeri (SPATH)	1		3	out
inflatum (COBBAN, HOOK, AND KENNEDY)	1		3	out
naviculare (MANTELL)	1		47	in
newboldi (KOSSMAT)	1		3	in
obrieni (YOUNG)	1		10	out
Conlinoceras (COBBAN AND SCOTT)	(7)		(41)	
tarrantense (ADKINS)	7	5.40	41	in
Metoicoceras (HYATT)	(33)		(247)	
crassicostae (STEPHENSON)	1		1	out
frontierense (COBBAN)	1		31	in
geslinianum (D'ORBIGNY)	7	0.38	84	in
latoventer (STEPHENSON)	1		31	out
mosbyense (COBBAN)	15	15.24	56	in
praecox (HAAS)	5	0	38	in
swallovi (SHUMARD)	3	0	6	out
Plesiacanthoceras (HAAS)	(9)		(42)	
bellsanum (STEPHENSON)	1		8	out
wyomingense (REAGAN)	8	0	34	in
Tarrantoceras (STEPHENSON)	(17)		(89)	
bentonianum (CRAGIN)	2	0.58	13	in
conlini (WRIGHT AND KENNEDY)	2	0	12	in
cuspidum (STEPHENSON)	1		10	in
exile (KENNEDY AND COBBAN)	1		1	in
sellardsi (ADKINS)	11	3.31	53	out

Table 2.2: Results of one-way MANOVA (Pillai's trace) for differences in morphospace occupation between species that occupied the WIS and those that did not for three genera. Morphospace occupation refers to scores along first two principal component axes after size standardization of aperture shapes as predictors. *Plesiacanthoceras*, shown in Figure 2.7, was excluded due to low sample size.

genus	predictor	Df	Pillai	approx F	Pr(>F)
Calycoceras	WIS status	1	0.785	9.111	0.022
	Residuals	6			
Metoicoceras	WIS status	1	0.48	13.847	< 0.005
	Residuals	31			
Tarrantoceras	WIS status	1	0.667	14.005	< 0.005
	Residuals	15			

Table 2.3: Results from linear discriminant function analyses species that occupied the WIS and those that did not for three genera. Accuracy is given as the sum of the diagonal of the confusion matrix when predicting all points divided by its total. *Plesiacanthoceras*, shown in Figure 2.7, was excluded due to low sample size.

genus	axis	LD scaled coefficient	group means		accuracy
			in	out	
Calycoceras	PC1	2.142	-0.141	-0.163	1
	PC2	-29.198	-0.027	-0.145	1
Metoicoceras	PC1	-12.319	0.239	0.029	0.782
	PC2	-0.328	0.001	0	0.782
Tarrantoceras	PC1	3.797	-0.059	-0.126	0.917
	PC2	-22.749	0.11	-0.023	0.917

Chapter 3

Testing Darwin's naturalization hypothesis using ongoing colonization of the San Joaquin Basin, California, during the late Cenozoic

Introduction

Understanding what determines the success or failure of non-native species to become established and thrive in new habitats is crucial for informing conservation efforts in a rapidly changing global environment. Active debate surrounds the role that evolutionary relatedness between colonizers and members of the native community may play in determining colonization success. One hypothesis, referred to as Darwin's naturalization hypothesis (Darwin 1859), posits that colonizers are less likely to become established in novel environments the more closely related they are to the native taxa. This is because closer relatives are more likely to be ecologically similar, intensifying the negative effects of competition. Alternatively, it has been suggested that the presence of closely related taxa in a new environment is in an indication of existing favorable conditions for the colonizer and thus colonization is more likely to succeed (Darwin 1859).

Advances in phylogenetic methods have allowed for large-scale analyses capable of incorporating measures of relatedness into tests of the tradeoff described above. Specifically, phylogenetic distance can serve as a proxy for ecological similarity, based on the assumption that functional traits tend to be phylogenetically conserved (Wiens and Graham 2005), although this may not always be the case (Losos 2008). Despite the increased focus on using phylogenetic relatedness to predict colonization success and subsequent ecosystem impact, there is no sign of a consensus favoring one hypothesis over the other. Previous studies have found invasion success associated with both distantly related invaders (Strauss et al. 2005, Schaefer et al. 2011, Park and Potter 2013) and closely related invaders (Duncan and Williams 2002, Li et al. 2015), leading to a question of how the spatial and temporal scale of the study as well as the observed stage of invasion affect the ability to detect competitive interactions and the influence of relatedness on these events (Procheş et al. 2007, Thuiller et al. 2010, Ma et al. 2016).

Most invasion biology studies have focused on the impacts of human-mediated introductions, which are limited to historic documentation and thus capture only short-term impacts of invasion and only successful invasions (see Zenni and Nuñez 2013). In contrast, the fossil record is capable not only of providing evidence that documents the complete aftermath of colonization events but also of establishing regional source pools of successful and unsuccessful colonizers, all in entirely natural systems. Furthermore, the abundance and high preservation potential of some morphologically conservative groups, such as mollusks, allows for Recent fossil taxa to be associated with extant taxonomic units. This opens up the possibility of incorporating prehistoric immigration, extirpation, and consequent evolutionary and ecosystem responses using explicit phylogenetic hypotheses (Fritz et al. 2013). Very few studies, however, have attempted to test Darwin's hypotheses in marine systems, and those that have relied on trait and invasiveness correlations in a non-phylogenetic framework (e.g., Azzurro et al. 2014). Marine systems, in general, have garnered less attention than terrestrial and freshwater systems in terms of generating large-scale phylogenetic and biogeographic datasets. Additionally, testing

naturalization hypothesis require a discretely defined geographic scope. While islands (e.g., Schaefer et al. 2011, Marx et al. 2016) or plots of land (e.g., Lim et al. 2014) have been common units in non-marine systems, identification of tractable marine analogs can be difficult.

This study takes advantage of sequential colonization from the Pacific Ocean into the flooded San Joaquin Basin (SJB), a restricted embayment that persisted for approximately 24.5 million years in the late Cenozoic in what is now part of the southern half of California's Central Valley. Covering a large geographic extent (175 km long by 100 km wide), the SJB had limited faunal and hydrological exchange with the adjacent open marine environment through a restricted opening, which was largely controlled eustatic sea level cycles, subsidence and infill of the basin, and the geographic consequences of seismic activity stemming from the bounding San Andreas Fault (Bartow 1991, Bowersox 2005). Paleoenvironmental studies reconstruct a number of freshwater sources entering the system from the surrounding uplifted ranges (Stanton and Dodd 1970) and indicate the SJB had generally brackish waters. Southward shifting ranges down the North American Pacific coast as a result of global climatic cooling provided new marine fauna access to the protected embayment of the SJB (Hall 2002). While this system has been the subject of faunal analyses, including well-characterized periodic episodes of regional extinction caused by environmental forcing (Bowersox 2005), little has been done to characterize determinants of colonization success in the basin and no treatment of this system has been done within a phylogenetic framework.

Here, I constructed a large phylogeny for Bivalvia representing several hundred extant genera using publicly available sequences. I then used this phylogeny to test Darwin's naturalization hypothesis, specifically whether colonization of new habitats is non-random with respect to the degree of relatedness to native fauna, in the late Cenozoic marine bivalve fossil record of the San Joaquin Basin and western coast of North America.

Methods

Phylogeny estimation

To assess the relationships among bivalve genera, I accessed available sequence data from GenBank (https://www.ncbi.nlm.nih.gov/) matching 335 bivalve genera for six loci: two mitochondrial ribosomal sub-units (12S and 16S), two nuclear ribosomal sub-units (18S and 28S), mitochondrial cytochrome c oxidase subunit I (COI), and one nuclear protein-encoding gene (histone H3). Up to thirty sequences of each locus were downloaded per genus and the longest sequence was retained for alignment regardless of species assignment (Appendix C.1). All loci were aligned individually using MUSCLE (v3.7, Edgar 2004) with non-overlapping regions trimmed to minimize the amount of missing data. The percentage of total missing data in the aligned sequences was approximately 76%.

Sequences belonging to members of the same genus were then concatenated after alignment (7,924 bp). This taxonomic sampling strategy increases the chance that a taxon is represented by more than one gene but assumes that combined species are monophyletic. However, because it is not uncommon for bivalve genera be rendered paraphyletic in molecular phylogenies with intrageneric sampling, I examined a number of species-level phylogenies published between

2000 and 2014 for instances of genus paraphyly (Appendix C.2). If monophyly was unsupported in an examined study, species in that genus were assigned to sub-groups so that no tip in the constructed phylogeny represented a known paraphyletic group. A paraphyletic genus is therefore represented in the final tree by multiple tips (e.g., "*Ctena* 1" and "*Ctena* 2").

An unconstrained maximum likelihood (ML) analysis of the concatenated sequences was conducted using RAxML (v8.2.9, Stamatakis 2014) using default settings as implemented in the CIPRES gateway (Miller et al. 2010). Node support was determined using 1,000 bootstrap replicates. Topological congruence with previously published species-level phylogenies was assessed using the normalized Robinson-Foulds distance (Robinson and Foulds 1981). The tree was rooted using the divergence between taxa of the subclass Protobranchia and remaining crown group Bivalvia, a placement supported by numerous molecular and morphological studies (Sharma et al. 2012, Bieler et al. 2014, González et al. 2015).

Divergence times were estimated for the resulting likelihood tree with a strict clock model using penalized likelihood (Sanderson 2002) as implemented in the R package ape (v4.1, Paradis et al. 2004). Ten fossil calibration points were used to constrain divergence times following Bieler et al. (2014). Uncertainty in fossil ages was incorporated through normally distributed priors on the minimum age for the following nodes: (1) A minimum age spanning 520.5-530 Myr for crown group Bivalvia based on the earliest reported crown group bivalve, *Fordilla troyensis* Barrande, 1881, from Tommotian (Pojeta et al. 1973, Parkhaev 2008). (2) A minimum age spanning 478.6-488.3 Myr for Anomalodesmata based on the report of *Ucumaris conradoi* Sánchez & Vaccari, 2003 from the Tremadocian (Sánchez and Vaccari 2003). (3) A minimum age spanning 471.8-488.6 Myr for Arcida based on the report of *Glyptarca serrata* Cope, 1996 from the Arenigian (Cope 1997). (4) A minimum age spanning 204-228 Myr for Cardiidae based on the report of *Tulongocardium nequam* Healey, 1908 from the Norian (Schneider 1995). (5) A minimum age spanning 112-125 Myr for Mactroidea based on the report of *Nelltia elliptica* Whitfield, 1891 from the Aptian (Saul 1973). (6) A minimum age spanning 197-201.6 Myr for Nucinellidae based on the report of *Nucinella liasina* Bistram, 1903 from the Hettangian (Conti 1954). (7) A minimum age spanning 237-245 Myr for Ostreoidea based on the Muschelkalk of Germany from the Anisian (Hautmann and Hagdorn 2013). (8) A minimum age spanning 471-478 Myr for Palaeoheterodonta based on the early Ordovician genus *Noradonta* Pojeta & Gilbert-Tomlinson, 1977 from the Arenigian (Cope 2000). (9) A conservative minimum age spanning 476-488.4 Myr for Pterida based on the Ordovician genus *Pterinea* Goldfuss, 1826 (Bassler 1915). (10) A minimum age spanning 197-201.6 Myr for Tellinoidea based on the report of *Tancredia securiformis* Dunker, 1846 from the Hettangian (Dunker 1846).

Phylogenetic relatedness and colonization of the San Joaquin Basin

To test for phylogenetic patterns in historic colonization events, range data for marine invertebrates along the Californian coast from the late Oligocene (27 Ma) to the late Pliocene (2.5 Ma) were obtained from Hall (2002). The Hall (2002) dataset provides species presences for mollusks binned temporally into six time bins (27-23, 23-17, 17-13, 13-8, 8-5, and 5-2.5 Ma) and spatially into east or west of the San Andreas Fault, where a designation of east of the San Andreas Fault indicates presence in the SJB. Presences are further binned into one-degree latitudinal bins spanning the modern 27-43º latitude north. The taxonomic treatment used by

Hall (2002) was updated to account for currently synonymized genera. Species of paraphyletic genera, as determined during the steps leading to phylogeny estimation, were assigned to genus groupings if possible. Those that could not be explicitly assigned to an existing genus group were disregarded. Taxa were then assigned one of three states in each time bin: present only outside of the SJB (non-colonizing), newly present in the SJB after having not been in the previous time bin (colonizing), or persistent in the SJB since the last time bin (native). Because I was unable to identify, using this dataset, which taxa are newly colonizing in the first time bin, it was excluded from further analyses.

For each time bin, the dated ML tree was reduced to include only taxa present in the Hall (2002) dataset during that interval. Terminal branches were truncated so as not to extend past the ending age of each bin, providing more accurate estimations of contemporaneous phylogenetic distances. The phylogenetic relatedness between a colonizing taxon and the native fauna was then quantified using two metrics: the mean phylogenetic distance (MPD) of a colonizer to each native taxon and the phylogenetic distance of a colonizer to its nearest native taxon (PNND). While MPD provides a measure of relatedness to the receiving community as a whole, PNND captures potential effects of close relatives.

To test whether colonizers were more or less closely related to native fauna than expected by chance, I simulated random colonization by sampling the non-native (i.e., colonizer and non-colonizer) taxa in each time bin equivalent to the number of colonizers observed, giving each potential colonizer equal chance of inclusion. The randomization approach allows for incorporation of information known about the regional taxon pool, including non-colonizing genera. I then calculated the mean MPD and PNND of the simulated assemblage and repeated this process 1,000 times, generating distributions of mean values for colonizers given the null model of random assembly. I then measured the standardized effect score (SES or z-score), which is the difference between the observed mean and the null mean for MPD and PNND divided by the standard deviation of the null distributions. Negative SES scores indicate overall closer relatedness of colonizers to the native fauna than expected from random, while positive scores indicate colonizers are less closely related to the native fauna than expected from random assembly. The null distributions themselves reflect the overall relatedness of the non-SJB fauna to the SJB fauna. Significance of the SES was assessed by calculating *p*-values from the proportion of simulated means that were as or more extreme than the observed mean for each metric and adjusting the significance level using the Bonferroni correction. To assess the impact of including co-colonizers as members of the native fauna, I repeated the above procedure including other colonizing fauna into the calculations of MPD and PNND. In effect, differences between the two treatments - including and excluding colonizers in calculations of relatedness metrics - reflect how closely related colonizers were to one another. Differences between the colonizing and non-colonizing fauna in the regional source pool were more explicitly tested for using Student's t-Test.

Unless otherwise noted, all analyses were conducted in the R programming environment (v3.4.0, R Core Team 2016). Tree manipulations were implemented in the R package ape (v4.1, Paradis et al. 2004).

Results

Bivalve phylogeny

The ML analysis and divergence time estimation using the six concatenated loci resulted in a time-calibrated phylogeny representing 335 bivalve genera on 388 tips (*ln*L = -1037798) (Figure 3.1). Due to the high proportion of missing data, bootstrap node support varied drastically across the tree (Appendix C.3). Despite this, the monophyly of major subclasses of Bivalvia were recovered. The relationships between the major subclasses reflects those that González et al. (2015) obtained using a phylogenomic (RNA-Seq) approach and including 34 genera, where Achiheterodonta is sister to a clade formed by Anomalodesmata and Imparidentia. The relationship between Palaeoheterodonta and these clades, particularly Archiheterodonta, has historically been a point of contention (see Sharma et al. 2012). In the ML tree produced here, Palaeoheterdonta is sister to the clade formed by Archiheterodonta, Anomalodesmata, and Imparidentia, similar to the findings of González et al. (2015). The normalized Robinson-Foulds distance between the González et al. (2015) tree and this tree is 0.31 out of 1, where 0 indicates complete topological congruence, suggesting some inconsistencies in taxon placement within subclasses but largely congruent topologies.

Phylogenetic patterns of colonization

Of the 211 bivalve genera documented in Hall (2002), 198 genera are still extant, and of those, 89 genera are represented in the ML tree (Figure 3.2). Despite fluctuations in overall genus richness, representation of fossil taxa in the bivalve phylogeny is consistent across time bins and between the SJB and open marine communities with 50-65% of genera represented in each case (Figure 3.3). Though no true extinction is captured given the use of a phylogeny containing only extant taxa, frequent extirpations in the SJB introduced variation to the composition of the native fauna over time.

The overall relatedness of the fauna outside of the SJB to native fauna appears temporally stable, with no drastic shifts in relatedness with turnover, as indicated by the large degree of overlap in null distributions over time (Figure 3.4). One departure from this is the apparent leftward shift of the expected means of PNND when considering native-only taxa from 23-17 Ma to 13-8 Ma. The leftward shift suggests that the relatedness between fauna inside and outside the SJB is increasing, regardless of observed colonizers. In other words, with each passing time bin, the regional source pool contained proportionally more taxa with existing close relatives within the SJB than in the previous time bin. This pattern counters the expectation that extension of terminal branch lengths over time given the addition of new time bins would consistently increase relatedness metrics.

This peak increase in overall relatedness between potential colonizers and their nearest native taxa coincides with a low observed PNND value. However, after Bonferroni correction was applied ($p \leq 0.0025$), I did not find any observed mean relatedness metrics to be significantly different from expected given random assembly. In cases where the probability of a more extreme value than that observed was low (less than 0.05), effect sizes tended to be negative. Similarly, logistic models predicting colonization status using non-colonizing and colonizing

MPD and PNND values recovered coefficients statistically indistinguishable from zero across all intervals following Bonferroni correction (Figure 3.5).

Unsurprisingly, the inclusion of colonizing taxa as part of the native fauna during calculation of relatedness metrics generally decreased both expected and observed values by virtue of filling in the tree (Figure 3.4). This overall had little effect on the direction and significance of observed values with respect to the null expectation. Additionally, despite the intention of reflecting somewhat similar ecological processes, the two metrics for phylogenetic relatedness appear decoupled in overall trajectory and in discriminatory strength over time (Figure 3.5). This pattern would be difficult to detect without the temporal context provided by the fossil record but suggests fundamental differences in the mechanisms driving changes in the two metrics of relatedness.

Discussion

I find little evidence in support of Darwin's naturalization hypothesis as a consistent rule during colonization events of the late Cenozoic San Joaquin Basin. Observed values of MPD and PNND are statistically indistinguishable from values obtained through random assembly from the regional source pool. However, the findings presented here tentatively suggest that successful colonizers were more closely related to the native fauna both when compared to randomly assembled taxa from the regional source pool. This presence of overall negative effect sizes is not significant nor is it consistent through time. Given the resolution of the time bins used in this study, colonization is likely not coincident across taxa. Thus, co-colonizers may play as much of a role in the process of naturalization within the SJB community as those strictly defined here as native taxa, highlighting the need to develop a better resolved temporal sequence of colonization in this system.

Though the majority of reported bivalve genera from the Hall (2002) dataset were represented on the phylogeny in any given time bin, this approach in its current state captured only a portion of the bivalve fauna known in the ecosystem. While the relationships and measures of relatedness between currently represented genera would not change with increased coverage, these metrics are meant to reflect the impact of specific relationships given the whole community on the likelihood of establishment. Thus, increasing the proportion of coverage should be a top priority and a promising one given that nearly all bivalve genera in Hall (2002) are extant (94%). It should be noted that use of an extant-only phylogeny in this study is adequate only because of the high proportion of fossil genera that are still extant. Use of an extant-only phylogeny in scenarios where the group has undergone substantial extinction would fail to recover a meaningful representation the co-occurring taxa.

The incorporation of deep time perspective is hampered by the difficulties reconciling fossil and modern data in phylogenetic analyses. Inclusion of fossils, however, has been shown to dramatically alter inferences of evolutionary and biogeographic histories (Slater et al. 2012, Wood et al. 2013). Efforts to build large-scale phylogenies for diverse group or for the entire tree of life have employed a variety of methods, including construction and analysis of a supermatrices containing genetic and/or morphological data (e.g., Jetz et al. 2012) or systematic merging of topologies generated through multiple focused analyses into a supertree (e.g., Davies

et al. 2014) or some combination of the both. Continuing development of these methods can hopefully succeed in integrating disparate sources of data for applications at all timescales. For example, because genus continuity in the SJB from the previous time bin was used to designate native fauna, the effects of limiting similarity between congeneric species is obscured. This is a true shortfall of the current approach and is best remedied by using a robust species-level tree including several hundred fossil and modern taxa.

The lack of consensus in whether Darwin's naturalization hypothesis is generalizable has often been attributed to two outstanding issues: first, the use of different temporal, phylogenetic, and spatial scales examined and, second, the underlying assumption that phylogenetic relatedness is a direct proxy of ecological similarity. Meta-analyses of invasion studies have found that the frequency at which a phylogenetic signal can be detected, and the direction of that relationship, is subject to the spatial scale used (e.g., Procheş et al. 2007, Thuiller et al. 2010, Ma et al. 2016). Other meta-analyses have found that the impact of relatedness is more detectable at larger spatial scales than smaller ones (Gallien and Carboni 2016).

The relationship between phylogenetic relatedness and functional similarity is a complex one requiring careful consideration on a case-by-case basis (Losos 2008). The inclusion of trait data provides valuable additional information to both measure the degree of functional overlap represented by phylogenetic relatedness and also potentially help explain ecological patterns of invasion potential not captured through relatedness metrics (Thuiller et al. 2010, Schaefer et al. 2011, Marx et al. 2016). For example, larger body sizes in marine bivalves has been linked to increased invasion success (Roy et al. 2002). Even if traits are phylogenetically conserved, inclusion of such information in addition to phylogenetic relatedness may improve future models of invasion.

Conclusions

Tests of Darwin's naturalization hypothesis in modern systems have returned mixed findings. Because of the richness of the molluscan fossil record, especially towards the Recent, there is clear potential for the application of phylogenetic methods towards understanding the evolutionary and environmental processes that have built up and torn down marine ecosystems leading to the present-day state. I find that colonizers of the late Cenozoic San Joaquin Basin from the Pacific Ocean are not significantly more or less closely related to native taxa than expected if randomly assembled from the source pool, though findings tentatively suggest successful colonizers may be more closely related to native taxa during some periods of time. This study demonstrates how modern phylogenetic and ecological theory may be applied to and benefit from fossil systems as well as the complexity of factors the affecting the success of invasion events.

Acknowledgments

I would like to thank Phillip Skipwith for his generous help with constructing the phylogeny used in this analysis.

References

Azzurro, E., Tuset, V.M., Lombarte, A., Maynou, F., Simberloff, D., Rodríguez-Pérez, A., and Solé, R.V. 2014. External morphology explains the success of biological invasions. Ecology Letters 17(11): 1455-1463.

Bartow, J.A. 1991. The Cenozoic evolution of the San Joaquin Valley, California. United States Geological Survey Professional Paper 1501.

Barucca, M., Olmo, E., Schiaparelli, S., and Canapa, A. 2004. Molecular phylogeny of the family Pectinidae (Mollusca: Bivalvia) based on mitochondrial 16S and 12S rRNA genes. Molecular Phylogenetics and Evolution 31(1): 89-95.

Bassler, R.S. 1915. Bibliographic index of American Ordovician and Silurian fossils, volume 2. United States National Museum Bulletin 92: 719-1521.

Bieler, R., Mikkelsen, P.M., Collins, T.M., Glover, E.A., González, V.L., Graf, D.L., Harper, E.M., Healy, J., Kawauchi, G.Y., Sharma, P.P., and Staubach, S. 2014. Investigating the Bivalve Tree of Life – an exemplar-based approach combining molecular and novel morphological characters. Invertebrate Systematics 28(1): 32-115.

Bowersox, J.R. 2005. Reassessment of extinction patterns of Pliocene molluscs from California and environmental forcing of extinction in the San Joaquin Basin. Palaeogeography, Palaeoclimatology, Palaeoecology 221(1): 55-82.

Conti, S. 1954. Stratigrafi e paleontologia della Val Solda (Lago di Lugano). Memorie Descrittive della Carta Geologica d'Italia 30: 1-248.

Cope, J.C. 1997. The early phylogeny of the class Bivalvia. Palaeontology 40: 713-746.

Cope, J.C. 2000. A new look at early bivalve phylogeny. Pp. 81-95 in Harper, E.M., Taylor, J.D., and Crame, J.A. eds. The Evolutionary Biology of the Bivalvia. Geological Society, London, Special Publications 177.

Davies, T.J., Barraclough, T.G., Chase, M.W., Soltis, P.S., Soltis, D.E., and Savolainen, V. 2004. Darwin's abominable mystery: insights from a supertree of the angiosperms. Proceedings of the National Academy of Sciences 101(7): 1904-1909.

Dunker, W. 1846. Ueber die in dem Lias bei Halberstadt vorkommenden Versteinerungen. Palaeontographica 1: 34-41.

Edgar, R.C. 2004. MUSCLE: multiple sequence alignment with high accuracy and high throughput. Nucleic Acids Research 32(5): 1792-1797.

Hall, Jr., C.A. 2002. Nearshore marine paleoclimatic regions, increasing zoogeographic provinciality, molluscan extinctions, and paleoshorelines, California: Late Oligocene (27 Ma) to late Pliocene (2.5 Ma). Geological Society of America Special Papers 357: 1-489.

Darwin, C. 1859. On the origins of species by means of natural selection. Murray, London.

Duncan, R.P. and Williams, P.A. 2002. Ecology: Darwin's naturalization hypothesis challenged. Nature 417(6889): 608-609.

Fritz, S.A., Schnitzler, J., Eronen, J.T., Hof, C., Böhning-Gaese, K., and Graham, C.H. 2013. Diversity in time and space: wanted dead and alive. Trends in Ecology and Evolution, 28(9): 509-516.

Gallien, L. and Carboni, M. 2017. The community ecology of invasive species: where are we and what's next? Ecography 40(2): 335-352.

Giribet, G. and Distel, D.L. 2003. Bivalve phylogeny and molecular data. Pp. 45-90 *in* Lydeard, C. and Lindberg, D.R. eds. Molecular Systematics and Phylogeography of Mollusks. Smithsonian Books, Washington, D.C.

Giribet, G. and Wheeler, W. 2002. On bivalve phylogeny: a high-level analysis of the Bivalvia (Mollusca) based on combined morphology and DNA sequence data. Invertebrate Biology 121(4): 271-324.
González, V.L., Andrade, S.C., Bieler, R., Collins, T.M., Dunn, C.W., Mikkelsen, P.M., Taylor, J.D., and Giribet, G. 2015. A phylogenetic backbone for Bivalvia: an RNA-seq approach. Proceedings of the Royal Society of London B 282: 20142332.
Goto, R., Kawakita, A., Ishikawa, H., Hamamura, Y., and Kato, M. 2012. Molecular phylogeny of the bivalve superfamily Galeommatoidea (Heterodonta, Veneroida) reveals dynamic evolution of symbiotic lifestyle and interphylum host switching. BMC Evolutionary Biology 12(1): 172.
Hautmann, M. and Hagdorn, H. 2013. Oysters and oyster-like bivalves from the Middle Triassic Muschelkalk of the Germanic Basin. Paläontologische Zeitschrift 87: 19-32.
Jetz, W., Thomas, G.H., Joy, J.B., Hartmann, K., and Mooers, A.O. 2012. The global diversity of birds in space and time. Nature 491(7424): 444-448.
Li, S.P., Cadotte, M.W., Meiners, S.J., Hua, Z.S., Shu, H.Y., Li, J.T., and Shu, W.S. 2015. The effects of phylogenetic relatedness on invasion success and impact: deconstructing Darwin's naturalisation conundrum. Ecology Letters 18(12):1285-1292.
Lim, J., Crawley, M.J., De Vere, N., Rich, T., and Savolainen, V. 2014. A phylogenetic analysis of the British flora sheds light on the evolutionary and ecological factors driving plant invasions. Ecology and Evolution 4(22): 4258-4269.
Losos, J.B. 2008. Phylogenetic niche conservatism, phylogenetic signal and the relationship between phylogenetic relatedness and ecological similarity among species. Ecology Letters 11(10): 995-1003.
Ma, C., Li, S.P., Pu, Z., Tan, J., Liu, M., Zhou, J., Li, H., and Jiang, L. 2016. Different effects of invader–native phylogenetic relatedness on invasion success and impact: a meta-analysis of Darwin's naturalization hypothesis. Proceedings of the Royal Society of London B 283: 20160663.
Marx, H.E., Giblin, D.E., Dunwiddie, P.W., and Tank, D.C. 2016. Deconstructing Darwin's Naturalization Conundrum in the San Juan Islands using community phylogenetics and functional traits. Diversity and Distributions 22(3): 318-331.
Matsumoto, M. 2003. Phylogenetic analysis of the subclass Pteriomorphia (Bivalvia) from mtDNA COI sequences. Molecular Phylogenetics and Evolution 27(3): 429-440.
Mikkelsen, P.M., Bieler, R., Kappner, I., and Rawlings, T.A. 2006. Phylogeny of Veneroidea (Mollusca: Bivalvia) based on morphology and molecules. Zoological Journal of the Linnean Society 148(3): 439-521.
Miller, M.A., Pfeiffer, W. and Schwartz, T. 2010. Creating the CIPRES Science Gateway for inference of large phylogenetic trees. Pp. 1-8 *in* Proceedings of the Gateway Computing Environments Workshop (GCE), 14 Nov. 2010, New Orleans, Louisiana.
Miyazaki, J.I., de Oliveira Martins, L., Fujita, Y., Matsumoto, H., and Fujiwara, Y. 2010. Evolutionary process of deep-sea *Bathymodiolus* mussels. PLoS one 5(4): e10363.
Paradis, E., Claude, J., and Strimmer, K. 2004. APE: analyses of phylogenetics and evolution in R language. Bioinformatics 20: 289-290.
Park, D.S. and Potter, D. 2013. A test of Darwin's naturalization hypothesis in the thistle tribe shows that close relatives make bad neighbors. Proceedings of the National Academy of Sciences 110(44): 17915-17920.

Parkhaev, P.Y. 2008. The Early Cambrian radiation of Mollusca. Pp. 33-69 *in* Ponder, W.F. and Lindberg, D.R. eds. Phylogeny and Evolution of the Mollusca. University of California Press, Berkeley, CA.
Plazzi, F., Ceregato, A., Taviani, M., and Passamonti, M. 2011. A molecular phylogeny of bivalve mollusks: ancient radiations and divergences as revealed by mitochondrial genes. PloS one 6(11): e27147.
Pojeta, Jr., J., Runnegar, B., and Kriz, J. 1973. *Fordilla troyensis* Barrande: the oldest known pelecypod. Science 180: 866-868
Procheş, Ş., Wilson, J.R., Richardson, D.M., and Rejmánek, M. 2008. Searching for phylogenetic pattern in biological invasions. Global Ecology and Biogeography 17(1): 5-10.
R Core Team. 2016. R: A language and environment for statistical computing. R Foundation for Statistical Computing, Vienna, Austria.
Robinson, D.F. and Foulds, L.R. 1981. Comparison of phylogenetic trees. Mathematical Biosciences 53: 131-147.
Roy, K., Jablonski, D., and Valentine, J.W. 2002. Body size and invasion success in marine bivalves. Ecology Letters 5(2): 163-167.
Sánchez, T.M. and Vaccari, N.E. 2003. Ucumariidae new family (Bivalvia, Anomalodesmata) and other bivalves from the Early Ordovician (Tremadocian) of northwestern Argentina. Ameghiniana 40(3): 415-424.
Sanderson, M.J. 2002. Estimating absolute rates of molecular evolution and divergence times: a penalized likelihood approach. Molecular Biology and Evolution 19(1): 101-109.
Saul, L.R. 1973. Evidence for the origin of the Mactridae (Bivalvia) in the Cretaceous. University of California Publications in Geological Sciences 97: 1-51.
Schaefer, H., Hardy, O.J., Silva, L., Barraclough, T.G., and Savolainen, V. 2011. Testing Darwin's naturalization hypothesis in the Azores. Ecology Letters 14(4): 389-396.
Schneider, J.A. 1995. Phylogeny of the Cardiidae (Mollusca, Bivalvia): Protocardiinae, Laevicardiinae, Lahilliinae, Tulongocardiinae subfam. n. and Pleuriocardiinae subfam. n. Zoologica Scripta 24(4): 321-346.
Sharma, P.P., González, V.L., Kawauchi, G.Y., Andrade, S.C., Guzmán, A., Collins, T.M., Glover, E.A., Harper, E.M., Healy, J.M., Mikkelsen, P.M., and Taylor, J.D. 2012. Phylogenetic analysis of four nuclear protein-encoding genes largely corroborates the traditional classification of Bivalvia (Mollusca). Molecular Phylogenetics and Evolution 65(1): 64-74.
Sharma, P.P., Zardus, J.D., Boyle, E.E., González, V.L., Jennings, R.M., McIntyre, E., Wheeler, W.C., Etter, R.J., & Giribet, G. 2013. Into the deep: A phylogenetic approach to the bivalve subclass Protobranchia. Molecular Phylogenetics and Evolution 69(1): 188-204.
Slater, G.J., Harmon, L.J., and Alfaro, M.E. 2012. Integrating fossils with molecular phylogenies improves inference of trait evolution. Evolution 66(12): 3931-3944.
Stamatakis, A. 2014. RAxML version 8: a tool for phylogenetic analysis and post-analysis of large phylogenies. Bioinformatics 30(9): 1312-1313.
Stanton, R.J. and Dodd, J.R. 1997. Lack of stasis in late Cenozoic marine faunas and communities, central California. Lethaia 30(3): 239-256.
Steiner, G. and Hammer, S. 2000. Molecular phylogeny of the Bivalvia inferred from 18S rDNA sequences with particular reference to the Pteriomorphia. Geological Society, London, Special Publications 177(1): 11-29.
Strauss, S.Y., Webb, C.O., and Salamin, N. 2006. Exotic taxa less related to native species are more invasive. Proceedings of the National Academy of Sciences 103(15): 5841-5845.

Taylor, J.D., Glover, E.A., Smith, L., Dyal, P., and Williams, S.T. 2011. Molecular phylogeny and classification of the chemosymbiotic bivalve family Lucinidae (Mollusca: Bivalvia). Zoological Journal of the Linnean Society 163(1): 15-49.
Taylor, J.D., Glover, E.A., and Williams, S.T. 2014. Diversification of chemosymbiotic bivalves: origins and relationships of deeper water Lucinidae. Biological Journal of the Linnean Society 111: 401–420.
Taylor, J.D., Williams, S.T., and Glover, E.A. 2007. Evolutionary relationships of the bivalve family Thyasiridae (Mollusca: Bivalvia), monophyly and superfamily status. Journal of the Marine Biological Association of the United Kingdom 87(2): 565-574.
Taylor, J.D., Williams, S.T., Glover, E.A., and Dyal, P. 2007. A molecular phylogeny of heterodont bivalves (Mollusca: Bivalvia: Heterodonta): new analyses of 18S and 28S rRNA genes. Zoologica Scripta 36(6): 587-606.
Tëmkin, I. 2010. Molecular phylogeny of pearl oysters and their relatives (Mollusca, Bivalvia, Pterioidea). BMC Evolutionary Biology 10(1): 342.
Thuiller, W., Gallien, L., Boulangeat, I., De Bello, F., Münkemüller, T., Roquet, C., and Lavergne, S. 2010. Resolving Darwin's naturalization conundrum: a quest for evidence. Diversity and Distributions 16(3): 461-475.
Tsubaki, R., Kameda, Y., and Kato, M. 2011. Pattern and process of diversification in an ecologically diverse epifaunal bivalve group Pterioidea (Pteriomorphia, Bivalvia). Molecular Phylogenetics and Evolution 58(1): 97-104.
Valdés, F., Sellanes, J., and D'Elia, G. 2012. Phylogenetic position of vesicomyid clams from a methane seep off central Chile (~36°S) with a molecular timescale for the diversification of the Vesicomyidae. Zoological Studies 51(7): 1154-1164.
Wiens, J.J. and Graham, C.H. 2005. Niche conservatism: integrating evolution, ecology, and conservation biology. Annual Review of Ecology, Evolution, and Systematics 36: 519-539.
Williams, S.T., Taylor, J.D., and Glover, E.A. 2004. Molecular phylogeny of the Lucinoidea (Bivalvia): non-monophyly and separate acquisition of bacterial chemosymbiosis. Journal of Molluscan Studies 70(2): 187-202.
Wood, H.M., Matzke, N.J., Gillespie, R.G., Griswold, C.E. 2013. Treating fossils as terminal taxa in divergence time estimation reveals ancient vicariance patterns in the Palpimanoidea spiders. Systematic Biology 62(2): 264-284.
Xu, K., Kanno, M., Yu, H., Li, Q., and Kijima, A. 2011. Complete mitochondrial DNA sequence and phylogenetic analysis of Zhikong scallop *Chlamys farreri* (Bivalvia: Pectinidae). Molecular Biology Reports 38(5): 3067-3074.
Zenni, R.D. and Nuñez, M.A. 2013. The elephant in the room: the role of failed invasions in understanding invasion biology. Oikos 122(6): 801-815.

Figure 3.1: Time-calibrated maximum-likelihood tree of Bivalvia based on concatenated sequences for six loci (12S, 16S, 18S, 28S, COI, and histone H3). Numbered nodes indicate fossil calibration points with labels corresponding to descriptions in the main text.

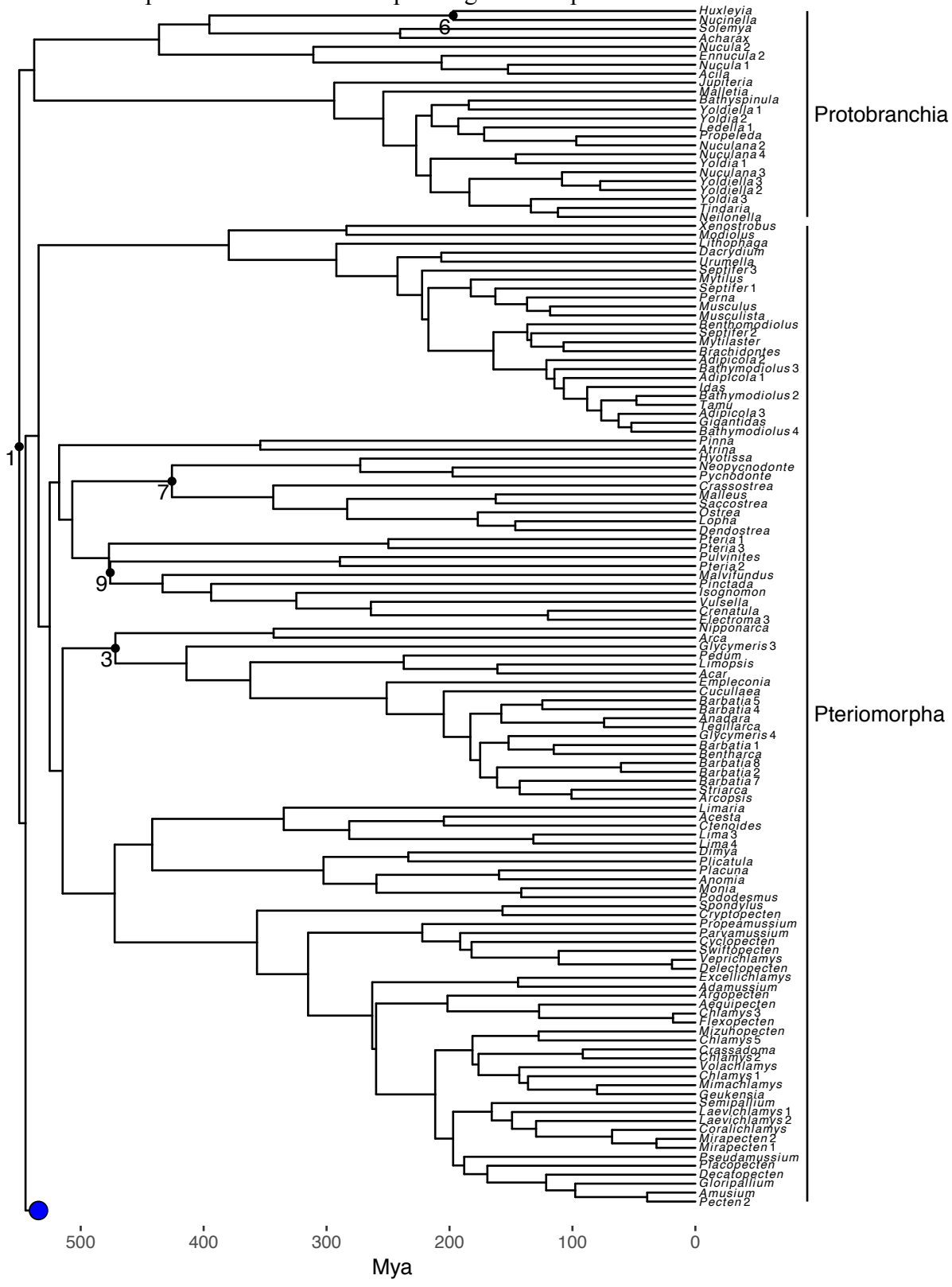

Figure 3.1: Phylogeny of Bivalvia (continued).

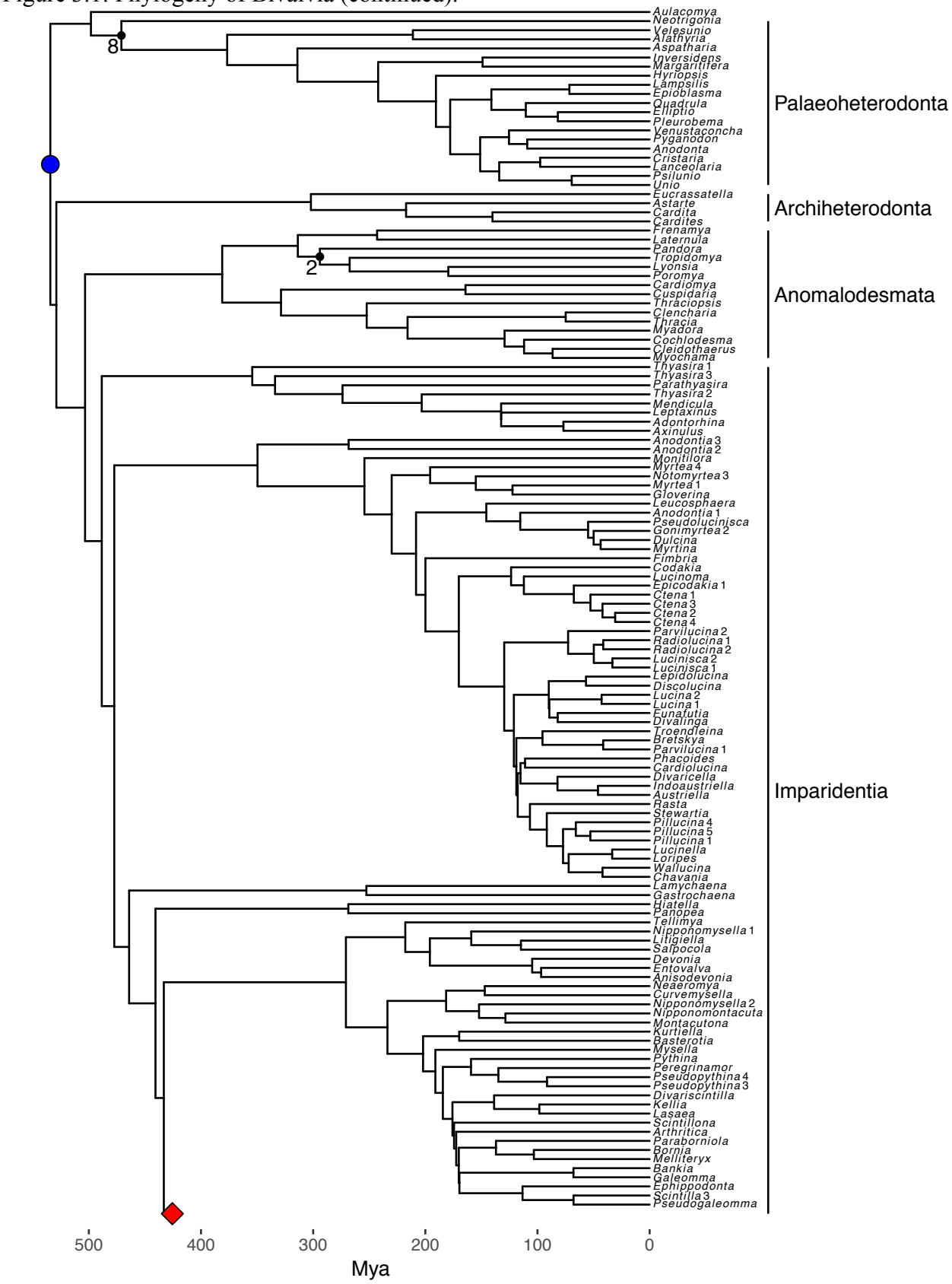

Figure 3.1: Phylogeny of Bivalvia (continued).

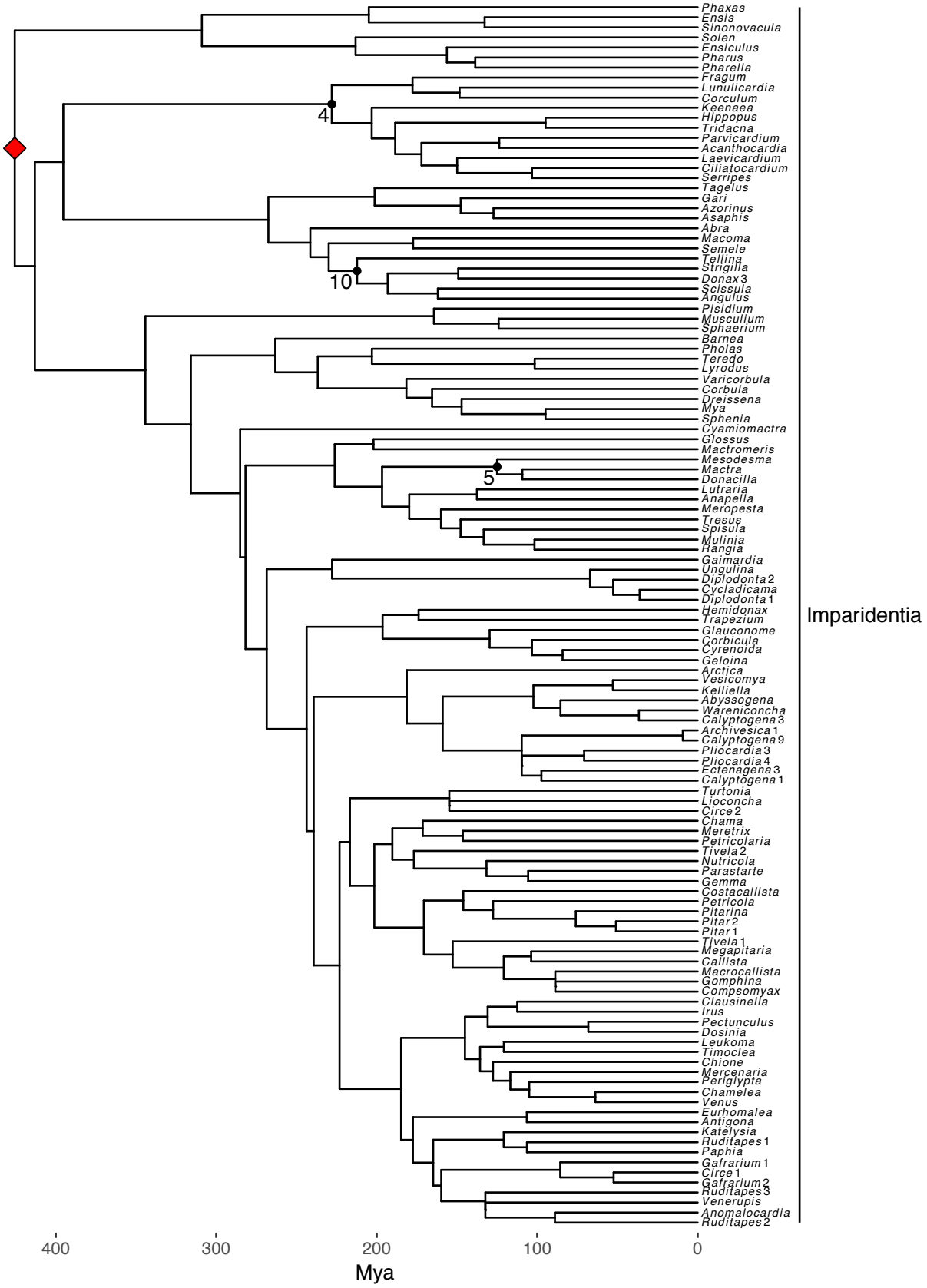

Figure 3.2: Subset of the dated bivalve phylogeny with taxa reported in Hall (2002). Colors indicate colonization status in the San Joaquin Basin of each taxon across six time bins. Blank spaces indicate no recorded presence of a taxon for that time interval.

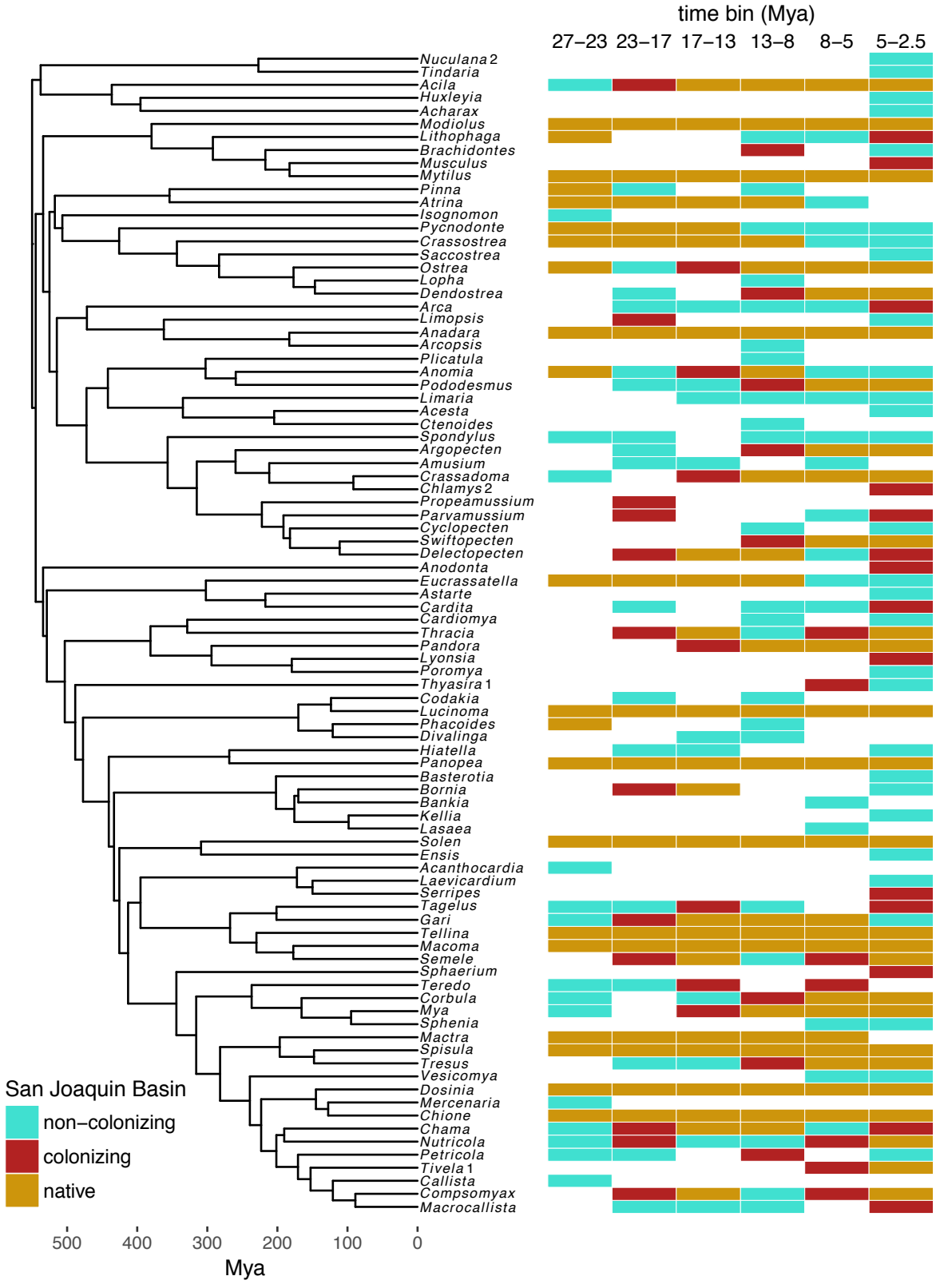

Figure 3.3: Bivalve genus richness over time of the San Joaquin Basin and nearby Pacific coast. Solid lines indicate richness calculated from the Hall (2002) dataset and dotted lines indicate the number of Hall (2002) taxa represented on the bivalve phylogeny. Note that some genera occur in both regions. Alternating gray and white shading indicate six late Cenozoic time bins defined by Hall (2002).

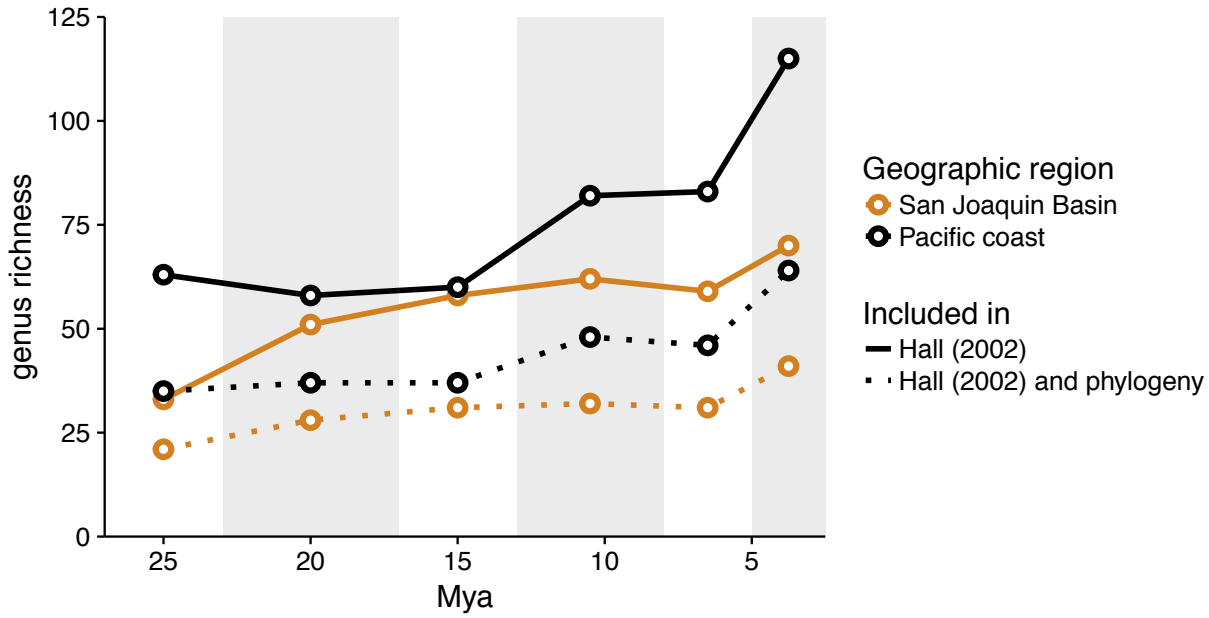

Figure 3.4: Null distributions showing mean values of mean phylogenetic distance (MPD) and phylogenetic nearest neighbor distance (PNND) given randomly selected colonizers from the regional taxon pool repeated 1,000 times. Vertical lines indicate observed values with standardized effect sizes (SES) and associated *p*-values shown. Colors indicate whether colonizers were treated as native fauna. Time bins are arranged from top to bottom.

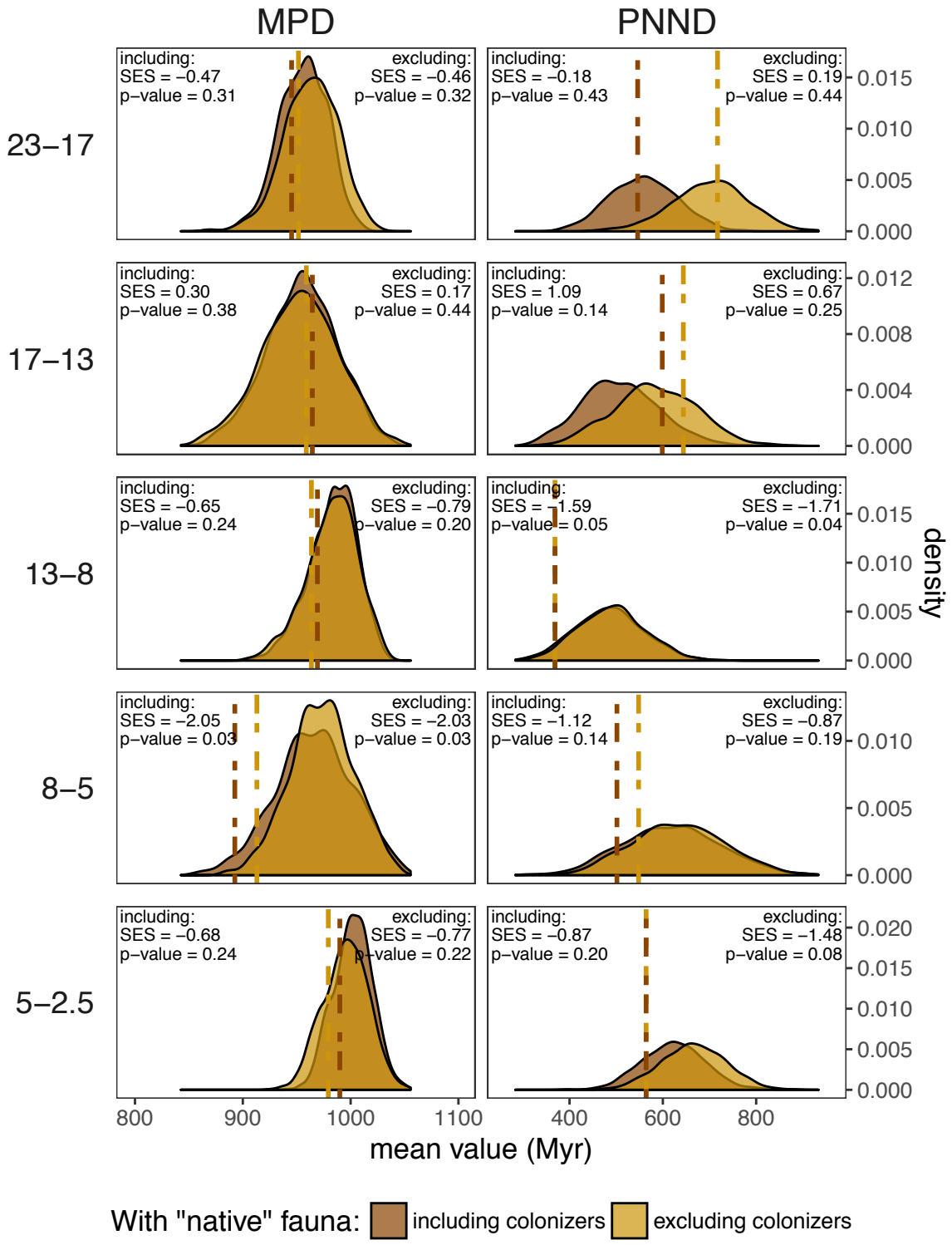

Figure 3.5: Mean phylogenetic distance (MPD) and phylogenetic nearest neighbor distance (PNND) of non-colonizing and colonizing taxa across time. Boxes contain second and third quartiles with median values marked by a horizontal line. Whiskers extend to values 1.5 times the interquartile range. Asterisks (*) indicate significantly non-zero slopes in fitted logistic models before Bonferroni correction for multiple comparisons ($p \leq 0.05$). No differences were significant following Bonferroni correction ($p \leq 0.005$).

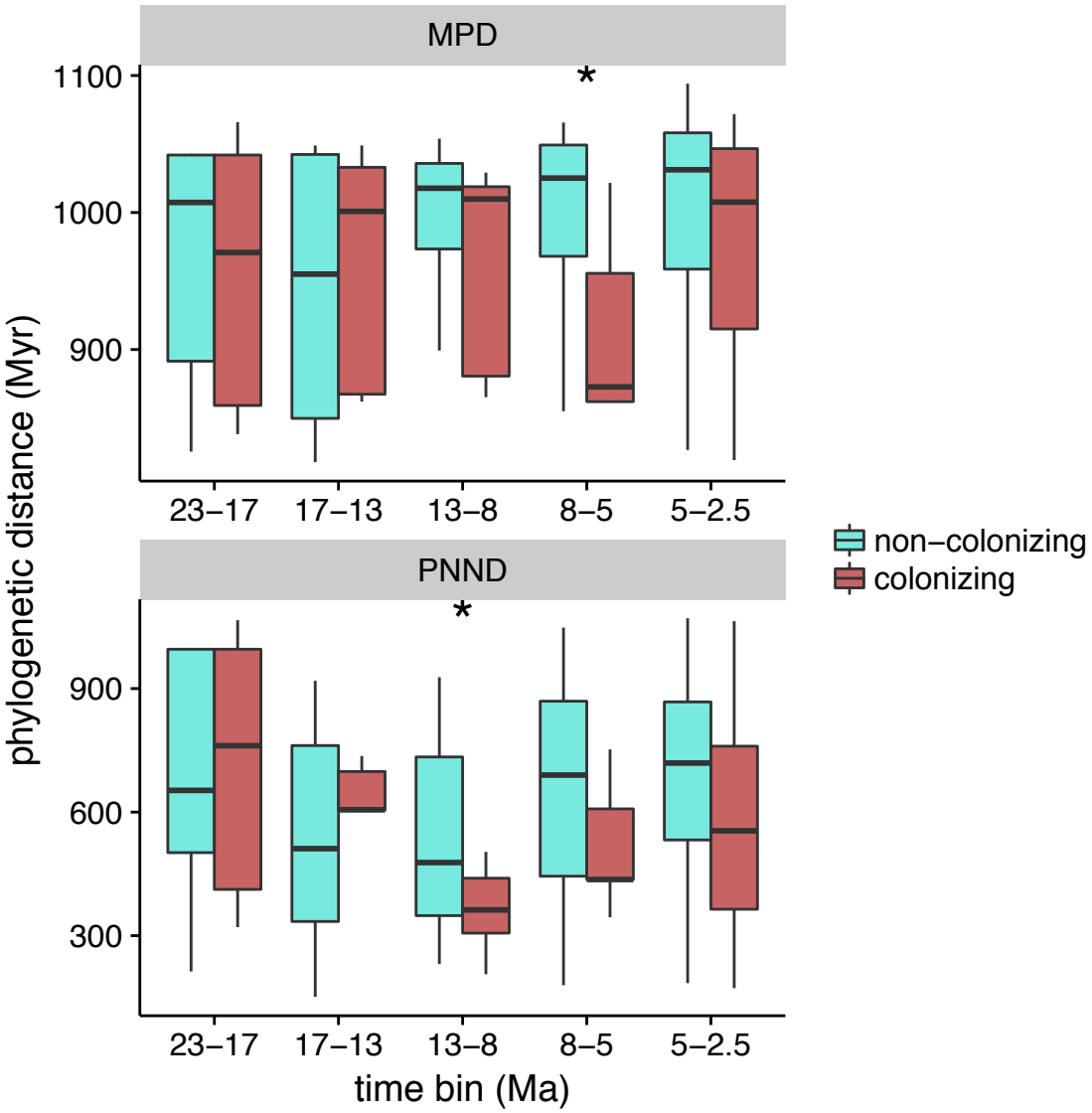

Appendix A

Supporting material for Chapter 1

Appendix A.1: Sources for measurements taken outside of Wright et al. (1996).

family	genus	subgenus	species	reference
Acanthoceratidae	*Acanthoceras*		*jukesbrownei*	Kennedy and Juignet 1993
Acanthoceratidae	*Codazziceras*		*ospinae*	Wright et al. 1983
Acanthoceratidae	*Eucalycoceras*		*pentagonum*	Cobban 1988
Acanthoceratidae	*Mammites*		*nodosoides*	Kennedy et al. 2008
Brancoceratidae	*Cantabrigites*		*spinosum*	Barragan et al. 2011
Cleoniceratidae	*Cymahoplites*		*hohendorfensis*	Lehmann et al. 2013
Coilopoceratidae	*Hoplitoides*		cf. *gibbosulus*	Kennedy and Cobban 1988
Collignoniceratidae	*Cibolaites*		*molenaari*	Kennedy et al. 2001
Collignoniceratidae	*Forresteria*	*Forresteria*	*alluaudi*	Benavides-Caceres 1956
Collignoniceratidae	*Menabites*	*Australiella*	cf. *besairiei*	Kennedy 1986
Collignoniceratidae	*Menabites*	*Delawarella*	*vanuxemi*	Kennedy and Cobban 1993
Collignoniceratidae	*Prionocyclus*		*wyomingensis*	Kennedy et al. 2001
Collignoniceratidae	*Submortoniceras*	*Submortoniceras*	*woodsi*	Kennedy 1981
Collignoniceratidae	*Subprionocyclus*		*neptuni*	Matsumoto 1959
Collignoniceratidae	*Yabeiceras*		*orientale*	Futakami et al. 2016
Desmoceratidae	*Abrytusites*		*neumayri*	Nikolov and Breskovski 1969
Desmoceratidae	*Boliteceras*		*perlatum*	Whitehouse 1928
Desmoceratidae	*Callizoniceras*	*Wollemanniceras*	*alaskanum*	Imlay 1960
Desmoceratidae	*Damesites*		*hetonaiensis fresnoensis*	Matsumoto 1959
Desmoceratidae	*Moremanoceras*		*costatum*	Cobban, Hook, and Kennedy 1989
Desmoceratidae	*Pachydesmoceras*		*kossmati*	Kennedy et al. 2015
Desmoceratidae	*Parasilesites*		*bullatus*	Imlay 1960
Desmoceratidae	*Pseudohaploceras*		*liptoviense*	Gonzalez-Arreola et al. 1996

family	genus	subgenus	species	reference
Desmoceratidae	*Pseudosilesites*		*russoi*	Medina and Riccardi 2005
Desmoceratidae	*Silesitoides*		*alicantensis*	Wiedmann 1966
Desmoceratidae	*Umsinenoceras*		*cardielense*	Medina and Riccardi 2005
Desmoceratidae	*Zuercherella*		*latecostata*	Bogdanova and Hoedemaeker 2004
Flickiidae	*Adkinsia*		*bosquensis*	Bose 1927
Holcodiscidae	*Parasaynoceras*		*mexicanum*	Imlay 1940
Hoplitidae	*Farnhamia*		*farnhamensis*	Casey 1954
Kossmaticeratidae	*Eomadrasites*		*nipponicus*	Matsumoto 1991
Kossmaticeratidae	*Eomarshallites*		*espinosum*	Medina and Riccardi 2005
Kossmaticeratidae	*Kossmaticeras*	*Natalites*	*africanus*	Kennedy and Klinger 1985
Kossmaticeratidae	*Marshallites*		*compressus*	Matsumoto 1991
Kossmaticeratidae	*Mikasaites*		*orbicularis*	Matsumoto 1991
Kossmaticeratidae	*Neograhamites*		*carnarvonensis*	Henderson and McNamara 1985
Kossmaticeratidae	*Protokossmaticeras*		*madagascariense*	Matsumoto 1991
Kossmaticeratidae	*Wellmanites*		*japonicus*	Matsumoto 1991
Kossmaticeratidae	*Yeharites*		*kobayashii*	Matsumoto 1991
Lyelliceratidae	*Stoliczkaia*	*Lamnayella*	*juigneti*	Kennedy and Juignet 1984
Muniericeratidae	*Tragodesmoceras*		*ashlandicum*	Matsumoto 1959
Neocomitidae	*Cuyaniceras*		*transgrediens*	Riccardi 1988
Neocomitidae	*Kilianella*		*submartini*	Wiedmann 1966
Neocomitidae	*Neohoploceras*		*arnoldi*	Aguirre-Urreta 1998
Neocomitidae	*Pseudofavrella*		*angulatiformis*	Aguirre-Urreta and Rawson 2010
Neocomitidae	*Stoicoceras*		*pitrei*	Mojon et al. 2013
Olcostephanidae	*Groebericeras*		*bifrons*	Aguirre-Urreta and Alvarez 1999
Olcostephanidae	*Valanginites*		*argentinicus*	Aguirre-Urreta and Rawson 1999
Pachydiscidae	*Eupachydiscus*		*arbucklensis*	Anderson 1958
Pachydiscidae	*Nowakites*		*klamathonis*	Anderson 1958

family	genus	subgenus	species	reference
Polyptychitidae	*Nikitinoceras*	*Nikitinoceras*	*inflatum*	Alsen 2006
Pseudotissotiidae	*Wrightoceras*		*munieri*	Kennedy et al. 2008
Silesitidae	*Miyakoceras*		sp.	Bogdanova and Hoedemaeker 2004
Silesitidae	*Neoastieria*		*patagonica*	Medina and Riccardi 2005
Sphenodiscidae	*Coahuilites*		*sheltoni*	Kennedy et al. 1996
Sphenodiscidae	*Sphenodiscus*		*pleurisepta*	Kennedy et al. 1996
Vascoceratidae	*Neoptychites*		*cephalotus*	Kennedy et al. 2008

Appendix A.2: Data used to generate morphospace and extinction predictors for Chapter 1.

family	genus	subgenus	species	*U*	*w*	*S*	FAD	LAD	size (mm)
Acanthoceratidae	*Acanthoceras*		*jukesbrownei*	0.28	2.12	1.28	Cenomanian	Cenomanian	94
Acanthoceratidae	*Acanthoceras*		*rhotomagense*	0.26	2.76	NA	Cenomanian	Cenomanian	94
Acanthoceratidae	*Acompsoceras*		*renevieri*	0.28	2.18	0.65	Cenomanian	Cenomanian	243
Acanthoceratidae	*Acompsoceras*		*sarthacense*	NA	NA	0.78	Cenomanian	Cenomanian	35
Acanthoceratidae	*Alzadites*		*westonensis*	0.3	2.01	0.86	Cenomanian	Cenomanian	15
Acanthoceratidae	*Benueites*		*benueensis*	NA	NA	NA	Turonian	Turonian	NA
Acanthoceratidae	*Benueites*		*spinosus*	0.29	2.15	0.79	Turonian	Turonian	20
Acanthoceratidae	*Buccinammonites*		*minimus*	NA	NA	NA	Cenomanian	Cenomanian	6
Acanthoceratidae	*Buchiceras*		*bilobatum*	0.21	1.72	0.77	Coniacian	Coniacian	60
Acanthoceratidae	*Calycoceras*	*Calycoceras*	*naviculare*	0.33	1.33	1.65	Cenomanian	Cenomanian	156
Acanthoceratidae	*Calycoceras*	*Calycoceras*	*naviculare*	0.33	1.33	1.65	Cenomanian	Cenomanian	156
Acanthoceratidae	*Calycoceras*	*Gentoniceras*	*gentoni*	0.35	2.31	1.1	Cenomanian	Cenomanian	68
Acanthoceratidae	*Calycoceras*	*Hourcqiceras*		NA	NA	NA	Cenomanian	Cenomanian	NA
Acanthoceratidae	*Calycoceras*	*Newboldiceras*	*asiaticum*	0.29	2.4	1	Cenomanian	Cenomanian	126
Acanthoceratidae	*Calycoceras*	*Proeucalycoceras*	*besairiei*	0.26	2	0.88	Cenomanian	Cenomanian	46
Acanthoceratidae	*Calycoceras*	*Proeucalycoceras*	*choffati*	0.25	2.5	0.98	Cenomanian	Cenomanian	80
Acanthoceratidae	*Codazziceras*		*ospinae*	0.44	1.26	0.95	Coniacian	Coniacian	102
Acanthoceratidae	*Codazziceras*		*scheibei*	0.46	1.44	NA	Coniacian	Coniacian	124
Acanthoceratidae	*Conlinoceras*		*gilberti*	0.3	2.06	1.03	Cenomanian	Cenomanian	129
Acanthoceratidae	*Cryptometoicoceras*			NA	NA	NA	Cenomanian	Cenomanian	NA
Acanthoceratidae	*Cunningtoniceras*		*cunningtoni*	0.31	3.28	1.11	Cenomanian	Cenomanian	150
Acanthoceratidae	*Dunveganoceras*	*Dunveganoceras*	*albertense montanense*	0.32	2.38	1.1	Cenomanian	Cenomanian	214
Acanthoceratidae	*Dunveganoceras*	*Plesiacanthoceras*	*wyomingense*	0.31	2.5	0.7	Cenomanian	Cenomanian	145
Acanthoceratidae	*Eucalycoceras*		*pentagonum*	0.28	1.86	1.12	Cenomanian	Cenomanian	34

family	genus	subgenus	species	*U*	*w*	*S*	FAD	LAD	size (mm)
Acanthoceratidae	*Eucalycoceras*		*pentagonum*	NA	NA	NA	Cenomanian	Cenomanian	110
Acanthoceratidae	*Euomphaloceras*		*euomphalum*	NA	NA	NA	Cenomanian	Cenomanian	45
Acanthoceratidae	*Euomphaloceras*		*septemseriatum*	0.28	2.25	1.26	Cenomanian	Cenomanian	98
Acanthoceratidae	*Graysonites*		*lozoi*	NA	NA	0.58	Cenomanian	Cenomanian	170
Acanthoceratidae	*Kamerunoceras*		*eschii*	NA	NA	NA	Turonian	Turonian	51
Acanthoceratidae	*Kamerunoceras*		*inaequicostatus*	NA	NA	0.97	Turonian	Turonian	67
Acanthoceratidae	*Kamerunoceras*		*turoniense*	0.44	2.35	0.72	Turonian	Turonian	217
Acanthoceratidae	*Kastanoceras*		*spinigerum*	0.38	1.96	1.35	Cenomanian	Cenomanian	11
Acanthoceratidae	*Kennediella*		*inopinata*	NA	NA	NA	Cenomanian	Cenomanian	48
Acanthoceratidae	*Lotzeites*		*aberrans*	0.37	2.47	1.7	Cenomanian	Cenomanian	49
Acanthoceratidae	*Mammites*		*nodosoides*	0.23	2.03	0.96	Turonian	Turonian	200
Acanthoceratidae	*Mammites*		*nodosoides*	0.26	1.61	NA	Turonian	Turonian	179
Acanthoceratidae	*Mantelliceras*		*mantelli*	0.25	2.39	1.17	Cenomanian	Cenomanian	48
Acanthoceratidae	*Metasigaloceras*		*rusticum*	0.35	3.94	0.94	Turonian	Turonian	502
Acanthoceratidae	*Metoicoceras*		*swallovi*	0.17	2.52	0.57	Cenomanian	Cenomanian	98
Acanthoceratidae	*Mhriliceras*		*lapparenti*	0.17	2.15	0.54	Cenomanian	Cenomanian	47
Acanthoceratidae	*Microsulcatoceras*			NA	NA	NA	Cenomanian	Cenomanian	NA
Acanthoceratidae	*Mitonia*		*venezolana*	0.41	2.01	1.25	Turonian	Turonian	30
Acanthoceratidae	*Morrowites*		*subdepressus*	NA	NA	NA	Turonian	Turonian	54
Acanthoceratidae	*Nannometoicoceras*		*acceleratum*	0.1	2.34	0.61	Cenomanian	Cenomanian	35
Acanthoceratidae	*Nebraskites*		*haresiceratiforme*	0.11	2.02	0.49	Turonian	Turonian	18
Acanthoceratidae	*Neocardioceras*		*juddii barroisi*	NA	NA	NA	Cenomanian	Turonian	39
Acanthoceratidae	*Neocardioceras*		*juddii juddii*	0.39	1.39	1.05	Cenomanian	Turonian	38
Acanthoceratidae	*Nigericeras*		*gignouxi*	0.29	2.11	1.05	Cenomanian	Cenomanian	67
Acanthoceratidae	*Paraburroceras*			NA	NA	NA	Cenomanian	Cenomanian	NA
Acanthoceratidae	*Paracompsoceras*		*landisi*	NA	NA	0.89	Cenomanian	Cenomanian	63

family	genus	subgenus	species	*U*	*w*	*S*	FAD	LAD	size (mm)
Acanthoceratidae	*Paraconlinoceras*		*leonense*	0.32	1.91	1.1	Cenomanian	Cenomanian	46
Acanthoceratidae	*Plesiacanthoceratoides*			NA	NA	NA	Cenomanian	Cenomanian	NA
Acanthoceratidae	*Protacanthoceras*		*bunburianum*	0.33	1.82	0.7	Cenomanian	Cenomanian	32
Acanthoceratidae	*Pseudaspidoceras*		*auriculatum*	0.25	2.73	NA	Turonian	Turonian	144
Acanthoceratidae	*Pseudaspidoceras*		*footeanum*	0.35	2.42	1.09	Turonian	Turonian	257
Acanthoceratidae	*Pseudocalycoceras*		*harpax*	0.32	1.84	0.84	Cenomanian	Cenomanian	101
Acanthoceratidae	*Quitmaniceras*		*reaseri*	NA	NA	NA	Turonian	Turonian	54
Acanthoceratidae	*Rhamphidoceras*		*saxatile*	0.27	1.52	1.02	Turonian	Turonian	28
Acanthoceratidae	*Romaniceras*	*Neomphaloceras*	*pseudomphalum*	0.29	2.34	1.12	Turonian	Turonian	34
Acanthoceratidae	*Romaniceras*	*Obiraceras*	*ornatum*	NA	NA	0.92	Turonian	Turonian	52
Acanthoceratidae	*Romaniceras*	*Romaniceras*	*deverianum*	0.32	2	0.84	Turonian	Turonian	112
Acanthoceratidae	*Romaniceras*	*Shuparoceras*	*yagii*	0.25	2.25	0.79	Turonian	Turonian	140
Acanthoceratidae	*Romaniceras*	*Yubariceras*	*ornatissimum*	0.33	2.4	1.16	Turonian	Turonian	100
Acanthoceratidae	*Sharpeiceras*		*laticlavium*	0.26	2.78	0.8	Cenomanian	Cenomanian	130
Acanthoceratidae	*Spathites*	*Ingridella*	*malladae*	0.43	2.13	1.35	Turonian	Turonian	120
Acanthoceratidae	*Spathites*	*Jeanrogericeras*	*revelierеanus*	0.17	2.49	0.99	Turonian	Turonian	109
Acanthoceratidae	*Spathites*	*Jeanrogericeras*	*subconciliatus*	0.31	1.77	1.22	Turonian	Turonian	103
Acanthoceratidae	*Spathites*	*Spathites*	*coahuilensis*	0.13	2.43	1.05	Turonian	Turonian	79
Acanthoceratidae	*Spathites*	*Spathites*	*sulcatus*	0.13	1.36	1.01	Turonian	Turonian	132
Acanthoceratidae	*Tarrantoceras*	*Sumitomoceras*	*faustum*	0.36	2.09	0.76	Cenomanian	Cenomanian	65
Acanthoceratidae	*Tarrantoceras*	*Tarrantoceras*	*sellardsi*	0.35	2.04	0.63	Cenomanian	Cenomanian	61
Acanthoceratidae	*Thomelites*		*sornayi*	NA	NA	NA	Cenomanian	Turonian	91
Acanthoceratidae	*Utaturiceras*		*vicinale*	0.21	1.87	0.6	Cenomanian	Cenomanian	142
Acanthoceratidae	*Watinoceras*		*amudariense*	0.41	2.01	0.88	Turonian	Turonian	33
Binneyitidae	*Binneyites*		*parkensis*	0.04	2.7	0.35	Turonian	Santonian	29
Binneyitidae	*Borissjakoceras*		*mirabilis*	0.32	2	0.62	Albian	Turonian	24

family	genus	subgenus	species	*U*	*w*	*S*	FAD	LAD	size (mm)
Binneyitidae	*Johnsonites*		*sulcatus*	0.07	2.23	0.46	Cenomanian	Cenomanian	21
Brancoceratidae	*Algericeras*	*Algericeras*	*boghariense*	0.26	2.91	NA	Cenomanian	Cenomanian	9
Brancoceratidae	*Algericeras*	*Sakondryella*	*remolinense*	0.31	2.17	1.14	Cenomanian	Cenomanian	42
Brancoceratidae	*Arestoceras*		*collinum*	NA	NA	0.66	Albian	Albian	102
Brancoceratidae	*Brancoceras*	*Brancoceras*	*senequieri*	0.38	2.04	0.84	Albian	Albian	56
Brancoceratidae	*Brancoceras*	*Eubrancoceras*	*aegoceratoides*	0.39	2.25	0.82	Albian	Albian	52
Brancoceratidae	*Cantabrigites*		*cantabrigense*	0.41	1.92	NA	Albian	Albian	36
Brancoceratidae	*Cantabrigites*		*spinosum*	0.35	0.77	0.71	Albian	Albian	23
Brancoceratidae	*Dipoloceras*	*Dipoloceras*	*cristatum*	0.36	2.52	0.86	Albian	Albian	64
Brancoceratidae	*Dipoloceras*	*Rhytidoceras*	*elegans*	0.38	1.83	0.81	Albian	Albian	159
Brancoceratidae	*Elobiceras*	*Craginites*	*serratescens*	0.38	1.72	NA	Albian	Albian	90
Brancoceratidae	*Elobiceras*	*Elobiceras*	*elobiense*	NA	NA	NA	Albian	Albian	196
Brancoceratidae	*Erioliceras*		*tenuis*	0.42	1.68	NA	Albian	Albian	69
Brancoceratidae	*Euhystrichoceras*		*nicaisei*	0.33	1.63	1.12	Cenomanian	Cenomanian	17
Brancoceratidae	*Falloticeras*		*proteus*	0.32	2.07	0.98	Albian	Albian	31
Brancoceratidae	*Goodhallites*		*goodhalli*	0.28	2.28	0.62	Albian	Albian	132
Brancoceratidae	*Goodhallites*		*liber*	0.33	2.5	0.55	Albian	Albian	60
Brancoceratidae	*Hysteroceras*		*antipodeum*	NA	NA	NA	Albian	Albian	NA
Brancoceratidae	*Hysteroceras*		*varicosum*	0.41	1.8	0.86	Albian	Albian	40
Brancoceratidae	*Mojsisoviczia*		*delaruei*	0.28	2.28	0.98	Albian	Albian	52
Brancoceratidae	*Mojsisoviczia*		*ventanillensis*	0.28	2.29	0.82	Albian	Albian	68
Brancoceratidae	*Mojsisoviczia*		*ventanillensis*	0.28	2.29	0.82	Albian	Albian	68
Brancoceratidae	*Mortoniceras*	*Angolaites*	*gregoryi*	0.46	0.98	1.08	Albian	Albian	110
Brancoceratidae	*Mortoniceras*	*Boesites*		NA	NA	NA	Albian	Albian	NA
Brancoceratidae	*Mortoniceras*	*Deiradoceras*	*prerostratum*	NA	NA	0.95	Albian	Albian	56
Brancoceratidae	*Mortoniceras*	*Drakeoceras*	*drakei*	0.37	2.79	1.03	Albian	Albian	93

family	genus	subgenus	species	*U*	*w*	*S*	FAD	LAD	size (mm)
Brancoceratidae	*Mortoniceras*	*Durnovarites*	*perinflatum*	0.28	1.94	1.3	Albian	Albian	122
Brancoceratidae	*Mortoniceras*	*Durnovarites*	*subquadratum*	0.44	1.84	1.05	Albian	Albian	31
Brancoceratidae	*Mortoniceras*	*Mortoniceras*	*inflatum*	0.44	2	0.97	Albian	Albian	106
Brancoceratidae	*Mortoniceras*	*Mortoniceras*	*inflatum*	0.44	2	0.97	Albian	Albian	106
Brancoceratidae	*Mortoniceras*	*Mortoniceras*	*rostratum*	0.36	1.72	NA	Albian	Albian	157
Brancoceratidae	*Mortoniceras*	*Mortoniceras*	*vespertinum*	0.47	1.7	NA	Albian	Albian	324
Brancoceratidae	*Mortoniceras*	*Pagoceras*	*amplificatum*	0.33	2.77	0.75	Albian	Albian	112
Brancoceratidae	*Neoharpoceras*		*hugardianum*	0.12	2.93	0.5	Albian	Albian	86
Brancoceratidae	*Neokentroceras*		*curvicornu*	0.39	2.49	0.77	Albian	Albian	29
Brancoceratidae	*Oxytropidoceras*	*Adkinsites*	*bravoense*	NA	NA	NA	Albian	Albian	55
Brancoceratidae	*Oxytropidoceras*	*Benavidesites*	*acutocarinatum*	0.33	2.4	NA	Albian	Albian	106
Brancoceratidae	*Oxytropidoceras*	*Benavidesites*	*harrisoni*	NA	NA	NA	Albian	Albian	89
Brancoceratidae	*Oxytropidoceras*	*Laraiceras*	*laraense*	NA	NA	0.45	Albian	Albian	133
Brancoceratidae	*Oxytropidoceras*	*Mirapelia*	*mirapelianum*	NA	NA	NA	Albian	Albian	104
Brancoceratidae	*Oxytropidoceras*	*Oxytropidoceras*	*manuanense*	0.14	2.91	0.31	Albian	Albian	90
Brancoceratidae	*Oxytropidoceras*	*Oxytropidoceras*	*roissyanum*	0.22	2.91	0.59	Albian	Albian	100
Brancoceratidae	*Oxytropidoceras*	*Venezoliceras*	*venezolanum*	NA	NA	0.66	Albian	Albian	57
Brancoceratidae	*Parabrancoceras*		*besairiei*	0.46	2.06	0.85	Albian	Albian	28
Brancoceratidae	*Parabrancoceras*		*besairiei*	0.46	2.06	0.85	Albian	Albian	28
Brancoceratidae	*Prohysteroceras*		*wordiei*	0.45	2.5	0.86	Albian	Albian	103
Cleoniceratidae	*Anadesmoceras*		*emendatum*	0.21	2.03	0.54	Albian	Albian	51
Cleoniceratidae	*Anadesmoceras*		*strangulatum*	NA	NA	NA	Albian	Albian	55
Cleoniceratidae	*Arcthoplites*		*belli*	0.26	2.02	0.85	Albian	Albian	43
Cleoniceratidae	*Arcthoplites*		*jachromensis*	NA	NA	NA	Albian	Albian	56
Cleoniceratidae	*Arcthoplites*		*probus*	0.2	3.08	0.7	Albian	Albian	58
Cleoniceratidae	*Brewericeras*		*breweri*	NA	NA	NA	Albian	Albian	134

family	genus	subgenus	species	*U*	*w*	*S*	FAD	LAD	size (mm)
Cleoniceratidae	*Brewericeras*		*hulenense*	NA	NA	NA	Albian	Albian	NA
Cleoniceratidae	*Cleoniceras*	*Anacleoniceras*	*caseyi*	0.23	2.27	0.66	Albian	Albian	57
Cleoniceratidae	*Cleoniceras*	*Cleoniceras*	*cleon*	0.14	3.58	0.5	Albian	Albian	70
Cleoniceratidae	*Cleoniceras*	*Grycia*	*besairei*	0.21	1.9	NA	Albian	Albian	72
Cleoniceratidae	*Cleoniceras*	*Grycia*	*sablei*	0.15	1.8	0.44	Albian	Albian	85
Cleoniceratidae	*Cleoniceras*	*Neosaynella*	*inornatum*	0.13	2.95	0.44	Albian	Albian	54
Cleoniceratidae	*Colvillia*		*crassicostata*	NA	NA	NA	Albian	Albian	32
Cleoniceratidae	*Colvillia*		*kenti*	NA	NA	NA	Albian	Albian	64
Cleoniceratidae	*Cymahoplites*		*hohendorfensis*	0.29	2.71	0.66	Albian	Albian	52
Cleoniceratidae	*Cymahoplites*		*kerenskianus*	0.31	2.39	NA	Albian	Albian	58
Cleoniceratidae	*Freboldiceras*		*singulare*	0.25	1.95	0.8	Albian	Albian	61
Cleoniceratidae	*Leconteites*		*lecontei*	0.22	2.43	NA	Albian	Albian	76
Cleoniceratidae	*Leconteites*		*sacramenticus*	0.29	2.49	0.79	Albian	Albian	120
Cleoniceratidae	*Lemuroceras*		*aburense*	0.34	1.83	0.77	Albian	Albian	42
Cleoniceratidae	*Moretella*		*madagascariensis*	0.35	1.84	0.92	Albian	Albian	38
Cleoniceratidae	*Tetrahoplitoides*		*stantoni*	0.24	3.41	NA	Albian	Albian	34
Coilopoceratidae	*Coilopoceras*		*colleti*	0.08	2.28	0.54	Turonian	Turonian	76
Coilopoceratidae	*Coilopoceras*		*glebosum*	0.02	7.91	NA	Turonian	Turonian	256
Coilopoceratidae	*Erichsenites*		*mirabilis*	0.03	2.38	0.49	Turonian	Turonian	156
Coilopoceratidae	*Hoplitoides*		*gibbosulus*	0.08	1.15	0.58	Turonian	Turonian	49
Coilopoceratidae	*Hoplitoides*		*gibbosulus bipartitus*	NA	NA	0.63	Turonian	Turonian	122
Coilopoceratidae	*Hoplitoides*		*ingens*	NA	NA	NA	Turonian	Turonian	134
Collignoniceratidae	*Aneuretoceras*			NA	NA	NA	Coniacian	Coniacian	NA
Collignoniceratidae	*Barroisiceras*		*colnacapi*	0.27	1.89	0.65	Turonian	Coniacian	112
Collignoniceratidae	*Barroisiceras*		*haberfellneri*	0.12	1.32	NA	Turonian	Coniacian	69

family	genus	subgenus	species	*U*	*w*	*S*	FAD	LAD	size (mm)
Collignoniceratidae	*Barroisiceras*		*mahafalense*	0.19	2.32	NA	Turonian	Coniacian	89
Collignoniceratidae	*Barroisiceras*		*minimum*	0.17	2.41	NA	Turonian	Coniacian	106
Collignoniceratidae	*Bevahites*		*quadratus*	0.39	2.19	0.9	Santonian	Campanian	91
Collignoniceratidae	*Cibolaites*		*molenaari*	0.22	2.26	1.21	Cenomanian	Turonian	42
Collignoniceratidae	*Cibolaites*		*molenaari*	0.26	3.18	NA	Cenomanian	Turonian	69
Collignoniceratidae	*Collignoniceras*		*woollgari*	0.4	2	0.67	Turonian	Turonian	135
Collignoniceratidae	*Cryptotexanites*			NA	NA	NA	Campanian	Campanian	NA
Collignoniceratidae	*Defordiceras*			NA	NA	NA	Santonian	Santonian	NA
Collignoniceratidae	*Diaziceras*		*tissotiaeforme*	0.1	1.65	1.11	Santonian	Santonian	56
Collignoniceratidae	*Forresteria*	*Forresteria*	*alluaudi*	0.31	2.82	0.83	Coniacian	Coniacian	48
Collignoniceratidae	*Forresteria*	*Forresteria*	*alluaudi*	NA	NA	1.39	Coniacian	Coniacian	24
Collignoniceratidae	*Forresteria*	*Harleites*	*petrocoriensis*	0.14	2.17	0.57	Coniacian	Coniacian	68
Collignoniceratidae	*Gauthiericeras*		*listeri*	NA	NA	0.99	Coniacian	Coniacian	65
Collignoniceratidae	*Gauthiericeras*		*margae*	0.33	1.97	0.84	Coniacian	Coniacian	99
Collignoniceratidae	*Germariceras*		*germari*	0.39	1.8	0.8	Turonian	Coniacian	22
Collignoniceratidae	*Haboroceras*		*haboroense*	0.34	1.69	0.66	Santonian	Campanian	21
Collignoniceratidae	*Ishikariceras*		*binodosum*	NA	NA	0.88	Coniacian	Coniacian	35
Collignoniceratidae	*Lecointriceras*		*fleuriausianum*	0.29	2.06	0.87	Turonian	Turonian	176
Collignoniceratidae	*Lymaniceras*		*planulatum*	0.31	2.33	0.72	Turonian	Turonian	50
Collignoniceratidae	*Menabites*	*Australiella*	*australe*	0.38	4.2	1.23	Campanian	Campanian	63
Collignoniceratidae	*Menabites*	*Australiella*	cf. *besairiei*	0.39	1.37	1.41	Campanian	Campanian	120
Collignoniceratidae	*Menabites*	*Bererella*		NA	NA	NA	Campanian	Campanian	NA
Collignoniceratidae	*Menabites*	*Delawarella*	*delawarensis*	NA	NA	NA	Campanian	Campanian	NA
Collignoniceratidae	*Menabites*	*Delawarella*	*vanuxemi*	0.25	2.57	0.7	Campanian	Campanian	130
Collignoniceratidae	*Menabites*	*Menabites*	*menabensis*	0.43	1.92	1.05	Campanian	Campanian	87
Collignoniceratidae	*Neogauthiericeras*		*zafimahovai*	0.49	1.57	1.1	Santonian	Campanian	117

family	genus	subgenus	species	*U*	*w*	*S*	FAD	LAD	size (mm)
Collignoniceratidae	*Niceforoceras*		*umbulaziforme*	0.15	2.32	0.48	Coniacian	Coniacian	50
Collignoniceratidae	*Paratexanites*		*serratomarginatus*	0.37	1.82	0.99	Coniacian	Santonian	45
Collignoniceratidae	*Paratexanites*		*zeilleri*	NA	NA	0.94	Coniacian	Santonian	147
Collignoniceratidae	*Peroniceras*	*Peroniceras*	*tanakai*	NA	NA	0.94	Coniacian	Coniacian	50
Collignoniceratidae	*Peroniceras*	*Peroniceras*	*tridorsatus*	0.52	1.72	0.89	Coniacian	Coniacian	95
Collignoniceratidae	*Peroniceras*	*Zuluiceras*	*modestum*	NA	NA	0.82	Coniacian	Coniacian	33
Collignoniceratidae	*Peroniceras*	*Zuluiceras*	*proteus*	NA	NA	0.9	Coniacian	Coniacian	27
Collignoniceratidae	*Peroniceras*	*Zuluiceras*	*zulu*	0.5	2.33	NA	Coniacian	Coniacian	349
Collignoniceratidae	*Pleurotexanites*		*superbus*	0.37	2.4	0.86	Santonian	Santonian	77
Collignoniceratidae	*Prionocycloceras*		*guayabanum*	0.28	2.66	0.7	Coniacian	Coniacian	57
Collignoniceratidae	*Prionocyclus*		*wyomingensis*	0.36	1.31	1.01	Turonian	Turonian	63
Collignoniceratidae	*Prionocyclus*		*wyomingensis*	NA	NA	NA	Turonian	Turonian	95
Collignoniceratidae	*Protexanites*	*Anatexanites*	*orientalis*	NA	NA	0.64	Santonian	Santonian	53
Collignoniceratidae	*Protexanites*	*Miotexanites*	*minimus*	0.4	1.83	0.86	Coniacian	Santonian	59
Collignoniceratidae	*Protexanites*	*Protexanites*	*bourgeoisi*	0.41	2.01	1.03	Coniacian	Santonian	55
Collignoniceratidae	*Pseudobarroisiceras*		*nagaoi*	0.17	2.46	0.67	Coniacian	Coniacian	93
Collignoniceratidae	*Reginaites*		*hataii*	0.45	2.02	0.89	Coniacian	Campanian	77
Collignoniceratidae	*Reginaites*		*quadrituberculatum*	0.5	1.08	NA	Coniacian	Campanian	151
Collignoniceratidae	*Submortoniceras*	*Ankilizatella*	*ankilizatense*	0.39	2.09	0.54	Campanian	Campanian	101
Collignoniceratidae	*Submortoniceras*	*Submortoniceras*	*woodsi*	0.33	2.19	0.73	Santonian	Campanian	46
Collignoniceratidae	*Submortoniceras*	*Submortoniceras*	*woodsi*	NA	NA	0.81	Santonian	Campanian	98
Collignoniceratidae	*Subprionocyclus*		*hitchinensis*	0.31	2.55	NA	Turonian	Turonian	39
Collignoniceratidae	*Subprionocyclus*		*neptuni*	0.3	2.68	0.67	Turonian	Turonian	109
Collignoniceratidae	*Subprionocyclus*		*neptuni*	0.31	2.64	NA	Turonian	Turonian	35
Collignoniceratidae	*Subprionotropis*		*colombianus*	0.27	2.06	0.66	Turonian	Coniacian	36
Collignoniceratidae	*Texanites*	*Eutexanites*		NA	NA	NA	Santonian	Santonian	NA

family	genus	subgenus	species	*U*	*w*	*S*	FAD	LAD	size (mm)
Collignoniceratidae	*Texanites*	*Plesiotexanites*	*kawasakii*	0.41	0.51	NA	Santonian	Campanian	98
Collignoniceratidae	*Texanites*	*Texanites*	*texanus*	0.41	1.79	0.56	Coniacian	Campanian	154
Collignoniceratidae	*Texanites*	*Texanites*	*texanus ?hispanica*	0.47	1.86	NA	Coniacian	Campanian	166
Collignoniceratidae	*Yabeiceras*		*orientale*	0.48	2.72	0.8	Coniacian	Coniacian	123
Collignoniceratidae	*Yabeiceras*		*orientale*	0.47	1.16	NA	Coniacian	Coniacian	67
Desmoceratidae	*Abrytusites*		*neumayri*	0.31	3.06	0.59	Barremian	Barremian	128
Desmoceratidae	*Abrytusites*		*neumayri*	0.31	2.57	NA	Barremian	Barremian	126
Desmoceratidae	*Achilleoceras*		*erasmusi*	0.3	2.3	0.79	Albian	Albian	992
Desmoceratidae	*Aioloceras*		*argentinum*	0.17	2.65	0.45	Aptian	Aptian	65
Desmoceratidae	*Barremites*		*chaputi*	0.26	1.62	0.72	Hauterivian	Barremian	55
Desmoceratidae	*Barremites*		*difficilis*	0.15	2.07	0.36	Hauterivian	Barremian	87
Desmoceratidae	*Barremites*		*raspaili*	0.16	1.95	0.71	Hauterivian	Barremian	72
Desmoceratidae	*Bassites*		*reesidei*	0.12	1.55	0.97	Turonian	Turonian	136
Desmoceratidae	*Beaudanticeras*	*Beudanticeras*	*beaudanti*	0.15	2.71	0.46	Albian	Albian	100
Desmoceratidae	*Beaudanticeras*	*Grantziceras*	*convergens*	NA	NA	NA	Albian	Albian	NA
Desmoceratidae	*Beaudanticeras*	*Grantziceras*	*multiconstrictum*	0.21	2.15	0.74	Albian	Albian	96
Desmoceratidae	*Boliteceras*		*perlatum*	0.35	0.36	0.94	Albian	Albian	130
Desmoceratidae	*Boliteceras*		*perlatum*	0.22	1.98	NA	Albian	Albian	138
Desmoceratidae	*Callizoniceras*	*Callizoniceras*	*hoyeri*	0.24	2.22	0.78	Barremian	Aptian	27
Desmoceratidae	*Callizoniceras*	*Wollemanniceras*	*alaskanum*	0.28	4	0.82	Albian	Albian	23
Desmoceratidae	*Callizoniceras*	*Wollemanniceras*	*keilhacki*	0.33	2.28	NA	Albian	Albian	33
Desmoceratidae	*Cophinoceras*		*ogilviei*	0.14	2.52	0.57	Albian	Albian	197
Desmoceratidae	*Damesites*		*hetonaiensis fresnoensis*	0.07	2.59	0.61	Cenomanian	Campanian	106
Desmoceratidae	*Damesites*		*semicostatus*	0.07	3.32	NA	Cenomanian	Campanian	51
Desmoceratidae	*Damesites*		*sugata*	0.12	2.53	NA	Cenomanian	Campanian	61

family	genus	subgenus	species	*U*	*w*	*S*	FAD	LAD	size (mm)
Desmoceratidae	*Desmoceras*	*Desmoceras*	*latidorsatum*	0.21	2.51	1.06	Aptian	Cenomanian	70
Desmoceratidae	*Desmoceras*	*Pseudouhligella*	*japonica*	0.19	2.61	0.77	Albian	Turonian	131
Desmoceratidae	*Desmophyllites*		*larteti*	0.09	2.17	0.45	Santonian	Maastrichtian	88
Desmoceratidae	*Epipuzosia*			NA	NA	NA	Cenomanian	Turonian	NA
Desmoceratidae	*Ferugliоceras*		*piatnitzkyi*	NA	NA	NA	Albian	Albian	55
Desmoceratidae	*Hauericeras*		*angustum*	0.4	1.83	NA	Coniacian	Maastrichtian	120
Desmoceratidae	*Hauericeras*		*pseudogardeni*	0.3	1.71	0.42	Coniacian	Maastrichtian	263
Desmoceratidae	*Jimboiceras*		*planulatiforme*	0.39	1.97	0.78	Turonian	Santonian	117
Desmoceratidae	*Kennicottia*		*bifurcata*	0.22	2.33	0.93	Albian	Albian	71
Desmoceratidae	*Kitchinites*		*japonica*	0.31	2.32	NA	Santonian	Maastrichtian	98
Desmoceratidae	*Kitchinites*		*pondycherryanus*	0.31	2.06	0.64	Santonian	Maastrichtian	57
Desmoceratidae	*Lytodiscoides*		*conduciensis*	0.32	1.87	1.37	Albian	Albian	700
Desmoceratidae	*Melchiorites*		*melchioris*	0.34	1.72	0.81	Barremian	Albian	47
Desmoceratidae	*Microdesmoceras*		*tetragonum*	0.41	1.98	1.03	Cenomanian	Cenomanian	21
Desmoceratidae	*Moremanoceras*		*costatum*	0.04	0.39	0.39	Cenomanian	Cenomanian	20
Desmoceratidae	*Moremanoceras*		*scotti*	0.09	2.46	NA	Cenomanian	Cenomanian	36
Desmoceratidae	*Onitshoceras*		*matsumotoi*	NA	NA	NA	Coniacian	Coniacian	NA
Desmoceratidae	*Pachydesmoceras*		*kossmati*	0.33	3.47	1.03	Albian	Turonian	46
Desmoceratidae	*Pachydesmoceras*		*kossmati*	NA	NA	0.94	Albian	Turonian	121
Desmoceratidae	*Parapuzosia*	*Austiniceras*	*austeni*	0.29	1.83	0.54	Cenomanian	Turonian	226
Desmoceratidae	*Parapuzosia*	*Grandidiericeras*	*grandidierorum*	0.28	2.29	0.53	Coniacian	Campanian	164
Desmoceratidae	*Parapuzosia*	*Parapuzosia*	*daubreei*	0.27	1.8	NA	Santonian	Campanian	236
Desmoceratidae	*Parasilesites*		*bullatus*	0.43	1.92	0.89	Albian	Albian	27
Desmoceratidae	*Parasilesites*		*bullatus*	0.42	1.63	NA	Albian	Albian	30
Desmoceratidae	*Plesiospitidiscus*		*ligatus*	0.23	2.3	0.7	Hauterivian	Hauterivian	53
Desmoceratidae	*Pseudohaploceras*		*liptoviense*	0.23	1.25	0.79	Barremian	Aptian	47

family	genus	subgenus	species	*U*	*w*	*S*	FAD	LAD	size (mm)
Desmoceratidae	*Pseudohaploceras*		*liptoviense*	0.23	2.47	NA	Barremian	Aptian	94
Desmoceratidae	*Pseudosaynella*		*bicurvata*	NA	NA	NA	Aptian	Aptian	NA
Desmoceratidae	*Pseudosaynella*		*raresulcata*	0.19	2.96	0.62	Aptian	Aptian	35
Desmoceratidae	*Pseudosilesites*		*russoi*	0.34	3.29	0.88	Aptian	Aptian	34
Desmoceratidae	*Pseudosilesites*		*seranoniformis*	0.44	1.5	NA	Aptian	Aptian	47
Desmoceratidae	*Puzosia*	*Anapuzosia*	*buenaventura*	NA	NA	NA	Albian	Cenomanian	124
Desmoceratidae	*Puzosia*	*Bhimaites*	*bhima*	0.32	2.19	0.84	Albian	Turonian	55
Desmoceratidae	*Puzosia*	*Mesopuzosia*	*pacifica*	0.33	1.77	0.66	Turonian	Campanian	125
Desmoceratidae	*Puzosia*	*Mesopuzosia*	*yubarensis*	0.32	1.67	NA	Turonian	Campanian	924
Desmoceratidae	*Puzosia*	*Puzosia*	*planulata*	0.34	1.83	0.76	Albian	Campanian	111
Desmoceratidae	*Puzosia*	*Puzosia*	*tamon*	0.39	1.35	NA	Albian	Campanian	431
Desmoceratidae	*Silesitoides*		*alicantensis*	0.44	1.7	1.33	Albian	Albian	10
Desmoceratidae	*Silesitoides*		*escragnollensis*	0.55	1.75	NA	Albian	Albian	34
Desmoceratidae	*Spitidiscus*		*rotula*	0.26	2.54	1.12	Valanginian	Hauterivian	30
Desmoceratidae	*Subsaynella*		*sayni*	0.18	3.08	0.56	Hauterivian	Barremian	25
Desmoceratidae	*Torcapella*		*fabrei*	0.25	1.36	0.48	Barremian	Barremian	220
Desmoceratidae	*Tragodesmoceroides*		*subcostatus*	0.08	2.19	0.79	Turonian	Santonian	37
Desmoceratidae	*Uhligella*		*clansayensis*	0.22	2.33	0.65	Aptian	Albian	98
Desmoceratidae	*Uhligella*		*clansayensis*	0.22	2.33	0.65	Aptian	Albian	98
Desmoceratidae	*Umsinenoceras*		*cardielense*	0.34	2.16	0.84	Albian	Albian	32
Desmoceratidae	*Umsinenoceras*		*linguatuberculatum*	0.37	2.54	NA	Albian	Albian	28
Desmoceratidae	*Valdedorsella*		*akuschaensis*	0.24	2.1	1.23	Hauterivian	Aptian	41
Desmoceratidae	*Valdedorsella*		*vacaensis*	0.29	2.12	NA	Hauterivian	Aptian	165
Desmoceratidae	*Zuercherella*		*latecostata*	0.26	2.04	0.84	Barremian	Aptian	27
Desmoceratidae	*Zuercherella*		*zuercheri*	0.22	3.03	NA	Barremian	Aptian	54
Flickiidae	*Adkinsia*		*bosquensis*	0.26	1.11	1.44	Cenomanian	Cenomanian	15

family	genus	subgenus	species	*U*	*w*	*S*	FAD	LAD	size (mm)
Flickiidae	*Adkinsia*		*bosquensis*	0.29	1.69	NA	Cenomanian	Cenomanian	16
Flickiidae	*Ficheuria*		*kiliani*	0.2	1.26	1.07	Albian	Cenomanian	19
Flickiidae	*Ficheuria*		*pernoni*	NA	NA	NA	Albian	Cenomanian	11
Flickiidae	*Flickia*		*simplex*	0.25	2.37	0.55	Albian	Cenomanian	13
Flickiidae	*Neosaynoceras*		*gazellae*	0.06	1.66	1.18	Cenomanian	Cenomanian	14
Flickiidae	*Salaziceras*		*salazacense*	0.23	1.95	1.15	Albian	Albian	22
Forbesiceratidae	*Forbesiceras*		*largilliertianum*	0.01	3.39	0.43	Cenomanian	Cenomanian	108
Forbesiceratidae	*Paradolphia*		*prisca*	NA	NA	NA	Albian	Albian	52
Haploceratidae	*Haploceras*		*carachtheis*	0.23	2.12	0.68	Kimmeridgian	Valanginian	44
Haploceratidae	*Haploceras*		*elimatum*	0.22	2.18	0.72	Kimmeridgian	Valanginian	72
Haploceratidae	*Neolissoceras*		*grasianum*	0.24	1.98	0.5	Tithonian	Barremian	96
Haploceratidae	*Neolissoceras*		*grasianum*	0.24	1.98	0.5	Tithonian	Barremian	96
Holcodiscidae	*Almohadites*		*subcamelinus*	0.33	2.63	1.2	Barremian	Barremian	18
Holcodiscidae	*Astieridiscus*		*morleti*	0.28	2.72	0.94	Barremian	Barremian	45
Holcodiscidae	*Holcodiscus*		*caillaudianus*	0.33	1.96	1.11	Barremian	Barremian	54
Holcodiscidae	*Metahoplites*	*Medjeziceras*	*collignoni*	0.25	2.07	0.64	Barremian	Barremian	18
Holcodiscidae	*Metahoplites*	*Metahoplites*	*henoni*	0.15	2.93	0.74	Barremian	Barremian	28
Holcodiscidae	*Parasaynoceras*		*horridum*	NA	NA	NA	Barremian	Barremian	27
Holcodiscidae	*Parasaynoceras*		*horridum*	NA	NA	NA	Barremian	Barremian	27
Holcodiscidae	*Parasaynoceras*		*mexicanum*	0.19	2.25	1.11	Barremian	Barremian	18
Hoplitidae	*Anahoplites*		*cantabrigensis*	NA	NA	NA	Albian	Albian	NA
Hoplitidae	*Anahoplites*		*planus*	0.16	2.58	0.53	Albian	Albian	53
Hoplitidae	*Callihoplites*		*patella*	NA	NA	NA	Albian	Albian	NA
Hoplitidae	*Callihoplites*		sp. aff. *C. patella*	0.26	2.56	0.74	Albian	Albian	62
Hoplitidae	*Dimorphoplites*		*biplicatus*	0.34	1.98	0.94	Albian	Albian	59
Hoplitidae	*Discohoplites*		*subfalcatus*	0.31	2.23	0.64	Albian	Albian	44

family	genus	subgenus	species	*U*	*w*	*S*	FAD	LAD	size (mm)
Hoplitidae	*Discohoplites*		*subfalcatus*	0.31	2.23	0.64	Albian	Albian	44
Hoplitidae	*Discohoplites*		*subfalcatus*	0.31	2.23	0.64	Albian	Albian	44
Hoplitidae	*Epihoplites*	*Epihoplites*	*trifidus*	0.31	2.38	0.88	Albian	Albian	53
Hoplitidae	*Epihoplites*	*Metaclavites*	*compressus*	0.23	2.38	0.58	Albian	Albian	53
Hoplitidae	*Euhoplites*		*truncatus*	0.29	2.54	1.13	Albian	Albian	42
Hoplitidae	*Farnhamia*		*farnhamensis*	0.28	2.2	0.79	Albian	Albian	155
Hoplitidae	*Farnhamia*		*farnhamensis*	0.29	2.03	NA	Albian	Albian	229
Hoplitidae	*Gastroplites*	*Gastroplites*	*arcticus*	NA	NA	NA	Albian	Albian	52
Hoplitidae	*Gastroplites*	*Gastroplites*	*canadensis*	0.24	1.73	NA	Albian	Albian	63
Hoplitidae	*Gastroplites*	*Gastroplites*	*canadensis*	0.24	1.73	NA	Albian	Albian	63
Hoplitidae	*Gastroplites*	*Gastroplites*	*crowensis*	NA	NA	NA	Albian	Albian	74
Hoplitidae	*Gastroplites*	*Gastroplites*	*tozeri*	0.19	1.93	0.71	Albian	Albian	62
Hoplitidae	*Gastroplites*	*Paragastroplites*	*spiekeri*	0.2	2.1	0.71	Albian	Albian	29
Hoplitidae	*Hoplites*	*Hoplites*	*dentatus*	0.24	2.43	0.83	Albian	Albian	115
Hoplitidae	*Hoplites*	*Isohoplites*	*steinmanni*	NA	NA	NA	Albian	Albian	58
Hoplitidae	*Hyphoplites*		*falcatus*	0.22	2.73	0.5	Albian	Cenomanian	44
Hoplitidae	*Neogastroplites*		*cornutus*	0.09	2.52	0.54	Albian	Cenomanian	69
Hoplitidae	*Otohoplites*		*raulinianus*	0.31	1.85	1.18	Albian	Albian	72
Hoplitidae	*Pleurohoplites*	*Arrhaphoceras*	*studeri*	0.28	2.19	1.12	Albian	Albian	42
Hoplitidae	*Pleurohoplites*	*Pleurohoplites*	*renauxianus*	0.28	1.71	0.9	Albian	Albian	153
Hoplitidae	*Protohoplites*	*Hemisonneratia*	*puzosianus*	0.27	2.42	1.12	Albian	Albian	89
Hoplitidae	*Protohoplites*	*Protohoplites*	*archiacianus*	NA	NA	1.52	Albian	Albian	73
Hoplitidae	*Pseudopulchellia*		*imlayi*	0.17	3.11	0.62	Albian	Albian	62
Hoplitidae	*Pseudopulchellia*		*pattoni*	NA	NA	NA	Albian	Albian	50
Hoplitidae	*Pseudosonneratia*		*typica*	NA	NA	NA	Albian	Albian	79
Hoplitidae	*Semenoviceras*		*michalskii*	0.19	2.65	0.45	Albian	Albian	72

family	genus	subgenus	species	*U*	*w*	*S*	FAD	LAD	size (mm)
Hoplitidae	*Sokolovites*		*aberrans*	0.19	2.2	0.7	Albian	Albian	44
Hoplitidae	*Sokolovites*		*subdragunovi*	0.27	1.67	0.56	Albian	Albian	59
Hoplitidae	*Sonneratia*		*dutempleana*	0.32	1.99	1.14	Albian	Albian	105
Hoplitidae	*Tetrahoplites*		*subquadratus*	0.37	1.64	1.17	Albian	Albian	76
Kossmaticeratidae	*Brahmaites*		*brahma*	0.48	1.6	1.19	Maastrichtian	Maastrichtian	93
Kossmaticeratidae	*Eogunnarites*		*alaskensis*	0.37	2.17	1.47	Albian	Cenomanian	132
Kossmaticeratidae	*Eogunnarites*		*unicus*	NA	NA	NA	Albian	Cenomanian	33
Kossmaticeratidae	*Eomadrasites*		*nipponicus*	0.26	2.35	0.89	Cenomanian	Cenomanian	41
Kossmaticeratidae	*Eomadrasites*		*nipponicus*	0.32	2.03	NA	Cenomanian	Cenomanian	47
Kossmaticeratidae	*Eomarshallites*		*espinosum*	0.32	1.37	0.97	Albian	Albian	28
Kossmaticeratidae	*Eomarshallites*		*espinosum*	0.4	1.51	NA	Albian	Albian	47
Kossmaticeratidae	*Grossouvreites*		*gemmatus*	0.2	2.35	0.7	Campanian	Campanian	105
Kossmaticeratidae	*Gunnarites*		*antarcticus*	0.33	2.2	1.04	Campanian	Campanian	117
Kossmaticeratidae	*Holcodiscoides*		*cliveanus*	0.39	2.79	0.91	Turonian	Turonian	60
Kossmaticeratidae	*Hulenites*		*reesidei*	0.3	2.06	NA	Aptian	Albian	41
Kossmaticeratidae	*Jacobites*	*Jacobites*	*anderssoni*	NA	NA	NA	Campanian	Campanian	80
Kossmaticeratidae	*Jacobites*	*Jacobites*	*nodulosus*	0.36	2.22	NA	Campanian	Campanian	62
Kossmaticeratidae	*Jacobites*	*Tainuia*	*aucklandica*	0.36	1.91	0.51	Campanian	Campanian	144
Kossmaticeratidae	*Kossmaticeras*	*Karapadites*	*karapadense*	NA	NA	NA	Campanian	Campanian	49
Kossmaticeratidae	*Kossmaticeras*	*Kossmaticeras*	*theobaldianum*	0.36	2.3	0.92	Turonian	Santonian	67
Kossmaticeratidae	*Kossmaticeras*	*Natalites*	*africanus*	0.31	1.59	0.71	Coniacian	Campanian	44
Kossmaticeratidae	*Kossmaticeras*	*Natalites*	*africanus*	0.34	1.85	NA	Coniacian	Campanian	80
Kossmaticeratidae	*Maccarthyites*		*gracilis*	0.23	2.71	0.6	Cenomanian	Cenomanian	24
Kossmaticeratidae	*Maorites*	*Caledonites*		NA	NA	NA	Campanian	Campanian	NA
Kossmaticeratidae	*Maorites*	*Maorites*	*tenuicostatum*	0.27	2.32	NA	Campanian	Campanian	132
Kossmaticeratidae	*Marshallites*		*compressus*	0.26	2.17	0.67	Aptian	Cenomanian	49

family	genus	subgenus	species	*U*	*w*	*S*	FAD	LAD	size (mm)
Kossmaticeratidae	*Marshallites*		*compressus*	0.28	2.03	NA	Aptian	Cenomanian	56
Kossmaticeratidae	*Mikasaites*		*orbicularis*	0.26	2.03	1.29	Cenomanian	Cenomanian	20
Kossmaticeratidae	*Mikasaites*		*orbicularis*	0.27	2.17	NA	Cenomanian	Cenomanian	20
Kossmaticeratidae	*Neograhamites*		*carnarvonensis*	0.41	1.74	0.82	Campanian	Campanian	49
Kossmaticeratidae	*Neograhamites*		*kiliani*	0.43	1.96	NA	Campanian	Campanian	71
Kossmaticeratidae	*Protokossmaticeras*		*madagascariense*	0.37	2.58	1.17	Albian	Cenomanian	14
Kossmaticeratidae	*Protokossmaticeras*		*madagascariense*	NA	NA	1.25	Albian	Cenomanian	31
Kossmaticeratidae	*Pseudokossmaticeras*		*pacificum*	0.48	1.72	0.53	Maastrichtian	Maastrichtian	52
Kossmaticeratidae	*Wellmanites*		*japonicus*	0.34	2.65	1.36	Cenomanian	Cenomanian	38
Kossmaticeratidae	*Wellmanites*		*japonicus*	0.35	1.92	NA	Cenomanian	Cenomanian	64
Kossmaticeratidae	*Wellmanites*		*zelandicus*	NA	NA	NA	Cenomanian	Cenomanian	44
Kossmaticeratidae	*Yakushiceras*		*takahashii*	0.4	2.28	0.76	Cenomanian	Cenomanian	51
Kossmaticeratidae	*Yeharites*		*kobayashii*	0.3	1.86	0.82	Albian	Cenomanian	82
Kossmaticeratidae	*Yeharites*		*kobayashii*	0.36	0.94	NA	Albian	Cenomanian	79
Kossmaticeratidae	*Yokoyamaoceras*		aff. *minimum*	0.35	1.3	NA	Turonian	Coniacian	23
Kossmaticeratidae	*Yokoyamaoceras*		*kotoi*	0.29	2.62	0.79	Turonian	Coniacian	37
Leymeriellidae	*Epileymeriella*		*hitzeli*	0.29	2.28	0.64	Albian	Albian	26
Leymeriellidae	*Epileymeriella*		*revili*	0.38	2.88	NA	Albian	Albian	42
Leymeriellidae	*Leymeriella*	*Leymeriella*	*tardefurcata*	0.31	2.59	0.61	Albian	Albian	39
Leymeriellidae	*Leymeriella*	*Neoleymeriella*	*consueta*	0.36	2.9	0.81	Albian	Albian	29
Leymeriellidae	*Proleymeriella*		*schrammeni*	0.3	2.2	0.77	Albian	Albian	43
Lyelliceratidae	*Budaiceras*		*hyatti*	0.23	2.03	0.74	Cenomanian	Cenomanian	55
Lyelliceratidae	*Cenisella*		*bonnetiana*	0.26	1.33	0.8	Albian	Albian	88
Lyelliceratidae	*Lyelliceras*		*lyelli*	0.5	1.97	1.17	Albian	Albian	79
Lyelliceratidae	*Neophlycticeras*		*blancheti*	0.13	2.23	0.52	Albian	Albian	51
Lyelliceratidae	*Neophlycticeras*		*brottianum*	0.19	2.59	0.77	Albian	Albian	50

family	genus	subgenus	species	*U*	*w*	*S*	FAD	LAD	size (mm)
Lyelliceratidae	*Ojinagiceras*			NA	NA	NA	Cenomanian	Cenomanian	NA
Lyelliceratidae	*Paracalycoceras*		*subvicinale*	0.22	2.13	NA	Cenomanian	Cenomanian	20
Lyelliceratidae	*Paracalycoceras*		*wiestii*	NA	NA	NA	Cenomanian	Cenomanian	74
Lyelliceratidae	*Prolyelliceras*		*prorsocurvatum*	0.37	2.01	0.9	Albian	Albian	76
Lyelliceratidae	*Protissotia*		*itierianus*	0.31	3	0.59	Albian	Albian	32
Lyelliceratidae	*Stoliczkaia*	*Lamnayella*	*juigneti*	0.31	1.28	0.72	Cenomanian	Cenomanian	61
Lyelliceratidae	*Stoliczkaia*	*Lamnayella*	*juigneti*	0.31	1.57	NA	Cenomanian	Cenomanian	69
Lyelliceratidae	*Stoliczkaia*	*Shumarinaia*	*hashimotoi*	0.28	2.37	0.72	Albian	Albian	46
Lyelliceratidae	*Stoliczkaia*	*Stoliczkaia*	*dispar*	0.11	1.49	0.5	Albian	Albian	175
Lyelliceratidae	*Tegoceras*		*camatteanum*	0.29	2.4	0.8	Albian	Albian	36
Lyelliceratidae	*Tegoceras*		*mosense*	NA	NA	NA	Albian	Albian	64
Lyelliceratidae	*Zuluscaphites*			NA	NA	NA	Albian	Albian	NA
Muniericeratidae	*Muniericeras*		*lapparenti*	NA	NA	NA	Coniacian	Santonian	69
Muniericeratidae	*Pseudoschloenbachia*	*Besairiella*	*besairiei*	0.33	2.13	NA	Campanian	Campanian	131
Muniericeratidae	*Pseudoschloenbachia*	*Buehrierella*	*buehreri*	0.17	2.19	0.48	Campanian	Campanian	162
Muniericeratidae	*Pseudoschloenbachia*	*Condamyella*	*condamyi*	0.25	2.65	0.68	Campanian	Campanian	98
Muniericeratidae	*Pseudoschloenbachia*	*Fournierella*	*fournieri*	0.23	1.87	0.53	Santonian	Campanian	84
Muniericeratidae	*Pseudoschloenbachia*	*Hirtziella*	*inornata*	0.13	2.93	0.48	Campanian	Campanian	79
Muniericeratidae	*Pseudoschloenbachia*	*Hourcqiella*	*bererensis*	0.27	1.92	NA	Campanian	Campanian	89
Muniericeratidae	*Pseudoschloenbachia*	*Pseudoschloenbachia*	*griesbachi*	NA	NA	NA	Santonian	Campanian	NA
Muniericeratidae	*Pseudoschloenbachia*	*Pseudoschloenbachia*	*umbulazi*	0.12	2.38	0.56	Santonian	Campanian	49
Muniericeratidae	*Pseudoschloenbachia*	*Rabenjanaharyella*	*rhomboidalis*	0.22	2.71	0.71	Campanian	Campanian	95
Muniericeratidae	*Pseudoschloenbachia*	*Rabiella*	*orthogona*	NA	NA	NA	Campanian	Campanian	113
Muniericeratidae	*Pseudoschloenbachia*	*Vendegiesiella*	*spinosa*	0.31	1.92	0.62	Campanian	Campanian	119
Muniericeratidae	*Texasia*		*dentatocarinata*	0.19	2.36	0.43	Santonian	Campanian	89
Muniericeratidae	*Texasia*		*sornayi*	0.25	2.41	NA	Santonian	Campanian	74

family	genus	subgenus	species	*U*	*w*	*S*	FAD	LAD	size (mm)
Muniericeratidae	*Tragodesmoceras*		*ashlandicum*	0.28	1.78	0.78	Turonian	Santonian	78
Muniericeratidae	*Tragodesmoceras*		*carlilense*	NA	NA	NA	Turonian	Santonian	NA
Muniericeratidae	*Tragodesmoceras*		*clypealoides*	0.21	2.52	NA	Turonian	Santonian	82
Neocomitidae	*Acanthodiscus*		*radiatus*	0.19	3.9	0.54	Hauterivian	Hauterivian	196
Neocomitidae	*Acantholissonia*		*gerthi*	NA	NA	NA	Valanginian	Valanginian	56
Neocomitidae	*Argentiniceras*		*malarguense*	0.36	1.67	0.95	Berriasian	Berriasian	109
Neocomitidae	*Banikoceras*		*involutum*	0.18	2.34	0.64	Berriasian	Berriasian	134
Neocomitidae	*Banikoceras*		*involutum*	0.18	2.34	0.64	Berriasian	Berriasian	134
Neocomitidae	*Berriasella*	*Berriasella*	*callistoides*	0.3	1.99	0.66	Tithonian	Berriasian	84
Neocomitidae	*Berriasella*	*Berriasella*	*privasensis*	NA	NA	NA	Tithonian	Berriasian	NA
Neocomitidae	*Berriasella*	*Elenaella*	*cularensis*	NA	NA	NA	Tithonian	Berriasian	65
Neocomitidae	*Breistrofferella*		*castellanensis*	0.21	2.94	0.66	Hauterivian	Hauterivian	44
Neocomitidae	*Calliptychoceras*		*calliptychum*	0.32	1.93	0.79	Berriasian	Valanginian	67
Neocomitidae	*Chamalocia*		*subaenigmatica*	0.32	2.25	0.62	Valanginian	Valanginian	30
Neocomitidae	*Criosarasinella*		*furcillata*	0.37	1.79	NA	Valanginian	Valanginian	106
Neocomitidae	*Cuyaniceras*		*transgrediens*	0.35	1.73	0.76	Berriasian	Berriasian	102
Neocomitidae	*Cuyaniceras*		*transgrediens*	0.32	1.56	NA	Berriasian	Berriasian	106
Neocomitidae	*Dalmasiceras*		*dalmasi*	0.31	1.51	0.47	Tithonian	Berriasian	46
Neocomitidae	*Distoloceras*		*hystrix*	0.36	2.92	0.92	Valanginian	Hauterivian	74
Neocomitidae	*Distoloceras*		*pavlowi*	NA	NA	NA	Valanginian	Hauterivian	NA
Neocomitidae	*Favrella*		*americana*	0.42	1.85	1	Hauterivian	Hauterivian	140
Neocomitidae	*Frenguelliceras*		*magister*	0.48	1.83	0.91	Berriasian	Berriasian	89
Neocomitidae	*Hannaites*		*riddlensis*	NA	NA	NA	Hauterivian	Hauterivian	87
Neocomitidae	*Karakaschiceras*		*biassalense*	0.3	2.15	1.01	Valanginian	Valanginian	63
Neocomitidae	*Kilianella*		*pexiptycha*	0.37	2.07	NA	Berriasian	Valanginian	45
Neocomitidae	*Kilianella*		*roubaudiana*	0.4	2.62	NA	Berriasian	Valanginian	42

family	genus	subgenus	species	*U*	*w*	*S*	FAD	LAD	size (mm)
Neocomitidae	*Kilianella*		*submartini*	0.33	4	1.1	Berriasian	Valanginian	9
Neocomitidae	*Kilianella*		*superba*	0.37	2.21	NA	Berriasian	Valanginian	80
Neocomitidae	*Leopoldia*		*leopoldina*	0.19	2.45	0.54	Hauterivian	Hauterivian	103
Neocomitidae	*Lissonia*		*riveroi*	NA	NA	NA	Valanginian	Valanginian	51
Neocomitidae	*Lyticoceras*		*amblygonium*	0.34	2	NA	Valanginian	Hauterivian	142
Neocomitidae	*Lyticoceras*		*colcanapi*	0.34	2.18	NA	Valanginian	Hauterivian	160
Neocomitidae	*Lyticoceras*		*cryptoceras*	0.32	2.1	0.63	Valanginian	Hauterivian	162
Neocomitidae	*Lyticoceras*		*cryptoceras*	0.32	2.1	0.63	Valanginian	Hauterivian	162
Neocomitidae	*Lyticoceras*		*regale*	0.29	2.36	0.62	Valanginian	Hauterivian	88
Neocomitidae	*Lyticoceras*		*stevrecensis*	NA	NA	NA	Valanginian	Hauterivian	131
Neocomitidae	*Lytohoplites*		*besairei*	0.37	3.08	1	Tithonian	Berriasian	28
Neocomitidae	*Lytohoplites*		*burckhardti*	NA	NA	1.02	Tithonian	Berriasian	50
Neocomitidae	*Malbosiceras*		*malbosi*	0.38	1.89	0.66	Tithonian	Berriasian	155
Neocomitidae	*Neocomites*	*Eristavites*	*platycostatus*	0.29	2.04	0.77	Valanginian	Hauterivian	43
Neocomitidae	*Neocomites*	*Neocomites*	*neocomiensis*	0.24	2.76	0.52	Valanginian	Hauterivian	32
Neocomitidae	*Neocomites*	*Neocomites*	*neocomiensis*	0.24	2.76	0.52	Valanginian	Hauterivian	32
Neocomitidae	*Neocomites*	*Teschenites*	*neocomiensiformis*	0.25	1.83	NA	Valanginian	Hauterivian	86
Neocomitidae	*Neocomites*	*Varlheidites*	*peregrinus*	0.32	1.88	0.84	Valanginian	Valanginian	129
Neocomitidae	*Neocosmoceras*		*sayni*	0.45	2.15	NA	Berriasian	Berriasian	78
Neocomitidae	*Neohoploceras*		*arnoldi*	0.35	3.13	0.78	Valanginian	Valanginian	55
Neocomitidae	*Neohoploceras*		*submartini*	NA	NA	NA	Valanginian	Valanginian	56
Neocomitidae	*Odontodiscoceras*		*odontodiscum*	NA	NA	NA	Berriasian	Valanginian	89
Neocomitidae	*Pseudargentiniceras*		*abscissum*	0.4	1.69	0.75	Tithonian	Berriasian	56
Neocomitidae	*Pseudofavrella*		*angulatiformis*	0.29	2.24	0.75	Hauterivian	Hauterivian	46
Neocomitidae	*Pseudofavrella*		*angulatiformis*	0.4	2.42	NA	Hauterivian	Hauterivian	84
Neocomitidae	*Riasanites*		*rjasanensis*	0.37	1.88	0.8	Berriasian	Berriasian	46

family	genus	subgenus	species	*U*	*w*	*S*	FAD	LAD	size (mm)
Neocomitidae	*Sarasinella*		*ambigua*	0.34	2.48	NA	Valanginian	Valanginian	71
Neocomitidae	*Sarasinella*		*variens*	0.33	2.54	0.83	Valanginian	Valanginian	99
Neocomitidae	*Saynella*		*clypeiformis*	0.15	2.95	0.38	Hauterivian	Hauterivian	376
Neocomitidae	*Stoicoceras*		*pitrei*	0.3	2.64	0.65	Valanginian	Valanginian	150
Neocomitidae	*Stoicoceras*		*teutobergense*	NA	NA	NA	Valanginian	Valanginian	250
Neocomitidae	*Stoicoceras*		*tuberculatum*	NA	NA	NA	Valanginian	Valanginian	111
Neocomitidae	*Subalpinites*		*fauriensis*	0.29	2.16	0.6	Tithonian	Valanginian	74
Neocomitidae	*Suboosterella*		*heliaca*	0.35	1.93	0.42	Hauterivian	Hauterivian	63
Neocomitidae	*Subthurmannia*		*fermori*	0.38	2.14	0.87	Tithonian	Valanginian	176
Neocomitidae	*Subthurmannia*		*gallica*	0.39	2	0.67	Tithonian	Valanginian	68
Neocomitidae	*Thurmanniceras*	*Clavithurmannia*	*foraticostatum*	NA	NA	NA	Valanginian	Valanginian	188
Neocomitidae	*Thurmanniceras*	*Thurmanniceras*	*thurmanni*	0.35	2.75	NA	Berriasian	Valanginian	66
Olcostephanidae	*Baronnites*			NA	NA	NA	Valanginian	Valanginian	NA
Olcostephanidae	*Capeloites*		*perelegans*	NA	NA	0.56	Hauterivian	Hauterivian	27
Olcostephanidae	*Ceratotuberculus*		*casitensis*	0.4	1.44	NA	Hauterivian	Hauterivian	31
Olcostephanidae	*Ceratotuberculus*		*linguituberculatus*	NA	NA	NA	Hauterivian	Hauterivian	27
Olcostephanidae	*Groebericeras*		*bifrons*	0.42	1.84	0.76	Berriasian	Berriasian	125
Olcostephanidae	*Groebericeras*		*rocardi*	0.37	1.55	NA	Berriasian	Berriasian	93
Olcostephanidae	*Negreliceras*		*negreli*	0.42	1.76	0.82	Tithonian	Berriasian	70
Olcostephanidae	*Olcostephanus*	*Jeannoticeras*	*jeannotii*	0.27	2.17	0.52	Valanginian	Hauterivian	59
Olcostephanidae	*Olcostephanus*	*Jeannoticeras*	*jeannotii*	0.27	2.17	0.52	Valanginian	Hauterivian	59
Olcostephanidae	*Olcostephanus*	*Mexicanoceras*	*kanesi*	0.21	2.22	1.3	Hauterivian	Hauterivian	23
Olcostephanidae	*Olcostephanus*	*Olcostephanus*	*astierianus*	0.27	1.71	NA	Valanginian	Hauterivian	99
Olcostephanidae	*Olcostephanus*	*Olcostephanus*	*atherstoni*	0.3	1.54	NA	Valanginian	Hauterivian	82
Olcostephanidae	*Olcostephanus*	*Olcostephanus*	*madagascariensis*	0.37	1.16	NA	Valanginian	Hauterivian	71
Olcostephanidae	*Olcostephanus*	*Olcostephanus*	*rogersi*	0.21	1.54	1.61	Valanginian	Hauterivian	84

family	genus	subgenus	species	*U*	*w*	*S*	FAD	LAD	size (mm)
Olcostephanidae	*Olcostephanus*	*Olcostephanus*	*sulcosus*	0.35	2.06	1.84	Valanginian	Hauterivian	23
Olcostephanidae	*Parastieria*		*peltoceroides*	0.27	2.44	0.98	Hauterivian	Hauterivian	19
Olcostephanidae	*Saynoceras*		*verrucosum*	0.24	1.96	1.3	Valanginian	Valanginian	18
Olcostephanidae	*Spiticeras*	*Kilianiceras*	*damesi*	0.47	2.13	1.04	Tithonian	Berriasian	147
Olcostephanidae	*Spiticeras*	*Spiticeras*	*gregoryi*	0.38	1.97	0.92	Tithonian	Berriasian	103
Olcostephanidae	*Spiticeras*	*Spiticeras*	*spitiense*	0.4	2.1	1.29	Tithonian	Berriasian	97
Olcostephanidae	*Valanginites*		*argentinicus*	0.22	1.49	1.69	Valanginian	Valanginian	35
Olcostephanidae	*Valanginites*		*nucleus*	0.19	0.98	NA	Valanginian	Valanginian	56
Olcostephanidae	*Valanginites*		*wilfridi*	0.2	1.99	NA	Valanginian	Valanginian	42
Oosterellidae	*Oosterella*		*cultrata*	0.28	3.09	0.49	Valanginian	Hauterivian	101
Oosterellidae	*Pseudosterella*		*fischeri*	0.38	1.77	0.87	Valanginian	Valanginian	13
Oppeliidae	*Aconeceras*	*Aconeceras*	*nisus*	0.11	3.04	0.38	Barremian	Albian	35
Oppeliidae	*Aconeceras*	*Gyaloceras*	*smithi*	NA	NA	NA	Aptian	Albian	NA
Oppeliidae	*Aconeceras*	*Sanmartinoceras*	*groenlandicum*	NA	NA	NA	Aptian	Albian	NA
Oppeliidae	*Aconeceras*	*Sinzovia*	*sazonovae*	0.13	2.3	0.5	Aptian	Albian	43
Oppeliidae	*Aconeceras*	*Theganoceras*	*scalatum*	NA	NA	NA	Aptian	Aptian	NA
Oppeliidae	*Bornhardticeras*		*discoidale*	NA	NA	NA	Hauterivian	Hauterivian	NA
Oppeliidae	*Cyrtosiceras*		*macrotelus*	NA	NA	0.8	Tithonian	Berriasian	43
Oppeliidae	*Doridiscus*		*rotulus*	0.2	2.34	0.53	Aptian	Aptian	48
Oppeliidae	*Falciferella*		*milbournei*	0.16	2.62	0.37	Albian	Albian	23
Oppeliidae	*Koloceras*			NA	NA	NA	Albian	Albian	NA
Oppeliidae	*Naramoceras*		*breadeni*	0.24	2.51	0.55	Albian	Albian	22
Oppeliidae	*Nothodiscus*			NA	NA	NA	Aptian	Aptian	NA
Oppeliidae	*Protaconeceras*		*patagoniense*	0.16	2.47	0.48	Hauterivian	Hauterivian	89
Oppeliidae	*Protaconeceras*		*patagoniense*	0.16	2.47	0.48	Hauterivian	Hauterivian	89
Oppeliidae	*Protaconeceras*		*patagoniense*	0.16	2.47	0.48	Hauterivian	Hauterivian	89

family	genus	subgenus	species	*U*	*w*	*S*	FAD	LAD	size (mm)
Oppeliidae	*Substreblites*		*zonarius*	0.11	3.06	0.4	Tithonian	Valanginian	47
Oppeliidae	*Uhligites*			NA	NA	NA	Valanginian	Valanginian	NA
Pachydiscidae	*Canadoceras*		*newberryanum*	0.27	1.97	0.74	Santonian	Campanian	156
Pachydiscidae	*Eopachydiscus*		*marcianus*	0.21	2.36	NA	Albian	Albian	140
Pachydiscidae	*Eupachydiscus*		*arbucklensis*	0.3	2.02	0.8	Coniacian	Campanian	132
Pachydiscidae	*Eupachydiscus*		*isculensis*	0.27	2.08	NA	Coniacian	Campanian	202
Pachydiscidae	*Lewesiceras*		*mantelli*	0.29	2.68	1.07	Cenomanian	Coniacian	52
Pachydiscidae	*Menabonites*		*anapadensis*	0.31	2.17	1.26	Turonian	Coniacian	97
Pachydiscidae	*Menuites*		*fascicostatus*	0.28	2.19	NA	Coniacian	Maastrichtian	96
Pachydiscidae	*Menuites*		*menu*	0.26	2.19	1.24	Coniacian	Maastrichtian	71
Pachydiscidae	*Nowakites*		*carezi*	0.32	2.16	NA	Coniacian	Santonian	59
Pachydiscidae	*Nowakites*		*klamathonis*	0.36	1.29	1	Coniacian	Santonian	170
Pachydiscidae	*Pachydiscoides*		*janeti*	0.25	2.3	1.22	Coniacian	Santonian	46
Pachydiscidae	*Pachydiscus*	*Neodesmoceras*		NA	NA	NA	Maastrichtian	Maastrichtian	NA
Pachydiscidae	*Pachydiscus*	*Pachydiscus*	*compressus*	0.22	2.24	0.56	Campanian	Maastrichtian	85
Pachydiscidae	*Patagiosites*		*patagiosus*	NA	NA	NA	Santonian	Maastrichtian	57
Pachydiscidae	*Pseudojacobites*		*farmeryi*	0.31	1.91	NA	Turonian	Coniacian	78
Pachydiscidae	*Teshioites*		*ryugasensis*	0.28	2.41	0.94	Campanian	Campanian	109
Pachydiscidae	*Tongoboryceras*		*tongoboryense*	0.29	2.22	1.48	Turonian	Coniacian	62
Pachydiscidae	*Tuberodiscoides*		*termierorum*	0.33	1.9	0.94	Santonian	Santonian	59
Pachydiscidae	*Urakawites*		*rotalinoides*	0.32	2.37	1.01	Campanian	Campanian	104
Placenticeratidae	*Hengestites*		*applanatus*	0.13	2.7	0.33	Albian	Albian	178
Placenticeratidae	*Hoplitoplacenticeras*		*plasticus*	0.2	2.16	0.93	Campanian	Maastrichtian	75
Placenticeratidae	*Metaplacenticeras*		*pacificum*	NA	NA	NA	Santonian	Campanian	80
Placenticeratidae	*Metaplacenticeras*		*subtilistriatum*	0.14	2.32	NA	Santonian	Campanian	68
Placenticeratidae	*Plancenticeras*		*bidorsatum*	0.19	1.96	NA	Albian	Campanian	93

family	genus	subgenus	species	*U*	*w*	*S*	FAD	LAD	size (mm)
Placenticeratidae	*Plancenticeras*		*fritschi*	0.13	2.13	0.53	Albian	Campanian	65
Placenticeratidae	*Plancenticeras*		*gradaloupae*	0.23	2.22	0.78	Albian	Campanian	162
Placenticeratidae	*Plancenticeras*		*grossouvrei*	NA	NA	NA	Albian	Campanian	114
Placenticeratidae	*Plancenticeras*		*mediasiaticum*	NA	NA	NA	Albian	Campanian	NA
Placenticeratidae	*Plancenticeras*		*placenta*	NA	NA	NA	Albian	Campanian	64
Polyptychitidae	*Borealites*	*Borealites*	*bidevexus*	NA	NA	NA	Berriasian	Berriasian	57
Polyptychitidae	*Borealites*	*Borealites*	*fedorovi*	0.35	1.45	1.01	Berriasian	Berriasian	58
Polyptychitidae	*Borealites*	*Ronkinites*	*rossicus*	0.37	1.34	0.89	Berriasian	Berriasian	74
Polyptychitidae	*Craspedites*	*Craspedites*	*okensis*	0.29	0.76	1.23	Berriasian	Berriasian	55
Polyptychitidae	*Craspedites*	*Kachpurites*	*fulgens*	0.4	1.7	0.89	Berriasian	Berriasian	51
Polyptychitidae	*Craspedites*	*Kachpurites*	*fulgens*	0.4	1.7	0.89	Berriasian	Berriasian	51
Polyptychitidae	*Craspedites*	*Kachpurites*	*nekrassovi*	0.32	1.8	0.84	Berriasian	Berriasian	49
Polyptychitidae	*Craspedites*	*Taimyroceras*	*taimyrensis*	0.28	1.8	0.87	Berriasian	Berriasian	61
Polyptychitidae	*Delphinites*		cf. *kurmyschensis*	0.21	2.22	NA	Valanginian	Valanginian	32
Polyptychitidae	*Delphinites*		*kurmyschensis*	NA	NA	0.67	Valanginian	Valanginian	81
Polyptychitidae	*Delphinites*		*ritteri*	0.28	3.35	NA	Valanginian	Valanginian	26
Polyptychitidae	*Delphinites*		*undulatoplicatile*	NA	NA	NA	Valanginian	Valanginian	131
Polyptychitidae	*Dichotomites*	*Dichotomites*	*bidichotomus*	0.27	1.49	NA	Valanginian	Valanginian	113
Polyptychitidae	*Dichotomites*	*Dichotomites*	*grotriani*	0.26	1.49	0.63	Valanginian	Valanginian	291
Polyptychitidae	*Dichotomites*	*Prodichotomites*	*polytomus*	0.21	2.13	0.71	Valanginian	Valanginian	137
Polyptychitidae	*Garniericeras*		*catenulatum*	0.14	1.89	0.5	Berriasian	Berriasian	75
Polyptychitidae	*Garniericeras*		*interjectum*	0.19	1.89	0.55	Berriasian	Berriasian	52
Polyptychitidae	*Hectoroceras*	*Hectoroceras*	*kochi*	0.12	2.04	0.37	Berriasian	Berriasian	85
Polyptychitidae	*Hectoroceras*	*Shulginites*	*tolijense*	0.23	1.95	0.58	Berriasian	Berriasian	75
Polyptychitidae	*Homolsomites*		*oregonensis*	0.12	2.2	NA	Valanginian	Hauterivian	107
Polyptychitidae	*Homolsomites*		*stantoni*	0.17	1.98	0.69	Valanginian	Hauterivian	51

family	genus	subgenus	species	*U*	*w*	*S*	FAD	LAD	size (mm)
Polyptychitidae	*Menjaites*		*certus*	0.23	2.23	0.8	Valanginian	Valanginian	54
Polyptychitidae	*Menjaites*		*imperceptus*	0.21	1.79	0.67	Valanginian	Valanginian	78
Polyptychitidae	*Nikitinoceras*	*Bodylevskiceras*	*elegans*	0.17	1.67	0.66	Valanginian	Valanginian	71
Polyptychitidae	*Nikitinoceras*	*Nikitinoceras*	*hoplitoides*	0.25	1.99	0.93	Valanginian	Valanginian	37
Polyptychitidae	*Nikitinoceras*	*Nikitinoceras*	*inflatum*	0.23	0.89	1.12	Valanginian	Valanginian	62
Polyptychitidae	*Nikitinoceras*	*Russanovia*	*diptychum*	0.31	1.45	1.76	Valanginian	Valanginian	58
Polyptychitidae	*Nikitinoceras*	*Russanovia*	*rudis*	0.29	1.71	1.14	Valanginian	Valanginian	52
Polyptychitidae	*Paquiericeras*	*Julianites*	*undulatum*	0.36	2.4	NA	Valanginian	Valanginian	37
Polyptychitidae	*Paquiericeras*	*Paquiericeras*	*paradoxum*	0.36	2.15	0.69	Valanginian	Valanginian	31
Polyptychitidae	*Paquiericeras*	*Paquiericeras*	*paradoxum tuberculatum*	0.43	2.04	0.5	Valanginian	Valanginian	55
Polyptychitidae	*Peregrinoceras*		cf. *albidum*	0.29	1.45	0.85	Berriasian	Berriasian	41
Polyptychitidae	*Peregrinoceras*		*pressulum*	0.24	1.66	NA	Berriasian	Berriasian	70
Polyptychitidae	*Platylenticeras*	*Platylenticeras*	*heteropleurum*	0.19	2.41	0.5	Valanginian	Valanginian	74
Polyptychitidae	*Platylenticeras*	*Platylenticeras*	*heteropleurum*	0.19	2.41	0.5	Valanginian	Valanginian	74
Polyptychitidae	*Platylenticeras*	*Tolypeceras*	*marcousianum*	0.31	2.19	0.59	Valanginian	Valanginian	102
Polyptychitidae	*Polyptychites*	*Astieriptychites*	*astieriptychus*	0.26	1.45	1.34	Valanginian	Valanginian	81
Polyptychitidae	*Polyptychites*	*Euryptychites*	*latissimus*	0.34	1.61	2	Valanginian	Valanginian	149
Polyptychitidae	*Polyptychites*	*Polyptychites*	*euomphalus*	0.32	1.98	NA	Valanginian	Valanginian	42
Polyptychitidae	*Polyptychites*	*Polyptychites*	*keyserlingi*	0.31	1.5	1.35	Valanginian	Valanginian	136
Polyptychitidae	*Polyptychites*	*Primitiviptychites*	*rectangulatum*	0.23	2.14	1.48	Valanginian	Valanginian	44
Polyptychitidae	*Polyptychites*	*Siberiptychites*	*stubendorffi*	0.22	1.68	1.25	Valanginian	Valanginian	107
Polyptychitidae	*Polyptychites*	*Siberites*	*savitzkii*	0.23	2.33	NA	Valanginian	Valanginian	60
Polyptychitidae	*Praetollia*		*maynci*	NA	NA	NA	Berriasian	Berriasian	73
Polyptychitidae	*Simbirskites*	*Craspedodiscus*	*clypeiformis*	0.09	1.97	0.34	Hauterivian	Hauterivian	164
Polyptychitidae	*Simbirskites*	*Craspedodiscus*	*discofalcatus*	0.18	2.14	0.49	Hauterivian	Hauterivian	142

family	genus	subgenus	species	*U*	*w*	*S*	FAD	LAD	size (mm)
Polyptychitidae	*Simbirskites*	*Hollisites*	*aguila*	0.29	1.51	NA	Hauterivian	Hauterivian	139
Polyptychitidae	*Simbirskites*	*Hollisites*	*dichotomus*	0.31	1.28	NA	Hauterivian	Hauterivian	41
Polyptychitidae	*Simbirskites*	*Hollisites*	*lucasi*	0.33	2.08	1.01	Hauterivian	Hauterivian	219
Polyptychitidae	*Simbirskites*	*Milanowskia*	*spetonensis*	0.26	1.9	0.87	Hauterivian	Hauterivian	37
Polyptychitidae	*Simbirskites*	*Simbirskites*	*arminius*	NA	NA	NA	Hauterivian	Hauterivian	87
Polyptychitidae	*Simbirskites*	*Simbirskites*	*decheni*	0.43	2.29	1.52	Hauterivian	Hauterivian	63
Polyptychitidae	*Simbirskites*	*Simbirskites*	*nodocinctus*	0.45	1.58	NA	Hauterivian	Hauterivian	47
Polyptychitidae	*Simbirskites*	*Simbirskites*	*picteti*	NA	NA	NA	Hauterivian	Hauterivian	79
Polyptychitidae	*Simbirskites*	*Speetoniceras*	*inverselobatus*	0.46	2	0.85	Hauterivian	Hauterivian	268
Polyptychitidae	*Simbirskites*	*Speetoniceras*	*inversum*	0.44	1.49	NA	Hauterivian	Hauterivian	83
Polyptychitidae	*Simbirskites*	*Speetoniceras*	*subbipliciformis*	0.43	1.65	NA	Hauterivian	Hauterivian	29
Polyptychitidae	*Subcraspedites*	*Runctonia*	*runctoni*	NA	NA	0.6	Berriasian	Berriasian	46
Polyptychitidae	*Subcraspedites*	*Subcraspedites*	*sowerbyi*	0.23	2.16	0.92	Berriasian	Berriasian	69
Polyptychitidae	*Subcraspedites*	*Swinnertonia*	*cristatus*	NA	NA	0.79	Berriasian	Berriasian	23
Polyptychitidae	*Subcraspedites*	*Swinnertonia*	*subundulatus*	0.43	1.28	NA	Berriasian	Berriasian	66
Polyptychitidae	*Surites*	*Bojarkia*	*mesezhnikowi*	0.3	1.87	0.81	Berriasian	Berriasian	100
Polyptychitidae	*Surites*	*Bojarkia*	*stenomphalus*	0.24	2.25	0.66	Berriasian	Berriasian	61
Polyptychitidae	*Surites*	*Caseyiceras*	*caseyi*	0.36	1.6	1.18	Berriasian	Berriasian	61
Polyptychitidae	*Surites*	*Externiceras*	*solowaticus*	0.4	1.57	0.84	Berriasian	Berriasian	57
Polyptychitidae	*Surites*	*Lynnia*	*icenii*	0.32	1.98	0.97	Berriasian	Berriasian	52
Polyptychitidae	*Surites*	*Praesurites*	*elegans*	0.21	1.59	0.76	Berriasian	Berriasian	46
Polyptychitidae	*Surites*	*Surites*	*pechorensis*	NA	NA	NA	Berriasian	Berriasian	73
Polyptychitidae	*Surites*	*Surites*	*pseudostenomphalus*	0.21	1.78	0.99	Berriasian	Berriasian	52
Polyptychitidae	*Surites*	*Surites*	*simplex*	0.23	1.58	1.02	Berriasian	Berriasian	37
Polyptychitidae	*Thorsteinssonoceras*		*ellesmerense*	0.3	2.15	1.3	Valanginian	Valanginian	92
Polyptychitidae	*Tollia*	*Neocraspedites*	*semilaevis*	0.17	1.58	0.78	Valanginian	Valanginian	80

family	genus	subgenus	species	*U*	*w*	*S*	FAD	LAD	size (mm)
Polyptychitidae	*Tollia*	*Tollia*	sp. aff. *tolli*	NA	NA	NA	Valanginian	Valanginian	36
Polyptychitidae	*Tollia*	*Tollia*	*tolli*	0.21	1.83	0.61	Valanginian	Valanginian	113
Polyptychitidae	*Virgatoptychites*	*Propolyptychites*	*pumilio*	0.27	2.07	NA	Valanginian	Valanginian	20
Polyptychitidae	*Virgatoptychites*	*Propolyptychites*	*quadrifidus*	0.28	1.82	1.15	Valanginian	Valanginian	65
Polyptychitidae	*Virgatoptychites*	*Virgatoptychites*	*pachsaensis*	0.22	1.6	0.58	Valanginian	Valanginian	113
Pseudotissotiidae	*Choffaticeras*	*Choffaticeras*	*meslei*	0.23	1.22	1.07	Turonian	Turonian	171
Pseudotissotiidae	*Choffaticeras*	*Leoniceras*	*luciae*	0.25	1.52	0.53	Turonian	Turonian	151
Pseudotissotiidae	*Donenriquoceras*		*forbesiceratiforme*	0.04	2.41	0.47	Turonian	Turonian	80
Pseudotissotiidae	*Eotissotia*		*simplex*	0.07	2.86	0.45	Turonian	Turonian	63
Pseudotissotiidae	*Hemitissotia*		*cazini*	NA	NA	NA	Coniacian	Coniacian	NA
Pseudotissotiidae	*Hemitissotia*		*galeppei*	0.15	2.31	0.5	Coniacian	Coniacian	141
Pseudotissotiidae	*Hemitissotia*		*michaleti*	0.14	1.84	NA	Coniacian	Coniacian	88
Pseudotissotiidae	*Hourcqia*		*ingens*	0.28	2.3	1.03	Turonian	Coniacian	81
Pseudotissotiidae	*Hourcqia*		*pacifica*	0.22	1.96	1.13	Turonian	Coniacian	57
Pseudotissotiidae	*Masiaposites*		*carinatus*	NA	NA	1.07	Turonian	Turonian	71
Pseudotissotiidae	*Pseudotissotia*		*galliennei*	0.23	1.79	0.76	Turonian	Turonian	133
Pseudotissotiidae	*Pseudotissotia*		*nigeriensis*	0.15	2.47	0.95	Turonian	Turonian	73
Pseudotissotiidae	*Thomasites*		*gongilense*	0.23	2.27	1.08	Turonian	Turonian	113
Pseudotissotiidae	*Thomasites*		*rollandi*	0.15	2.86	0.92	Turonian	Turonian	56
Pseudotissotiidae	*Wrightoceras*		*munieri*	0.07	2.92	0.53	Turonian	Turonian	62
Pseudotissotiidae	*Wrightoceras*		*wallsi*	0.17	3.25	0.99	Turonian	Turonian	53
Pulchelliidae	*Buergliceras*		*buerglii*	0.07	2.86	0.77	Barremian	Barremian	68
Pulchelliidae	*Coronites*			NA	NA	NA	Barremian	Barremian	NA
Pulchelliidae	*Lopholobites*		*cotteaui*	0.12	2.22	NA	Barremian	Barremian	11
Pulchelliidae	*Nicklesia*		*communis*	0.12	2.42	0.48	Barremian	Barremian	50
Pulchelliidae	*Nicklesia*		*dumasiana*	0.06	2.09	0.59	Barremian	Barremian	118

family	genus	subgenus	species	*U*	*w*	*S*	FAD	LAD	size (mm)
Pulchelliidae	*Psilotissotia*		*chalmasi*	0.07	2.91	0.52	Hauterivian	Aptian	20
Pulchelliidae	*Pulchellia*	*Carstenia*	*lindigi*	NA	NA	NA	Barremian	Barremian	82
Pulchelliidae	*Pulchellia*	*Heinzia*	*galeatoides*	0.28	1.61	0.78	Hauterivian	Barremian	91
Pulchelliidae	*Pulchellia*	*Heinzia*	*provincialis*	0.24	3.56	0.57	Hauterivian	Barremian	38
Pulchelliidae	*Pulchellia*	*Pulchellia*	*caicedi*	0.12	1.9	0.99	Hauterivian	Barremian	45
Pulchelliidae	*Pulchellia*	*Pulchellia*	*galeata*	0.37	1.81	NA	Hauterivian	Barremian	34
Pulchelliidae	*Pulchellia*	*Pulchellia*	*orbignyi*	0.09	2.39	0.6	Hauterivian	Barremian	72
Pulchelliidae	*Subpulchellia*		*oehlerti*	0.1	3.07	0.54	Barremian	Aptian	20
Pulchelliidae	*Subpulchellia*		*prisca*	0.07	2.25	0.46	Barremian	Aptian	61
Schloenbachiidae	*Schloenbachia*		*varians*	0.26	2.3	0.8	Cenomanian	Cenomanian	66
Silesitidae	*Miyakoceras*		sp.	0.43	2.15	0.91	Aptian	Aptian	20
Silesitidae	*Miyakoceras*		*tanohatense*	0.44	2.1	NA	Aptian	Aptian	13
Silesitidae	*Neoastieria*		*patagonica*	0.4	2.43	1.26	Aptian	Aptian	52
Silesitidae	*Neoastieria*		*reliqua*	0.37	2.16	NA	Aptian	Aptian	14
Silesitidae	*Neosilesites*		*balearensis*	0.46	1.85	1.12	Aptian	Albian	20
Silesitidae	*Neosilesites*		*balearensis*	0.46	1.85	1.12	Aptian	Albian	20
Silesitidae	*Neosilesites*		*nepos*	0.48	1.32	NA	Aptian	Albian	21
Silesitidae	*Silesites*		*seranonis*	0.46	2.17	0.82	Barremian	Barremian	77
Sphenodiscidae	*Coahuilites*		*cavinsi*	NA	NA	NA	Campanian	Maastrichtian	55
Sphenodiscidae	*Coahuilites*		*sheltoni*	0.04	2.17	0.42	Campanian	Maastrichtian	111
Sphenodiscidae	*Daradiceras*		*gignouxi*	NA	NA	NA	Maastrichtian	Maastrichtian	107
Sphenodiscidae	*Eulophoceras*		*austriaca*	NA	NA	0.43	Coniacian	Campanian	82
Sphenodiscidae	*Eulophoceras*		*jacobi*	0.02	3.19	0.34	Coniacian	Campanian	69
Sphenodiscidae	*Indoceras*		*baluchistanense*	NA	NA	NA	Maastrichtian	Maastrichtian	87
Sphenodiscidae	*Lenticeras*		*andii*	0.03	1.87	0.98	Coniacian	Santonian	91
Sphenodiscidae	*Libycoceras*		*ismaeli*	0.05	2.02	0.47	Campanian	Maastrichtian	114

family	genus	subgenus	species	*U*	*w*	*S*	FAD	LAD	size (mm)
Sphenodiscidae	*Manambolites*	*Manambolites*	*piveteaui*	0.06	1.51	0.41	Campanian	Maastrichtian	74
Sphenodiscidae	*Manambolites*	*Praemanambolites*	*hourcqui*	0.04	1.23	0.62	Campanian	Campanian	202
Sphenodiscidae	*Paralenticeras*		*sieversi*	NA	NA	NA	Coniacian	Santonian	64
Sphenodiscidae	*Paralenticeras*		*spathi*	NA	NA	NA	Coniacian	Santonian	19
Sphenodiscidae	*Sphenodiscus*		*lobatus*	NA	NA	0.5	Campanian	Maastrichtian	291
Sphenodiscidae	*Sphenodiscus*		*pleurisepta*	0.06	2.08	0.32	Campanian	Maastrichtian	92
Tissotiidae	*Metatissotia*		*bakundu*	NA	NA	NA	Coniacian	Coniacian	NA
Tissotiidae	*Metatissotia*		*fourneli*	0.09	2.71	0.74	Coniacian	Coniacian	110
Tissotiidae	*Metatissotia*		*fourneli*	0.09	2.71	0.74	Coniacian	Coniacian	110
Tissotiidae	*Paratissotia*		*regularis*	0.16	2.06	0.74	Coniacian	Coniacian	42
Tissotiidae	*Tissotia*	*Subtissotia*	*inflata*	NA	NA	1.45	Coniacian	Coniacian	74
Tissotiidae	*Tissotia*	*Tissotia*	*tissoti*	0.09	1.43	NA	Coniacian	Coniacian	124
Tissotiidae	*Tissotioides*		*haplophyllus*	0.18	2.4	0.77	Coniacian	Coniacian	90
Tissotiidae	*Tissotioides*		*haplophyllus*	0.18	2.4	0.77	Coniacian	Coniacian	90
Vascoceratidae	*Ezilloella*			NA	NA	NA	Turonian	Turonian	NA
Vascoceratidae	*Fagesia*		*catinus*	NA	NA	2.29	Turonian	Turonian	83
Vascoceratidae	*Fagesia*		*superstes*	0.35	1.72	2.29	Turonian	Turonian	105
Vascoceratidae	*Infabricaticeras*			NA	NA	NA	Turonian	Turonian	NA
Vascoceratidae	*Neoptychites*		*andinus*	0.13	2.19	NA	Turonian	Turonian	38
Vascoceratidae	*Neoptychites*		*cephalotus*	0.1	1.81	0.88	Turonian	Turonian	126
Vascoceratidae	*Neoptychites*		*cephalotus*	0.07	1.65	NA	Turonian	Turonian	195
Vascoceratidae	*Rubroceras*		*alatum*	0.22	2.74	1.11	Cenomanian	Cenomanian	66
Vascoceratidae	*Vascoceras*		*chevalieri*	0.18	2.35	NA	Cenomanian	Turonian	127
Vascoceratidae	*Vascoceras*		*gamai*	0.32	2.07	1.18	Cenomanian	Turonian	151

Appendix A.3: Three-dimensional morphospace showing results of kernel density estimation for the Cenomanian. Contours indicate 75% (dark orange), 50% (light orange), and 25% (yellow) density levels. Positions of taxa in morphospace are shown as black dots.

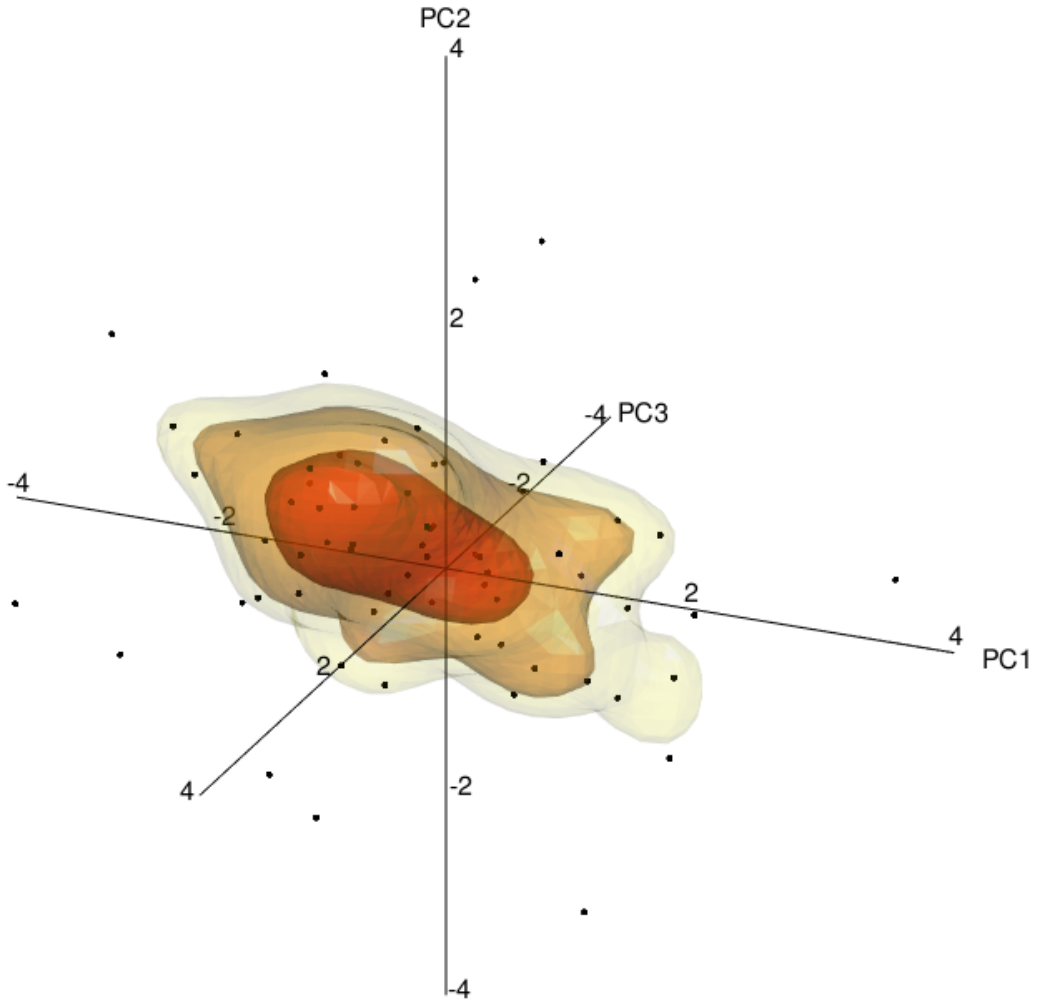

Appendix A.4: Results of hyperparameter grid search showing values used to fit final extinction models.

stage	number of trees	interaction depth	shrinkage	number of minimum observations per node
Berriasian	820	7	0.05	3
Valanginian	460	1	0.01	1
Hauterivian	760	9	0.1	1
Barremian	20	9	0.01	1
Aptian	20	7	0.0005	1
Albian	1720	3	0.05	1
Cenomanian	180	1	0.0005	3
Turonian	1560	5	0.1	5
Coniacian	140	7	0.1	5
Santonian	20	7	0.1	3
Campanian	40	1	0.1	1

Appendix A.5: Plot showing stage durations and the associated model's performance (AUROC). Gray shading indicates 95% confidence interval around the linear regression line. See Figure 1.2 for stage abbreviations.

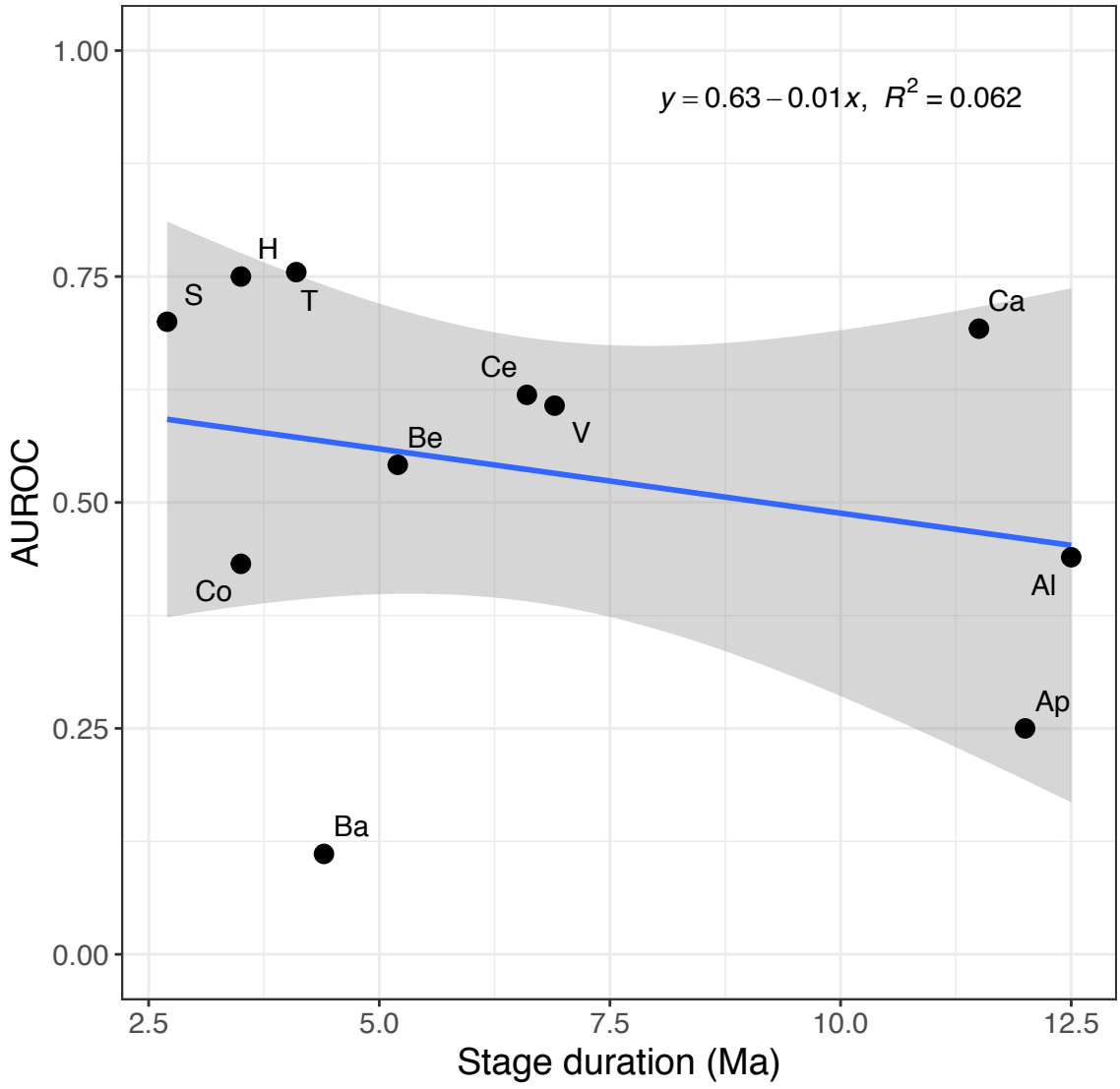

Appendix B

Supporting material for Chapter 2

Appendix B.1: List of specimens used in elliptic Fourier analysis of aperture shapes. Specimens denoted with an asterisk (*) are missing geographic coordinate data and were excluded from intraspecific shape versus latitude analyses but included in size standardization and intraspecific comparisons.

species	USNM catalog no. (PAL #)	county	state	latitude	longitude	height (cm)	centroid size
Acanthoceras amphibolum	108826	Johnson	TX	32.38	-97.36	(1) 3.00, (2) 1.16	(1) 1.64, (2) 0.55
Acanthoceras amphibolum	239766	McKinley	NM	35.57	-108.26	1.02	0.59
Acanthoceras amphibolum	239768	McKinley	NM	35.57	-108.26	1.08	0.52
Acanthoceras amphibolum	239769	Valencia	NM	34.72	-106.81	1.68	0.85
Acanthoceras amphibolum	239771	Valencia	NM	34.72	-106.81	2.49	1.23
Acanthoceras amphibolum	239772	Valencia	NM	34.72	-106.81	1.68	0.84
Acanthoceras amphibolum	239773	Valencia	NM	34.72	-106.81	2.75	1.30
Acanthoceras amphibolum	252729	Niobara	WY	43.06	-104.47	2.07	1.05
Acanthoceras amphibolum	416063	Dona Ana	NM	32.35	-106.83	3.18	1.62
Acanthoceras amphibolum	420216	Johnson	TX	32.38	-97.36	1.78	0.79
Acanthoceras amphibolum	420218	Johnson	TX	32.38	-97.36	1.97	0.99
Acanthoceras amphibolum	420220	Johnson	TX	32.38	-97.36	5.07	2.50
Acanthoceras amphibolum	420221	Johnson	TX	32.38	-97.36	3.78	1.83
Acanthoceras amphibolum	420223	Grayson	TX	33.62	-96.68	2.26	1.09
Acanthoceras amphibolum	420224	Bell	TX	31.04	-97.48	2.59	1.41
Acanthoceras amphibolum	420226	Johnson	TX	32.38	-97.36	0.66	0.32
Acanthoceras amphibolum	420227	Johnson	TX	32.38	-97.36	0.71	0.34
Acanthoceras amphibolum	420230	Johnson	TX	32.38	-97.36	1.72	0.81
Acanthoceras amphibolum	420231	Johnson	TX	32.38	-97.36	5.52	2.80
Acanthoceras bellense	388094	Weston	WY	43.85	-104.57	0.67	0.37
Acanthoceras bellense	388095	Weston	WY	43.85	-104.57	0.87	0.45
Acanthoceras bellense	388097	Weston	WY	43.85	-104.57	0.47	0.23
Acanthoceras bellense	388098	Weston	WY	43.85	-104.57	1.56	0.84
Acanthoceras bellense	388100	Weston	WY	43.85	-104.57	3.42	1.88
Acanthoceras bellense	388102	Weston	WY	43.85	-104.57	1.79	0.95
Acanthoceras bellense	388103	Weston	WY	43.85	-104.57	2.06	1.10
Acanthoceras bellense	388104	Weston	WY	43.85	-104.57	1.18	0.61
Acanthoceras bellense	388109	Weston	WY	43.85	-104.57	2.10	1.14
Acanthoceras muldoonense	388112	Johnson	WY	44.04	-106.59	0.90	0.43
Acanthoceras muldoonense	388113	Johnson	WY	44.04	-106.59	1.13	0.55

species	USNM catalog no. (PAL #)	county	state	latitude	longitude	height (cm)	centroid size
Acanthoceras muldoonense	388114	Johnson	WY	44.04	-106.59	1.26	0.58
Acanthoceras muldoonense	388115	Johnson	WY	44.04	-106.59	0.57	0.30
Acanthoceras muldoonense	388116	Johnson	WY	44.04	-106.59	1.41	0.70
Acanthoceras muldoonense	388118	Johnson	WY	44.04	-106.59	1.28	0.63
Acanthoceras muldoonense	388119	Johnson	WY	44.04	-106.59	2.30	1.06
Acanthoceras muldoonense	388121	Johnson	WY	44.04	-106.59	2.76	1.37
Alzadites alzadensis	423709	Carter	MT	45.52	-104.52	0.97	0.39
Alzadites alzadensis	423710	Carter	MT	45.52	-104.52	0.80	0.35
Alzadites alzadensis	423712	Carter	MT	45.52	-104.52	0.66	0.32
Alzadites alzadensis	423713	Carter	MT	45.52	-104.52	0.58	0.26
Calycoceras canitaurinum	422690	Big Horn	WY	44.53	-107.99	2.51	1.33
Calycoceras canitaurinum	422691	Carbon	WY	41.70	-106.93	2.63	1.42
Calycoceras canitaurinum	422697	Big Horn	WY	44.53	-107.99	6.38	3.47
Calycoceras guerangeri	425182	Luna	NM	32.18	-107.75	3.08	1.68
Calycoceras inflatum	425180	Luna	NM	32.18	-107.75	4.13	2.23
Calycoceras naviculare	166374	Las Animas	CO	37.32	-104.04	6.78	3.13
Calycoceras newboldi	376908	Natrona	WY	42.97	-106.76	9.38	5.36
Calycoceras obrieni	422681	Apache	AZ	35.39	-109.49	5.29	2.96
Conlinoceras tarrantense	105962	Tarrant	TX	32.77	-97.29	5.19	2.71
Conlinoceras tarrantense	105964	Tarrant	TX	32.77	-97.29	5.49	2.80
Conlinoceras tarrantense	105965	Denton	TX	33.21	-97.12	4.93	2.56
Conlinoceras tarrantense	105968	Tarrant	TX	32.77	-97.29	3.53	1.68
Conlinoceras tarrantense	163913	Pueblo	CO	38.17	-104.49	1.26	0.60
Conlinoceras tarrantense	239763	Valencia	NM	34.72	-106.81	3.98	1.97
Conlinoceras tarrantense	239764	Valencia	NM	34.72	-106.81	4.82	2.47
Metoicoceras crassicostae	106003	Grayson	TX	33.62	-96.68	4.04	1.91
Metoicoceras frontierense	376927	Johnson	WY	44.04	-106.59	3.90	1.57
*Metoicoceras geslinianum**	29498		UT			6.25	2.45
Metoicoceras geslinianum	411503	Ellis	TX	32.35	-96.80	7.41	2.64
*Metoicoceras geslinianum**	411504		TX			8.00	3.05
*Metoicoceras geslinianum**	411506		TX			10.47	3.95
Metoicoceras geslinianum	411507	Ellis	TX	32.35	-96.80	10.66	3.98
Metoicoceras geslinianum	425303	Grant	NM	32.73	-108.38	2.20	0.88
Metoicoceras geslinianum	427950	Ellis	TX	32.35	-96.80	6.85	2.29

species	USNM catalog no. (PAL #)	county	state	latitude	longitude	height (cm)	centroid size
Metoicoceras latoventer	106001	Grayson	TX	33.62	-96.68	1.17	0.56
Metoicoceras mosbyense	108316a	Petroleum	MT	47.14	-108.23	0.74	0.32
Metoicoceras mosbyense	108317a	Petroleum	MT	47.14	-108.23	2.13	0.87
Metoicoceras mosbyense	108317b	Petroleum	MT	47.14	-108.23	4.28	1.48
Metoicoceras mosbyense	108318a	Petroleum	MT	47.14	-108.23	4.79	1.70
Metoicoceras mosbyense	108318b	Petroleum	MT	47.14	-108.23	3.40	1.22
Metoicoceras mosbyense	108319b	Petroleum	MT	47.14	-108.23	6.40	2.44
Metoicoceras mosbyense	108321	Petroleum	MT	47.14	-108.23	8.59	3.00
Metoicoceras mosbyense	108322a	Petroleum	MT	47.14	-108.23	7.21	2.60
Metoicoceras mosbyense	108323b	Petroleum	MT	47.14	-108.23	6.40	2.22
Metoicoceras mosbyense	220382	Petroleum	MT	47.14	-108.23	4.47	1.59
Metoicoceras mosbyense	423759	Crook	WY	44.59	-104.57	1.04	0.43
Metoicoceras mosbyense	425308	Hidalgo	NM	31.90	-108.75	2.10	0.84
Metoicoceras mosbyense	427947	Petroleum	MT	47.14	-108.23	2.61	0.93
Metoicoceras mosbyense	427949	Petroleum	MT	47.14	-108.23	5.12	2.21
Metoicoceras mosbyense	443802	Natrona	WY	42.97	-106.76	2.10	0.77
Metoicoceras praecox	427908	Big Horn	WY	44.53	-107.99	2.31	0.91
Metoicoceras praecox	427909	Big Horn	WY	44.53	-107.99	2.52	0.99
Metoicoceras praecox	427915	Big Horn	WY	44.53	-107.99	3.74	1.32
Metoicoceras praecox	427918	Big Horn	WY	44.53	-107.99	4.24	1.53
Metoicoceras praecox	427936	Big Horn	WY	44.53	-107.99	4.99	2.09
Metoicoceras swallovi	105992b	Lamar	TX	33.67	-95.57	3.35	1.42
Metoicoceras swallovi	427941	Lamar	TX	33.67	-95.57	1.31	0.61
Metoicoceras swallovi	427942	Lamar	TX	33.67	-95.57	2.22	1.01
Plesiacanthoceras bellsanum	105984	Grayson	TX	33.62	-96.68	3.47	1.61
Plesiacanthoceras wyomingense	220381	Carter	MT	45.52	-104.52	3.18	1.55
Plesiacanthoceras wyomingense	388156	Carter	MT	45.52	-104.52	0.83	0.41
Plesiacanthoceras wyomingense	388157	Carter	MT	45.52	-104.52	1.01	0.47
Plesiacanthoceras wyomingense	388158	Carter	MT	45.52	-104.52	1.12	0.50
Plesiacanthoceras wyomingense	388162	Carter	MT	45.52	-104.52	1.26	0.56
Plesiacanthoceras wyomingense	388163	Carter	MT	45.52	-104.52	1.20	0.54
Plesiacanthoceras wyomingense	388168	Carter	MT	45.52	-104.52	3.77	1.75
Plesiacanthoceras wyomingense	388169	Carter	MT	45.52	-104.52	5.72	2.72
Tarrantoceras bentonianum	400813	Luna	NM	32.18	-107.75	1.03	0.49

species	USNM catalog no. (PAL #)	county	state	latitude	longitude	height (cm)	centroid size
Tarrantoceras bentonianum	411489	Dallas	TX	32.77	-96.78	1.71	0.76
Tarrantoceras conlini	400805	Grant	NM	32.73	-108.38	1.04	0.46
Tarrantoceras conlini	400808	Grant	NM	32.73	-108.38	1.59	0.74
Tarrantoceras cuspidum	105974	Grayson	TX	33.62	-96.68	1.15	0.60
Tarrantoceras exile	423698	Weston	WY	43.85	-104.57	0.47	0.23
Tarrantoceras sellardsi	108841	Johnson	TX	32.38	-97.36	2.04	1.00
Tarrantoceras sellardsi	108855	Tarrant	TX	32.77	-97.29	1.03	0.49
Tarrantoceras sellardsi	108861	Tarrant	TX	32.77	-97.29	(1) 1.13, (2) 0.50, (3) 0.42	(1) 0.57, (2) 0.29, (3) 0.23
Tarrantoceras sellardsi	239761	Sandoval	NM	35.69	-106.88	0.75	0.35
Tarrantoceras sellardsi	400761	Santa Fe	NM	35.51	-105.97	2.94	1.42
Tarrantoceras sellardsi	400765	Johnson	TX	32.38	-97.36	1.69	0.80
Tarrantoceras sellardsi	400766	Tarrant	TX	32.77	-97.29	0.82	0.43
Tarrantoceras sellardsi	400767	Tarrant	TX	32.77	-97.29	0.56	0.29
Tarrantoceras sellardsi	400769	Johnson	TX	32.38	-97.36	1.68	0.78

Appendix B.2: Results of Procrustes ANOVA for assessing measurement error through repeated measurements of three specimens indicating highly significant inter-specimen differences ($p << 0.01$) and little remaining variation attributed to intra-specimen differences.

	Df	SS	MS	Rsq	F	Z	Pr(>F)
specimen	2	0.0195	0.0098	0.9642	161.7974	6.751	0.001
Residuals	12	0.0007	0.0001				
Total	14	0.0203					

Appendix B.3: Elliptical Fourier descriptors of ammonite aperture shapes before size standardization. Specimen numbers are arranged according to Appendix 2.1. Descriptors consist of four coefficients (here referred to as A-D) for the first seven harmonics (1-7).

USNM catalog no. (PAL #)	A1	A2	A3	A4	A5	A6	A7
108826(1)	0.2305	0.0273	0.0175	0.0087	0.0008	0.0065	0.011
108826(2)	0.421	-0.0048	0.0268	0.0121	0.0355	0.0729	0.0598
239766	0.5352	-0.0778	-0.0356	0.029	-0.0121	0.0159	0.052
239768	0.3266	-0.0687	0.039	-0.0752	-0.05	0.0255	0.0123
239769	0.0044	0.0254	-0.0105	0.0026	-0.0062	0.0005	0.0102
239771	0.2794	-0.0279	0.0396	-0.0402	0.0022	0.0287	0.0179
239772	0.8326	-0.081	0.0064	-0.078	0.0376	0.1405	0.0543
239773	0.4559	-0.016	0.0227	-0.0517	-0.0246	0.0254	0.0251
252729	0.1441	0.0056	0.0142	0.0056	0.0437	0.0792	0.0671
416063	0.6351	-0.0893	0.0101	-0.1211	-0.041	0.0476	0.05
420216	0.2364	0.0114	-0.0049	0.002	0.0015	-0.0024	0.0193
420218	-0.0961	0.114	0.0278	0.0321	0.0073	-0.0103	-0.0006
420220	0.1595	0.0144	-0.0035	-0.0207	-0.0092	0.0097	0.0145
420221	0.4694	-0.0318	0.0109	-0.0331	-0.0208	0.0479	0.0523
420223	0.0673	-0.0139	-0.008	-0.0082	0.0101	0.0091	-0.0024
420224	0.405	-0.0715	-0.0097	-0.0562	-0.0306	0.0228	0.0162
420226	0.7519	-0.1154	-0.0162	0.0285	0.0354	0.0898	0.1177
420227	0.5943	-0.0568	0.0545	-0.0133	0.0636	0.1279	0.0159
420230	-0.0492	0.0689	-0.0231	0.0207	0.0023	-0.0423	-0.0081
420231	0.5295	-0.074	-0.022	-0.0152	-0.0077	0.054	0.0304
388094	0.326	-0.016	-0.0424	-0.0076	0.0369	0.0425	0.0259
388095	0.198	-0.0333	-0.0161	-0.0024	-0.0157	-0.0059	0.0335
388097	0.7508	0.0461	-0.0485	-0.051	0.0271	0.0397	0.0586
388098	-0.0233	0.0373	0.017	0.0234	0.0163	-0.0001	-0.0102
388100	0.4265	-0.0417	0.0275	-0.0425	-0.0235	0.0062	0.0032
388102	0.4766	-0.0649	-0.0023	-0.0331	-0.0028	0.0593	0.0196
388103	0.2236	-0.0708	-0.012	-0.0421	-0.035	0.0123	-0.0046
388104	0.2472	-0.0095	-0.0007	-0.006	0	0.0126	0.022
388109	0.4665	-0.054	-0.0112	0.0066	-0.0194	0.023	0.0356
388112	0.4478	-0.062	0.0178	-0.0165	0.0407	0.0727	0.0283
388113	0.0253	0.0493	0.0414	0.0243	0.0057	0.0001	0.0038
388114	0.0975	-0.0175	0.0399	0.0149	0.0211	0.0123	0.0103
388115	0.2225	-0.0392	-0.0035	0.0048	0.024	0.0245	0.0014
388116	0.4678	-0.0468	0.0414	-0.0224	0.0105	0.0647	0.0262

USNM catalog no. (PAL #)	A1	A2	A3	A4	A5	A6	A7
388118	-0.1246	0.049	0.0328	0.0415	0.0541	0.0517	0.0228
388119	0.4429	-0.0482	-0.005	-0.0348	0.0007	0.0001	0.0026
388121	0.2218	-0.022	0.0004	-0.0401	0.0038	-0.0023	0.0034
423709	0.3958	-0.1159	0.124	0.0526	0.0437	0.0583	0.0451
423710	0.7652	-0.1602	0.157	0.1204	0.0866	0.1322	0.0383
423712	1.1466	-0.1672	0.1317	-0.0093	0.0049	0.1219	0.1474
423713	0.9249	-0.2526	0.3727	0.2287	0.1657	0.1243	-0.0092
422690	0.6619	-0.1774	-0.0751	-0.0751	-0.0607	0.0025	0.0479
422691	0.1513	-0.0065	-0.0033	-0.0158	-0.0069	0.0061	0.0072
422697	0.3236	0.0228	-0.007	-0.0372	-0.004	0.022	0.0158
425182	0.3214	-0.0045	-0.0183	-0.0232	-0.0156	0.0185	0.0307
425180	0.4962	-0.0552	-0.0476	-0.099	0.0306	0.0987	0.0408
166374	0.4369	-0.068	0.0281	-0.0528	-0.024	-0.001	0.0035
376908	0.2381	0.0008	-0.028	-0.0298	-0.0241	0.0037	0.018
422681	0.1528	0.0484	-0.0022	0.0055	0.0111	0.0054	0.0155
105962	0.2279	-0.0105	-0.023	0.0018	0.0071	0.0061	0.0187
105964	0.1799	-0.0163	-0.0088	-0.0003	0.0108	0.0226	0.0201
105965	0.1651	0.0084	0.0063	-0.0084	-0.0072	-0.002	0.0018
105968	0.6115	-0.0728	0.0636	-0.1257	-0.0493	0.0079	0.0111
163913	0.4076	-0.0783	0.0246	0.0208	0.0174	0.0133	0.0045
239763	0.2516	-0.0161	-0.0101	-0.0016	-0.008	-0.0084	0.0217
239764	-0.2408	0.0765	0.0584	0.0622	0.0535	0.0107	-0.0132
106003	0.3182	-0.0281	0.0101	-0.0412	-0.0104	0.0269	0.0326
376927	0.2624	-0.0643	0.0472	-0.0189	0.0234	0.0414	0.028
29498	0.1659	-0.0555	0.0529	-0.0019	0.0361	0.0194	0.0093
411503	0.1158	-0.0052	0.031	0.0017	0.0366	0.0178	0.0174
411504	0.1692	-0.0425	0.0475	-0.0226	0.0309	0.0199	0.0163
411506	0.0455	0.021	0.0169	0.0121	0.0122	0.0086	0.004
411507	0.1576	-0.0324	0.0431	-0.009	0.0253	0.0191	0.0081
425303	0.0052	-0.0128	0.0045	-0.011	0.0026	-0.0044	-0.0086
427950	0.2478	-0.0277	0.0257	-0.018	0.0831	0.0079	0.0828
106001	0.4716	-0.0947	0.0231	-0.0854	-0.0016	0.0769	0.0347
108316a	0.2347	-0.11	0.0123	-0.0381	0.0426	0.0239	0.0078
108317a	0.294	-0.1044	0.0384	0.0243	0.0409	0.058	0.0088
108317b	0.2591	-0.0277	0.0603	0.0101	0.0624	0.035	0.0625
108318a	0.1094	-0.0253	0.016	-0.014	0.0244	0.0047	0.0189
108318b	0.1947	-0.0386	0.0219	-0.0222	0.0499	0.0202	0.0499

USNM catalog no. (PAL #)	A1	A2	A3	A4	A5	A6	A7
108319b	0.2388	-0.0694	0.0514	0.0112	0.0423	0.0209	0.0261
108321	0.2656	-0.086	0.0368	-0.0516	0.0461	0.0004	0.0747
108322a	0.1892	-0.0487	0.0068	-0.0026	0.0477	0.0049	0.0502
108323b	0.1501	-0.0458	0.0289	-0.0116	0.0367	-0.0078	0.0327
220382	0.0483	0.0154	0.0025	0.016	0.0139	0.0171	0.0016
423759	0.0891	-0.0141	0.0168	-0.0197	0.0145	0.0021	0.0118
425308	0.3579	-0.0597	-0.0032	-0.0629	0.0755	0.0753	0.0491
427947	0.3535	-0.0696	0.0332	-0.0422	0.0864	0.0264	0.0711
427949	-0.1169	0.0326	-0.005	0.0168	0.0101	-0.0023	0.0031
443802	0.3718	-0.0888	-0.015	-0.0173	0.0671	0.0558	0.0693
427908	0.0535	0.0046	-0.0257	-0.0171	-0.0093	0.0057	0.0085
427909	0.138	-0.0103	0.0149	-0.0223	0.0183	0.0086	0.0205
427915	0.2676	-0.0371	0.0319	-0.0442	0.0663	0.011	0.0532
427918	0.3278	-0.0284	0.0665	-0.0397	0.0735	0.0194	0.0674
427936	0.1637	-0.0246	0.0141	-0.0025	0.0084	0.0227	0.0268
105992b	0.1213	0.0312	0.0295	0.0008	0.0081	0.0172	0.0137
427941	0.2192	-0.0542	-0.0064	0.0013	0.0412	0.026	0.0142
427942	0.1689	-0.0158	0.0068	-0.0218	0.0111	0.0322	0.0205
105984	0.3893	-0.04	0.0169	-0.027	0.0425	0.0506	0.0286
220381	0.1762	0.0105	0.0039	-0.0271	0.0016	0.0271	0.0221
388156	0.7538	-0.0405	-0.1059	-0.0378	0.0038	0.1594	0.0772
388157	0.0382	0.0247	0.0442	0.0546	0.0194	0.0208	0.035
388158	0.1882	0.0056	0.0023	0.005	0.0171	0.0424	0.0551
388162	0.5786	-0.0874	0.0933	-0.0229	0.0966	0.1225	0.0457
388163	0.0039	0.0187	-0.0074	0.0072	0.0009	0.0086	0.0066
388168	0.2262	-0.101	0.0543	0.0004	-0.0069	0.0363	0.0334
388169	0.632	-0.0671	0.0135	-0.06	-0.0221	0.0155	0.0317
400813	0.3874	0.0537	0.0096	-0.0471	-0.0928	-0.0798	0.0015
411489	0.1129	0.0346	-0.0056	-0.0166	-0.0352	-0.0247	-0.0108
400805	0.2155	0.1098	0.0184	0.011	0.0044	0.0181	0.0193
400808	-0.0397	0.0131	-0.007	-0.0004	0.0003	0.0004	-0.0031
105974	1.0625	0.0711	0.0447	-0.1918	-0.0827	0.0634	0.0675
423698	0.118	0.039	0.0134	-0.0044	-0.0134	-0.0041	0.0003
108841	0.0601	-0.008	0.0065	-0.0014	-0.002	-0.005	-0.002
108855	0.6969	-0.1166	0.0711	-0.0339	-0.0573	0.0027	0.0487
108861(1)	0.27	0.0151	0.0155	-0.0325	-0.0243	-0.0024	0.0224
108861(2)	0.0192	0.1072	-0.0647	0.0019	-0.0186	-0.021	0.02

USNM catalog no. (PAL #)	A1	A2	A3	A4	A5	A6	A7
108861(3)	1.3676	-0.1664	-0.0765	0.1272	-0.0041	0.0704	0.1679
239761	0.8443	-0.0421	0.0821	-0.072	-0.008	0.0596	0.0718
400761	-0.0506	0.0081	0.0298	0.0207	0.0247	0.0118	-0.0052
400765	0.3786	-0.0154	0.0123	-0.0548	-0.0534	-0.0066	0.0213
400766	0.3017	-0.0041	0.0177	-0.0171	-0.0187	-0.0038	0.0047
400767	0.5106	-0.0784	0.0225	-0.0056	-0.0093	0.0368	-0.0081
400769	0.2858	-0.0149	-0.0191	0.0235	-0.0148	0.0217	-0.0227

USNM catalog no. (PAL #)	B1	B2	B3	B4	B5	B6	B7
108826(1)	-105.5199	2.2587	-0.5517	0.8835	0.7522	-0.3936	-0.4429
108826(2)	-101.8559	3.2982	-1.274	0.8769	-1.0196	-2.9216	-2.0447
239766	-116.252	2.6016	4.4453	-0.4608	-0.5097	-0.4169	-1.2878
239768	-99.0788	2.7349	-5.3513	2.9777	0.1733	-2.7621	-1.0724
239769	-101.169	-1.027	-2.2948	4.8342	1.1976	-1.3019	-1.0247
239771	-98.9197	3.3971	-3.1794	3.4064	-0.2523	-2.0171	-1.2139
239772	-102.336	5.824	-0.5467	2.2834	-0.8213	-2.9426	-0.9021
239773	-98.2024	-2.3461	-2.2156	2.8519	1.3822	-0.7022	-0.8766
252729	-102.035	4.1663	-2.3736	2.3566	-0.6763	-3.1274	-1.3275
416063	-100.2087	2.1355	-1.966	3.2362	0.5151	-1.5917	-1.3665
420216	-94.3753	4.1547	-4.927	0.3952	0.113	-2.3704	-2.032
420218	-99.6569	0.5897	-4.7838	4.033	1.3609	-2.4604	-0.8653
420220	-100.9131	0.2316	-0.5721	2.4768	1.0354	-1.1361	-0.7963
420221	-100.3494	3.4217	-1.7943	0.6629	0.379	-1.9935	-1.5558
420223	-98.7997	0.7244	-0.9596	3.5351	-0.0839	-1.6562	-1.0261
420224	-104.9639	2.1292	-0.0491	2.8416	1.3222	-0.9308	-0.7763
420226	-106.8527	5.2172	1.3451	-0.9041	-1.2727	-2.289	-2.6249
420227	-106.6384	7.2134	-3.6318	0.3831	-2.2175	-3.599	-0.2682
420230	-94.7607	1.9421	-4.5328	0.9446	0.6211	-1.2815	-0.5708
420231	-104.1242	2.8265	0.2625	0.1329	-0.117	-1.7273	-0.9265
388094	-113.5463	4.5744	2.9636	0.4802	-1.1353	-1.8914	-1.6151
388095	-108.1629	0.6084	0.3188	0.9864	-0.0492	-0.7148	-3.4672
388097	-110.4558	-1.1978	1.56	1.4236	-0.7383	-1.0605	-1.2508
388098	-106.7046	2.7491	-0.6567	1.4699	1.3936	-0.5856	-1.1371
388100	-105.8532	1.6665	-0.8573	2.4345	1.2677	-0.1074	-0.4967
388102	-106.1714	4.6069	-1.0484	2.11	0.4764	-1.8751	-0.5925
388103	-104.939	3.823	-2.18	1.5036	1.2714	-1.3408	-0.2787

USNM catalog no. (PAL #)	B1	B2	B3	B4	B5	B6	B7
388104	-105.1653	3.2631	-1.2539	0.5246	0.2414	-1.1034	-1.4251
388109	-108.0587	3.1813	0.2023	0.0594	1.1517	-0.8957	-1.3276
388112	-103.3248	6.0161	-1.5791	0.7927	-1.9343	-3.1018	-1.1141
388113	-106.4937	7.5584	0.3013	-1.0545	-2.4091	-3.2189	-1.586
388114	-99.7107	6.6857	-1.5291	0.1312	-2.6505	-2.0077	-1.7851
388115	-113.0197	7.7445	0.5582	-0.6713	-2.8755	-2.7724	-0.5128
388116	-103.816	4.4555	-3.2098	1.1229	-0.5389	-2.3898	-0.9128
388118	-101.119	5.825	-3.2001	1.014	0.1183	-1.7524	-0.7551
388119	-95.8656	3.2622	-1.4115	1.2956	-0.507	-0.5629	-0.7639
388121	-99.8734	2.3498	-0.6677	2.104	-1.5214	-0.4203	-0.3707
423709	-92.2179	13.7325	-9.7171	-2.6823	-2.1953	-2.1596	-1.4297
423710	-104.2081	11.7211	-7.167	-4.2441	-2.3844	-3.0247	-0.6501
423712	-101.6762	6.1237	-2.3893	0.8689	0.3487	-1.703	-2.3499
423713	-104.3581	9.876	-6.99	-2.3682	-2.1726	-2.4138	-0.5914
422690	-106.857	6.4654	1.3868	1.3325	0.8694	-0.6051	-1.4842
422691	-105.9166	1.4025	0.3731	2.7554	1.0081	-0.8921	-0.9034
422697	-107.5309	0.594	0.1974	2.8639	0.1151	-1.3478	-0.5246
425182	-111.4337	-0.1717	2.0849	2.1854	0.9949	-1.145	-1.5521
425180	-112.6689	1.161	3.3583	4.7958	-2.0648	-3.8985	-1.5657
166374	-96.1258	3.9623	-2.1152	2.1081	0.7499	-0.1698	-0.3334
376908	-110.2377	-1.5813	2.4367	2.1212	1.4898	-0.7165	-1.3823
422681	-111.9479	2.8467	2.9862	1.2885	-0.6636	-0.7493	-1.021
105962	-105.7733	7.2598	1.03	-0.3006	-0.6689	-1.1797	-1.2981
105964	-105.8668	3.4756	-0.8588	0.369	-0.1363	-1.8451	-1.404
105965	-102.2976	1.0003	-1.6389	0.9457	1.1297	0.2256	-0.3693
105968	-94.1754	0.8963	-4.918	2.7551	0.6701	-0.5769	-0.4081
163913	-101.2852	5.9993	-2.3663	-1.9806	-1.0263	-0.5536	-0.462
239763	-100.4692	3.1818	-0.8121	1.5646	0.7111	-0.2583	-0.9187
239764	-100.2391	2.3055	-1.6409	0.7731	1.4422	-0.4655	-1.0254
106003	-99.5089	3.1777	-2.1161	1.7747	-0.2784	-2.2523	-1.8132
376927	-83.5353	10.0846	-4.82	1.4874	-1.6948	-2.3449	-1.3407
29498	-84.0109	10.7906	-8.6672	-0.586	-3.8494	-2.0399	-0.9314
411503	-79.7793	7.876	-4.1337	1.3799	-5.6956	-1.5593	-2.0211
411504	-78.683	6.8902	-8.7346	1.6975	-2.5332	-1.4915	-1.8504
411506	-80.4223	4.9903	-4.5379	-0.5681	-2.8232	-0.9148	-1.6315
411507	-81.655	3.5718	-8.1565	-0.0704	-2.8672	-1.5411	-1.152
425303	-86.1833	5.5356	-3.7068	2.9564	-3.4003	-1.9197	-2.3512

USNM catalog no. (PAL #)	B1	B2	B3	B4	B5	B6	B7
427950	-71.9991	3.8818	-2.3538	1.2799	-4.7993	-0.4605	-3.5005
106001	-101.3222	2.6288	-1.3306	2.824	-1.3846	-3.2406	-1.5901
108316a	-95.4499	4.6483	-4.5171	1.4191	-3.6815	-2.6456	-1.1725
108317a	-97.4866	16.0321	-4.2032	-2.5702	-2.7389	-3.2811	-0.6892
108317b	-77.8475	5.1291	-4.6855	0.489	-3.7271	-2.0434	-2.8258
108318a	-79.4093	5.8313	-3.6494	1.1101	-4.1131	-1.4921	-2.2781
108318b	-77.0548	6.8414	-2.6117	1.9089	-3.9407	-1.674	-2.9646
108319b	-82.734	11.8503	-5.9071	-1.0572	-2.9032	-1.179	-1.3404
108321	-72.9623	8.9737	-4.477	3.1608	-2.7239	-0.1832	-3.1816
108322a	-78.8429	11.0053	-1.4406	0.5812	-4.1659	-0.3815	-2.9761
108323b	-69.7329	8.51	-4.9273	0.8025	-3.5643	0.2659	-2.2409
220382	-75.2603	3.7076	-1.7479	2.9569	-4.8991	-0.9793	-2.3877
423759	-92.9066	5.6498	-2.9529	3.3727	-4.4338	-2.5826	-1.7825
425308	-91.2023	3.2932	-3.2875	2.0465	-5.7287	-3.4964	-2.5637
427947	-81.8543	4.0733	-3.2505	0.9669	-4.7688	-1.6387	-2.9179
427949	-90.0791	6.026	-3.8005	1.3328	0.3214	-1.0704	-0.9557
443802	-79.4744	9.3788	-1.3151	0.426	-3.7687	-1.6169	-2.3913
427908	-83.6319	2.1035	-3.2426	2.8511	-3.6561	-1.2637	-2.9621
427909	-83.1228	2.7339	-3.8907	3.2036	-2.298	-0.8032	-1.7785
427915	-74.9387	4.2795	-2.6825	2.7947	-3.8677	-0.9709	-2.3796
427918	-75.8358	2.3	-4.8371	2.4882	-3.4445	-0.7899	-2.2974
427936	-90.4856	7.2272	-2.6383	0.3804	-0.8694	-2.0776	-2.0802
105992b	-86.7031	-0.1923	-4.5896	5.0715	-0.6928	-1.161	-2.1315
427941	-104.3525	9.534	2.3188	-0.713	-3.6889	-2.6529	-1.9037
427942	-98.0952	5.6589	-2.4064	2.951	-1.4159	-3.1725	-1.5996
105984	-97.2992	6.4514	-1.5977	1.6595	-1.9431	-2.0132	-1.0214
220381	-96.7513	4.3559	-2.7695	3.4756	-0.5504	-2.2254	-1.0469
388156	-103.918	3.9825	-0.1226	1.382	-1.2356	-2.6985	-1.6462
388157	-100.7147	7.7189	-3.6188	-0.4482	-1.8743	-2.9646	-1.4367
388158	-94.6424	9.6592	-4.4531	1.1736	-1.062	-3.124	-2.2898
388162	-96.2937	7.5785	-3.3356	1.4951	-2.8274	-3.4157	-1.3007
388163	-98.7987	3.6018	-2.1591	0.9954	-2.4981	-2.6026	-0.6116
388168	-91.4898	7.1108	-4.1668	2.6861	0.5792	-1.8993	-1.4002
388169	-95.6943	4.5293	-1.7378	1.694	0.2364	-0.6269	-0.7875
400813	-94.4975	-0.0291	-3.2167	1.8798	1.9979	1.276	-0.2304
411489	-90.808	0.337	-4.1808	1.7376	1.4829	0.4923	0.0686
400805	-90.7398	-0.8668	-4.6932	2.714	1.1421	0.2879	-0.5102

USNM catalog no. (PAL #)	B1	B2	B3	B4	B5	B6	B7
400808	-92.8543	2.1691	-5.0771	1.1915	2.4136	0.424	-0.3966
105974	-101.6622	-2.6907	-2.1294	4.4032	1.857	-0.9157	-0.9739
423698	-98.3684	1.5018	-2.1121	-1.1301	1.1366	0.8646	-0.9719
108841	-97.0831	-1.0313	-3.162	0.555	0.8316	0.6804	-0.2695
108855	-97.283	0.0219	-2.3508	1.6994	1.6226	-0.1368	-1.1925
108861(1)	-99.8023	-2.1316	-2.4587	3.0113	1.8644	0.1432	-1.111
108861(2)	-110.6089	1.5188	1.944	2.7367	1.014	-0.8084	-1.3159
108861(3)	-115.2477	4.4123	1.6785	-2.314	-0.154	-1.2015	-2.0328
239761	-97.7619	3.3581	-3.2593	2.1607	0.0906	-1.111	-1.227
400761	-98.3392	2.1263	-2.3301	1.3485	1.8859	-0.6075	-1.0621
400765	-95.6808	-0.2048	-2.4267	2.5132	1.5086	-0.2061	-0.8852
400766	-102.576	0.7573	-1.7308	1.5653	1.1911	0.38	-0.1821
400767	-106.4836	3.7696	-1.3574	0.6142	0.4556	-1.1067	0.1046
400769	-93.1493	-2.8997	-3.4799	2.3166	0.5067	0.6334	-0.3721

USNM catalog no. (PAL #)	C1	C2	C3	C4	C5	C6	C7
108826(1)	-94.9266	7.28	8.8075	3.7326	4.272	1.3109	1.2389
108826(2)	-97.3675	23.9153	13.5873	9.4783	3.4519	0.6762	-1.3389
239766	-82.9793	16.7898	13.6552	6.1683	0.9238	-0.2503	-1.8077
239768	-99.879	21.8482	14.2541	7.4674	4.7333	-0.7736	-1.3416
239769	-98.4947	15.7071	9.2829	6.4423	4.4928	0.5353	0.895
239771	-100.5945	16.7747	11.6794	6.9587	5.891	0.6561	1.1454
239772	-96.796	17.2279	13.184	6.7517	6.3709	1.2157	1.2421
239773	-102.0385	15.2607	7.6058	8.2595	3.6903	1.8954	0.2216
252729	-97.6797	17.1861	12.3342	6.026	4.674	-0.2926	-0.4093
416063	-100.058	12.9381	9.1647	5.4523	4.5012	0.6711	0.9538
420216	-105.4306	20.6961	11.964	9.0251	4.3665	1.1118	-0.959
420218	-100.5459	14.0297	10.2051	5.8512	5.9907	1.0225	0.6006
420220	-99.2355	13.8614	8.3734	7.0105	3.8817	1.9636	0.545
420221	-99.5214	16.086	11.2669	7.5315	4.2929	1.8471	-0.3638
420223	-101.0164	15.957	8.7845	7.7799	4.6637	1.6968	1.0018
420224	-94.6351	12.2358	10.2498	5.0101	3.9279	0.6635	0.3822
420226	-91.5736	26.5286	15.2269	9.582	2.2968	0.4296	-1.4531
420227	-88.8461	35.0665	20.8971	8.2006	2.8041	-2.8782	-2.1769
420230	-105.8201	9.6298	6.923	4.8962	4.0713	1.3973	0.6493
420231	-96.0007	13.8474	9.825	6.1507	2.9957	1.2301	-1.0801

USNM catalog no. (PAL #)	C1	C2	C3	C4	C5	C6	C7
388094	-85.0495	21.2422	14.8856	6.8948	3.0801	0.1646	-0.279
388095	-89.8841	27.0228	14.1538	9.0242	0.6263	-1.1936	-1.1114
388097	-87.6277	28.4735	14.111	9.622	0.3535	-1.4752	-2.2172
388098	-93.0271	14.9465	12.6409	6.2766	3.7697	0.3766	-0.4925
388100	-93.9774	12.0903	10.6502	5.1218	4.3265	-0.0458	0.6758
388102	-92.3969	18.3538	15.2338	6.4143	5.1298	-0.4181	-0.4813
388103	-94.3512	15.3022	13.2609	5.711	4.2146	0.4167	-1.0054
388104	-94.2106	18.0758	13.4168	7.5687	4.1923	0.5411	-0.5077
388109	-91.7552	12.611	12.7226	6.1658	3.9262	1.6908	-0.4561
388112	-94.3557	28.292	16.9945	9.7139	4.4146	-0.3672	-1.4871
388113	-91.5895	27.5775	16.8899	9.2136	3.5018	-0.0647	-1.7427
388114	-98.2938	27.462	14.9219	10.8471	4.6771	0.4939	-0.7894
388115	-83.6318	29.7915	19.9143	7.4525	2.6481	-1.9106	-1.8682
388116	-94.5474	23.5912	16.1933	7.7716	4.1188	-1.095	-1.479
388118	-97.619	19.0995	14.5783	7.5476	5.6978	0.513	-0.3899
388119	-103.4036	16.8417	8.7475	8.7357	4.5891	2.3042	0.7686
388121	-99.7585	13.6307	8.1514	7.0001	5.0742	1.4799	1.7644
423709	-100.4538	44.4267	21.6462	13.1858	3.7117	-2.4171	-2.9126
423710	-87.5506	47.5513	23.1222	9.22	-0.3274	-3.7079	-3.38
423712	-96.5207	24.5034	15.8116	9.3514	4.5009	0.3804	-0.7775
423713	-88.2684	45.1279	22.3188	8.7466	0.2682	-3.7408	-2.3926
422690	-92.0025	18.9308	14.0916	7.2566	4.0594	0.5433	-0.2572
422691	-93.871	13.7614	10.6379	6.2009	4.1464	1.1822	0.8458
422697	-92.3906	13.9304	10.4404	6.1754	4.6829	0.8922	0.6565
425182	-87.2196	19.3928	13.6144	7.7692	2.4982	0.6257	-0.8894
425180	-85.4833	27.6978	12.8032	7.9309	3.2178	0.4019	0.5057
166374	-102.3535	19.8302	11.7273	10.2283	5.9681	2.6913	0.9016
376908	-89.4987	9.996	7.8595	3.827	0.7373	0.6277	-0.3311
422681	-87.215	17.7051	13.1634	7.3055	4.0023	0.4903	0.201
105962	-93.6398	16.6622	12.5668	6.7251	4.2946	0.5704	-0.5479
105964	-93.6052	17.659	13.4595	7.6402	4.1748	0.97	-0.8593
105965	-97.7701	10.1429	8.1617	5.5528	4.3112	1.7136	1.2557
105968	-106.0026	12.0856	7.0344	6.1262	4.9331	1.3106	1.169
163913	-97.1708	21.6088	13.1134	8.6728	3.8801	0.3434	-1.73
239763	-98.879	14.8525	10.228	7.8609	5.2787	2.4676	1.6316
239764	-100.1223	6.529	6.6892	3.6873	3.4274	1.7019	1.0776
106003	-99.61	21.6374	12.5206	8.5901	3.7336	0.0816	-1.0435

USNM catalog no. (PAL #)	C1	C2	C3	C4	C5	C6	C7
376927	-114.1826	22.426	11.2487	10.8165	7.1321	3.5958	1.6075
29498	-110.9202	34.7428	16.8126	13.1315	6.3212	0.3827	-1.4336
411503	-114.2327	43.6786	17.0899	17.3626	4.4981	1.0271	-2.2321
411504	-118.5023	28.3679	13.3147	13.2442	7.134	2.0852	-0.0287
411506	-117.1449	25.8433	9.7824	13.3869	5.0026	3.7835	-0.5624
411507	-116.5689	31.6446	12.53	13.8388	3.797	1.1111	-2.74
425303	-111.0272	29.9785	13.6761	13.5774	5.8919	1.7114	0.007
427950	-121.2909	43.7081	16.5526	19.503	3.973	2.466	-2.086
106001	-98.5661	20.6968	12.1414	8.0031	5.1558	0.1012	0.4513
108316a	-101.8417	32.6267	16.3147	11.7541	4.1789	-1.0464	-1.6313
108317a	-95.4571	46.7641	22.6023	11.5717	2.3369	-1.7349	-3.1319
108317b	-117.6458	42.5436	16.7859	17.7246	3.4204	1.8232	-2.919
108318a	-115.1706	42.3123	16.8032	17.0838	3.629	1.276	-2.3371
108318b	-117.4439	40.1378	17.2999	17.0177	5.643	1.7604	-0.7739
108319b	-112.8321	34.1369	15.2269	14.7781	6.4795	2.3828	-1.1115
108321	-121.1273	39.7625	16.2837	17.9479	5.9197	2.5726	-1.0278
108322a	-115.5416	39.2419	15.7699	17.6501	5.5248	2.9633	-1.2311
108323b	-123.0876	36.4829	14.7094	17.3714	6.9095	2.9186	-0.4625
220382	-118.7764	39.2065	15.7932	17.6585	5.5782	1.7334	-0.8494
423759	-102.8653	38.2092	17.2946	13.8144	4.1971	-0.5655	-0.9849
425308	-105.6184	37.751	15.5245	13.4612	2.8193	-1.1234	-2.5085
427947	-113.3195	42.3759	17.1392	17.1892	3.3564	0.9029	-2.279
427949	-109.6906	16.7769	8.9503	9.0962	6.0807	3.5034	1.6868
443802	-115.5736	37.3327	15.8467	16.0911	5.4489	1.9299	-1.3006
427908	-113.3405	29.9391	12.3567	14.7831	5.4124	2.4626	-0.125
427909	-114.9549	27.2503	11.1141	14.2293	5.9032	3.0916	0.2727
427915	-120.7567	34.1224	12.48	17.2305	5.8201	3.9998	-0.4046
427918	-120.963	29.7394	11.0141	15.8303	5.9645	3.8044	0.0553
427936	-108.6996	22.4015	11.0555	11.2774	5.8022	3.5926	0.5708
105992b	-112.2848	20.7258	7.5889	10.2202	4.7432	1.7725	0.4599
427941	-92.7968	31.8567	16.3728	10.9972	3.4492	0.3164	-1.122
427942	-99.5147	29.0846	16.5664	11.2246	5.2664	0.387	-0.7902
105984	-101.3723	20.4813	12.1352	9.1527	6.0384	1.6673	0.5953
220381	-102.3117	16.3958	9.7786	6.1328	4.4714	0.0041	0.2346
388156	-95.0952	21.3004	13.8978	7.9478	4.9726	0.2866	0.5119
388157	-97.0721	28.179	16.831	9.8577	3.9951	-0.0787	-1.8731
388158	-103.0499	25.7348	16.1716	10.0266	6.4241	0.9324	-0.1768

USNM catalog no. (PAL #)	C1	C2	C3	C4	C5	C6	C7
388162	-101.1596	28.7561	16.4925	10.6463	5.6009	0.216	-0.7721
388163	-99.6367	26.4486	13.536	10.7735	4.5525	0.8898	-1.0551
388168	-107.8773	13.5695	9.7417	5.8339	5.8127	1.6234	1.6825
388169	-103.6262	12.8249	8.1608	6.6358	4.8869	2.1453	1.4338
400813	-105.6367	10.8507	6.2322	7.1875	4.3057	2.7141	1.8394
411489	-109.7239	11.0895	5.0141	7.2885	4.2248	3.0136	1.4499
400805	-109.5449	13.2937	5.7975	7.935	4.2634	2.4298	1.282
400808	-107.6243	9.4292	6.8364	5.9961	5.0782	2.9428	1.8872
105974	-98.4346	12.2629	5.7207	5.2427	3.4568	1.1561	1.1796
423698	-102.1544	5.7848	4.3188	4.6867	3.2705	2.4825	1.7767
108841	-103.4773	7.2672	4.5808	5.01	3.3267	1.8446	1.5758
108855	-102.9078	13.5938	7.798	7.9245	4.0825	2.5392	0.9731
108861(1)	-100.3515	10.4925	6.1013	5.1903	3.0721	0.7983	0.7596
108861(2)	-88.4683	13.8604	13.1699	3.8305	3.3214	-1.7625	-0.1844
108861(3)	-83.9872	18.0818	15.8864	7.2818	1.4109	-0.3502	-1.5556
239761	-100.7321	21.4005	12.3246	8.6088	4.0909	-0.1409	-0.8089
400761	-101.6997	11.7527	8.5016	6.4093	4.3853	2.5022	1.113
400765	-104.6393	11.3279	5.2724	6.6408	3.581	2.3424	1.2981
400766	-97.3423	10.4393	8.5543	5.0327	3.7511	0.3989	0.6761
400767	-92.8342	15.5536	13.3913	5.8704	4.5947	-0.0968	-1.0863
400769	-107.2294	10.0159	4.0398	6.7157	4.0383	2.1827	2.011

USNM catalog no. (PAL #)	D1	D2	D3	D4	D5	D6	D7
108826(1)	-0.1796	0.0239	0.0647	0.0458	0.0533	0.0263	0.0241
108826(2)	-0.4278	0.2275	0.1767	0.1338	0.0704	0.0186	-0.0313
239766	-0.3257	0.1593	0.1211	0.1206	0.0195	-0.0128	-0.0383
239768	-0.4391	0.1943	0.1633	0.0582	0.0682	-0.0188	-0.0005
239769	0.0109	-0.02	0.0005	0.0073	0.012	0.0054	-0.0004
239771	-0.2575	0.0945	0.0704	0.0524	0.0665	0.0216	0.032
239772	-0.7913	0.2722	0.3241	0.234	0.2689	0.0617	0.0756
239773	-0.56	0.1926	0.1095	0.1314	0.0511	0.0355	0.0069
252729	-0.1546	0.0855	0.1318	0.1223	0.1012	0.0074	-0.0375
416063	-0.6958	0.1753	0.1667	0.1216	0.1258	0.01	0.0378
420216	-0.2074	0.0537	0.0697	0.0679	0.0339	0.0006	-0.0116
420218	0.1686	0.0289	0.0473	0.019	0.0398	0.0263	0.0121
420220	-0.15	0.0295	0.0458	0.0482	0.0391	0.0164	0.0084

USNM catalog no. (PAL #)	D1	D2	D3	D4	D5	D6	D7
420221	-0.4457	0.1059	0.1555	0.177	0.1141	0.0497	-0.0145
420223	-0.1258	0.0205	0.0256	0.0289	0.0145	-0.014	-0.0083
420224	-0.4062	0.1107	0.1074	0.0562	0.055	0.0031	0.0077
420226	-0.6511	0.408	0.2967	0.2558	0.0724	0.0232	-0.076
420227	-0.4918	0.3872	0.3695	0.201	0.0829	-0.1018	-0.0884
420230	0.0798	-0.0537	0.0204	0.0357	0.0285	-0.0064	0.0033
420231	-0.5239	0.1535	0.1377	0.1123	0.0656	0.0357	-0.0418
388094	-0.2999	0.0963	0.1679	0.0972	0.0533	-0.0087	-0.0101
388095	-0.3913	0.159	0.1852	0.0857	-0.0873	-0.0672	0.0496
388097	-0.5762	0.3661	0.2915	0.2698	0.0224	-0.0675	-0.106
388098	0.0089	-0.0202	0.0212	0.0136	-0.0008	-0.0056	-0.0057
388100	-0.3466	0.1197	0.1018	0.0527	0.0798	0.0069	0.0182
388102	-0.4646	0.1554	0.2056	0.1083	0.107	-0.0232	-0.0214
388103	-0.2024	0.0495	0.0699	0.0595	0.0434	-0.0066	-0.0237
388104	-0.2187	0.0795	0.096	0.0754	0.0499	0.0062	-0.0073
388109	-0.4463	0.111	0.1783	0.1058	0.073	0.0316	-0.0234
388112	-0.4097	0.2474	0.2098	0.1602	0.0889	-0.0104	-0.043
388113	0.0966	0.0062	-0.0179	-0.0005	0.0168	0.0331	0.0084
388114	-0.066	0.0643	0.0088	0.0079	0.0038	0.0104	-0.0043
388115	-0.1639	0.1199	0.1128	0.0544	0.026	-0.0243	-0.027
388116	-0.4291	0.2153	0.2196	0.1387	0.0919	-0.0288	-0.0456
388118	0.0836	-0.0284	-0.11	-0.1335	-0.0621	-0.0119	0.0118
388119	-0.4615	0.0834	0.1071	0.1529	0.0823	0.0347	0.0142
388121	-0.2113	0.0356	0.0514	0.0793	0.055	0.0201	0.0256
423709	-0.4317	0.3804	0.2888	0.2282	0.0792	-0.0642	-0.0909
423710	-0.6492	0.6979	0.5218	0.2786	-0.0115	-0.1647	-0.1726
423712	-1.0351	0.5794	0.4664	0.3792	0.2462	0.0376	-0.0689
423713	-0.8238	1.1193	0.6901	0.4296	0.0555	-0.3115	-0.2272
422690	-0.6429	0.246	0.2348	0.146	0.0983	-0.0105	-0.0403
422691	-0.1347	0.0401	0.0452	0.0354	0.0299	0.01	0.009
422697	-0.2724	0.0677	0.0991	0.0887	0.0863	0.0226	0.0136
425182	-0.2543	0.1138	0.1172	0.0879	0.033	0.0112	-0.0174
425180	-0.3936	0.2471	0.1472	0.1208	0.0509	0.0126	0.0138
166374	-0.4536	0.2013	0.1333	0.1612	0.1165	0.077	0.0187
376908	-0.1998	0.043	0.0541	0.0369	0.0096	0.01	-0.0049
422681	-0.0883	0.0629	0.058	0.0341	0.0459	0.022	0.0095
105962	-0.2469	0.0385	0.0901	0.0612	0.0319	0.0014	-0.0077

USNM catalog no. (PAL #)	D1	D2	D3	D4	D5	D6	D7
105964	-0.1947	0.0486	0.0788	0.0582	0.0333	0.0014	-0.0152
105965	-0.1524	0.0012	0.04	0.0587	0.0439	0.013	0.0106
105968	-0.7444	0.1301	0.1268	0.1781	0.1629	0.0388	0.0322
163913	-0.3867	0.1861	0.1306	0.1237	0.0733	0.0113	-0.0507
239763	-0.2792	0.0897	0.0935	0.0701	0.0765	0.0388	0.0287
239764	0.3669	0.0146	-0.026	-0.0136	-0.0226	-0.0096	-0.0157
106003	-0.2949	0.1468	0.1167	0.1126	0.0652	0.0116	-0.0233
376927	-0.3584	0.1406	0.1034	0.1356	0.1117	0.0671	0.0352
29498	-0.2126	0.1402	0.0849	0.0958	0.0616	0.0037	-0.0188
411503	-0.125	0.179	0.0576	0.071	0.0342	0.0277	-0.018
411504	-0.3019	0.1371	0.048	0.084	0.0748	0.0133	-0.0014
411506	-0.0252	0.0326	0.037	0.0435	0.0257	0.0146	-0.0002
411507	-0.2676	0.1435	0.04	0.0828	0.0324	0.0276	-0.027
425303	-0.0045	0.0133	-0.0137	-0.0132	-0.0094	0.0002	-0.0021
427950	-0.418	0.3016	0.1675	0.2657	0.0672	0.0518	-0.0508
106001	-0.4826	0.218	0.1356	0.1072	0.082	0.0031	0.0296
108316a	-0.3101	0.1169	0.1182	0.1349	0.0388	-0.0302	-0.0408
108317a	-0.2879	0.2856	0.1921	0.1379	0.0369	-0.0301	-0.0656
108317b	-0.3765	0.3223	0.1634	0.2182	0.05	0.0526	-0.0578
108318a	-0.1729	0.142	0.029	0.0585	0.0157	0.023	-0.0205
108318b	-0.2964	0.208	0.1229	0.1619	0.0652	0.0258	-0.0151
108319b	-0.3263	0.1981	0.1314	0.1702	0.0937	0.0412	-0.0225
108321	-0.4972	0.3083	0.1364	0.2412	0.0956	0.0476	-0.0353
108322a	-0.2763	0.1843	0.1188	0.173	0.066	0.0425	-0.0203
108323b	-0.2629	0.1623	0.0862	0.1431	0.0724	0.0382	-0.0082
220382	-0.0726	0.0605	0.0567	0.0729	0.0324	0.0082	-0.0069
423759	-0.0415	0.0848	0.0431	0.0393	0.022	0.0148	-0.0042
425308	-0.5027	0.3461	0.1901	0.2072	0.0363	-0.0473	-0.0841
427947	-0.5152	0.3848	0.2151	0.2847	0.063	0.0208	-0.0778
427949	0.1512	-0.0778	-0.0122	-0.0178	-0.0382	-0.0256	-0.0064
443802	-0.5901	0.3542	0.2937	0.3568	0.1432	0.0641	-0.0344
427908	-0.0909	0.0253	0.052	0.0827	0.0479	0.0114	-0.0053
427909	-0.1912	0.0907	0.0574	0.0969	0.0498	0.0318	0.0038
427915	-0.4361	0.2508	0.1246	0.2375	0.0973	0.0886	-0.0115
427918	-0.5437	0.3034	0.1102	0.2291	0.1078	0.1022	0.0038
427936	-0.1976	0.0807	0.0612	0.0829	0.0532	0.0391	0.0072
105992b	-0.1347	0.0744	0.0395	0.0516	0.0317	0.0222	0.0204

USNM catalog no. (PAL #)	D1	D2	D3	D4	D5	D6	D7
427941	-0.1981	0.1477	0.0798	0.079	0.0258	0.0032	-0.0218
427942	-0.1698	0.0973	0.0862	0.0804	0.0454	0.0035	-0.0102
105984	-0.4071	0.1584	0.1491	0.1535	0.125	0.0391	0.0167
220381	-0.1931	0.0617	0.0565	0.0315	0.0505	0.0065	0.0064
388156	-0.8266	0.3075	0.3588	0.2717	0.1926	-0.009	-0.0034
388157	0.0138	-0.0314	0.0677	0.0784	0.0026	-0.0107	0.0068
388158	-0.2853	0.1324	0.1514	0.0985	0.1058	0.0081	-0.0021
388162	-0.5719	0.3492	0.2593	0.2166	0.1458	0.013	-0.0232
388163	0.0125	-0.0136	0.0121	0.0092	0.0137	0.0006	0
388168	-0.3209	0.0678	0.111	0.1029	0.1247	0.0643	0.0451
388169	-0.7095	0.1965	0.1525	0.1495	0.1676	0.0903	0.0676
400813	-0.4588	0.0288	0.1108	0.1538	0.1108	0.0655	0.0751
411489	-0.1466	-0.0077	0.0355	0.0617	0.0487	0.0229	0.0201
400805	-0.226	-0.0029	0.0617	0.1221	0.1254	0.0409	0.0214
400808	0.041	-0.0164	-0.008	-0.0038	-0.0045	-0.0065	-0.0064
105974	-1.088	0.2385	0.1807	0.2361	0.2071	0.0599	0.0742
423698	-0.1682	-0.0706	0.0765	0.0578	0.0093	0.0392	0.0439
108841	-0.0627	-0.0237	0.0111	0.0341	0.0151	0.0041	0.0027
108855	-0.7648	0.3281	0.0881	0.1381	0.1115	0.112	0.018
108861(1)	-0.2685	0.0558	0.0491	0.0581	0.0417	0.0142	0.0151
108861(2)	-0.0705	0.0344	0.0659	-0.005	0.0183	0.0299	-0.0108
108861(3)	-0.995	0.4456	0.4972	0.2986	0.0427	-0.032	-0.108
239761	-0.8656	0.3558	0.3301	0.3099	0.1958	-0.0063	-0.0491
400761	0.1333	-0.0279	-0.0398	-0.0001	-0.0183	-0.0093	0.0022
400765	-0.4571	0.1322	0.0697	0.0796	0.0554	0.0535	0.0493
400766	-0.2885	0.0629	0.0751	0.0594	0.0546	0.0083	0.0123
400767	-0.431	0.214	0.1206	0.0292	0.1282	0.0085	-0.0498
400769	-0.2262	-0.0029	-0.0143	-0.0135	-0.0388	-0.0031	-0.006

Appendix B.4: Superimposed original (dashed line) and size-standardized (solid line) aperture outlines for specimens used in this study. Outlines are scaled by centroid size, colored by genus, and arranged alphabetically by genus and species. USNM catalog numbers (PAL #) provided, with multiple individuals of the same number indicated in parentheses. See Appendix 2.1 for additional specimen information.

Appendix B.5: Intraspecific shape change with latitude with geographic outliers removed for species with greater than five specimens. Shape is measured as scores along the first two principal components axes. Gray shading indicates 95% confidence interval around the regression line. Reported coefficients and support values are estimated using multivariate linear regression.

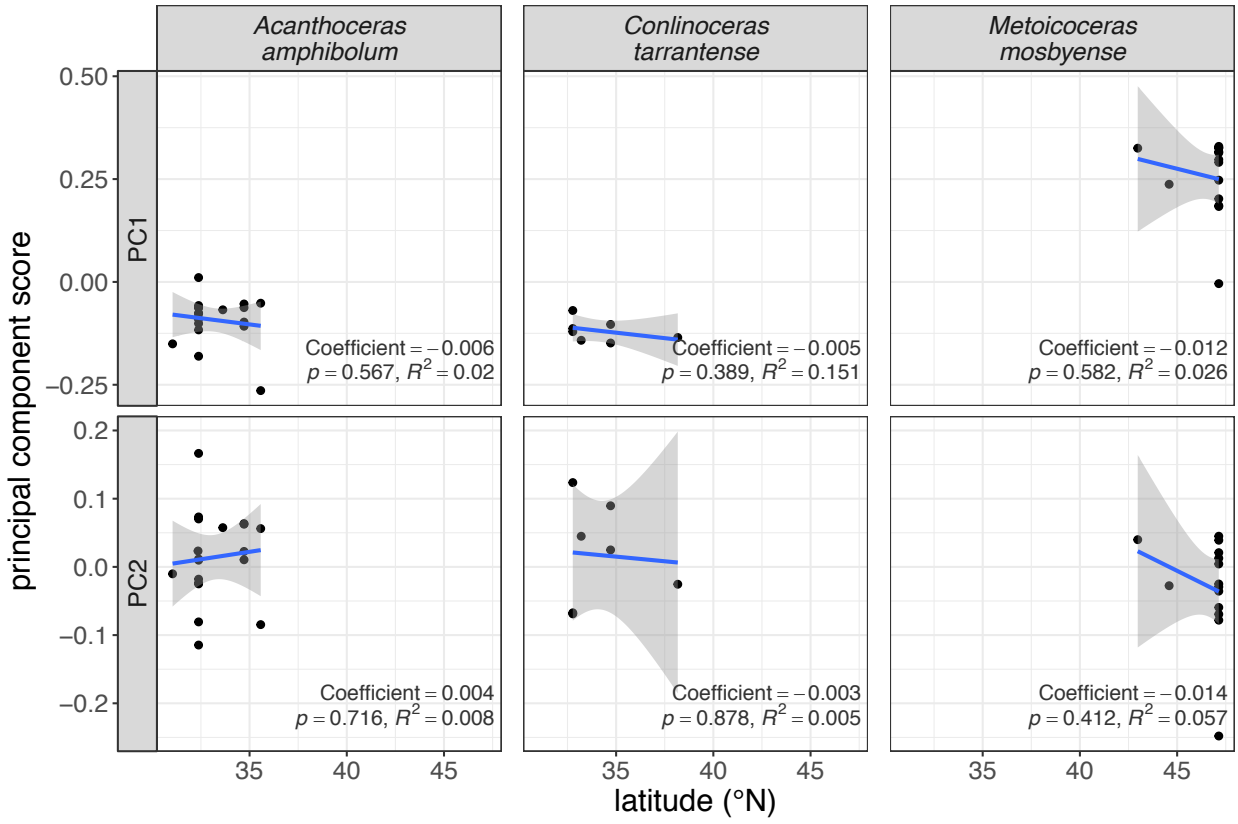

Appendix C

Supporting material for Chapter 3

Appendix C.1: GenBank accession numbers for bivalve sequences used to generate a maximum likelihood tree.

genus	species	12S	16S	18S	28S	COI	H3
Abra	*alba*	-	-	AM774533	AM779707	-	KC429228
Abra	*nitida*	-	-	-	-	KR084796	-
Abyssogena	*phaseoliformis*	-	-	-	-	-	KX010147
Abyssogena	*southwardae*	-	-	-	-	KX949734	-
Acanthocardia	*echinata*	-	-	-	-	KR084830	-
Acanthocardia	*tuberculata*	-	-	AM774522	AM779696	-	-
Acar	*domingensis*	-	-	-	-	FJ480682	KT757861
Acar	*plicata*	-	-	AJ389630	AJ307533	-	-
Acesta	*excavata*	-	AM494899	-	-	KX713441	-
Acesta	*oophaga*	AM494887	-	-	-	-	-
Acharax	sp.	-	-	AJ563761	HE863781	LC186997	-
Acila	*castrensis*	-	-	-	-	KC429087	-
Adamussium	*colbecki*	AJ571589	AJ243882	AJ242534	-	-	-
Adipicola 1	*iwaotakii*	-	HF545099	-	HF545021	EU702322	-
Adipicola 2	*pacifica*	-	HF545066	-	HF545040	AB539005	HF545161
Adipicola 3	*crypta*	-	HF545084	-	HF545041	EU702321	HF545134
Adontorhina	*cyclia*	-	-	AM392455	AM392438	-	-
Aequipecten	*opercularis*	AJ571591	AM494413	AJ310482	AJ307543	KR084493	-
Alathyria	*profuga*	-	-	-	-	KP184914	-
Amusium	*pleuronectes*	AJ571592	AJ571616	-	-	GU120019	-
Anadara	*broughtonii*	-	-	-	-	-	JN974601
Anadara	*inaequivalvis*	-	-	-	FN667990	-	-
Anadara	*kagoshimensis*	-	-	-	-	HQ258853	-
Anapella	*cycladea*	-	-	AM774556	AM779730	-	-
Angulus	*tenuis*	-	-	AM774524	AM779698	KR084511	-
Anisodevonia	*ohshimai*	-	-	-	-	AB714878	AB714838

genus	species	12S	16S	18S	28S	COI	H3
Anodonta	*californiensis*	-	-	-	-	AY785396	-
Anodonta	*cygnea*	-	-	AM774476	AM779650	-	-
Anodontia 1	*alba*	-	-	AM774498	LT614738	-	-
Anodontia 2	*bullula*	-	-	AM774495	AM779668	-	-
Anodontia 2	*omissa*	-	-	-	-	KC429120	KC429199
Anodontia 3	*fragilis*	-	-	AJ581842	AJ581877	-	-
Anomalocardia	*producta*	-	-	-	-	HM124616	HM124670
Anomia	*ephippium*	-	-	AJ389661	AJ307556	-	-
Anomia	sp.	-	-	-	-	GQ166573	-
Antigona	*lamellaris*	-	-	-	-	HM124608	HM124660
Arca	*noae*	-	-	-	AJ307563	-	-
Arca	*ventricosa*	-	-	-	-	AB076935	-
Arca	*zebra*	-	-	-	-	-	KT757872
Archivesica 1	*gigas*	-	-	-	-	KF990208	KX010138
Arcopsis	*interplicata*	-	-	-	-	HQ258879	JN974621
Arctica	*islandica*	-	-	AM774563	AM779737	KR084887	DQ184901
Argopecten	*irradians*	-	-	L11265	-	GU120025	HQ329247
Argopecten	*purpuratus*	-	AJ972426	-	-	-	-
Argopecten	*ventricosus*	AM039765	-	-	-	-	-
Arthritica	*japonica*	-	-	-	-	AB714879	AB714839
Asaphis	*deflorata*	-	-	-	-	KC429144	KC429227
Asaphis	*violascens*	-	-	AM774531	AM779705	-	-
Aspatharia	*pfeifferiana*	-	-	-	-	KC429107	KC429184
Astarte	*borealis*	-	AJ586485	-	-	-	-
Astarte	*castanea*	-	-	-	-	AF120662	-
Astarte	*elliptica*	-	-	-	-	-	KP113596
Astarte	*sulcata*	-	-	AM774480	AM779654	-	-
Atrina	*pectinata*	-	-	-	AJ307557	-	-

genus	species	12S	16S	18S	28S	COI	H3
Atrina	*rigida*	-	-	-	-	KX713446	-
Atrina	*seminuda*	-	-	-	-	-	HQ329249
Aulacomya	*ater*	-	-	-	-	JF301757	-
Austriella	*corrugata*	-	-	AM774502	AJ581882	-	-
Axinulus	*hadalis*	-	-	-	-	LC187042	-
Axinulus	sp.	-	-	AM392441	AM392440	-	-
Azorinus	*minutus*	-	-	-	-	AB714905	AB714864
Bankia	*carinata*	-	-	-	-	AF120671	-
Barbatia 1	*barbata*	-	-	-	-	AF120645	KC429161
Barbatia 2	*virescens*	-	-	-	-	HQ258841	KT757879
Barbatia 4	*lacerata*	-	-	-	-	HQ258836	JN974611
Barbatia 5	*reeveana*	-	-	-	-	AF253491	-
Barbatia 7	*lima*	-	-	-	-	HQ258838	JN974613
Barbatia 8	*parva*	-	-	-	-	GQ166575	-
Barnea	*candida*	-	-	-	-	-	KC429237
Barnea	*davidi*	-	-	-	-	KJ125426	-
Barnea	*parva*	-	-	AM774542	AM779716	-	-
Basterotia	sp.	-	-	-	-	AB714904	AB714863
Bathymodiolus 2	*aduloides*	-	-	-	HF545036	-	-
Bathymodiolus 2	*manusensis*	-	HF545059	-	-	-	-
Bathymodiolus 3	*heckerae*	-	-	-	-	LT841270	-
Bathymodiolus 3	*puteoserpentis*	-	HF545053	-	HF545033	-	-
Bathymodiolus 3	*septemdierum*	-	-	-	-	-	KP881000
Bathymodiolus 4	*japonicus*	-	-	-	HF545039	-	-
Bathymodiolus 4	*mauritanicus*	-	HF545083	-	-	-	HF545126
Bathymodiolus 4	*tangaroa*	-	-	-	-	AY608439	-
Bathyspinula	*filatovae*	-	-	-	-	-	KC993889
Bathyspinula	*hilleri*	-	-	-	-	KC984733	-

genus	species	12S	16S	18S	28S	COI	H3
Bentharca	sp.	-	-	-	-	AB076938	-
Benthomodiolus	*geikotsucola*	-	-	-	-	AB679346	-
Benthomodiolus	*lignocola*	-	HF545050	-	-	-	KF720596
Benthomodiolus	sp.	-	-	-	HF545022	-	-
Bornia	*sebetia*	-	-	-	-	KC429125	KC429206
Brachidontes	*rostratus*	-	-	-	-	KT804891	-
Brachidontes	*variabilis*	-	-	AJ389643	AJ307536	-	-
Bretskya	*scapula*	-	-	FR686722	-	-	-
Callista	*brevisiphonata*	-	-	-	-	JN898931	HM124623
Callista	*chione*	-	AJ548772	AJ007613	-	-	-
Callista	*disrupta*	-	-	-	AM779741	-	-
Calyptogena 1	*magnifica*	-	-	-	-	-	KX010150
Calyptogena 3	*pacifica*	-	-	AM774564	AM779738	-	KX010145
Calyptogena 9	*extenta*	-	-	-	-	KX420935	KT345595
Cardiolucina	*semperiana*	-	-	AJ389655	-	-	-
Cardiolucina	sp.	-	-	-	FR686788	-	-
Cardiomya	*costellata*	-	-	-	-	KR084474	-
Cardiomya	sp.	-	-	-	-	-	KC429198
Cardita	*calyculata*	-	-	-	-	AF120660	KC429189
Cardita	*leana*	-	-	AM774481	AM779655	-	-
Cardites	*antiquata*	-	-	-	-	AF120661	-
Chama	*aspersa*	-	-	-	AM779735	-	-
Chama	*gryphoides*	-	-	-	-	AF120656	-
Chama	*macerophylla*	-	-	-	-	-	KC429202
Chama	*semipurpurata*	-	-	AM774562	-	-	-
Chamelea	*gallina*	-	AM085110	-	-	KR084939	DQ184886
Chavania	sp.	-	-	FR686726	FR686790	-	-
Chione	*elevata*	-	-	-	-	KC429136	KC429219

genus	species	12S	16S	18S	28S	COI	H3
Chlamys 1	*varia*	AJ571593	AJ586480	-	-	-	-
Chlamys 2	*islandica*	AJ571605	AJ243573	-	-	-	-
Chlamys 3	*glabra*	AJ571590	AJ243574	-	-	-	-
Chlamys 5	*farreri*	-	-	-	-	GU120000	DQ418455
Ciliatocardium	*ciliatum*	-	-	-	-	HQ919142	-
Circe 1	cf. *rivularis*	-	-	-	-	-	DQ184891
Circe 2	*scripta*	-	-	-	-	HM124612	HM124666
Clausinella	*isabellina*	-	-	-	-	EU117995	-
Cleidothaerus	*albidus*	-	-	-	-	KC429117	-
Clencharia	*abyssorum*	-	-	-	-	-	KC429154
Cochlodesma	*praetenue*	-	-	-	-	KC429114	KC429193
Codakia	*orbicularis*	-	-	AM774500	LT614754	-	-
Codakia	*orbiculata*	-	-	-	-	AF120657	-
Compsomyax	*subdiaphana*	-	-	-	-	-	DQ184893
Coralichlamys	*madreporarum*	AJ571598	AJ571608	-	-	-	-
Corbicula	*fluminea*	-	-	AM774558	AM779732	KX192354	-
Corbula	*gibba*	-	-	-	-	HG005371	-
Corbula	*sinensis*	-	-	AM774545	AM779719	-	-
Corbula	*tunicata*	-	-	-	-	-	KC429236
Corculum	*cardissa*	-	-	-	-	FJ745334	-
Costacallista	*erycina*	-	-	-	-	JN898943	HM124622
Crassadoma	*gigantea*	AM039774	AJ972437	-	-	-	-
Crassostrea	*gigas*	-	-	AM182263	-	KX345128	-
Crassostrea	sp.	-	HF549057	-	AJ553915	-	-
Crassostrea	*virginica*	-	-	-	-	-	DQ901547
Crenatula	*avicularis*	-	-	-	-	-	HQ329251
Cristaria	*plicata*	-	-	-	-	KY561634	-
Cryptopecten	*nux*	-	-	-	-	-	KP300497

genus	species	12S	16S	18S	28S	COI	H3
Ctena 1	*chiquita*	-	-	-	FR686830	-	-
Ctena 1	*mexicana*	-	-	AM774496	-	-	-
Ctena 2	*bella*	-	-	-	FR686824	-	-
Ctena 2	*delicatula*	-	-	AM774494	-	-	-
Ctena 3	*eburnea*	-	-	FR686707	FR686827	-	-
Ctena 4	*divergens*	-	-	AJ389656	AJ307559	-	-
Ctenoides	*annulata*	-	-	AJ389653	-	-	-
Ctenoides	*annulatus*	-	-	-	AJ307550	-	-
Ctenoides	*mitis*	-	-	-	-	-	KT757881
Ctenoides	sp.	-	-	-	-	KU496287	-
Cucullaea	*labiata*	-	-	-	-	-	JN974615
Cucullaea	sp.	-	-	-	-	HQ258880	-
Curvemysella	*paula*	-	-	-	-	AB714881	AB714841
Cuspidaria	*rostrata*	-	-	-	-	GQ166580	-
Cyamiomactra	*laminifera*	-	-	-	-	KC429131	-
Cycladicama	*cumingi*	-	-	AM774548	AM779722	-	-
Cycladicama	*cumingii*	-	-	-	-	KX713453	-
Cyclopecten	*ryukyuensis*	-	-	-	-	AB076952	-
Cyrenoida	*floridana*	-	-	FM999789	-	KC429123	KC429201
Cyrenoida	sp.	-	-	-	LT614733	-	-
Dacrydium	*zebra*	-	-	-	-	AB076945	-
Decatopecten	*plica*	-	-	-	-	GU120030	-
Decatopecten	*strangei*	-	-	-	-	-	KP300501
Delectopecten	*fosterianus*	-	-	-	-	-	KP300482
Delectopecten	*greenlandicus*	-	-	-	-	KF643856	-
Delectopecten	*vitreus*	-	AJ571618	-	-	-	-
Dendostrea	*folium*	-	LM993885	-	-	-	-
Dendostrea	*frons*	-	-	-	-	AB084109	-

genus	species	12S	16S	18S	28S	COI	H3
Devonia	*semperi*	-	-	-	-	AB714882	AB714842
Dimya	*lima*	-	-	-	-	-	KC429181
Diplodonta 1	*subrotundata*	-	-	AJ389654	-	-	-
Diplodonta 2	*circularis*	-	-	AM774549	AM779723	-	-
Discolucina	*virginea*	-	-	AM774497	AM779671	-	-
Divalinga	*bardwelli*	-	-	-	FR686793	-	-
Divalinga	*weberi*	-	-	LT614690	-	-	-
Divaricella	*irpex*	-	-	FR686730	FR686784	-	KX375952
Divariscintilla	*toyohiwakensis*	-	-	-	-	AB714869	AB714831
Donacilla	*cornea*	-	-	-	-	KC429148	KC429233
Donax 3	*trunculus*	-	-	AJ309018	-	-	KC429226
Dosinia	*lupinus*	-	AJ548771	-	-	-	-
Dosinia	*troscheli*	-	-	-	-	HM124576	HM124630
Dreissena	*polymorpha*	-	-	AM774543	AM779717	KX537632	KC429234
Dulcina	*karubari*	-	-	FR686697	-	-	-
Dulcina	sp.	-	-	-	FR686777	-	-
Ectenagena 3	*elongata*	-	-	-	-	KT345568	KX010149
Electroma 3	*alacorvi*	-	-	AJ389641	AJ307549	-	HQ329254
Elliptio	*dilatata*	-	-	-	-	AF156507	-
Empleconia	*cumingii*	-	-	-	-	AB076930	-
Ennucula 2	*granulosa*	-	-	-	-	KC984749	-
Ensiculus	*cultellus*	-	-	AM774508	AM779682	-	-
Ensis	*americanus*	-	-	AM182264	-	-	-
Ensis	*arcuatus*	-	-	-	AJ966692	-	-
Ensis	*directus*	-	HF970449	-	-	-	-
Ensis	*siliqua*	-	-	-	-	EU523685	-
Entovalva	*lessonothuriae*	-	-	-	-	-	AB714843
Entovalva	sp.	-	-	-	-	FJ629377	-

genus	species	12S	16S	18S	28S	COI	H3
Ephippodonta	*gigas*	-	-	-	-	AB714870	AB714832
Epicodakia 1	*tatei*	-	-	FR686712	FR686828	-	-
Epioblasma	*triquetra*	-	-	-	-	AF156528	-
Eucrassatella	*cumingi*	-	-	-	-	-	KC429187
Eucrassatella	*cumingii*	-	-	AM774479	AM779653	-	-
Eucrassatella	*nana*	-	-	-	-	HM180574	-
Eurhomalea	*lenticularis*	-	-	-	-	DQ458480	DQ184870
Excellichlamys	*spectabilis*	-	-	AJ389648	AJ307544	AB076911	-
Fimbria	*fimbriata*	-	-	AM774505	AM779679	-	-
Flexopecten	*flexuosus*	-	FN667664	-	-	-	-
Flexopecten	*glaber*	-	-	AJ389662	AJ307545	-	-
Fragum	*mundum*	-	-	-	-	FJ745350	-
Fragum	*unedo*	-	-	-	-	-	KC429239
Frenamya	*elongatus*	-	-	AM774486	AM779660	-	KC429190
Funafutia	cf. *levukana*	-	-	LT614693	-	-	-
Funafutia	*levukana*	-	-	-	FR686782	-	-
Gafrarium 1	*tumidum*	-	-	-	-	-	DQ184892
Gafrarium 2	*dispar*	-	-	-	-	-	HM124664
Gaimardia	*trapesina*	-	-	-	-	KX713464	-
Gaimardia	*trapezina*	-	-	AM774546	AM779720	-	KC429215
Galeomma	sp.	-	-	-	-	-	AB714833
Galeomma	*turtoni*	-	-	-	-	AF120658	-
Gari	*intermedia*	-	-	AM774530	AM779704	-	-
Gari	*maculosa*	-	-	-	-	KX713465	-
Gastrochaena	*cuneiformis*	-	-	-	-	-	AB714865
Gastrochaena	*dubia*	-	-	-	-	AF120670	-
Gastrochaena	*gigantea*	-	-	AM774515	AM779689	-	-
Geloina	*erosa*	-	-	-	-	AB076927	-

genus	species	12S	16S	18S	28S	COI	H3
Gemma	*gemma*	-	-	-	-	KU905996	DQ184894
Geukensia	*demissa*	-	AJ586484	-	-	-	-
Geukensia	*granosissima*	-	-	-	-	AY621927	-
Gigantidas	*crypta*	-	-	-	-	-	KF720613
Gigantidas	*mauritanicus*	-	-	-	-	KU597621	-
Gigantidas	sp.	-	HF545088	-	HF545044	-	-
Glauconome	*chinensis*	-	-	-	-	-	DQ184899
Glauconome	*rugosa*	-	-	-	-	KC429140	-
Glauconome	*virens*	-	-	AM774559	AM779733	-	-
Gloripallium	*pallium*	AJ571599	AJ571609	-	-	-	-
Glossus	*humanus*	-	-	-	-	KX713466	KC429212
Gloverina	cf. *rectangularis*	-	-	-	FR686772	-	-
Gloverina	cf. *vestifex*	-	-	LT614713	-	-	-
Glycymeris 3	*pedunculus*	-	-	-	AJ307534	-	-
Glycymeris 4	*glycymeris*	-	-	-	FN667988	KX785213	KT757884
Gomphina	*undulosa*	-	-	-	-	-	DQ184869
Gonimyrtea 2	*ferruginea*	-	-	LT614714	LT614755	-	-
Hemidonax	*pictus*	-	-	AM774560	AM779734	-	KC429218
Hiatella	*arctica*	-	-	-	-	-	KC429208
Hiatella	*australis*	-	-	AM774512	AM779686	-	-
Hiatella	sp.	-	-	-	-	KP977967	-
Hippopus	*hippopus*	-	AM909765	-	-	KJ202106	-
Huxleyia	*munita*	-	-	-	-	-	KC429157
Hyotissa	*hyotis*	-	LM993887	AJ389632	-	-	-
Hyotissa	*imbricata*	-	-	-	-	AB076917	-
Hyotissa	*mcgintyi*	-	-	-	-	-	KC429171
Hyriopsis	sp.	-	-	-	-	KX865953	-
Idas	*argenteus*	-	-	-	-	-	LM992897

genus	species	12S	16S	18S	28S	COI	H3
Idas	sp.	-	HF545062	-	HF545024	FJ158587	-
Indoaustriella	*dalli*	-	-	-	AM774135	-	-
Indoaustriella	*plicifera*	-	-	AM774132	-	-	-
Inversidens	*brandtii*	-	-	-	-	AB040827	-
Irus	*crenatus*	-	-	-	-	-	DQ184871
Irus	*irus*	-	-	AM774572	AM779670	-	-
Irus	*mitis*	-	-	-	-	AB714906	-
Isognomon	*ephippium*	-	-	-	-	KU341975	-
Isognomon	*legumen*	-	-	AJ389639	AJ307551	-	KT757894
Jupiteria	sp.	-	-	-	-	-	KC993886
Katelysia	*hiantina*	-	-	-	-	JN898939	HM124657
Keenaea	*samarangae*	-	-	-	-	AB076947	-
Kellia	cf. *jacksoniana*	-	-	AM774517	AM779691	-	-
Kellia	*porculus*	-	-	-	-	AB714884	AB714844
Kelliella	sp.	-	-	-	-	KC429129	KC429213
Kurtiella	aff. *bidentata*	-	-	-	-	-	AB714849
Kurtiella	*bidentata*	-	-	-	-	KJ183014	-
Laevicardium	*serratum*	-	-	-	-	KX713470	-
Laevichlamys 1	*cuneata*	AJ571594	AJ571610	-	-	-	-
Laevichlamys 2	*wilhelminae*	AJ571595	AJ571611	-	-	-	-
Lampsilis	*ovata*	-	-	-	-	EF033262	-
Lamychaena	*hians*	-	-	-	-	KX713473	KC429209
Lanceolaria	*grayana*	-	-	-	-	KJ434525	-
Lasaea	*adansoni*	-	-	-	-	-	KC429203
Lasaea	*rubra*	-	-	AM774516	AM779690	-	-
Lasaea	sp.	-	-	-	-	AF120659	-
Laternula	*elliptica*	-	-	-	-	-	KC429192
Laternula	*marilina*	-	-	AM774487	AM779661	AB076923	-

genus	species	12S	16S	18S	28S	COI	H3
Ledella 1	*jamesi*	-	-	-	-	KC984739	-
Lepidolucina	*venusta*	-	-	FR686739	FR686806	-	-
Leptaxinus	*indusarium*	-	-	AM392454	-	-	-
Leucosphaera	cf. *diaphana*	-	-	FR686699	FR686781	-	-
Leukoma	*staminea*	-	-	AM774570	AM779744	KF643722	-
Lima 3	*lima*	-	-	AJ389652	AJ307558	AF120649	KC429174
Lima 4	*fujitai*	-	-	-	-	AB076913	-
Limaria	*fragilis*	-	-	-	-	AB076953	-
Limaria	*hemphilli*	-	-	-	-	-	KP300487
Limopsis	*marionensis*	-	-	AJ422058	-	-	-
Limopsis	sp.	-	-	-	-	-	KC429164
Lioconcha	*annettae*	-	-	-	-	HQ703158	-
Lithophaga	*lithophaga*	-	-	-	-	AF120644	-
Lithophaga	*purpurea*	X75529	-	-	-	-	-
Litigiella	*pacifica*	-	-	-	-	AB714886	AB714846
Lopha	*cristagalli*	-	-	AJ389635	-	AB076908	-
Loripes	*clausus*	-	-	FR686737	-	-	-
Loripes	*lucinalis*	-	-	-	FR686794	-	-
Lucina 1	*pensylvanica*	-	-	AM774127	FR686805	KC429119	-
Lucina 2	*adansoni*	-	-	FR686731	FR686803	-	-
Lucinella	*divaricata*	-	-	FR686733	FR686801	-	-
Lucinisca 1	*fenestrata*	-	-	FR686734	FR686811	-	-
Lucinisca 2	*nassula*	-	-	FR686736	FR686812	-	-
Lucinoma	*aequizonata*	-	-	-	FR686820	-	-
Lucinoma	*borealis*	-	-	AM774501	-	-	-
Lunulicardia	*hemicardia*	-	-	-	-	FJ745352	-
Lutraria	*lutraria*	-	-	AM774553	AM779727	KR084641	-
Lyonsia	*floridana*	-	-	-	-	-	KC429191

genus	species	12S	16S	18S	28S	COI	H3
Lyonsia	*kawamurai*	-	-	-	-	AB084108	-
Lyrodus	*pedicellatus*	-	-	AM774540	AM779714	KU201137	-
Macoma	*nasuta*	-	-	AM774527	AM779701	-	-
Macoma	*petalum*	-	-	-	-	KY050188	-
Macrocallista	*nimbosa*	-	-	-	-	-	DQ184867
Macrocallista	*squalida*	-	-	-	-	DQ458485	-
Mactra	*chinensis*	-	-	-	-	EU118000	-
Mactra	*eximia*	-	-	AM774550	AM779724	-	-
Mactromeris	*polynyma*	-	-	L11230	-	KF643868	-
Malletia	*johnsoni*	-	-	-	-	-	KC993888
Malleus	*albus*	-	-	-	-	KC429097	KC429169
Malvifundus	*regulatus*	-	-	AJ389640	AJ307547	-	-
Margaritifera	*laosensis*	-	-	-	-	KJ943555	-
Margaritifera	*margaritifera*	-	-	AM774475	AM779649	-	-
Margaritifera	*middendorffi*	-	-	-	-	-	KU763372
Megapitaria	*squalida*	-	-	-	-	-	DQ184868
Melliteryx	*puncticulata*	-	-	-	-	AB714887	AB714847
Mendicula	*ferruginosa*	-	-	AM774483	AM779657	LC187041	-
Mercenaria	*mercenaria*	-	AJ548773	AM774566	AM779740	JN898950	HM124672
Meretrix	*lyrata*	-	AJ548769	-	-	-	-
Meretrix	*meretrix*	-	-	-	-	JN898949	-
Meretrix	*petechialis*	-	-	-	-	-	HM124637
Meropesta	*nicobarica*	-	-	AM774551	AM779725	JN674606	AB714867
Mesodesma	*donacium*	-	-	-	-	JF301797	-
Mimachlamys	*nobilis*	AJ571606	-	-	-	JN974583	-
Mimachlamys	*varia*	-	FN667674	AJ534979	AJ307546	-	HM469534
Mirapecten 1	*mirificus*	AJ571600	AJ571612	-	-	-	-
Mirapecten 2	*rastellum*	AJ571601	AJ571613	-	-	-	-

genus	species	12S	16S	18S	28S	COI	H3
Mizuhopecten	*yessoensis*	-	-	-	-	GU119997	-
Modiolus	*auriculatus*	-	-	AJ389644	AJ307537	-	-
Modiolus	*elongatus*	-	-	-	-	GQ480318	-
Modiolus	*modiolus*	-	HF545048	-	-	-	KF720595
Monia	*patelliformis*	-	-	-	-	-	KC429179
Monia	*umbonata*	-	-	-	-	AB076951	-
Monitilora	*ramsayi*	-	-	AM774504	AM779678	-	-
Montacutona	sp.	-	-	-	-	AB714888	AB714848
Mulinia	*edulis*	-	-	-	-	JF301809	-
Mulinia	*lateralis*	-	-	L11268	-	-	-
Musculista	*senhousia*	-	-	HG005362	-	HG005372	-
Musculium	*indicum*	-	-	-	-	KU376202	-
Musculium	*lacustre*	-	-	AM774538	AM779712	-	KU376222
Musculus	*discors*	-	-	-	-	KR084795	KP113647
Mya	*arenaria*	-	-	FM999791	FM999792	-	KC429235
Mya	*uzenensis*	-	-	-	-	KX534204	-
Myadora	*brevis*	-	-	-	-	KX713483	-
Myadora	*pandoriformis*	-	-	AM774489	AM779662	-	-
Myochama	*anomioides*	-	-	-	-	KC429116	KC429195
Myrtea 1	*spinifera*	-	-	LT614720	LT614758	-	-
Myrtea 4	*flabelliformis*	-	-	FR686694	FR686775	-	-
Myrtina	sp.	-	-	LT614723	LT614761	-	-
Mysella	*charcoti*	-	-	-	-	-	KC429205
Mysella	*vitrea*	-	-	AM774519	AM779693	-	-
Mytilaster	*minimus*	-	-	-	-	KU697745	-
Mytilus	*edulis*	-	-	-	-	KX925570	-
Mytilus	*galloprovincialis*	-	-	-	-	-	AY267739
Mytilus	sp.	-	AM904599	-	-	-	-

genus	species	12S	16S	18S	28S	COI	H3
Neaeromya	*rugifera*	-	-	-	-	JQ712869	-
Neilonella	*salicensis*	-	-	-	-	-	KC993887
Neilonella	*whoii*	-	-	-	-	KC984732	-
Neopycnodonte	*cochlear*	-	-	-	-	AB076939	-
Neotrigonia	*lamarckii*	-	-	AM774478	AM779652	KC429105	KC429182
Nipponarca	*bistrigata*	-	-	-	-	AB076936	-
Nipponomontacuta	*actinariophila*	-	-	-	-	AB714891	AB714850
Nipponomysella 1	*subtruncata*	-	-	-	-	AB714893	AB714852
Nipponomysella 2	*oblongata*	-	-	-	-	AB714892	AB714851
Notomyrtea 3	*botanica*	-	-	AJ581862	AJ581896	-	-
Nucinella	sp.	-	-	-	-	KC429089	KC429158
Nucula 1	*sulcata*	-	-	-	-	KF369160	-
Nucula 2	*atacellana*	-	-	-	-	-	KT757893
Nucula 2	*proxima*	-	-	-	-	AF120641	-
Nuculana 2	*minuta*	-	-	-	-	AF120643	-
Nuculana 3	*pella*	-	-	AJ389665	AJ307553	-	-
Nuculana 4	*commutata*	-	-	-	-	GQ166587	-
Nutricola	*tantilla*	-	-	AM774569	AM779743	-	DQ184862
Ostrea	*lurida*	-	-	-	-	KT317529	-
Pandora	*glacialis*	-	-	-	-	-	KP113605
Pandora	*pinna*	-	-	-	-	GQ166588	-
Panopea	*abrupta*	-	-	AM774514	AM779688	-	-
Panopea	*generosa*	-	-	-	-	KC429126	KC429207
Paphia	*papilionacea*	-	-	-	-	JN898946	HM124668
Paphia	*undulata*	-	AM085109	-	-	-	-
Paraborniola	*matsumotoi*	-	-	-	-	AB714894	AB714853
Parastarte	*triquetra*	-	-	-	-	-	DQ184895
Parathyasira	*equalis*	-	-	AM774482	AM779656	KC429122	KC429200

genus	species	12S	16S	18S	28S	COI	H3
Parvamussium	*crypticum*	-	-	-	-	AB084106	-
Parvicardium	*exiguum*	-	-	-	-	AF120664	-
Parvilucina 1	*pectinella*	-	-	LT614711	LT614753	-	-
Parvilucina 2	*costata*	-	-	FR686727	FR686809	-	-
Pecten 2	*jacobaeus*	-	FN667671	-	-	-	-
Pecten 2	*maximus*	AJ571597	-	AJ534978	AJ534978	KC429102	KC429175
Pectunculus	*exoleta*	-	-	-	-	DQ458478	-
Pectunculus	*exoletus*	-	-	-	-	-	DQ184857
Pedum	*spondyloideum*	-	-	AJ389649	AJ311560	-	-
Peregrinamor	*gastrochaenans*	-	-	-	-	AB714895	-
Peregrinamor	*ohshimai*	-	-	-	-	-	AB714854
Periglypta	*puerpera*	-	-	-	-	HM124621	HM124674
Perna	*perna*	-	-	HG005364	-	KU743156	-
Petricola	*lapicida*	-	-	-	-	KC429138	DQ184896
Petricolaria	*pholadiformis*	-	-	AM774565	AM779739	-	DQ184897
Phacoides	*pectinatus*	-	-	AM774503	AM779677	KX713490	-
Pharella	*javanica*	-	-	AM774509	AM779683	-	-
Pharus	*legumen*	-	-	AM774510	AM779684	-	-
Phaxas	*pellucidus*	-	-	-	-	KR084896	KC429231
Pholas	*dactylus*	-	-	AJ309017	-	-	-
Pholas	*orientalis*	-	-	-	-	KJ125423	-
Pillucina 1	*pisidium*	-	-	AJ581865	AJ581898	-	-
Pillucina 4	*vietnamica*	-	-	AM774493	FR686796	-	-
Pillucina 5	*australis*	-	-	FR686743	FR686800	-	-
Pinctada	*chemnitzi*	-	-	-	-	KU341958	-
Pinctada	*margaritifera*	-	-	AJ389638	-	-	-
Pinctada	*martensi*	-	-	-	-	-	JN974634
Pinna	*carnea*	-	-	-	-	-	KC429172

genus	species	12S	16S	18S	28S	COI	H3
Pinna	*muricata*	-	-	AJ389636	AJ307560	-	-
Pinna	*nobilis*	-	-	-	-	KY321811	-
Pisidium	*kuiperi*	-	-	-	-	KU376218	-
Pisidium	*obtusale*	-	-	AM774539	AM779713	-	-
Pisidium	*zugmayeri*	-	-	-	-	-	KU376247
Pitar 1	*simpsoni*	-	-	-	-	-	DQ184865
Pitar 2	*fulminatus*	-	-	-	-	-	DQ184863
Pitarina	*japonica*	-	-	-	-	HQ703206	DQ184864
Placopecten	*magellanicus*	AM039780	AJ972443	-	-	-	-
Placuna	*placenta*	-	-	-	-	KC429104	KC429180
Pleurobema	*sintoxia*	-	-	-	-	EF033253	-
Plicatula	*australis*	-	-	-	-	-	KC429178
Plicatula	*plicata*	-	-	AJ389651	AJ307539	-	-
Pliocardia 3	*krylovata*	-	-	-	-	-	KX010160
Pliocardia 4	*stearnsii*	-	-	-	-	JX196993	KX010157
Pododesmus	*caelata*	-	-	AJ389650	AJ307555	-	-
Pododesmus	*macrochisma*	-	-	-	-	KF644022	-
Poromya	*illevis*	-	-	AM774492	AM779665	-	KC429197
Propeamussium	*maorium*	-	-	-	-	-	KP300493
Propeamussium	sp.	-	-	-	-	KC429103	-
Propeleda	*carpenteri*	-	-	-	-	KC984735	-
Pseudamussium	*peslutrae*	-	-	-	-	KR084848	-
Pseudogaleomma	*japonica*	-	-	AM774518	AM779692	-	-
Pseudogaleomma	sp.	-	-	-	-	AB714872	AB714834
Pseudolucinisca	*lacteola*	-	-	AJ581867	AJ581900	-	-
Pseudopythina 3	*macrophthalmensis*	-	-	-	-	AB714898	AB714857
Pseudopythina 4	*ochetostomae*	-	-	-	-	-	AB714855
Psilunio	*littoralis*	-	-	-	-	AF120652	-

genus	species	12S	16S	18S	28S	COI	H3
Pteria 1	*hirundo*	-	-	-	FN667991	AF120647	KC429167
Pteria 2	*macroptera*	-	-	AJ389637	AJ307548	-	-
Pteria 3	*penguin*	-	-	-	-	KU341960	HQ329314
Pulvinites	*exempla*	-	-	AJ414640	AJ307540	-	-
Pycnodonte	*taniguchii*	-	-	-	-	AB076916	-
Pyganodon	*grandis*	-	-	-	-	EF488189	-
Pythina	*deshayesiana*	-	-	-	-	-	KX375910
Quadrula	*quadrula*	-	-	-	-	KX853969	-
Radiolucina 1	*cancellaris*	-	-	FR686746	FR686814	-	-
Radiolucina 2	*amianta*	-	-	FR686745	FR686813	-	-
Rangia	*cuneata*	-	-	-	-	KT959440	KC429232
Rasta	*lamyi*	-	-	AM774506	AM779680	-	-
Ruditapes 1	*decussatus*	-	AJ417846	-	-	KX981455	-
Ruditapes 2	*philippinarum*	-	AJ417847	AM774568	AM779742	KU252878	JN807355
Ruditapes 3	*bruguieri*	-	-	-	-	-	DQ184879
Saccostrea	*cucullata*	-	-	AJ389634	AJ344329	-	-
Saccostrea	*palmula*	-	-	-	-	KT317604	-
Saccostrea	*scyphophilla*	-	LM993883	-	-	-	-
Salpocola	*philippinensis*	-	-	-	-	AB714901	AB714860
Scintilla 3	*rosea*	-	-	-	-	AB714873	-
Scintillona	*cryptozoica*	-	-	-	-	-	KC429204
Scissula	*similis*	-	-	-	-	KC429142	KC429225
Semele	*carnicolor*	-	-	AM774535	AM779709	-	-
Semele	*purpurascens*	-	-	-	-	KX713499	-
Semipallium	*amicum*	-	AJ571614	-	-	-	-
Semipallium	*dringi*	AJ571603	-	-	-	-	-
Semipallium	*fulvicostatum*	-	-	-	-	-	KP300483
Septifer 1	*excisus*	-	-	-	-	AB076922	-

genus	species	12S	16S	18S	28S	COI	H3
Septifer 2	*virgatus*	-	-	-	-	AB076941	-
Septifer 3	*bilocularis*	-	-	AJ389645	-	-	-
Serripes	*laperousii*	-	-	-	-	KF643682	-
Sinonovacula	*constricta*	-	-	-	-	AY874534	-
Solemya	sp.	-	HG942545	-	AM293673	-	-
Solemya	*togata*	-	-	AJ389658	-	-	-
Solemya	*velum*	-	-	-	-	JN165237	KC429159
Solen	*marginatus*	-	AJ586473	-	-	-	-
Solen	sp.	-	-	-	-	KP252996	-
Solen	*vaginoides*	-	-	AM774507	AM779681	-	KC429230
Sphaerium	*corneum*	-	-	AM774537	AM779711	-	-
Sphaerium	*nucleus*	-	-	-	-	-	KC429216
Sphaerium	*striatinum*	-	-	-	-	AF120667	-
Sphenia	*perversa*	-	-	AM774544	AM779718	-	-
Spisula	*solida*	-	-	-	AM779726	-	-
Spisula	*subtruncata*	-	AJ548774	L11271	-	KR084884	-
Spondylus	*gaederopus*	AJ571607	AJ571621	-	-	-	-
Spondylus	*hystrix*	-	-	AJ389647	AJ307561	-	-
Spondylus	*varius*	-	-	-	-	AB076909	-
Spondylus	*wrightianus*	-	-	-	-	-	KP300508
Stewartia	*floridana*	-	-	FR686749	FR686797	-	-
Striarca	*lactea*	-	-	-	-	AF120646	KT757897
Strigilla	*euronia*	-	-	AM774525	AM779699	-	-
Swiftopecten	*swiftii*	-	-	-	-	-	KP300502
Tagelus	*californianus*	-	-	AM774536	AM779710	-	-
Tagelus	*plebeius*	-	-	-	-	KU906110	KC429229
Tamu	*fisheri*	-	HF545065	-	HF545030	HF545104	HF545148
Tegillarca	*granosa*	-	-	-	-	HQ896817	KT757898

genus	species	12S	16S	18S	28S	COI	H3
Tellimya	*ferruginosa*	-	-	-	-	KC429153	KC429240
Tellina	*zyonoensis*	-	-	-	-	JX503037	-
Teredo	*clappi*	-	-	-	-	-	KC429238
Teredo	*navalis*	-	-	-	-	KU201203	-
Thracia	*alciope*	-	-	AM774490	AM779663	-	-
Thracia	*phaseolina*	-	-	-	-	KF808177	KC429194
Thraciopsis	*angustata*	-	-	AM774491	AM779664	-	-
Thyasira 1	cf. *subovata*	-	-	-	AM392435	-	-
Thyasira 1	*flexuosa*	-	-	-	-	KR084646	-
Thyasira 1	*polygona*	-	-	AM774484	-	-	-
Thyasira 2	*sarsi*	-	-	AM774485	AM779659	-	-
Thyasira 3	*perplicata*	-	-	AM392448	AM392432	-	-
Timoclea	*ovata*	-	-	-	-	KR084861	-
Timoclea	sp.	-	-	-	-	-	HM124662
Tindaria	*kennerlyi*	-	-	-	-	KC984731	-
Tivela 1	*stultorum*	-	-	-	-	-	DQ184859
Tivela 2	*mactroides*	-	-	-	-	-	DQ184858
Trapezium	*sublaevigatum*	-	-	AM774557	AM779731	KC429128	KC429211
Tresus	*capax*	-	-	L11267	-	KF643926	-
Tridacna	*crocea*	-	AM909764	-	-	DQ269479	-
Tridacna	*maxima*	-	-	-	AM779697	-	-
Tridacna	sp.	-	-	X91972	-	-	-
Troendleina	cf. *musculator*	-	-	FR686720	FR686807	-	-
Tropidomya	*abbreviata*	-	-	AJ389657	-	-	-
Turtonia	*minuta*	-	-	-	-	-	DQ184898
Ungulina	*cuneata*	-	-	AM774547	AM779721	-	-
Unio	*delphinus*	-	-	-	-	KP217927	-
Unio	*pictorum*	-	-	AM774477	AM779651	-	KC429186

genus	species	12S	16S	18S	28S	COI	H3
Urumella	*concava*	-	-	-	-	AB076946	-
Varicorbula	*dissimilis*	-	-	-	-	AF120669	-
Velesunio	*ambiguus*	-	-	-	-	-	KC429183
Velesunio	sp.	-	-	-	-	AY387020	-
Venerupis	*corrugata*	-	-	-	-	KX018583	-
Venerupis	*philippinarum*	AB065374	AB065375	-	-	-	EF670667
Venerupis	*saxatilis*	-	-	AM774571	AM779728	-	-
Venus	*casina*	-	-	-	-	KR084893	-
Venus	*verrucosa*	-	AJ548763	AJ007614	-	-	DQ184884
Venustaconcha	*ellipsiformis*	-	-	-	-	AY785401	-
Veprichlamys	*kiwaensis*	-	-	-	-	-	KP300489
Vesicomya	sp.	-	-	-	-	EU403476	KX010137
Volachlamys	*singaporina*	-	-	-	-	GU120011	-
Vulsella	sp.	-	-	AJ389642	AJ307562	-	-
Vulsella	*vulsella*	-	-	-	-	KX713508	HQ329322
Wallucina	*assimilis*	-	-	AJ581869	FR686791	-	-
Wareniconcha	*lepta*	-	-	-	-	JX256251	KX010142
Xenostrobus	*securis*	-	-	-	-	KU714835	-
Yoldia 1	*limatula*	-	-	-	-	AF120642	KC429156
Yoldia 2	*myalis*	-	-	-	-	KF644002	-
Yoldia 3	*eightsi*	-	-	-	-	KC984730	-
Yoldiella 1	*americana*	-	-	-	-	KC984726	-
Yoldiella 2	*orcia*	-	-	-	-	KC984728	-
Yoldiella 3	*nana*	-	-	AJ389659	-	HQ919200	-

Appendix C.2: Names and references for genera found to be paraphyletic in previously published phylogenies. This table was used to assign species to genus groupings/tree tips that are not known to be paraphyletic.

genus	species	source trees
Adipicola 1	*iwaotakii*	Miyazaki et al. 2010
Adipicola 2	*pacifica*	Miyazaki et al. 2010
Adipicola 3	*crypta*	Miyazaki et al. 2010
Anodontia 1	*alba*	Taylor, Williams, Glover, and Dyal 2007; Taylor, Williams, and Glover 2007; Taylor et al. 2011; Taylor et al. 2014; Williams et al. 2004
Anodontia 2	*bullula*	Taylor, Williams, Glover, and Dyal 2007; Williams et al. 2004
Anodontia 2	*omissa*	Williams et al. 2004
Anodontia 2	*philippiana*	Taylor, Williams, Glover, and Dyal 2007; Williams et al. 2004
Anodontia 2	sp.	Williams et al. 2004
Anodontia 3	*fragilis*	Williams et al. 2004
Anodontia 3	*ovum*	Taylor, Williams, and Glover 2007; Williams et al. 2004
Archivesica 1	*gigas*	Valdés et al. 2012
Archivesica 2	sp.	Valdés et al. 2012
Barbatia 1	*barbata*	Bieler et al. 2014; Giribet and Distel 2003; Giribet and Wheeler 2002; Plazzi et al. 2011
Barbatia 2	*virescens*	Giribet and Distel 2003; Steiner and Hammer 2000
Barbatia 3	*amygdalumtostum*	Matsumoto 2003
Barbatia 4	*lacerata*	Matsumoto 2003
Barbatia 5	cfr. *setigera*	Plazzi et al. 2011
Barbatia 5	*reeveana*	Plazzi et al. 2011
Barbatia 6	*cancelllaria*	Steiner and Hammer 2000
Barbatia 7	*lima*	Matsumoto 2003
Barbatia 8	*parva*	Plazzi et al. 2011
Bathymodiolus 1	sp. NZ3	Miyazaki et al. 2010
Bathymodiolus 2	*aduloides*	Miyazaki et al. 2010
Bathymodiolus 2	*manusensis*	Miyazaki et al. 2010
Bathymodiolus 2	sp. Lau1	Miyazaki et al. 2010
Bathymodiolus 2	sp. Ne1	Miyazaki et al. 2010
Bathymodiolus 3	aff. *thermophilus*	Miyazaki et al. 2010
Bathymodiolus 3	*azoricus*	Miyazaki et al. 2010
Bathymodiolus 3	*brevior* MT	Miyazaki et al. 2010
Bathymodiolus 3	*brevior* NF	Miyazaki et al. 2010
Bathymodiolus 3	*brooksi*	Miyazaki et al. 2010

genus	species	source trees
Bathymodiolus 3	*heckerae*	Miyazaki et al. 2010
Bathymodiolus 3	*marisindicus*	Miyazaki et al. 2010
Bathymodiolus 3	*puteoserpentis*	Miyazaki et al. 2010
Bathymodiolus 3	*septemdierum*	Miyazaki et al. 2010
Bathymodiolus 3	sp. BR1	Miyazaki et al. 2010
Bathymodiolus 3	sp. EF1	Miyazaki et al. 2010
Bathymodiolus 3	*thermophilus*	Miyazaki et al. 2010
Bathymodiolus 4	*childressi*	Miyazaki et al. 2010
Bathymodiolus 4	*hirtus*	Miyazaki et al. 2010
Bathymodiolus 4	*japonicus*	Miyazaki et al. 2010
Bathymodiolus 4	*mauritanicus*	Miyazaki et al. 2010
Bathymodiolus 4	*platifrons*	Miyazaki et al. 2010
Bathymodiolus 4	*securiformis*	Miyazaki et al. 2010
Bathymodiolus 4	sp. C1	Miyazaki et al. 2010
Bathymodiolus 4	sp. Kikaijima	Miyazaki et al. 2010
Bathymodiolus 4	sp. Si11	Miyazaki et al. 2010
Bathymodiolus 4	sp. Si21	Miyazaki et al. 2010
Bathymodiolus 4	sp. Si33	Miyazaki et al. 2010
Bathymodiolus 4	*tangaroa*	Miyazaki et al. 2010
Calyptogena 1	*magnifica*	Bieler et al. 2014; Giribet and Distel 2003; Giribet and Wheeler 2002; Mikkelsen et al. 2006; Taylor, Williams, and Glover 2007; Valdés et al. 2012; Williams et al. 2004
Calyptogena 2	*packardana*	Valdés et al. 2012
Calyptogena 3	*pacifica*	Taylor, Williams, Glover, and Dyal 2007; Valdés et al. 2012
Calyptogena 4	sp. mtV	Valdés et al. 2012
Calyptogena 5	*fausta*	Valdés et al. 2012
Calyptogena 5	*gallardoi*	Valdés et al. 2012
Calyptogena 5	sp. mtII	Valdés et al. 2012
Calyptogena 5	sp. mtIII	Valdés et al. 2012
Calyptogena 6	undesc. sp. 2	Valdés et al. 2012
Calyptogena 7	*magnocultellus*	Valdés et al. 2012
Calyptogena 7	undesc. sp. 1	Valdés et al. 2012
Calyptogena 8	*tsubasa*	Valdés et al. 2012
Calyptogena 9	*extenta*	Valdés et al. 2012
Calyptogena 1*0*	*similaris*	Valdés et al. 2012
Calyptogena 1*0*	undesc. sp. 3	Valdés et al. 2012
Chlamys 1	*multistriata*	Barucca et al. 2004

genus	species	source trees
Chlamys 1	*varia*	Barucca et al. 2004; Giribet and Distel 2003; Giribet and Wheeler 2002
Chlamys 2	*hastata*	Giribet and Distel 2003
Chlamys 2	*islandica*	Barucca et al. 2004; Giribet and Distel 2003; Matsumoto 2003; Plazzi et al. 2011; Steiner and Hammer 2000
Chlamys 3	*glabra*	Barucca et al. 2004
Chlamys 4	*livida*	Plazzi et al. 2011
Chlamys 5	*farreri*	Plazzi et al. 2011; Xu et al. 2011
Circe 1	cf. *rivularis*	Mikkelsen et al. 2006
Circe 1	*nummulina*	Mikkelsen et al. 2006
Circe 1	*plicatina*	Mikkelsen et al. 2006
Circe 2	*rivularis*	Mikkelsen et al. 2006
Circe 2	*scripta*	Mikkelsen et al. 2006
Ctena 1	*chiquita*	Taylor et al. 2011; Taylor et al. 2014
Ctena 1	*imbricatula*	Taylor et al. 2011; Taylor et al. 2014
Ctena 1	*mexicana*	Taylor, Williams, Glover, and Dyal 2007; Taylor et al. 2011; Taylor et al. 2014
Ctena 1	*orbiculata*	Taylor et al. 2011; Taylor et al. 2014; Williams et al. 2004
Ctena 2	*bella*	Taylor et al. 2011; Taylor et al. 2014
Ctena 2	*delicatula*	Taylor, Williams, Glover, and Dyal 2007; Taylor et al. 2011; Taylor et al. 2014
Ctena 2	sp.	Taylor et al. 2011
Ctena 3	*decussata*	Taylor et al. 2011; Taylor et al. 2014
Ctena 3	*eburnea*	Taylor et al. 2011; Taylor et al. 2014
Ctena 4	*divergens*	Giribet and Distel 2003; Steiner and Hammer 2000
Diplodonta 1	*subrotundata*	Giribet and Distel 2003; Steiner and Hammer 2000; Taylor, Williams, and Glover 2007
Diplodonta 2	*circularis*	Taylor, Williams, Glover, and Dyal 2007; Taylor, Williams, and Glover 2007
Donax 1	*faba*	Taylor, Williams, Glover, and Dyal 2007
Donax 2	*veruinus*	Taylor, Williams, Glover, and Dyal 2007
Donax 3	*trunculus*	Bieler et al. 2014; Giribet and Distel 2003
Donax 4	*variabilis*	Steiner and Hammer 2000
Donax 5	sp.	Plazzi et al. 2011
Ectenagena 1	*nautilei*	Valdés et al. 2012
Ectenagena 2	*laubieri*	Valdés et al. 2012
Ectenagena 3	*elongata*	Valdés et al. 2012
Electroma 1	*zebra*	Tsubaki et al. 2011
Electroma 2	*ovata*	Tsubaki et al. 2011

genus	species	source trees
Electroma 3	*alacorvi*	Giribet and Distel 2003; Steiner and Hammer 2000; Tëmkin 2010
Ennucula 1	cf. *cardara*	Sharma et al. 2013
Ennucula 1	*tenuis expansa*	Sharma et al. 2013
Ennucula 2	*granulosa*	Sharma et al. 2013
Epicodakia 1	*tatei*	Taylor et al. 2011; Taylor et al. 2014
Epicodakia 2	*falklandica*	Taylor et al. 2014
Gafrarium 1	*tumidum*	Mikkelsen et al. 2006
Gafrarium 2	*dispar*	Mikkelsen et al. 2006
Gafrarium 3	*alfredense*	Plazzi et al. 2011
Glycymeris 1	*reevei*	Matsumoto 2003
Glycymeris 2	*rotunda*	Matsumoto 2003
Glycymeris 3	*insubrica*	Giribet and Distel 2003; Giribet and Wheeler 2002
Glycymeris 3	*pedunculus*	Giribet and Distel 2003; Steiner and Hammer 2000
Glycymeris 3	sp.	Steiner and Hammer 2000
Glycymeris 4	*glycymeris*	Bieler et al. 2014; Sharma et al. 2012
Gonimyrtea 1	sp. VAN	Taylor et al. 2014
Gonimyrtea 2	*ferruginea*	Taylor et al. 2014
Laevichlamys 1	*cuneata*	Barucca et al. 2004
Laevichlamys 2	*wilhelminae*	Barucca et al. 2004
Laevichlamys 3	*squamosa*	Matsumoto 2003
Ledella 1	*jamesi*	Sharma et al. 2013
Ledella 1	sp.	Sharma et al. 2013
Ledella 1	*ultima*	Sharma et al. 2013
Ledella 2	*ecaudata*	Sharma et al. 2013
Ledella 2	*pustulosa*	Sharma et al. 2013
Lima 1	*pacifica galapagensis*	Plazzi et al. 2011
Lima 2	sp.	Plazzi et al. 2011
Lima 3	*lima*	Bieler et al. 2014; Giribet and Distel 2003; Giribet and Wheeler 2002; Sharma et al. 2012; Steiner and Hammer 2000
Lima 4	*fujitai*	Matsumoto 2003
Lucina 1	*pensylvanica*	Bieler et al. 2014; Taylor, Williams, and Glover 2007; Taylor et al. 2011; Taylor et al. 2014; Williams et al. 2004
Lucina 2	*adansoni*	Taylor et al. 2011; Taylor et al. 2014
Lucinisca 1	*fenestrata*	Taylor et al. 2011; Taylor et al. 2014
Lucinisca 2	*centrifuga*	Taylor et al. 2011; Taylor et al. 2014
Lucinisca 2	*nassula*	Taylor et al. 2011; Taylor et al. 2014

genus	species	source trees
Mirapecten 1	*mirificus*	Barucca et al. 2004
Mirapecten 2	*rastellum*	Barucca et al. 2004
Myrtea 1	*spinifera*	Giribet and Distel 2003; Taylor, Williams, and Glover 2007; Taylor et al. 2011; Taylor et al. 2014; Williams et al. 2004
Myrtea 2	sp.	Taylor et al. 2011
Myrtea 3	sp.	Taylor et al. 2014
Myrtea 4	*flabelliformis*	Taylor et al. 2011
Nipponomysella 1	*subtruncata*	Goto et al. 2012
Nipponomysella 2	*oblongata*	Goto et al. 2012
Notomyrtea 1	*flabelliformis*	Taylor et al. 2014
Notomyrtea 2	*mayi*	Taylor et al. 2011; Taylor et al. 2014
Notomyrtea 3	*botanica*	Taylor, Williams, and Glover 2007; Williams et al. 2004
Notomyrtea 4	sp.	Taylor et al. 2014
Notomyrtea 5	*vincentia*	Taylor et al. 2014
Nucula 1	*sulcata*	Bieler et al. 2014; Giribet and Distel 2003; Sharma et al. 2013
Nucula 2	*atacellana*	Sharma et al. 2013
Nucula 2	*profundorum*	Sharma et al. 2013
Nucula 2	*proxima*	Giribet and Distel 2003; Giribet and Wheeler 2002; Sharma et al. 2012; Sharma et al. 2013; Steiner and Hammer 2000
Nucula 3	*decipiens*	Plazzi et al. 2011
Nucula 3	*nucleus*	Plazzi et al. 2011
Nucula 3	sp.	Plazzi et al. 2011
Nuculana 1	*conceptionis*	Sharma et al. 2013
Nuculana 2	*minuta*	Giribet and Distel 2003; Giribet and Wheeler 2002; Sharma et al. 2013
Nuculana 2	*pernula*	Giribet and Distel 2003; Giribet and Wheeler 2002; Sharma et al. 2013
Nuculana 3	*pella*	Giribet and Distel 2003; Goto et al. 2012; Sharma et al. 2013; Steiner and Hammer 2000
Nuculana 4	*commutata*	Plazzi et al. 2011
Parvilucina 1	*crenella*	Taylor et al. 2011; Taylor et al. 2014
Parvilucina 1	*pectinella*	Taylor et al. 2011; Taylor et al. 2014
Parvilucina 2	*costata*	Taylor et al. 2014
Pecten 1	*albicans*	Matsumoto 2003
Pecten 2	*jacobaeus*	Barucca et al. 2004; Giribet and Distel 2003; Plazzi et al. 2011

genus	species	source trees
Pecten 2	*maximus*	Barucca et al. 2004; Bieler et al. 2014; Giribet and Distel 2003; Giribet and Wheeler 2002; Matsumoto 2003; Sharma et al. 2012; Steiner and Hammer 2000
Phreagena 1	*nankeiensis*	Valdés et al. 2012
Phreagena 2	*kilmeri*	Valdés et al. 2012
Phreagena 2	*okutanii*	Valdés et al. 2012
Pillucina 1	*pisidium*	Taylor et al. 2014; Williams et al. 2004
Pillucina 2	sp.	Taylor et al. 2011
Pillucina 3	sp.	Taylor et al. 2014
Pillucina 4	*vietnamica*	Taylor, Williams, Glover, and Dyal 2007; Williams et al. 2004
Pillucina 5	*australis*	Taylor et al. 2011; Taylor et al. 2014
Pitar 1	*simpsoni*	Mikkelsen et al. 2006
Pitar 2	*fulminatus*	Mikkelsen et al. 2006
Pitar 3	sp.	Plazzi et al. 2011
Pliocardia 1	*cordata*	Valdés et al. 2012
Pliocardia 2	*crenulomarginata*	Valdés et al. 2012
Pliocardia 2	*kuroshimana*	Valdés et al. 2012
Pliocardia 3	*krylovata*	Valdés et al. 2012
Pliocardia 3	*ponderosa*	Valdés et al. 2012
Pliocardia 4	*stearnsii*	Valdés et al. 2012
Pseudopythina 1	aff. *nodosa*	Goto et al. 2012
Pseudopythina 2	aff. *ariake*	Goto et al. 2012
Pseudopythina 3	*macrophthalmensis*	Goto et al. 2012
Pseudopythina 3	*subsinuata*	Goto et al. 2012
Pseudopythina 4	*ochetostomae*	Goto et al. 2012
Pteria 1	*hirundo*	Bieler et al. 2014; Giribet and Distel 2003; Giribet and Wheeler 2002; Plazzi et al. 2011; Sharma et al. 2012; Steiner and Hammer 2000
Pteria 2	*macroptera*	Giribet and Distel 2003; Steiner and Hammer 2000
Pteria 3	*brevialata*	Steiner and Hammer 2000; Tsubaki et al. 2011
Pteria 3	*colymbus* 1	Tëmkin 2010
Pteria 3	*dendronephythya*	Tsubaki et al. 2011
Pteria 3	*loveni*	Matsumoto 2003; Tëmkin 2010; Tsubaki et al. 2011
Pteria 3	*penguin*	Tsubaki et al. 2011
Pteria 3	*stema*	Tëmkin 2010
Radiolucina 1	*cancellaris*	Taylor et al. 2011; Taylor et al. 2014
Radiolucina 2	*amianta*	Taylor et al. 2011; Taylor et al. 2014
Ruditapes 1	*decussatus*	Mikkelsen et al. 2006

genus	species	source trees
Ruditapes 2	*philippinarum*	Mikkelsen et al. 2006; Taylor, Williams, Glover, and Dyal 2007
Ruditapes 3	*bruguieri*	Mikkelsen et al. 2006
Scintilla 1	aff. *hydatina*	Goto et al. 2012
Scintilla 2	sp.1	Goto et al. 2012
Scintilla 3	*rosea*	Goto et al. 2012
Scintilla 4	sp.2	Goto et al. 2012
Septifer 1	*excisus*	Matsumoto 2003
Septifer 2	*virgatus*	Matsumoto 2003
Septifer 3	*bilocularis*	Giribet and Distel 2003; Steiner and Hammer 2000
Silicula 1	*rouchi*	Sharma et al. 2013
Silicula 2	sp.A	Sharma et al. 2013
Silicula 3	sp.B	Sharma et al. 2013
Thyasira 1	cf. *subovata*	Taylor, Williams, and Glover 2007
Thyasira 1	*flexuosa*	Sharma et al. 2012; Taylor, Williams, and Glover 2007; Williams et al. 2004
Thyasira 1	*gouldi*	Taylor, Williams, and Glover 2007; Williams et al. 2004
Thyasira 1	*polygona*	Taylor, Williams, Glover, and Dyal 2007; Taylor, Williams, and Glover 2007; Taylor et al. 2011; Taylor et al. 2014
Thyasira 2	*methanophila*	Taylor, Williams, and Glover 2007
Thyasira 2	*sarsi*	Giribet and Distel 2003; Taylor, Williams, Glover, and Dyal 2007; Taylor, Williams, and Glover 2007
Thyasira 2	vent sp.	Taylor, Williams, and Glover 2007
Thyasira 3	*perplicata*	Taylor, Williams, and Glover 2007
Thyasira 4	*equalis*	Bieler et al. 2014; Taylor, Williams, Glover, and Dyal 2007
Tivela 1	*stultorum*	Mikkelsen et al. 2006
Tivela 2	*mactroides*	Mikkelsen et al. 2006
Yoldia 1	*limatula*	Bieler et al. 2014; Giribet and Distel 2003; Giribet and Wheeler 2002; Sharma et al. 2012; Sharma et al. 2013; Steiner and Hammer 2000
Yoldia 2	*myalis*	Giribet and Distel 2003; Giribet and Wheeler 2002; Sharma et al. 2013
Yoldia 2	*scissurata*	Sharma et al. 2013
Yoldia 3	*eightsi*	Sharma et al. 2013
Yoldiella 1	*americana*	Sharma et al. 2013
Yoldiella 2	*inconspicua inconspicua*	Sharma et al. 2013
Yoldiella 2	*orcia*	Sharma et al. 2013
Yoldiella 3	*nana*	Giribet and Distel 2003; Steiner and Hammer 2000

Appendix C.3: Maximum likelihood tree of Bivalvia based on concatenated sequences (12S, 16S, 18S, 28S, COI, and H3). Bootstrap support values ≥ 70% and < 90% (white nodes) and ≥ 90% (gray nodes) are shown.

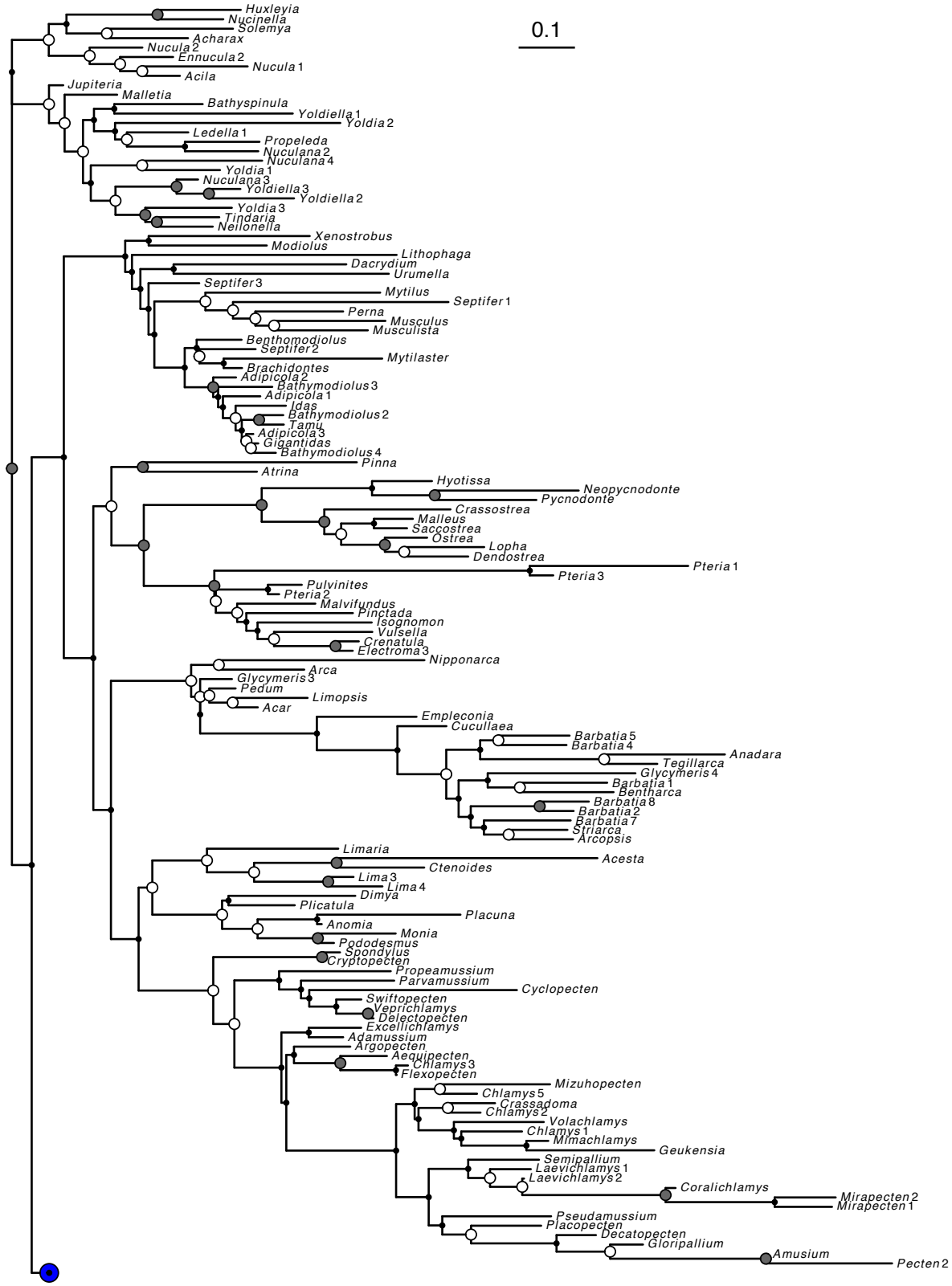

Appendix C.3: Maximum likelihood tree of Bivalvia (continued).

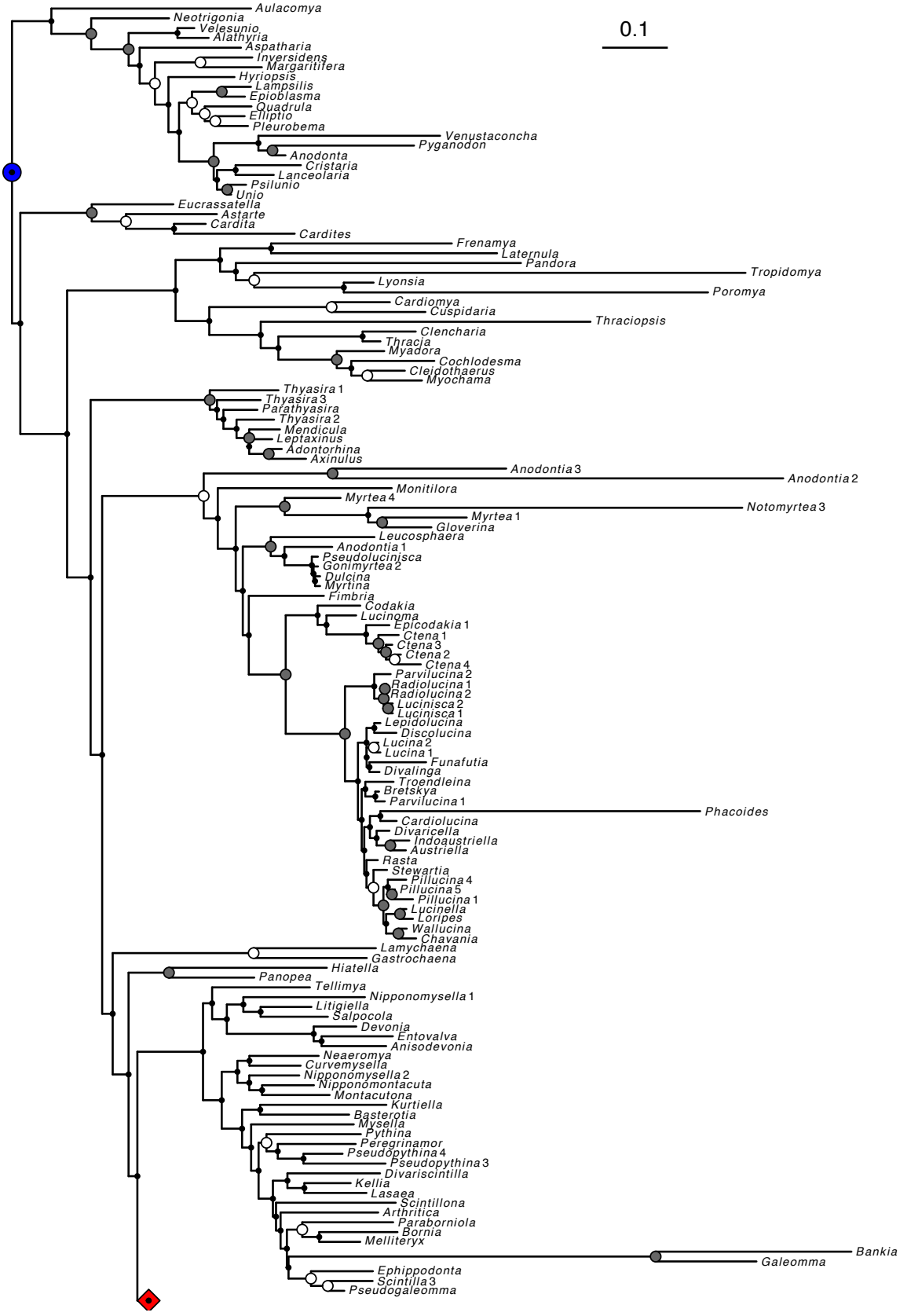

Appendix C.3: Maximum likelihood tree of Bivalvia (continued).